AD NUMBER
AD878074
LIMITATION CHANGES
TO: **Approved for public release; distribution is unlimited.**
FROM: **Distribution authorized to U.S. Gov't. agencies and their contractors; Critical Technology; OCT 1970. Other requests shall be referred to Army Aviation Materiel Laboratory, Fort Eustis, VA 23604. This document contains export-controlled technical data.**
AUTHORITY
usaamrdl ltr, 10 sep 1971

USAAVLABS TECHNICAL REPORT 70-55

20

APPLICATION OF COMPOSITE MATERIALS TO AN AIRCRAFT WING SECTION

By

Fred E. Bauch

Robert C. Lair

October 1970

U. S. ARMY AVIATION MATERIEL LABORATORIES
FORT EUSTIS, VIRGINIA

CONTRACT DA 44-177-AMC-407(T)
GOODYEAR AEROSPACE CORPORATION
AKRON, OHIO

DISCLAIMERS

The findings in this report are not to be construed as an official Department of the Army position unless so designated by other authorized documents.

When Government drawings, specifications, or other data are used for any purpose other than in connection with a definitely related Government procurement operation, the United States Government thereby incurs no responsibility nor any obligation whatsoever; and the fact that the Government may have formulated, furnished, or in any way supplied the said drawings, specifications, or other data is not to be regarded by implication or otherwise as in any manner licensing the holder or any other person or corporation, or conveying any rights or permission, to manufacture, use, or sell any patented invention that may in any way be related thereto.

DISPOSITION INSTRUCTIONS

Destroy this report when no longer needed. Do not return it to the originator.

DEPARTMENT OF THE ARMY
HEADQUARTERS US ARMY AVIATION MATERIEL LABORATORIES
FORT EUSTIS, VIRGINIA 23604

This report describes research conducted to develop fabrication techniques with fiberglass-resin systems and to apply small specimen test results to the design of a full-scale wing section. A 7-foot composite wing section was fabricated and subjected to bending and torsion loadings up to 200 percent of the design ultimate loading without failure.

The results of this research have been reviewed by the U.S. Army Aviation Materiel Laboratories and are considered to be technically sound. The report is published for the exchange of information and the stimulation of future research.

Task 1F162204A17003
Contract DA 44-177-AMC-407(T)
USAAVLABS Technical Report 70-55
October 1970

APPLICATION OF COMPOSITE MATERIALS TO AN AIRCRAFT WING SECTION

Final Report

GER 14892

By

Fred E. Bauch
Robert C. Lair

Prepared by

Goodyear Aerospace Corporation
Akron, Ohio

for

U. S. ARMY AVIATION MATERIEL LABORATORIES
FORT EUSTIS, VIRGINIA

SUMMARY

A 7-foot-long aircraft wing test section was fabricated with fiber glass reinforced plastic materials and subjected to static and dynamic tests. This was the third wing fabricated by Goodyear Aerospace and tested by the Naval Air Development Center (Aero Structures Department). However, this was the first wing to incorporate the higher strength, higher stiffness S glass material in roving and cloth form. The wing section performed in a very satisfactory manner with a good correlation between the predicted and actual test values.

TABLE OF CONTENTS

LIST OF ILLUSTRATIONS

Figure		Page

LIST OF TABLES

Table		Page

Table		Page
LII	Comparison of Experimental and Calculated Shear Stresses at Rosette No. 5 (Upper Skin of Aft Cell at BL 28.0)	194
LIII	Comparison of Experimental and Calculated Shear Stresses at Rosette No. 6 (Lower Skin of Aft Cell at BL 28.0)	195
LIV	Comparison of Experimental and Calculated Shear Stresses at Rosette No. 7 (Upper Skin of Aft Cell at BL 48.0)	196
LV	Comparison of Experimental and Calculated Shear Stresses at Rosette No. 8 (Upper Skin of Aft Cell at BL 68.0)	197
LVI	Comparison of Experimental and Calculated Shear Stresses at Rosette No. 9 (Lower Skin of Aft Cell at BL 68.0)	198
LVII	Comparison of Experimental and Calculated Shear Stresses at Rosette No. 10 (Main Spar at BL 28.0).	199
LVIII	Comparison of Experimental and Calculated Shear Stresses at Rosette No. 11 (Main Spar at BL 68.0).	200
LIX	Comparison of Experimental and Calculated Shear Stresses at Gages No. 34 and 35 (Aft Spar at BL 68.0)	201

LIST OF SYMBOLS

A	area, in.^{2}
a	unloaded side of compression panel, in.
BL	butt line
b	loaded side of compression panel, in.
C_1	$\dfrac{EI_{xy}}{EI_x EI_y - E^2 I^2_{xy}}$
C_2	$\dfrac{EI_y}{EI_x EI_y - E^2 I^2_{xy}}$
C_3	$\dfrac{EI_x}{EI_x EI_y - E^2 I^2_{xy}}$
D	dimension; also, skin bending stiffness, per inch
DUL	design ultimate load
d	sandwich skin thickness, in.
E	modulus of elasticity, psi
e	distance to shear center, in.
F	ultimate strength, psi
F_s	ultimate shear strength, psi
f	calculated stress, psi
G	shear modulus, psi
H	concentrated load, lb
Hz	cycles per second

I	moment of inertia, $in.^4$
K	constant; also, dimension
L	length, in.
M	bending moment, in.-lb
MS	margin of safety
N	allowable buckling load of panel, lb/in.; also, load factor
P	concentrated load, lb
p	load, lb
q	shear flow, lb/in.
R	stress ratio
T	torque, in.-lb.
t	thickness, in.
U	parameter involving shear stiffness
V	shear load, lb
V'	parameter relating shear and bending stiffness
WL	water line
x	distance to Y-Y axis, in.; also, horizontal distance, in.
y	distance to X-X axis, in.; also, deflection, in.
Z	dimension
γ	shear strain, radians or μ in./in.
Δ	incremental change
Δs	element length, in.
ϵ	strain, μ in./in.

μ	Poisson's ratio
σ_{cr}	buckling stress of panel, psi
ϕ	angular deflection, rad or deg

<u>SUBSCRIPTS</u>

a	forward cell
all	allowable
avg	average
b	aft cell; also, bending, buckling
br	bearing
c	compression; also, core
cg	center of gravity
cr	critical
l	longitudinal
max	maximum
n	number of cycles
pri	primary
s	shear
sc	shear center
sec	secondary
t	transverse; also, tensile, torsion
x	related to horizontal axis; also, spanwise
y	related to vertical axis; also, chordwise
vert	vertical
horiz	horizontal

BLANK PAGE

INTRODUCTION

GENERAL

Goodyear Aerospace Corporation fabricated three 7-foot-long fiber glass reinforced plastic aircraft wing test sections to verify that conventional methods of analysis will accurately predict the load-carrying capability of a composite structure. The design, fabrication, testing, and test analysis of the third wing test section are covered in this report. This program is a continuation of the research that is reported in USAAVLABS Technical Report 68-66.[1] The program has been funded by the U.S. Army Aviation Materiel Laboratories; the U.S. Naval Air Development Center, Aero Structures Department; and Goodyear Aerospace Corporation (GAC).

PROGRAM OBJECTIVE

The objective of this program was to apply data generated from small specimen tests of bidirectional and unidirectional S glass composites to the design of a large test structure to determine the stress distributions within the structure due to moment, shear, and torque and to predict the structure's deflections and rotations under specified loading conditions.

PROGRAM BACKGROUND

In the initial phase of the program, a design configuration for the first wing test section was established and construction materials were screened and tested. Also, a stress analysis was made, material allowables were established (from laminate and sandwich specimens), and wing section tools were fabricated.

The design of the test section was selected primarily to provide an established aerodynamic section (NACA23015) for which the actual moment-torque and moment-shear ratios were known. The skin and core construction was established on the basis of a three-ply minimum practical outer skin thickness.

Materials were chosen on the basis of availability, ease of processing, and cost. Since there were no designated design requirements with respect to magnitude of moments, shears, and torques, the materials for the first two wings were not oriented to optimize for any particular loading condition but were arranged to minimize the variables in construction, which would affect correlation of test data with analytical data.

The design and fabrication concepts followed in this program were to integrally mold sandwich skin, honeycomb core, spar caps, and shear webs to produce a typical airplane wing assembly utilizing the fewest individual parts. Only two large moldings were required to produce the first two wing test assemblies. This is in contrast to typical designs where skins, spar caps, and spar webs are fabricated separately, resulting in the assembly of a large number of detail parts.

The initial structural design approaches for the wing test section employed the use of optimistic values and assumptions. With this approach, critical areas could be better determined in the static tests, and design modifications could be accomplished for subsequent test wings. The results of the static tests for the first two wings showed that certain assumptions were overly optimistic, since both wings failed at approximately 80 percent design ultimate load (DUL).

It was concluded that the failure mode of the first wing was a buckling failure of the aft box compression skin. The stress calculation for the buckling stress of this panel was based on the assumption of fixed edge supports. Test data indicated that buckling was initiated at 40 percent DUL, and failure occurred at 80 percent. An analysis using simply supported edge criteria showed much closer correlation with test data.

For both the first and second wings, comparison showed that the calculated stresses and the stresses computed from test strain measurements corresponded quite closely. Plotted comparisons of calculated and measured test deflections of the first two wings also showed good correlation.

In designing the second wing, several transverse stiffeners were added to the critical area of the compression skins to prevent the buckling failure such as occurred in the first wing. This proved to be successful, as no buckling of the upper surface panel was noted throughout the test. Failure of the second wing also occurred at 80 percent DUL; however, this was a tension failure of the entire lower surface of the wing. It was concluded that failure was initiated due to a stress concentration in the skin at the bolted attachment to the center spar. Subsequent testing of tensile specimens confirmed a stress concentration factor of approximately 1.5 at the bolt hole.

PROGRAM PLAN

The program was divided into three tasks, which are outlined below.

Task A - Development of Design Criteria

1. Establish the design criteria of a full-scale wing test section with an optimized use of glass-reinforced plastic for the following conditions at the root section:

   a. Maximum moment condition

   $M = 862{,}500$ in.-lb

   $V = 20{,}200$ lb (ultimate)

   $T = 0$

   b. Maximum torque condition

   $M = 600{,}000$ in.-lb

   $V = 15{,}600$ lb (ultimate)

   $T = 500{,}000$ in.-lb

2. Perform preliminary evaluation of preimpregnated glass laminates in unidirectional and bidirectional form for application to the full-scale wing test section.

3. Evaluate selected types of bonded joints for their ability to meet load transfer requirements of the structure.

4. Develop methods to redistribute loads from unidirectional to bidirectional laminates in areas of attachment and loading points.

5. Design rib support boxes to investigate methods of transferring external loads into the wing structure.

Task B - Design and Fabrication of Wing Test Structure

1. Investigate methods of transferring external loads into the structure by constructing two 34-inch-long specimens representative of the aft box of the cross section, using the same skin and spar construction as the total wing specimen. Install a loading rib near one end to provide loading points external to both spars.

Ribs and attachments shall be designed and tested to the following ultimate load requirements:

a. Total down load = 8630 lb (4315 lb/attachment)
Total side load = 1130 lb (565 lb/attachment)
Total aft load = 1000 lb (1000 lb on one attachment)

b. Total down load = 4500 lb (2250 lb/attachment)
Total side load = 5270 lb (2635 lb/attachment)
Total aft load = 1000 lb (1000 lb on one attachment)

2. Design, fabricate, and test a full-size 7-foot wing test specimen. Testing to be performed at the U.S. Naval Air Development Center, Aero Structures Department.

Task C - Data Analysis

Prepare a final report.

TEST PLAN

The program test plan was developed by the U.S. Naval Air Development Center, Aero Structures Department, and Goodyear Aerospace Corporation.

MATERIAL PROPERTIES - SPECIMEN DESIGN, FABRICATION, AND TESTING

GENERAL

Reinforcement materials that were evaluated for possible use in the design of the No. 3 wing test section are listed as follows:

1. 1543 S glass unidirectional woven fabric
2. 1581 S glass bidirectional woven fabric
3. S glass unidirectional tapes

1543 S GLASS FABRIC

Initially, it was felt that Style 1543 S glass might be employed as the primary unidirectional reinforcement in the wing design. Style 1543 S/901 fabric preimpregnated with E293 epoxy resin was used in the construction of laminate tensile, sandwich tensile, sandwich compression, and sandwich flatwise tensile specimens.

Data from laminate tensile tests of this material were reproducible, and failures occurred in the specimen test sections. It was noted that during loading, those specimens tested at 90 degrees to the fabric warp direction began to exhibit cracking and erratic elongation at approximately 60 percent of ultimate strength.

When tested parallel to the fabric warp, sandwich tensile specimens employing 1543 S glass reinforcement showed appreciably lower ultimate strengths than the laminate specimens. These reduced values can be attributed primarily to specimen design. Failures occurred in the grip areas or at the edges of reinforcing pads. Good correlation existed between sandwich and laminate tensile modulus values.

Ultimate strengths obtained from 1543 S glass fabric sandwich compression specimens were conservative, as failures occurred at the edges of reinforcing pads rather than in the test section.

Flatwise tensile tests of sandwich specimens yielded acceptable test results. The ultimate tensile strength of the aluminum core was realized.

The average ply thickness of the 1543 laminates was greater than expected, even though individual plies of prepreg were within thickness tolerance and resin content of the material was within specified limits. The unidirectional woven fabric apparently does not nest well when laminated. This results in a 0.013-inch average laminated ply thickness rather than the 0.010-inch which would be expected from a similar weight bidirectional fabric.

Investigations involving 1543 S glass were discontinued after the foregoing evaluations were performed, because material costs were considered excessive and average laminated ply thickness could not be reduced using current processing pressures.

1581 S GLASS FABRIC

Design data were generated from laminate and sandwich specimens using 1581 S/901 glass preimpregnated with E293 epoxy as the reinforcement. Laminate specimens were tested in tension, edgewise shear, and interlaminar shear. Sandwich specimens were tested in tension, compression, and flatwise tension. This material presented no processing problems and very few testing problems. Panel quality was usually high, and test results showed the least scatter of the materials tested. The one test in which ultimate strength values were difficult to obtain for this material was the edgewise shear test in which the load was applied at 45 degrees to the fabric warp. Test fixture jaw slippage occurred frequently at high loads, and shear failures could not always be induced in the laminates.

Comparisons were made between properties derived from specimens made of 1581 S/901 glass and 481 E/550 glass. In general, it can be stated that the 1581 S/901 glass proved to be the superior reinforcement material.

S GLASS TAPES

Preliminary evaluations were run on several tape prepregs. Sandwich compression specimens were fabricated using Ferro Corporation's 1014 glass tape preimpregnated with E293 resin. The supplier's literature indicated that 1014 glass has properties equivalent to S glass. The 1014 tape was supported by a dry ply of Style 112 E glass fabric to facilitate handling and layup.

Ply thickness, including the backing material, was 0.013 to 0.014 inch per ply. Resin content of the tapes was quite low. Adequate filleting of resin between the skins and core was not in evidence, and compression specimens failed in the skin-to-core bonds. Tests were rerun with a ply of 1581 S/901 fabric prepreg substituted next to the core as a tie ply, but failures again occurred in the skin-to-core bonds.

Sandwich flatwise tensile screening tests were then run using several adhesive films. The Whittaker Corporation's N328 supported adhesive film was selected for incorporation between tape skins and core material to assure adequate skin-to-core bonds.

A limited evaluation was also made of an S glass tape epoxy prepreg supplied by Chicago Printed String Company (CPS). This tape was supported on a paper backing that was stripped from each ply after it was laid up. Handling characteristics of the material were good. Average laminated ply thickness was 0.007 inch. Sandwich compression specimens were fabricated using the CPS tape in conjunction with N328 adhesive film. Problems were encountered in molding high quality parts from this material. Apparently the glass yarns had not received a uniform coating of resin. Light-colored streaks, which were attributed to dry glass fibers, appeared in the panel skins. Compressive strengths in the order of 90,000 psi were obtained from these tapes when tested parallel to the filament direction.

S glass 901 finish tapes preimpregnated with E293 resin were procured for the remainder of the material properties investigation. Tapes were aligned and deposited on a preimpregnated Style 104 E glass carrier. Ply thickness of the tapes was 0.011 to 0.012 inch, and the resin content was 28 to 30 percent by weight. The tapes were procured in sheet form 18 inches wide by 8 feet long.

Laminate tensile, laminate edgewise shear, sandwich tensile, and sandwich compression specimens were fabricated from this material. Laminate tensile tests produced acceptable test results. In the laminate shear tests, failures could not be induced in the ±45-degree oriented tapes. All the tests were terminated when slippage occurred between the specimen and fixture jaws. A comparison of ultimate tensile strengths between laminate and sandwich specimens tested parallel to the filament direction showed a reduction from 260,000 psi for the laminate specimens to 184,000 psi for the sandwich specimens. The zero-degree sandwich specimens showed some evidence of shear failure outside of the test section. The sandwich compression strength of 102,000 psi (specimens tested parallel to the direction of filaments) derived on this program is a reduced value for this material, as the test specimens failed in a combination of buckling and compression.

Specimens were also made up from various combinations of 1581 S/901 fabric and S/901 tapes. Results of the tests of these coupons are discussed in the following sections of this report.

Figures 1 through 5 show the configurations of specimens fabricated and tested on this program.

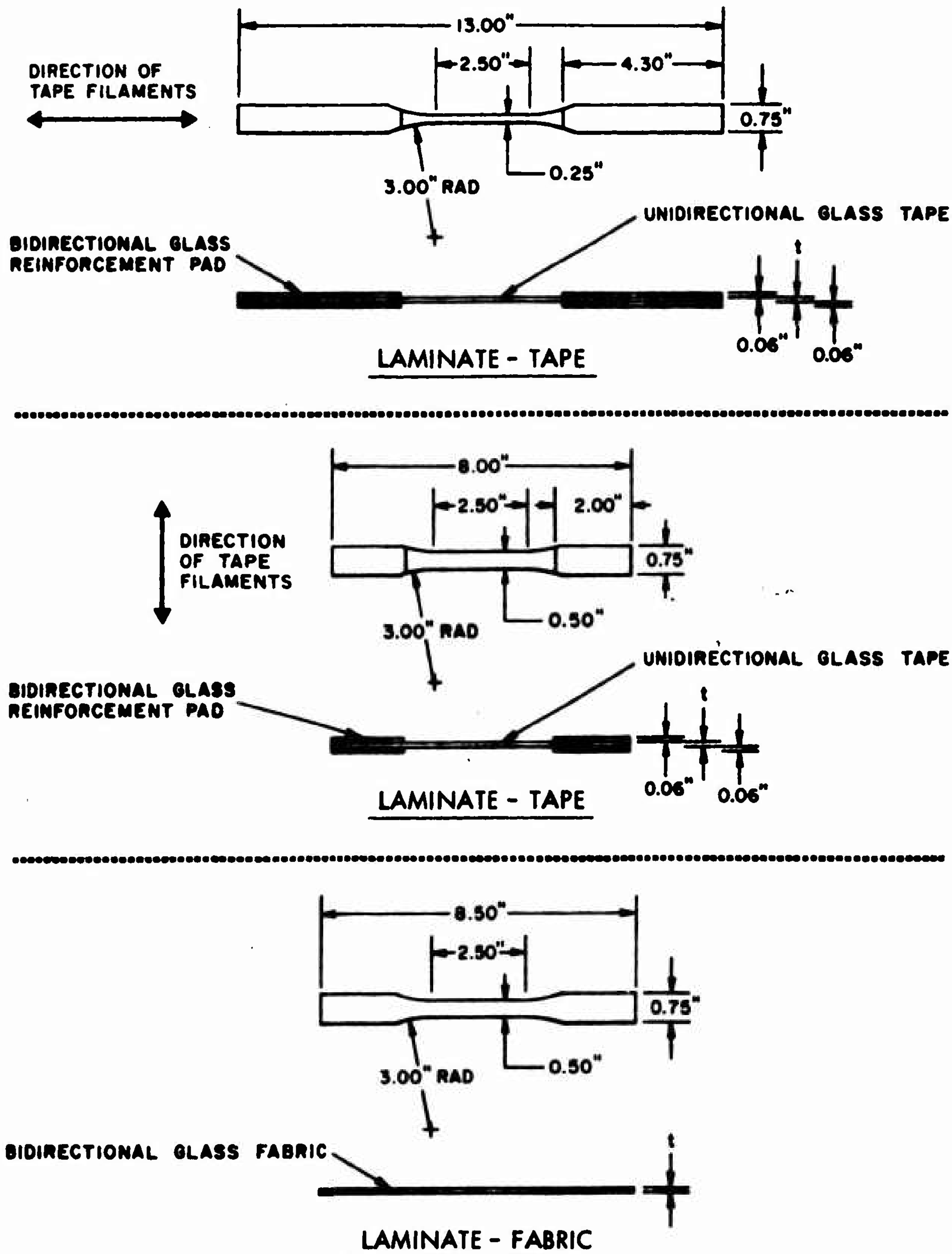

Figure 1. Laminate Tensile Specimens.

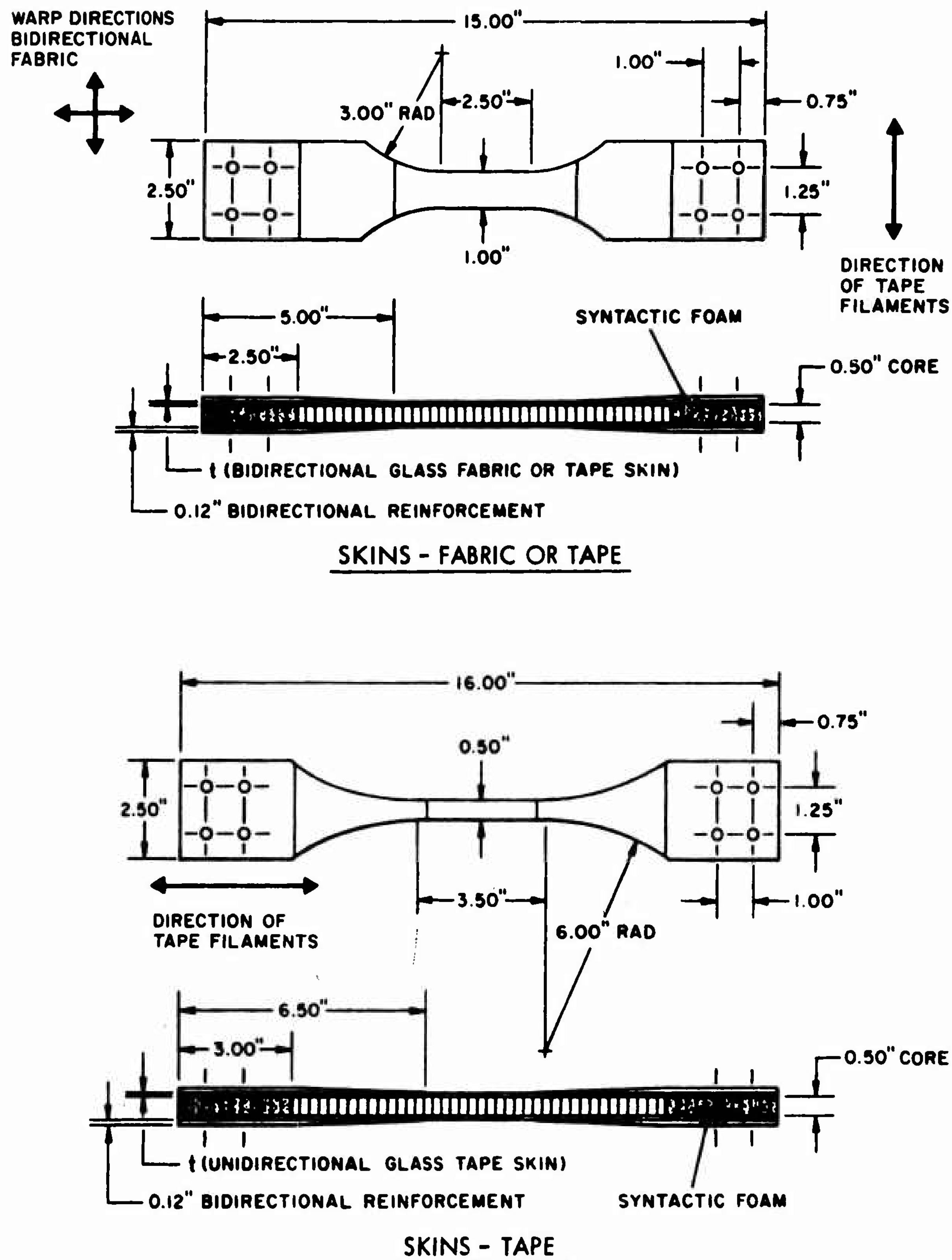

Figure 2. Sandwich Tensile Specimens.

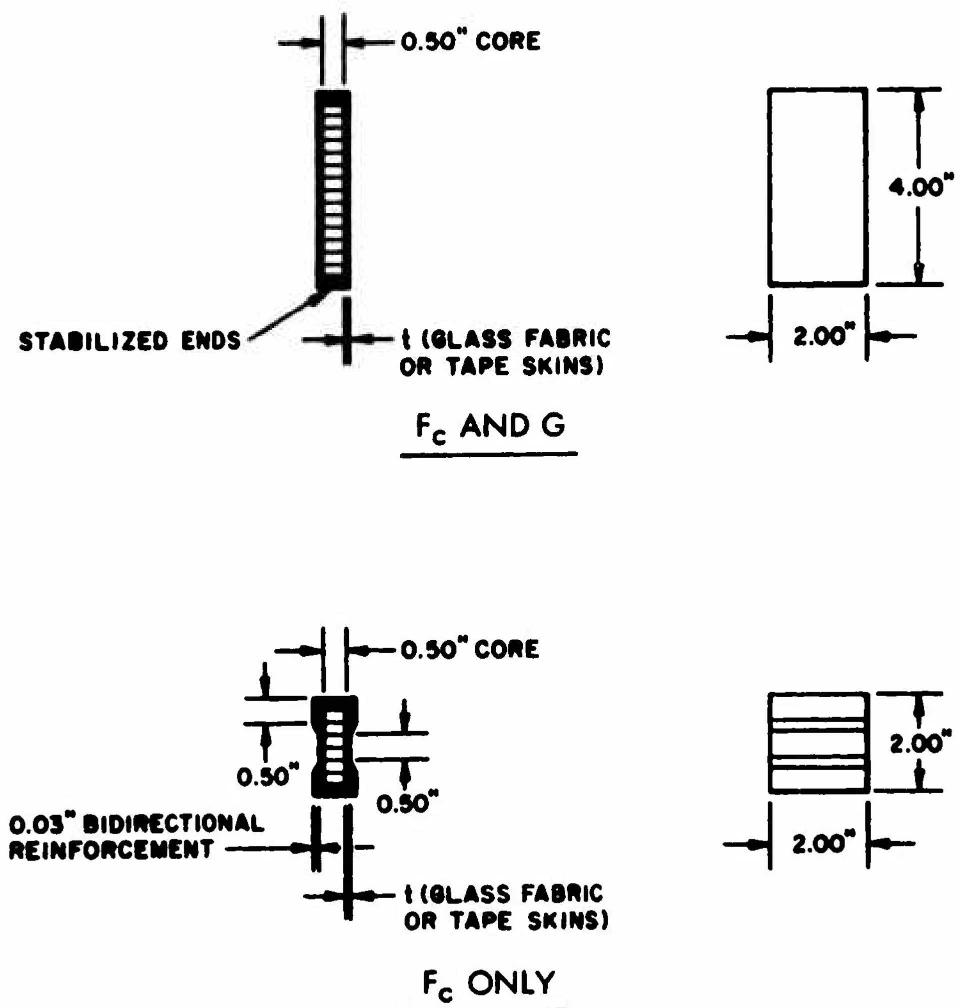

Figure 3. Sandwich Compression Specimens.

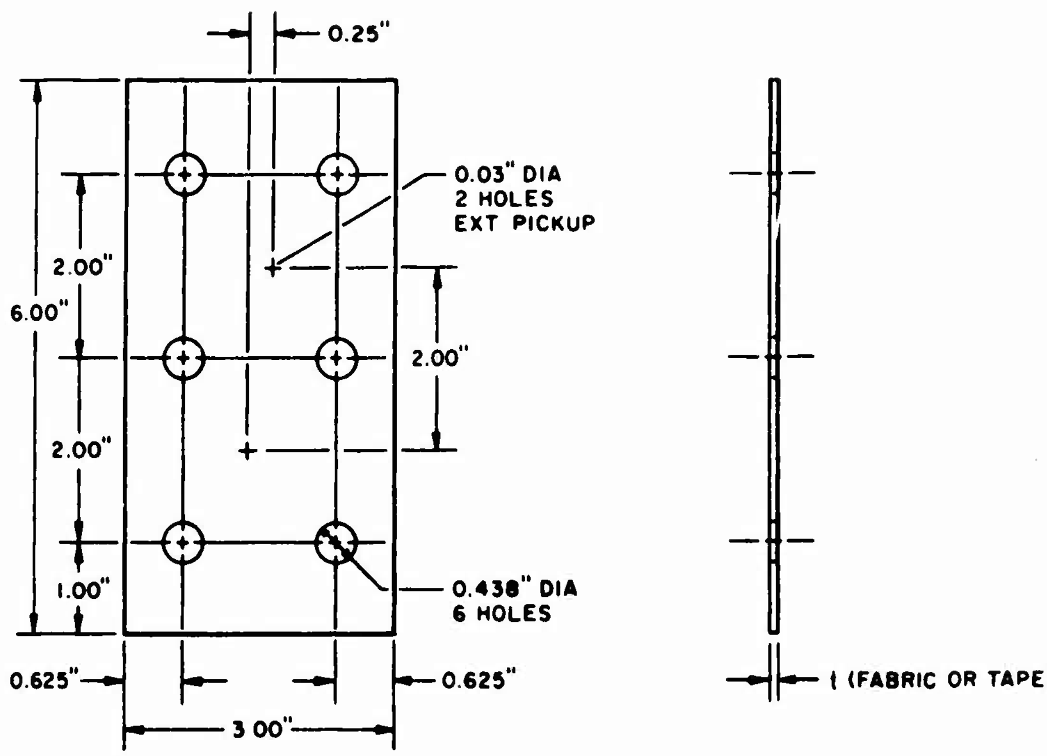

SPECIMEN CONFIGURATION

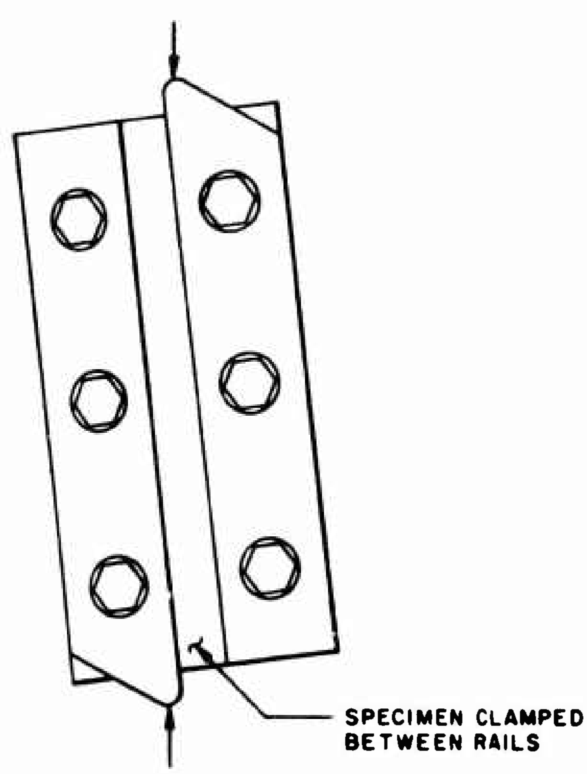

Figure 4. Shear Test.

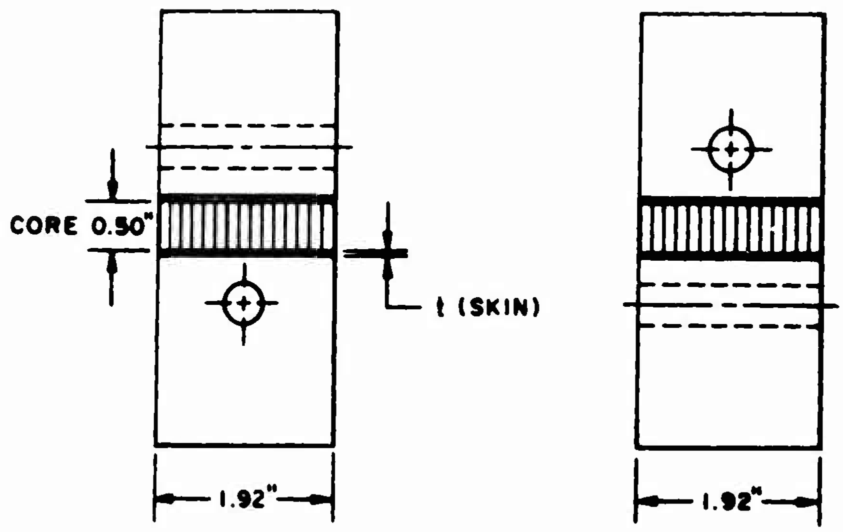

Figure 5. Sandwich Flatwise Tensile Specimen.

SUMMARY

Table I is a summary of material properties that were developed on this program for three glass fiber reinforcements.

E293 S/901 tape and E293 1581 S/901 fabric were selected as the reinforcement materials to be used in the fabrication of the 7-foot wing test section.

TABLE I. SUMMARY OF MATERIAL PROPERTIES

Material	Angle (deg)	Ultimate Strength (psi)				Primary Modulus (psi x 10^6)				Secondary Modulus (psi x 10^6)				Poisson's Ratio		
		LT	ST	SC	LS	LT	ST	SC	LS	LT	ST	SC	LS	LT	ST	SC
481 E Glass	0	64,200	57,500	48,200	14,700	3.87	3.70	3.80	0.72	2.72	2.60	3.28	0.45	-	-	-
	90	55,100	-	-	12,200	3.75	-	-	0.55	2.40	-	-	0.36	-	-	-
	45	24,400	-	-	-	2.13	-	-	-	1.38	-	-	-	-	-	-
1581 S Glass	0	91,800	81,800	73,200	15,600	3.74	4.10	4.24	0.69	2.96	2.60	3.82	0.45	0.110	0.122	-
	90	76,900	68,200	66,000	-	3.53	4.00	4.21	-	2.63	2.21	3.70	-	-	0.112	-
	45	30,900	34,200	36,800	30,000	2.04	2.40	2.24	1.49	1.48	1.60	1.77	1.08	-	-	-
S Glass Tape	0	260,500	185,700	102,600	9,000	6.95	6.37	6.63	0.69	6.95	5.59	6.63	0.40	0.259	0.243	0.289
	90	8,880	6,800	26,800	10,400	2.21	2.30	2.38	0.74	2.21	1.95	1.68	0.40	0.081	0.063	0.093
	±45	20,400	-	40,400	-	2.05	-	2.68	1.73	1.50	-	1.60	1.02	-	-	-
	±5	112,300	-	-	-	6.82	-	-	-	6.82	-	-	-	-	-	-
	+45	16,000	-	34,400	-	2.42	-	2.20	-	1.50	-	1.61	-	-	-	-

Note: LT-Laminate Tensile. ST-Sandwich Tensile. SC-Sandwich Compression. LS-Laminate Shear.

COMPARISON OF EMPIRICAL AND ANALYTICAL VALUES

A materials properties subprogram was undertaken in which a comparison was made between calculated and test values of four composite reinforcement configurations (panel types A, B, C, and D). Laminate tensile, sandwich compression, and sandwich tensile specimens of each type were fabricated and tested at a zero-degree angle.

To estimate the strength of the four different composites, calculated values were obtained by averaging the material properties of the individual plies at their correct angle to the test angle. Each ply was weighed according to its thickness in the average calculation. The calculated and the measured values are compared in Table II.

TABLE II. COMPARISON OF CALCULATED AND TEST VALUES

Panel Type	Method	Laminate Tensile F_t (psi)	Laminate Tensile E_t (pri) (psi x 10^6)	Laminate Tensile E_t (sec) (psi x 10^6)	Sandwich Compression F_c (psi)	Sandwich Compression E_c (pri) (psi x 10^6)	Sandwich Compression E_c (sec) (psi x 10^6)	Sandwich Tensile F_t (psi)	Sandwich Tensile E_t (pri) (psi x 10^6)	Sandwich Tensile E_t (sec) (psi x 10^6)
A	Exp	56,800	2.88	1.27	60,200	2.95	2.26	43,100	3.09	2.06
	Calc	58,700	2.81	2.15	53,500	3.15	2.70	51,200	3.17	2.05
B	Exp	68,100	4.18	3.61	81,500	4.66	4.07	60,100	4.23	4.23
	Calc	75,300	4.65	4.40	72,700	4.63	4.42	73,200	4.58	3.77
C	Exp	132,500	5.35	5.35	82,200	5.63	5.04	117,400	5.55	5.02
	Calc	133,300	5.83	5.70	88,500	5.67	5.57	114,700	5.51	4.72
D	Exp	-	-	-	56,000	4.51	3.93	52,600	4.49	3.84
	Calc	92,300	4.43	4.15	69,800	4.44	4.20	73,400	4.39	3.60

A Two-ply 1581 S glass at 0°; Two-ply S glass tape at $\pm45^{\circ}$
B Two-ply S glass tape at $\pm5^{\circ}$; Two-ply 1581 S glass at 45°
C Two-ply S glass tape at $\pm5^{\circ}$; One-ply S glass tape at 0°; One-ply 1581 S glass at 45°
D Two-ply S glass tape at $\pm5^{\circ}$; Two-ply S glass tape at $\pm45^{\circ}$

This method of calculating strength and stiffness values of composite laminates is not considered to be a refined method. However, in most cases it results in values quite close to the test values. Thus, this method appears practical for preliminary work where a more refined analysis is not available.

A sample calculation for panel type B laminate tensile values is given on page 14.

Two-ply 0.024 in. (t) at 112,300 psi	=	2695	two-ply S glass tape at ±5°
Two-ply 0.020 in. (t) at 30,900 psi	=	618	two-ply 1581 S glass at 45°
0.044 in. (t)	=	3313	
F_t	=	75,300 psi	

Two-ply 0.024 in. (t) at 6.82×10^6 psi	=	0.1637×10^6
Two-ply 0.020 in. (t) at 2.04×10^6 psi	=	0.0408×10^6
0.044 in. (t)	=	0.2045×10^6
$E_{t\ (pri)}$	=	4.65×10^6 psi

Two-ply 0.024 in. (t) at 6.82×10^6 psi	=	0.1637×10^6
Two-ply 0.020 in. (t) at 1.48×10^6 psi	=	0.0296×10^6
0.044 in. (t)	=	0.1933×10^6
$E_{t\ (sec)}$	=	4.40×10^6 psi

WING DESIGN

For a more refined analysis of a composite structure, a computer program has been developed at GAC. This program, as defined in GER 13860,[2] determines the gross composite properties of the laminate as they are affected by the properties and the orientation of the individual plies and determines the stresses within the individual plies due to edge loadings applied to the total composite.

To use this program, it is necessary that the orientation of each ply plus its properties in the directions parallel and perpendicular to its natural axis be known, along with the edge loadings on the total composite. This computer program will then obtain (1) the stiffness matrix, (2) the compliance matrix, (3) the composite principal properties, and (4) the individual ply stresses. The present program is limited to the elastic range of the material.

For this wing design program, the computer program has been used to determine the composite principal properties, which in turn are used in the development of the wing section properties. These section properties are used to determine the spanwise bending and shear loadings in the composite. The individual ply stresses due to these loadings are then determined by the computer program, and the results are compared with allowable stresses of the ply to determine margins of safety.

As with any other computer program, this program is only as good as the data supplied. Therefore, it is necessary that a complete and accurate test program be conducted on the basic material in parallel and perpendicular directions prior to utilizing the computer.

JOINT DESIGN EVALUATION

GENERAL

The objective of this task was to evaluate selected types of bonded joints for their ability to meet the load transfer requirements of the wing structure. Bonded-only joints are often considered to be somewhat unreliable because of secondary stresses that can produce tension on the bond. Bolted joints are quite reliable; however, they are not generally considered to provide the potential efficiency of reliable bonded joints for an all-reinforced plastic structure. A combination of the two joint types, where the bond carries the shear load and the clamping screws carry any secondary tension stresses, may be the most practical. The bonded joint with clamping screws has smaller bolts and larger bolt spacing than an all-bolted joint. The clamping screws are not considered to carry any of the shear load through the joint.

DISCUSSION

Figure 6 is a drawing of a typical double lap shear, bonded joint specimen used for this investigation.

Several different bonding systems were incorporated into the test program. The first system used Epon 901 adhesive with a B-1 curing agent. Both the straps and the base plates of the test specimens were made from fully cured laminates prior to the bonding operation. The straps were bonded to the base plates under light clamping pressure in a 125^{o}F oven for 8 hours.

The second bonding system involved layup of the strap materials directly on the cured base plates. This is considered to be a semiprimary bond, as one material is cured and the other is not cured at the time of attachment. The bonding resin in this case is actually the laminating resin. After layup,the strap material and the bond were cured under 50-psi autoclave pressure at a temperature of 325^{o}F for 3 hours.

The third bond system was a variation of the second, in which an N328 epoxy adhesive film was placed between the cured base plates and the uncured strap material.

There was also a variation in the installation of the clamping screws. For all secondarily bonded specimens using clamping screws, the screws were installed during the bonding operation. For all semiprimary bonds where clamping screws were used, the screws were installed subsequent to curing.

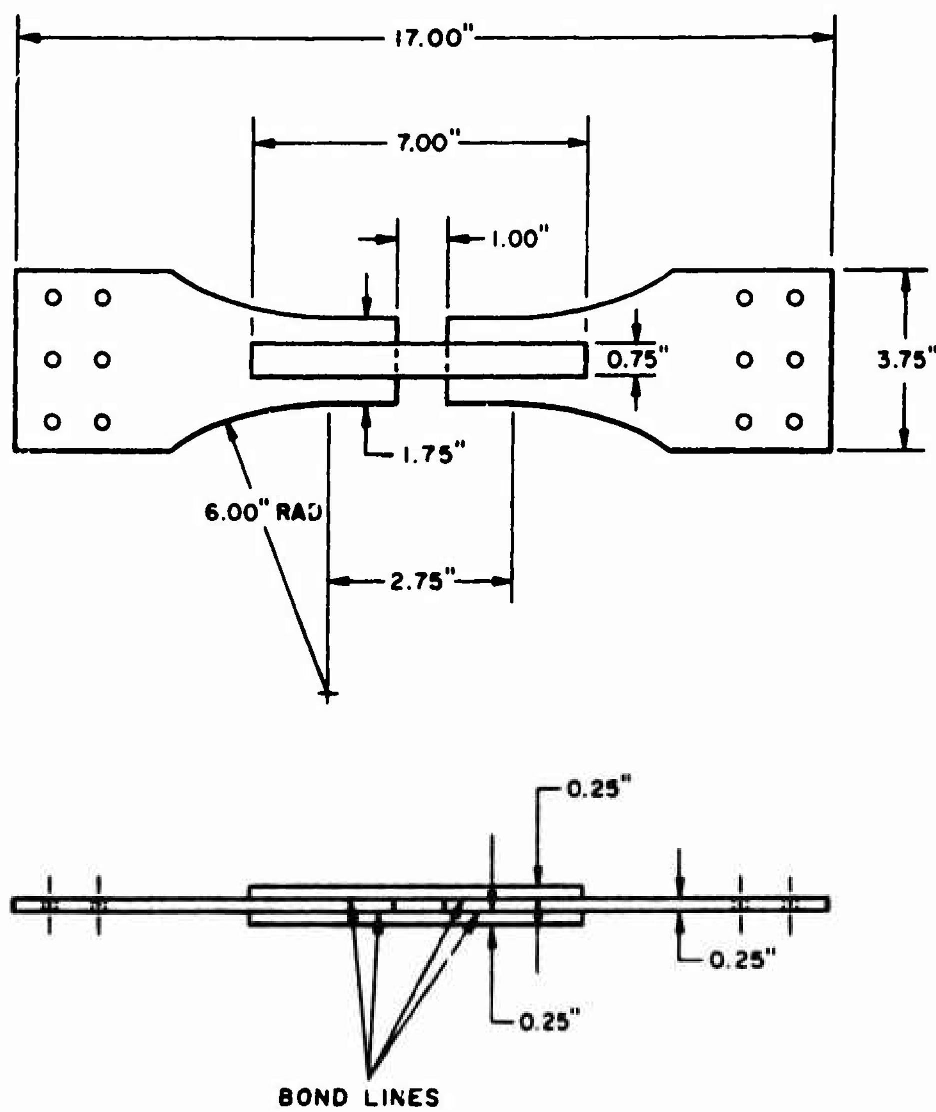

Figure 6. Typical Double Lap Shear Joint Specimen.

In the design of bonded joints, the fit of mating parts to be bonded together has been a subject for debate. Consequently, three different types of fit were incorporated into the test program for the secondary bonded joint specimens. Prior to bonding, the straps were premolded flat, concave, or convex. Cross sections of the joints are shown in Table III. Comparative values of bond strengths for the three types of joints were obtained.

A bolted joint specimen was designed using 1/4-inch AN bolts at 1-inch spacing. One set of tests was also conducted using only the clamping screws. This was not considered to be a joint design, but the test was conducted to obtain a strength value for comparison purposes only.

TABLE III. SUMMARY OF JOINT TESTS							
Item No.	Panel No.	Type of Joint	Adhesive Bond	Mechanical Fasteners	Relation of Straps to Base[d]	Failure Load (lb)	Bond Stress (psi)
1	102	Secondary bond	Epon 901-B1	None	Flat	3,814	847
2	103	Secondary bond	Epon 901-B1	None	Convex	4,262	947
3	104	Secondary bond	Epon 901-B1	None	Concave	4,935	1096
4	105	Secondary bond	Epon 901-B1	2-3/16 screws	Flat	9,600	2132
5	106	Secondary bond	Epon 901-B1	2-3/16 screws	Convex	9,604	2133
6	107	Secondary bond	Epon 901-B1	2-3/16 screws	Concave	10,176	2261
7	109a	Semiprimary bond[a]	481 Epoxy[b]	None	Flat	10,267	2207
8	109	Semiprimary bond	481 Epoxy[b]	2-3/16 screws	Flat	12,150	2697
9	110a	Semiprimary bond	N-328[c]	None	Flat	8,413	1869
10	110	Semiprimary bond	N-328[c]	2-3/16 screws	Flat	11,740	2608
11	108	Bolted	None	3-1/4 bolts	Flat	10,256	-
12	106a	Clamping screws	None	2-3/16 screws	Convex	8,660	-

[a] The straps were laid up uncured on the cured base plates, and the bond was made during primary cure of strap laminate.

[b] The laminating resin served as the adhesive.

[c] A layer of film adhesive was applied between the cured base plate and the uncured strap layup.

[d] The fit of the straps to the base plates was purposely varied.

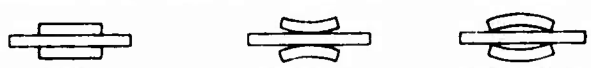

FLAT CONVEX CONCAVE

TEST RESULTS

A summary of failure loads for the laminate joint specimens that were tested is given in Table III.

The specimens utilizing a secondary bond only (items 1, 2, and 3) failed at a bond shear stress of approximately 1000 psi. The secondary bond specimens with clamping screws failed at a bond shear stress of approximately 2000 psi. The variation in test results among the flat, convex, and concave straps was not significant.

The specimens fabricated by the semiprimary bond method failed at about the same load as the secondary bond specimens with clamping screws. The addition of clamping screws to the semiprimary bond specimens did improve their load-carrying capability, but the increase was not as significant as in the secondary bond specimens. The use of a bonding film with the semiprimary bond specimens did not increase their strength.

The bolted specimen strength was equivalent to the strength of the secondary bond specimens with clamping screws and semiprimary bond specimens without clamping screws.

The strength of the specimens with clamping screws only was greater than the secondary bond specimens.

The type of failure experienced during testing was of considerable interest. The bonded-only specimen failures were quite sudden and ultimate after bond failure. The specimens with clamping screws could in some cases be loaded higher after initial failure of the bond. In some cases, only the bond on one strap would fail; the additional load was carried by a combination of bond shear and clamping screw shear.

The bolted specimens failed in strap tension at an average load of 10,256 pounds. Calculations had predicted bearing failure at 8,400 pounds in the base plate. Actually, bearing failure was evident in the base plate as whitening and crushing; however, this did not cause the specimen to fail. Failure actually occurred as strap tension at 10,256 pounds as compared to a calculated strap strength of 11,250 pounds. There was considerable whitening under the bolt hole in the strap, indicating stress concentration at the bolt hole. This stress concentration was responsible for reducing the strap strength approximately 10 percent.

The test specimens using clamping screws only also failed in strap tension at 8,660 pounds. The strap tension strength was calculated to be 8,500 pounds. Again, bearing occurred under the bolt hole prior to failure.

CONCLUSIONS

The following conclusions are presented based on the work performed on this program:

1. Secondary bonded joints with clamping screws achieved double the shear strength of secondary bonded joints without clamping screws.

2. The bolted-only joint specimens were equivalent in strength to the secondary bonded and clamped specimens.

3. The semiprimary bonded specimens achieved about the same shear strength as the secondary bonded and clamped specimens.

4. Addition of a bonding film in the semiprimary bonded specimens did not increase the shear strength.

5. Mismatching of parts to be secondary bonded did not decrease the shear strength of the bond.

TRANSITION AREA TESTS

LAMINATE SPECIMENS

A series of laminate tensile tests was conducted to explore the effects of changes of materials and material orientations in a fiber glass reinforced plastic structure. The tensile specimens were designed so that the transition areas fall at the centers of the specimens. Figure 7 shows the specimen configuration, and the test results are summarized in Tables IV and V. Efficiencies of the various transitions are reported. These efficiencies are the ratio of the specimen failing stress to the strength of the weakest end of the specimen, as reported in the Material Properties section of this report.

Two types of specimens were investigated. The first type, called the "splice type," had cuts in all major plies. The transition areas of these specimens represented either a construction splice or a splice required for a basic material change. In the first case the material is the same on both sides of the splice, while in the second case the materials for the two sides are different.

The second type is referred to as the "buildup type" and represents transition areas where extra plies are required, such as along panel edges and ends or at spar caps. In this case the basic plies are not cut, but additional plies are added to one end of the specimen. This produces a

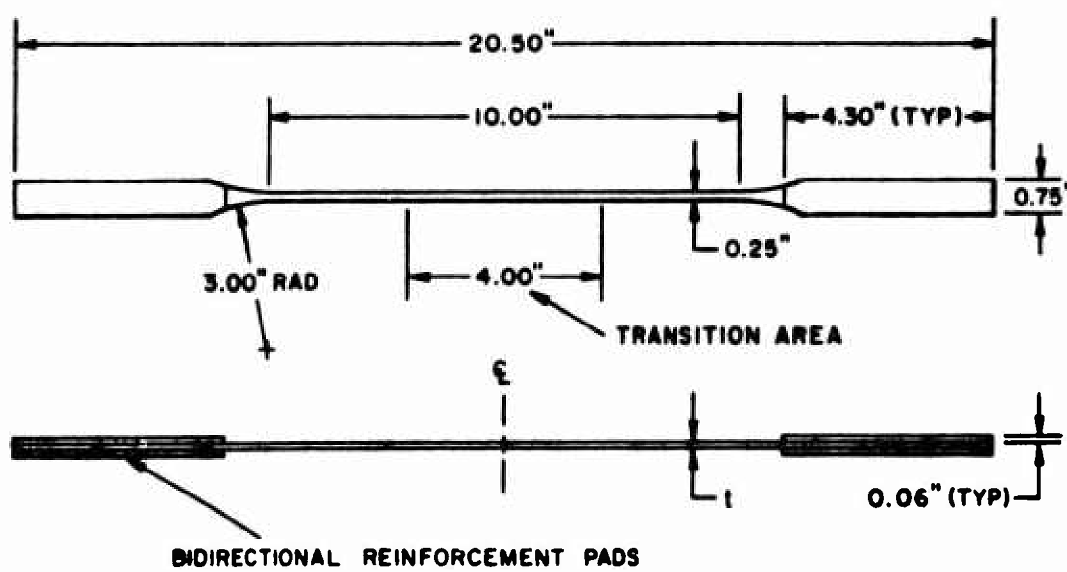

Figure 7. Laminate Transition - Tensile Specimen.

TABLE IV. SUMMARY OF SPLICE TYPE TESTS

Specimen No.	Left Side			Right Side			Transition Area Cross Section	Percent Efficiency	Remarks
	No. of Plies	Material Type	Angle (deg)	No. of Plies	Material Type	Angle (deg)			
111	5	481 E glass	0	5	481 E glass	0	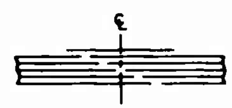	68	1/2" stagger on cut plies. One splice ply added.
112	5	S glass tape	0	5	S glass tape	0		45	1" stagger on cut plies. One splice ply added.
119	5	1581 S glass	0	2 2	1581 S glass S glass tape	±45 ±45	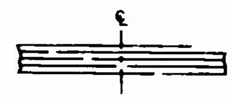	72*	1" stagger on cut plies. Additional ply overlaps splice.
120	5	1581 S glass	0	1 1 2	1581 S glass 1581 S glass S glass tape	0 ±45 ±45	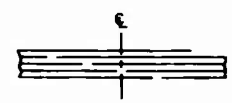	67	1" stagger on cut plies. Additional ply overlaps splice.

* Actual failure did not occur in transition area but as tensile failure in the basic $\pm 45^{\circ}$ plies. Therefore, efficiency of the transition configuration is greater than tabulated above.

TABLE V. SUMMARY OF BUILDUP TYPE TESTS

Specimen No.	Left Side: No. of Plies	Left Side: Material Type	Left Side: Angle (deg)	Right Side: No. of Plies	Right Side: Material Type	Right Side: Angle (deg)	Transition Area Cross Section	Percent Efficiency	Remarks
113	5	481 E glass	0	5 5	481 E glass 481 E glass	0 0	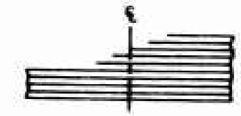	80	1 2" stagger on buildup. Additional plies all on bag side.
114	5	481 E glass	0	5 5	481 E glass 481 E glass	0 ±45	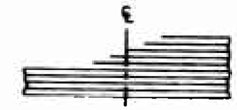	80	1 2" stagger on buildup. Additional plies all on bag side.
115	4	1581 S glass	0	4 3	1581 S glass S glass tape	0 0	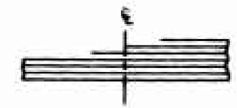	90	1" stagger on buildup. Additional plies all on bag side.
117	4	1581 S glass	0	4 3	1581 S glass S glass tape	0 0	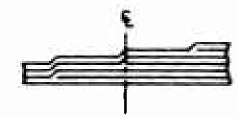	87	2" stagger on buildup. Additional plies intermixed.
118	4	1581 S glass	0	4 3	1581 S glass S glass tape	0 0	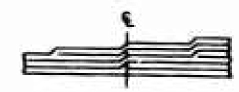	96	2" alternate stagger on buildup. Additional plies intermixed.
116	5	1581 S glass	0	5 4	1581 S glass S glass tape	0 ±45	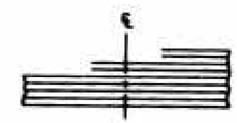	96	2" double ply stagger. Additional plies all on bag side.
121	5	1581 S glass	0	5 4	1581 S glass S glass tape	0 ±45	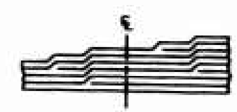	98	2" alternate stagger on buildup. Additional plies intermixed.
122	4	S glass tape	0	4 3	S glass tape 1581 S glass	0 0	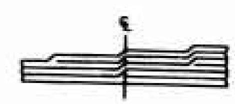	84	2" alternate stagger on buildup. Additional plies intermixed.
123	4	S glass tape	0	4 3	S glass tape 1581 S glass	0 ±45	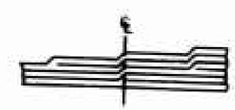	88	2" alternate stagger on buildup. Additional plies intermixed.

specimen that is thicker at one end than the other. A number of transition design variations were included in the investigation.

The splice type specimens had strength efficiencies ranging from 45 to 72 percent. These efficiencies are considered to be quite low for design purposes. The lowest efficiency was obtained with the unidirectional material, which is generally the most difficult to splice. It was concluded that longer stagger distances are required for the cut plies.

The buildup type specimens had strength efficiencies ranging from 80 to 98 percent. The basic specimen design differences included variations in material, layup angle of material, length of ply stagger, method of ply stagger, and position of buildup plies, either all on the bag side or intermixed.

Specimens 113 and 114 permit a comparison of 0- and 45-degree layup of the material where all materials are bidirectional. When the buildup material was unidirectional material laid up at 0 degrees (specimen 115), a higher efficiency resulted. When the basic material was unidirectional and the buildup material bidirectional (specimens 122 and 123), slightly better efficiencies were obtained with the 45-degree buildup layup angle.

The comparison of intermixed buildup design and positioning of buildup plies on the bag side did not yield conclusive results because of the number of variables involved in the test program.

It is concluded that although nine different types of specimens were tested, additional tests are required to provide direct comparisons for the large number of variables involved. The completed program is considered a preliminary test program.

SANDWICH SPECIMENS

Discussion

Two sandwich transition area specimens were designed, fabricated, and tested. Specimen 131 simulated a rib-to-spar joint where the rib attachment is made to a spar web that has transitioned from sandwich to solid laminate. Specimen 132 simulated a rib-to-surface panel joint where the rib attachment is made to a sandwich surface panel. The sandwich skins of both specimens were constructed of unidirectional tape (three plies - S glass E293 prepreg) and fabric (one ply next to core - 1581 S glass E293 prepreg). Doubler plies and bearing strips were 1581 S glass fabric. Aluminum honeycomb (1/8-0.001-5052) served as the core material. Narmco 328 adhesive film was used to make the skin-to-core bonds. Figures 8 and 9 show specimen geometry.

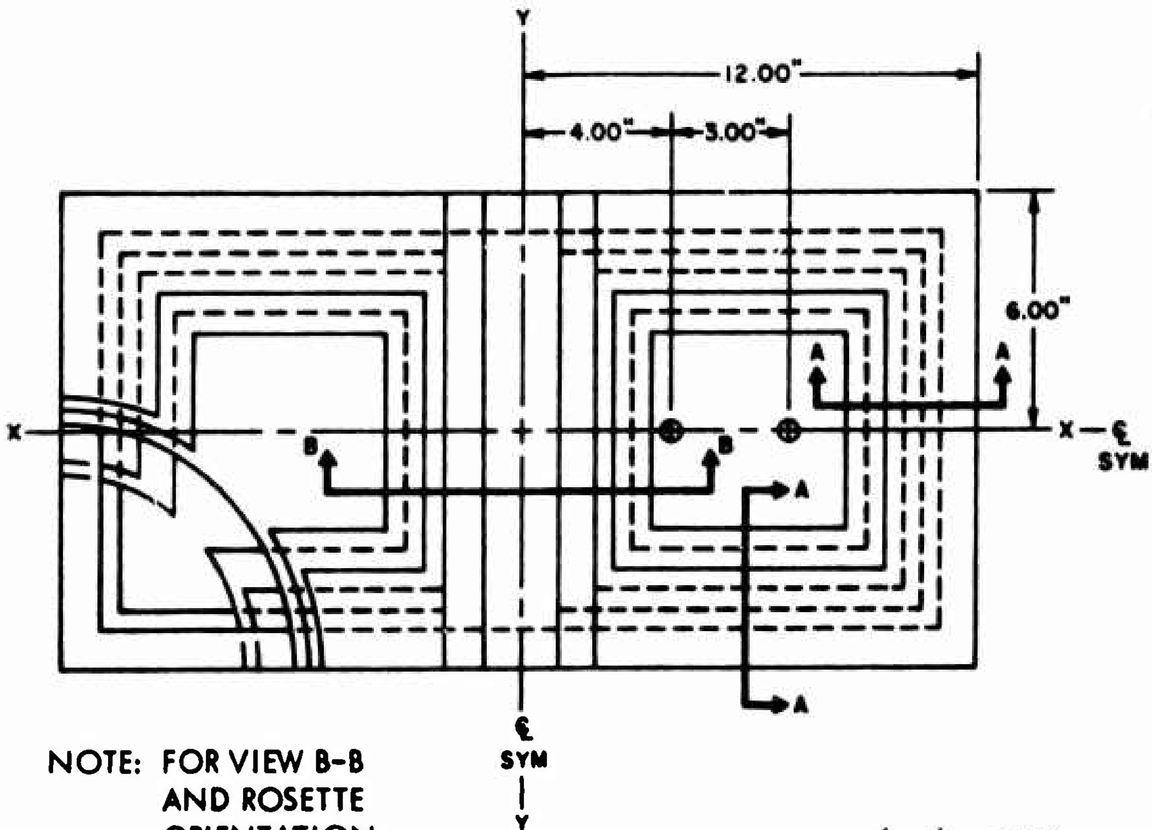

NOTE: FOR VIEW B-B AND ROSETTE ORIENTATION, SEE FIGURE 9.

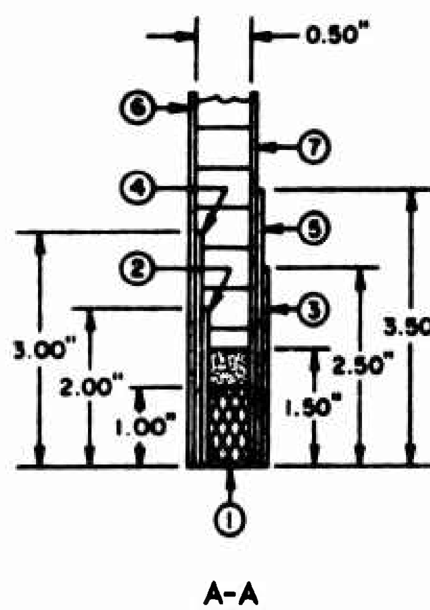

① 481 E GLASS, WARP PARALLEL TO SPAN.

②③④⑤ 1581 S GLASS, WARP ±45° TO SPAN (ONE PLY EACH).

⑥⑦ 1581 S GLASS NEXT TO CORE, WARP PARALLEL TO SPAN; S GLASS TAPE AT -60° TO SPAN, AT 0° TO SPAN, AND AT +60° TO SPAN (ONE PLY EACH).

Figure 8. Shear Beam Specimen Geometry Common to Specimens 131 and 132.

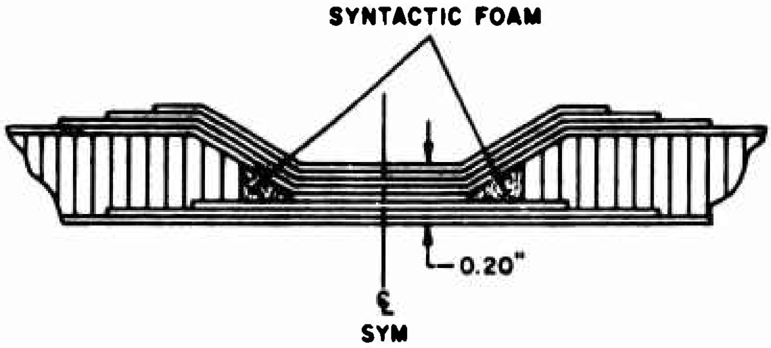

SPECIMEN 131

(B-B)

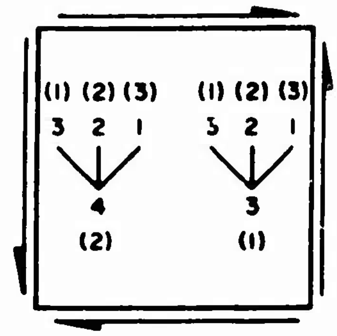

ROSETTE LOCATIONS

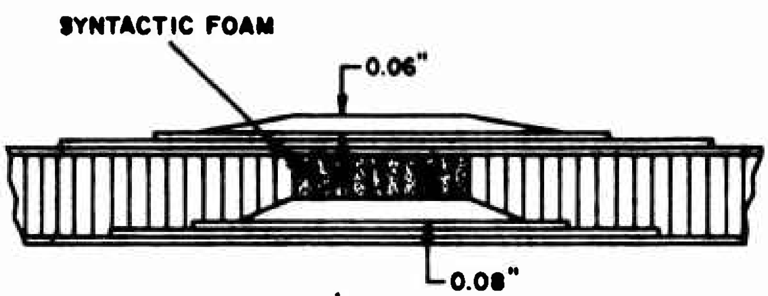

SPECIMEN 132

(B-B)

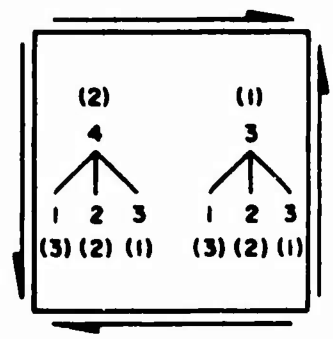

ROSETTE LOCATIONS

NOTE: NUMBERS SHOWN IN PARENTHESES REFER TO GAGE AND ROSETTE NUMBERS ON MOLD SURFACE.

Figure 9. Transition Area Geometry and Strain Rosette Identification for Shear Beam Specimens 131 and 132.

The test panels were mounted in a test fixture as shown in Figure 10 and subjected to an edgewise shear load by means of an 8-inch hydraulic actuator calibrated in 2000-pound increments to 40,000 pounds. The test fixture was arranged in such a way that the line of pull (centerline of actuator) was centered laterally on the specimen and fell in the plane of the bag surface at the mounting point.

Hydraulic pressure was applied by means of a hand pump. A momentary hold was made at each 2000-pound increment to allow recording of strain data.

Strain gages installed in accordance with Figure 9 were used to monitor strain at each increment of load to failure. The strain gages were Wm. T. Bean Type EA-06-250RA-120, rosette ($\pm 45^{\circ}$) configured. The strain gage output signals were continually recorded via CEC1-113B amplifiers and a CEC5-124 oscillograph.

During the installation of each specimen into the test fixture, the strain instrumentation was monitored to prevent any specimen preloading.

Test Results

The results of the sandwich specimen tests are summarized in the following paragraphs.

Run No. 1 - Specimen 131. Load was applied from 0 to a maximum of 40,000 pounds in 2000-pound increments. When no failure occurred, the load was released and the specimen was removed.

Run No. 2 - Specimen 132. Load was applied from 0 to a maximum of 28,000 pounds in 2000-pound increments, when a rotation in the specimen occurred due to eccentric loading. The load was released, and a slide stop apparatus was installed to maintain specimen alignment.

Run No. 3 - Specimen 132. Load was applied from 0 to a maximum of 40,000 pounds in 2000-pound increments; then the load was increased steadily to failure. Failure occurred at a 44,650-pound load.

Run No. 4 - Specimen 131. Load was applied from 0 to a maximum of 40,000 pounds in 2000-pound increments; then the load was increased steadily to failure. Failure occurred at a 49,300-pound load.

Figures 11 and 12 show the specimens after testing.

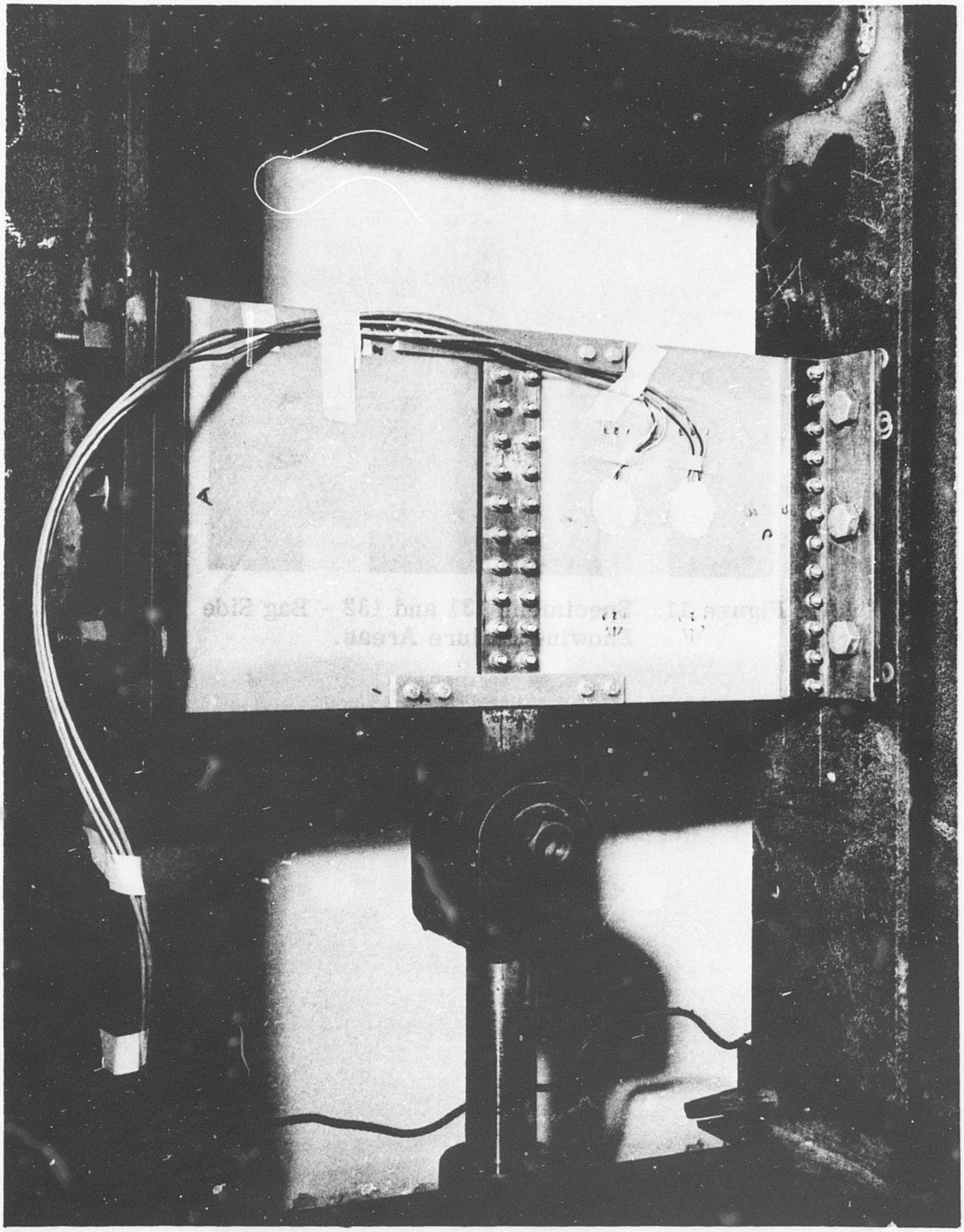

Figure 10. Details of Specimen Mounting.

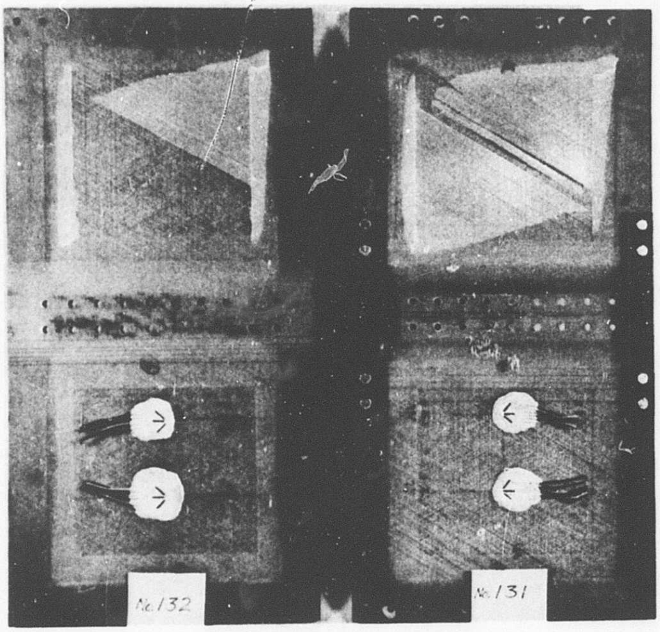

Figure 11. Specimens 131 and 132 - Bag Side Showing Failure Areas.

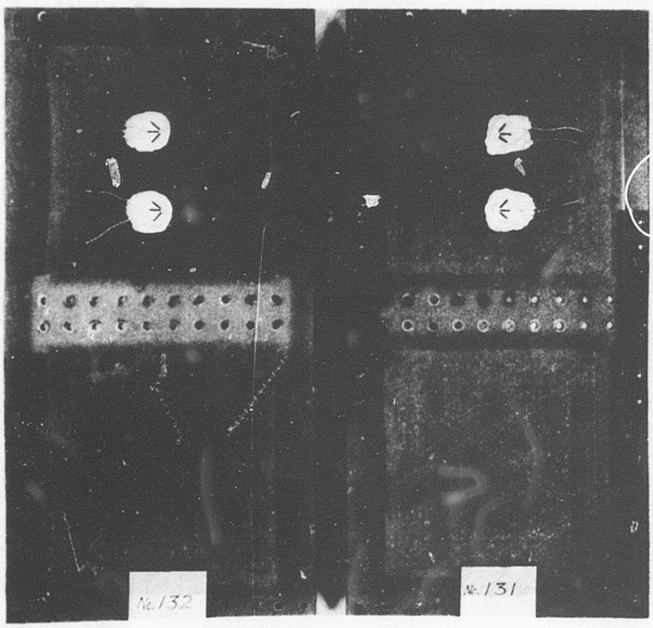

Figure 12. Specimens 131 and 132 - Mold Side.

These tests were performed to accomplish the following:

1. Compare strengths of the two attachment methods and transition areas.
2. Compare laminate shear strength and modulus with estimated properties.
3. Determine shear distribution in two faces for the two types of loading.
4. Observe shear stress variation along the beam axis.

Analysis

The analysis of the shear beams was obtained by the following procedure:

1. Properties of the constituent skin plies were used to obtain elastic properties of the gross composite.
2. These properties were used with those of the doubler material and spar cap materials to obtain section properties of the beam cross section at the rosette locations.
3. Shear flow for a unit shear load was then obtained at the gage locations. This shear flow was used to obtain principal stresses in each of the face sheets.
4. These principal stresses were converted to stresses along the principal strength axes of the separate plies, and Hill's criterion for failure was used to obtain a value for the failing load.

Because of the manner of support and the restraints to face sheet curvature offered by the core, the face sheets are assumed to remain flat and have zero strain in the axial direction.

With the 1581 fabric and tape elastic properties reported for shear and tension loading, the composite properties for the four laminate face sheets were determined by GAC's computer program for analysis of orthotropic laminates and are summarized below:

$E_x = 3.664 \times 10^6$ psi $\qquad E_y = 3.237 \times 10^6$ psi

$\mu_{xy} = -0.2665 \qquad \mu_{yx} = -0.2354$

$G_{xy} = 1.072 \times 10^6$ psi

The compliance and stiffness matrices were also determined in order to determine the effects of restraints to the face sheet tendency to bend and twist under shear. This tendency results from the elastically nonsymmetrical construction of the layup.

The average shear stress f_s at any point Z inches above the neutral axis is given by

$$f_s = \frac{q}{t} = \frac{V}{EIt} \sum_{i=1}^{n} \Delta(EA\bar{Z})_i \tag{1}$$

where $\bar{Z}$ is the centroidal distance to the incremental area from the neutral axis. The average shear stresses are calculated in Table VI.

TABLE VI. SHEAR FLOW CALCULATIONS FOR 10,000-POUND SHEAR LOAD

Z (in.)	ΔL (in.)	$\bar{Z}$ (in.)	ΣEt (lb/in. x 10^6)	Δ(EA$\bar{Z}$) (lb/in. x 10^6)	ΣΔ(EA$\bar{Z}$) (lb/in. x 10^6)	q (lb/in.)	Avg f_s (psi)	Shear Flow Distribution: Spar Cap (lb/in.)	Shear Flow Distribution: Doublers (lb/in.)	Shear Flow Distribution: Skins (lb/in.)
5.5	0.5	5.75	2.2810	6.5579	6.5579	382.2	624	311.3	14.3	56.7
5.0	0.5	5.25	2.2810	5.9876	12.5455	731.1	5,539	0	147.0	584.1
4.5	0.5	4.75	0.4238	1.0065	13.5520	789.8	6,474	0	158.2	630.9
4.0	0.5	4.25	0.4238	0.9006	14.4526	842.3	6,904	0	133.7	708.5
3.5	0.5	3.75	0.4025	0.7547	15.2073	886.2	7,734	0	99.0	787.1
3.0	0.5	3.25	0.3812	0.6194	15.8267	922.3	9,042	0	54.6	867.6
2.5	0.5	2.75	0.3599	0.4949	16.3216	951.2	10,339	0	0	951.2
0	2.5	1.25	0.3386	1.0581	17.3797	1012.8	11,009	0	0	1012.8

Also shown in Table VI is the shear flow distribution to the various plies making up the total cross section. This distribution is based on stiffness ratios involving G and t.

The shear strength of the doubler plies based on shear tests is 15,600 psi (see Table I). Assume that Z = 2.5 inches, q = 951.2 lb/in., and the doubler ply is still effective. Then shear stress in the doubler ply is

$$f_s = \frac{951.2}{0.3599} (0.3812 - 0.3599) \left(\frac{1}{0.010}\right) = 5650 \text{ psi} \tag{2}$$

and the allowable shear is

$$V_{all} = (15,600/5650)\ 10,000 = 27,600 \text{ lb} \tag{3}$$

or the maximum load on the beam to cause shear failure in the doublers is

$$P_{max} = 2V_{all} = 55,200 \text{ lb} \tag{4}$$

Since no shear tests were made for a laminate plied up as in the test specimen skins, the skin shear strength is calculated based on the shear strength of the individual plies. Failure is assumed to occur when the following condition is met in any ply within the laminate:

$$\left(\frac{f_l}{F_l}\right)^2 + \left(\frac{f_t}{F_t}\right)^2 + \left(\frac{f_{lt}}{F_{lt}}\right)^2 - \left(\frac{f_l f_t}{F_l^{\,2}}\right) = 1.0 \tag{5}$$

From the beam analysis, a shear load of 10,000 pounds gives an average shear stress at the gage locations of 11,009 psi (see Table VI). Using allowable strengths from tests and the failure criteria above, a load factor was determined for each ply:

1. For 1581 fabric at 0 degrees, N = 2.46.
2. For tape at 0 degrees, N = 1.47.
3. For tape at +60 degrees, N = 2.32.
4. For tape at -60 degrees, N = 1.213.

The minimum load factor is 1.213, which implies failure of the -60 degree ply at a shear load of 12,130 pounds or a beam load of 24,260 pounds. A tension failure occurs in the transverse direction for this ply.

Comparison with Test Data

The load factors determined by testing were 2.23 for specimen 132 and 2.46 for specimen 131. The higher value is equal to the maximum of 2.46 for the fabric ply calculated above. The lower value is slightly less than the 2.32 calculated for the zero-degree ply of tape.

On the basis of the lowest load factor (1.213), discontinuity in strain versus load data should become evident in the strain gage readings at about 24,260 pounds. The strain gage readings are plotted in Figures 13 through 19.

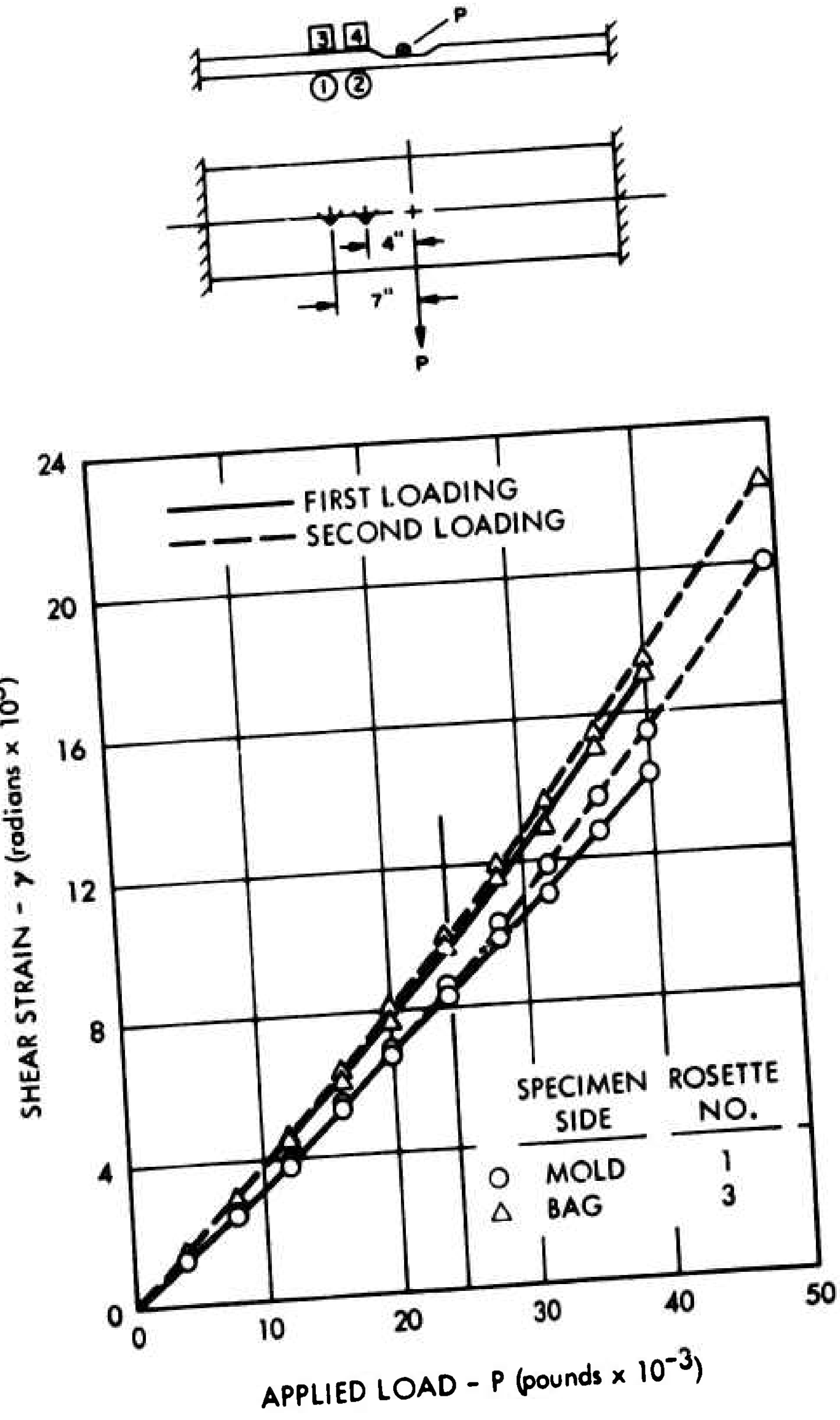

Figure 13. Shear Strains in Tapered-Thickness Sandwich Specimen 131 - Seven Inches From Mid-Span.

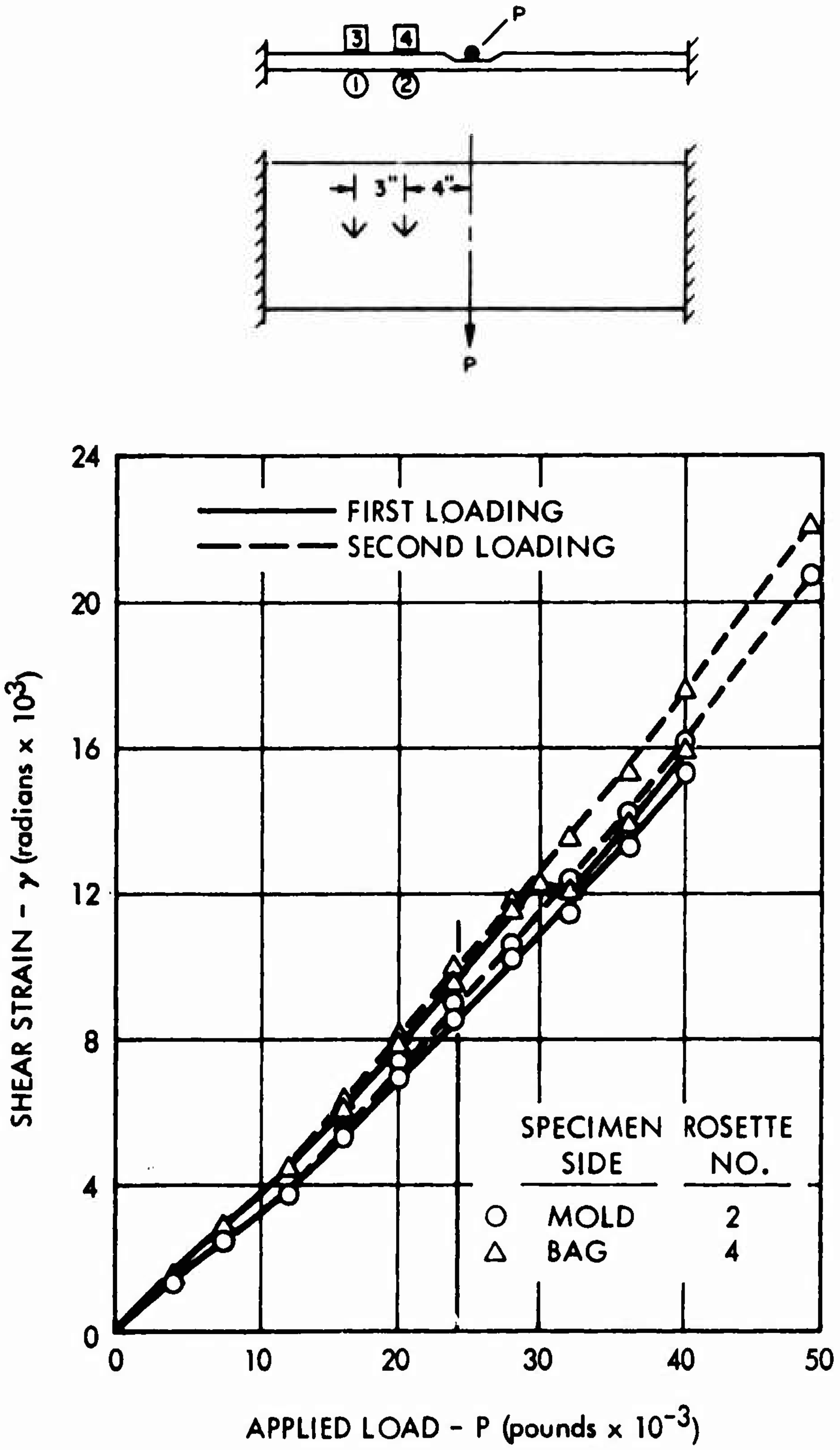

Figure 14. Shear Strains in Tapered-Thickness Sandwich Specimen 131 - Four Inches From Mid-Span.

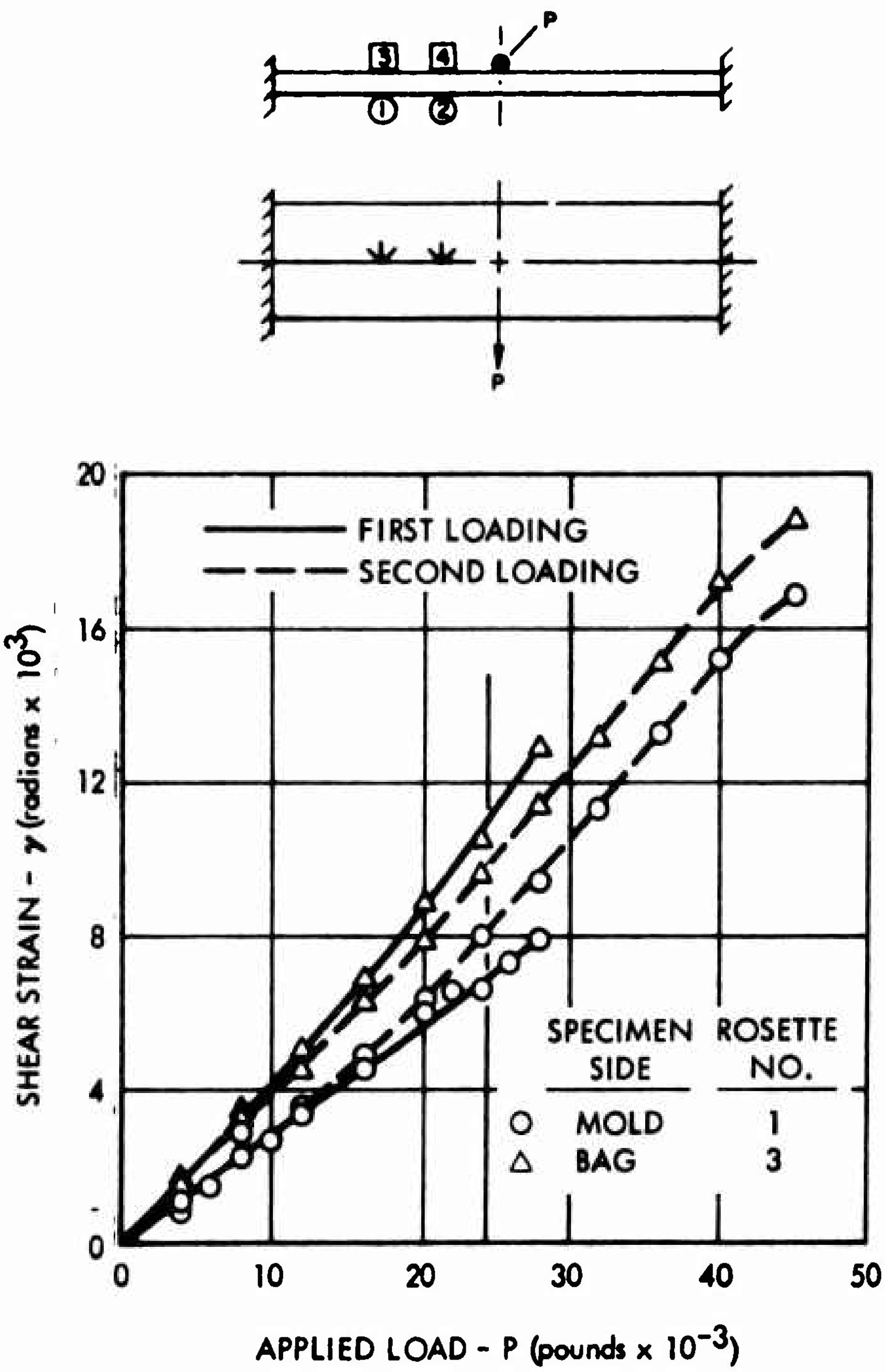

Figure 15. **Shear Strains in Constant-Thickness Sandwich Specimen 132 - Seven Inches From Mid-Span.**

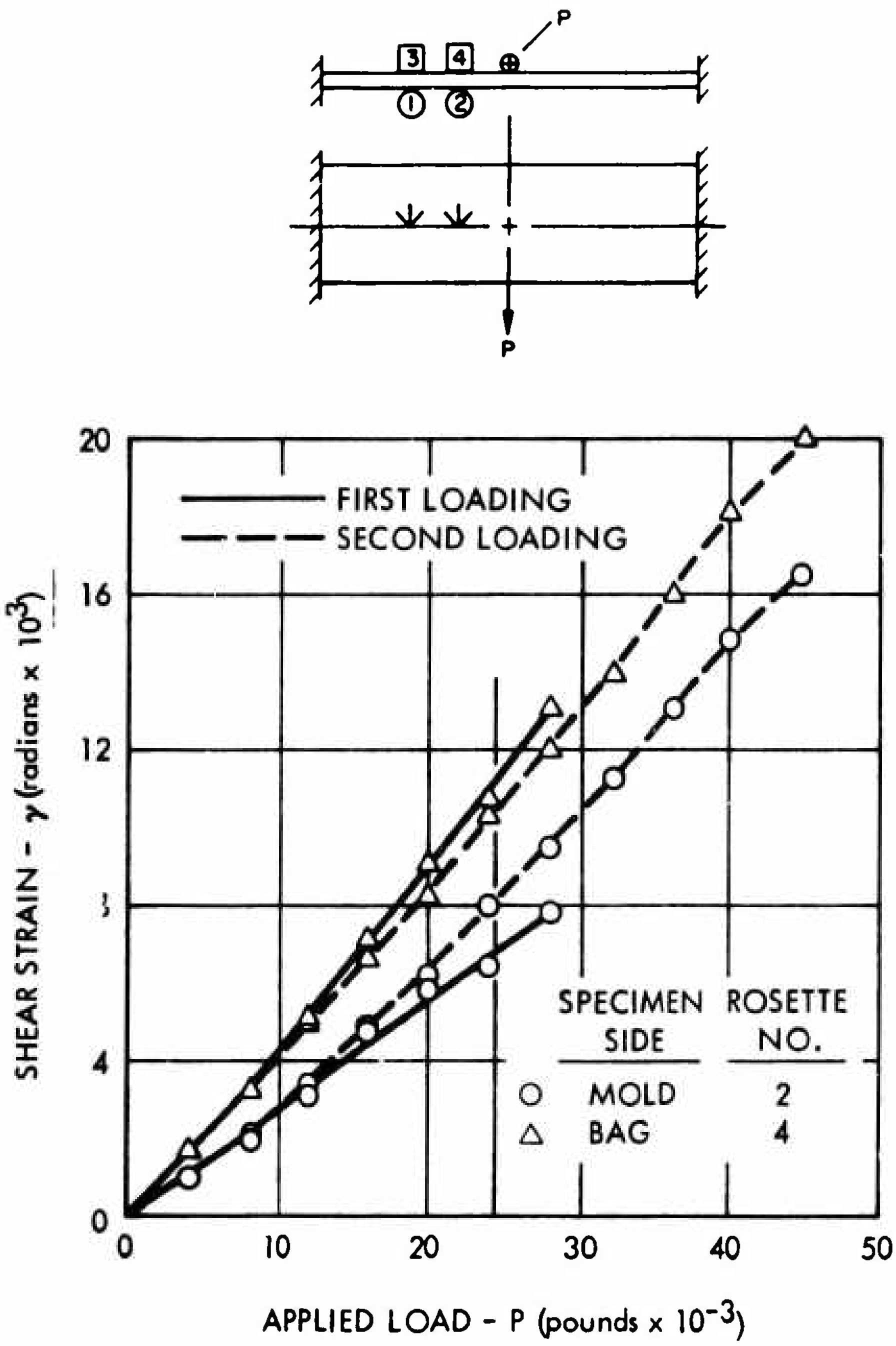

Figure 16. Shear Strains in Constant-Thickness Sandwich Specimen 132 - Four Inches From Mid-Span.

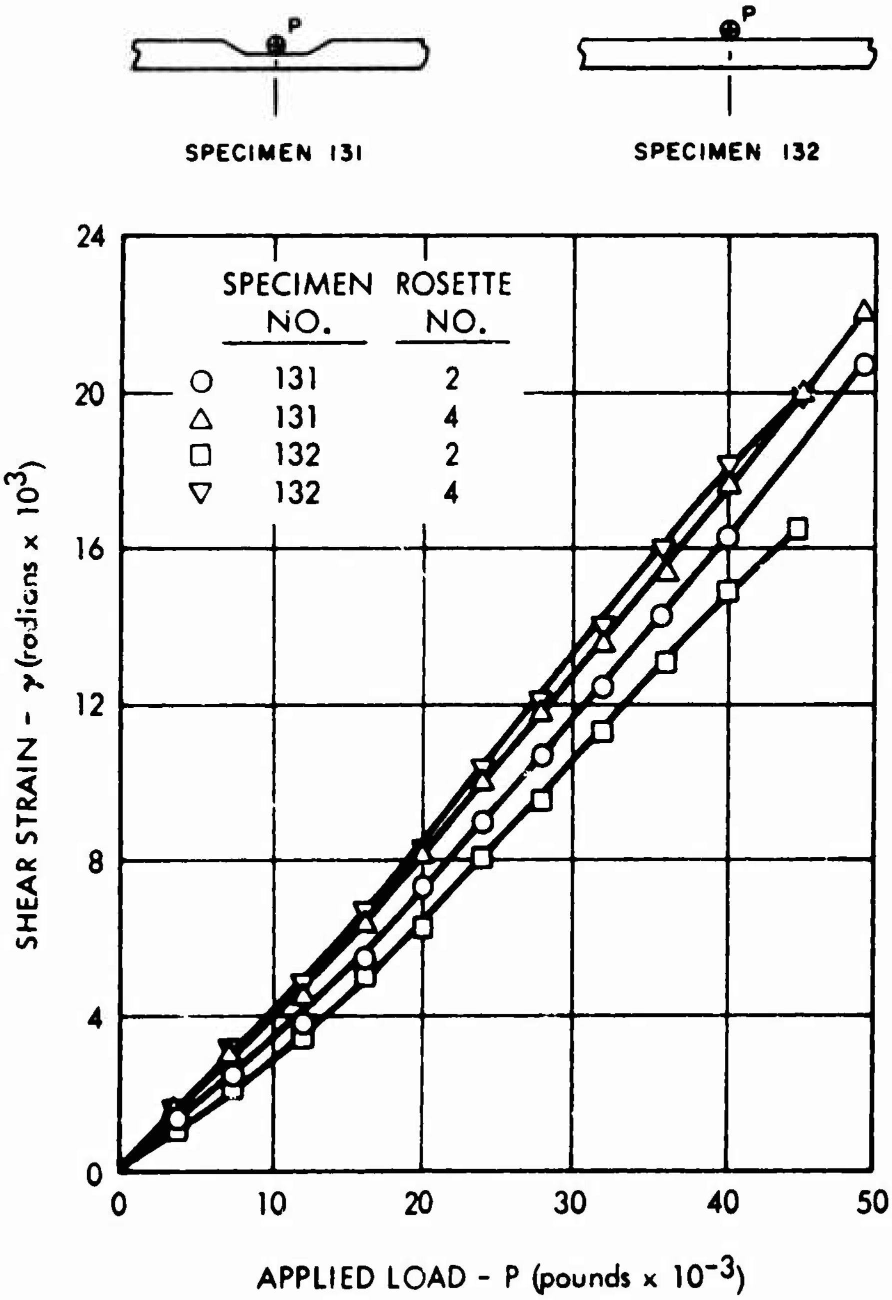

Figure 17. Comparison of Shear Strains in Sandwich Beam Specimens - Four Inches From Mid-Span.

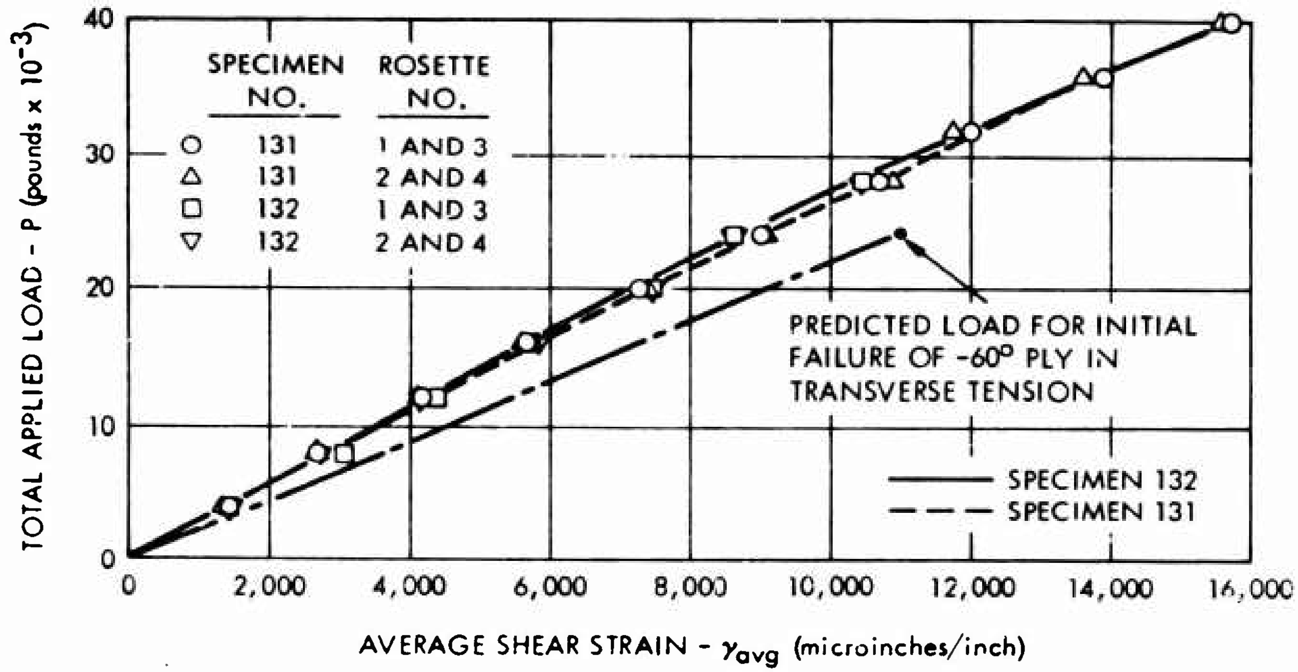

Figure 18. Results of Shear Beam Specimen Tests and Comparison With Theoretical Calculations - Proof Load Test.

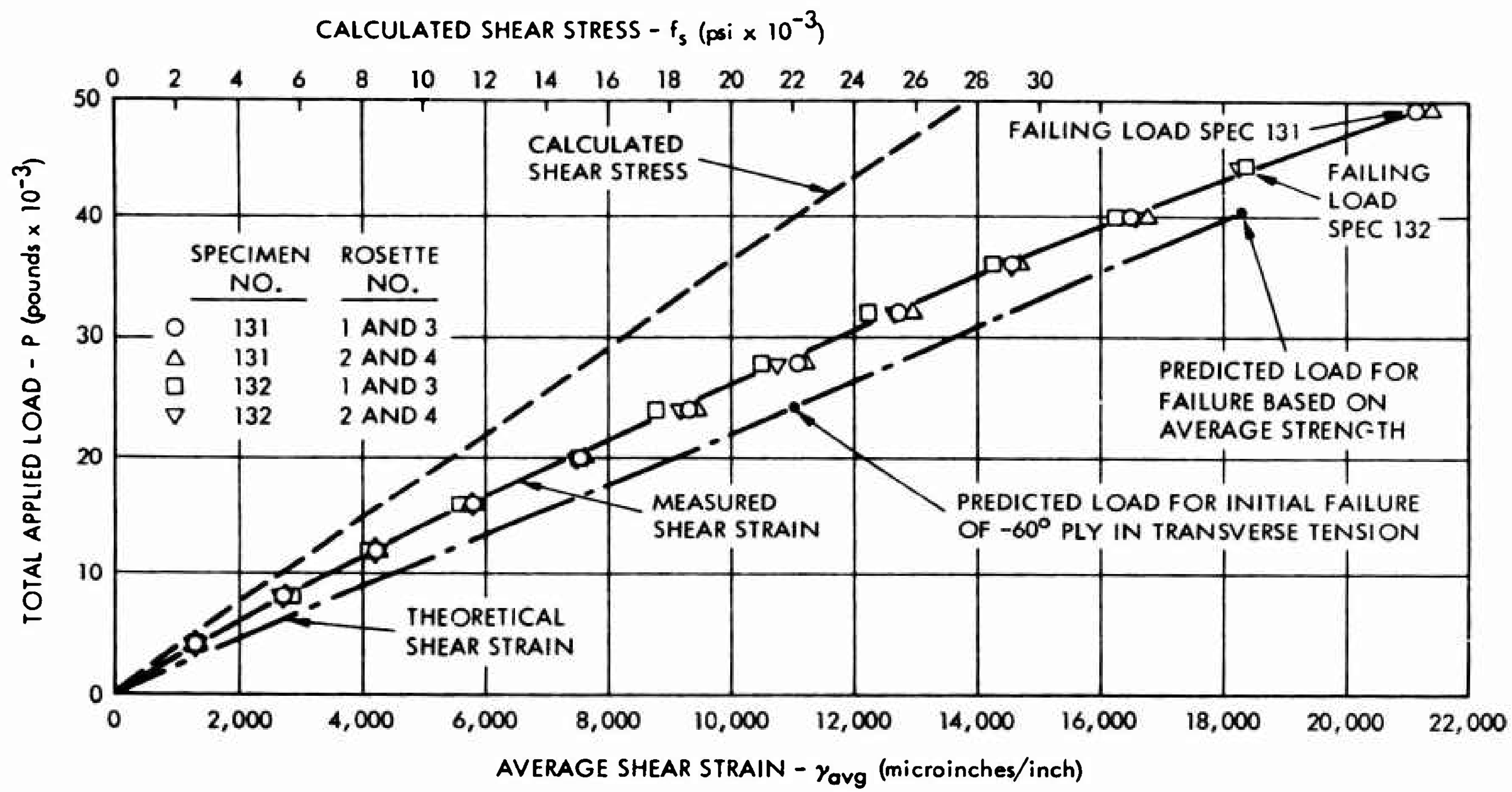

Figure 19. Results of Shear Beam Specimen Tests and Comparison With Theoretical Calculations - Failing Load Test.

In Figure 18 there appears to be a discontinuity in the load versus strain curve at 28,000 pounds for specimen 131 during the proof load test. For this reason, Figure 20 was prepared, which shows the slope of the load versus average shear strain curve as the beam load is increased. The data plotted in Figure 20 are based on the strain gage readings and a 2000-pound load increment for both the proof and ultimate load tests. Although there is considerable scatter in the data, two observations are of interest.

1. In the proof load test, there was a large change in the load versus strain rate between 25,000 and 30,000 pounds, which tends to support the calculations of an initial failure at 24,260 pounds.

2. The same thing is observed in the ultimate load test, but the change is not as pronounced as during the proof load test.

Figures 18 and 19 are plots of the average shear strains of the two faces at the two rosette locations for each beam. The initial portion of the curve suggests a shear modulus for the composite of 1.6×10^6 psi. Between 11,000 and 19,000 psi, the tangent shear modulus is very close to the theoretical value of 1.21×10^6 psi. Also shown in Figure 18 is a failing load based on the average load factor for the four plies. This predicted load falls below the test failing loads of the two beams and is 81 percent of specimen 131 and 90 percent of specimen 132 actual ultimate strengths.

Conclusions

Although a relatively simple beam analysis was made for the specimens, comparison of the analysis with test results is encouraging. The shear modulus comparison suggests that some additional stiffness may be imparted to the structure by virtue of the layer of resin at the core skin interface. This should be investigated by shear testing of sandwich specimens, using the rail shear method and comparing the results with data derived from laminates tested by the same method.

The stress calculations indicated initial failure in the -60-degree ply at a beam load of 24,260 pounds, and experimental data implies some change in the structural behavior at a load of 25,000 pounds.

The failing loads of both beams exceeded the ultimate load calculated on the basis of average strength, and although this is encouraging, it cannot justify the use of an average strength for design. Additional strength testing of orthotropic laminates is required, preferably in actual structural components. The testing should be directed toward verification of initial failure predictions based on the stress condition in single plies and ultimate strength comparisons with average strength.

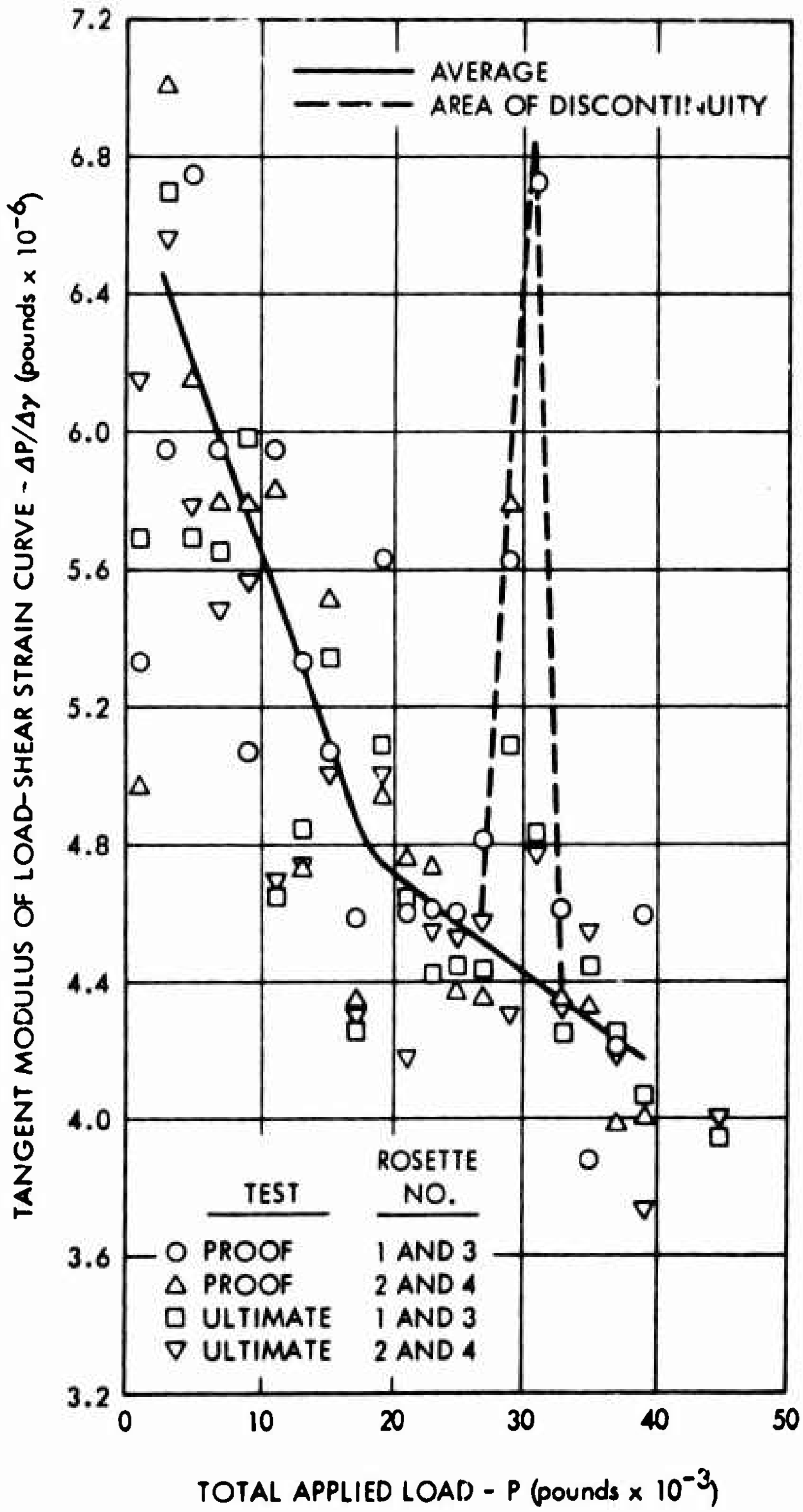

Figure 20. Variation of Slope of Shear Strain Versus Load Curve for Specimen 131 - Based on Average Strain Rosette Readings.

RIB SUPPORT BOXES

GENERAL

The primary purpose of this subprogram was to investigate methods of transferring external loads into the wing structure by means of a rib. These loads were to simulate external store or hinge loads that might be induced by a movable surface such as an aileron.

The effort involved basically the development of rib design, installation, and attachment concepts. A rib was installed in the aft cell of each of two reduced span sections of the 7-foot wing test article. The sections were mounted on a test jig. Loads were applied to fittings attached to ribs. The two test sections were fabricated using two different rib designs.

A secondary purpose of this program was to incorporate the more advanced S glass materials into the wing section design. These materials included both woven cloth and unidirectional tapes. This exercise provided experience in handling these materials prior to the fabrication of the No. 3 wing test section.

DESIGN LOADS

The rib loads originally specified in GAP 3417 S/9[2] represent inertia load factors for a 500-pound wing-mounted store (per Specification MIL-A-8591C) except for the moments and torques that would result from an eccentricity between the plane of attachments and the store center of gravity. The two loading conditions shown in Figure 21 were specified.

During the preliminary analysis of the test specimen, it was concluded that a revision of the loading conditions was desirable to achieve better test information. The changes include application of load at one spar only and elimination of the wing axial loads. The revised test conditions are shown in Figure 22.

Condition I loads are considered to be design ultimate loads. The test plan called for first testing to 100 percent test load for Condition II, followed by testing to design ultimate load for Condition I. At the conclusion of these tests, Condition I loads were to be increased until a failure occurred.

The vertical load change involved moving the center spar load to the aft spar. Thus,the same total load was maintained. This change eliminated the need for a set of fittings at each spar. It also produced a more realistic torsional load on the rib.

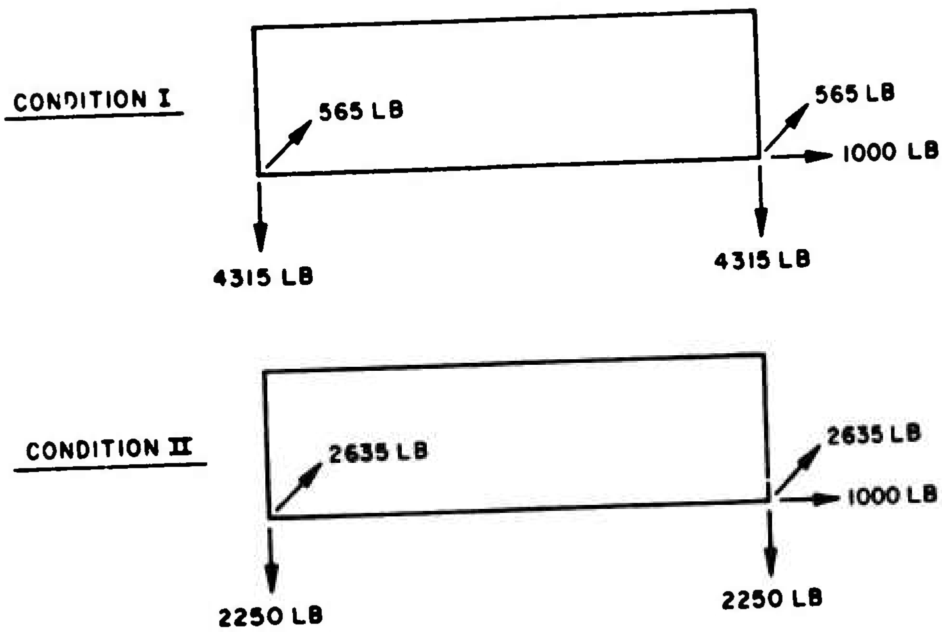

Figure 21. Specified Loading Conditions.

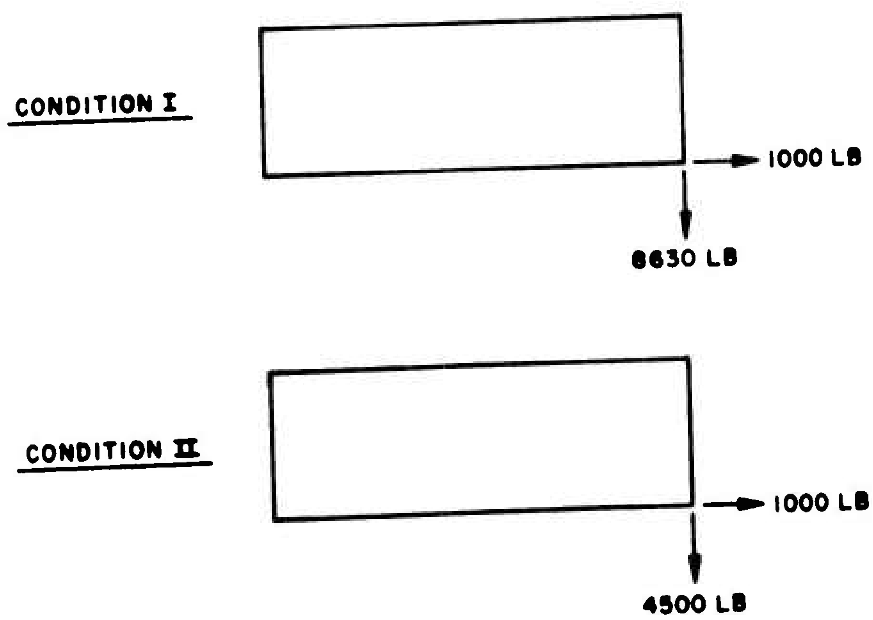

Figure 22. Modified Loading Conditions.

Elimination of the axial load was recommended for this program. Distribution of this load into the wing test section involves shear lag effects, because the rib is not stiff in the plane of this loading. It is felt that the results of the test can be more accurately analyzed when only down and aft loads are applied.

TEST SPECIMEN CONFIGURATION

The basic test specimen was similar to the aft box section of the completed No. 1 and 2 wing test sections, with the exception that it was approximately one-half the length. Existing tools were used for fabrication.

During preliminary design, consideration was given to two types of support. Both a cantilever test section with a rib at the unsupported end and a test specimen simulating a simple beam with supports at both ends and a rib at the center were considered. The cantilever test specimen was selected because it required support fittings at only one end. It also allowed for visual inspection of the rib during testing. The box sections were subjected to higher stresses for the cantilever tests; however, the bending and shears in the sections were not considered critical.

RIB DESIGN

The program provided for two separate test specimens utilizing two different rib designs. The first design is considered the more conventional, and the second design the more unique. Figures 23 and 24 are photographs of the rib support boxes.

The first design (Figure 23) incorporated four different methods of attaching the rib to the wing section. Basically, a solid laminate shear web approximately 0.10 inch thick was attached to the wing skins by angles and fittings. The top skin attachment was made by a semiprimary bonding method, and the forward spar attachment by a secondary bonding method utilizing clamping screws. The lower skin attachment was a bolted attachment, whereas the aft spar attachment was also bolted using the load application fittings.

The assembly sequence involved layup of the attachment angles on the actual wing section to assure proper fit. The rib web was first positioned in the open box section with the lower skin not attached. The upper skin attachment and the forward spar attachment were then laid up in place and cured. The upper skin angles were cured to the top skin, whereas the forward spar angle had a separator between the angle and the spar and rib so that it could be removed after curing. The forward spar angle was next removed, trimmed, and then bonded back into place.

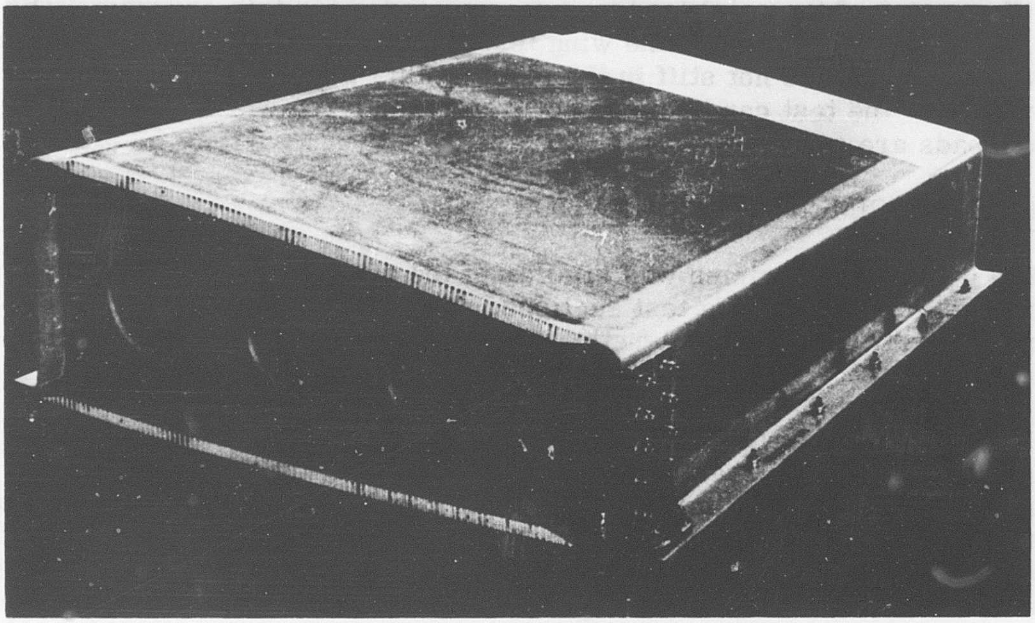

Figure 23. Laminate Rib Box.

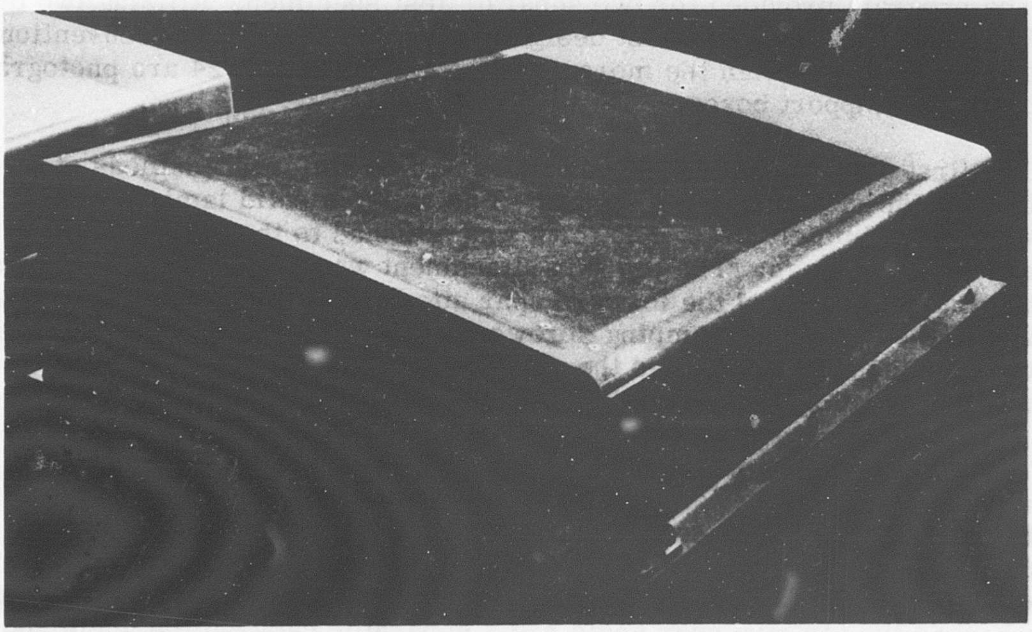

Figure 24. Sandwich Rib Box.

The lower skin angle was laid up and cured on the lower skin panel, again using a separator. The angle was then removed, trimmed, and located onto the rib web in its proper position. Then both rib fittings were installed at the aft spar and connected to the rib web.

The final assembly procedure involved locating the lower skin on the completed assembly and drilling the holes through the lower skin and lower rib angle and through the lower skin and lower spar caps. The lower rib angle was then bonded to the rib web, and the lower skin was bolted to the assembly.

The second rib design concept included a sandwich type of rib web with 0.50-inch core and 0.05-inch skins on each side. The outer 1 inch of the periphery contained solid laminate sections as thick as the core. This rib was laid up and cured on a flat plate and subsequently fitted to the inside of the wing box with approximately 0.05-inch clearance. The rib was positioned, and attachment holes were drilled through the wing skin and into the solid part of the rib. The rib was removed, and metal screw inserts were installed in the rib. The rib was then placed back in the assembly for subsequent bonding. The bonding material was placed between the rib and the skins. The attaching screws were then installed, and the bonding adhesive was cured. It should be noted that the screw attachments were used for clamping only, and the bond was considered to transfer the total shear load.

In both rib support box designs, the lower surface panels were attached to the lower spar caps by secondary bonding plus clamping screws.

Weights of the boxes with their loading point hardware attached were as follows:

Box	Wt (lb)
Laminate Rib	40.30
Sandwich Rib	41.55

From a fabrication standpoint, the sandwich rib was the better of the two designs. The process used to construct this box proved to be trouble-free. The laminate rib design presented fabrication problems in the areas of the rib attachment angles. Several attachment angle moldings were rejected. Since these angles are molded to the inside contours of the honeycomb surface panels, remolding of the angles subjected the surface panels to multiple cures in excess of their normal cures. Each additional cure of the assembly involved an element of risk. It was therefore concluded that even though the laminate rib design was lighter, the full-scale test article would be designed with a sandwich rib.

TEST SECTION DESIGN

The sandwich skins for the surface panels and spar webs of both test boxes were made from a combination of S glass cloth and S glass tapes. Orientations were prescribed to achieve the best balance between axial tension and compression stresses and shear stresses caused by both shear and torsional loadings.

The two upper corners of the box sections required additional laminate thicknesses to allow for splices at the junction of the unidirectional material in the skins and spar webs.

The skin thicknesses used in the top and bottom skins were equalized to best react the test loadings, which were primarily shear and torsion. The No. 2 wing used a greater skin thickness in the upper skin, since it was critical for compression stability.

The ply orientations prescribed for the test sections are shown in Figure 25.

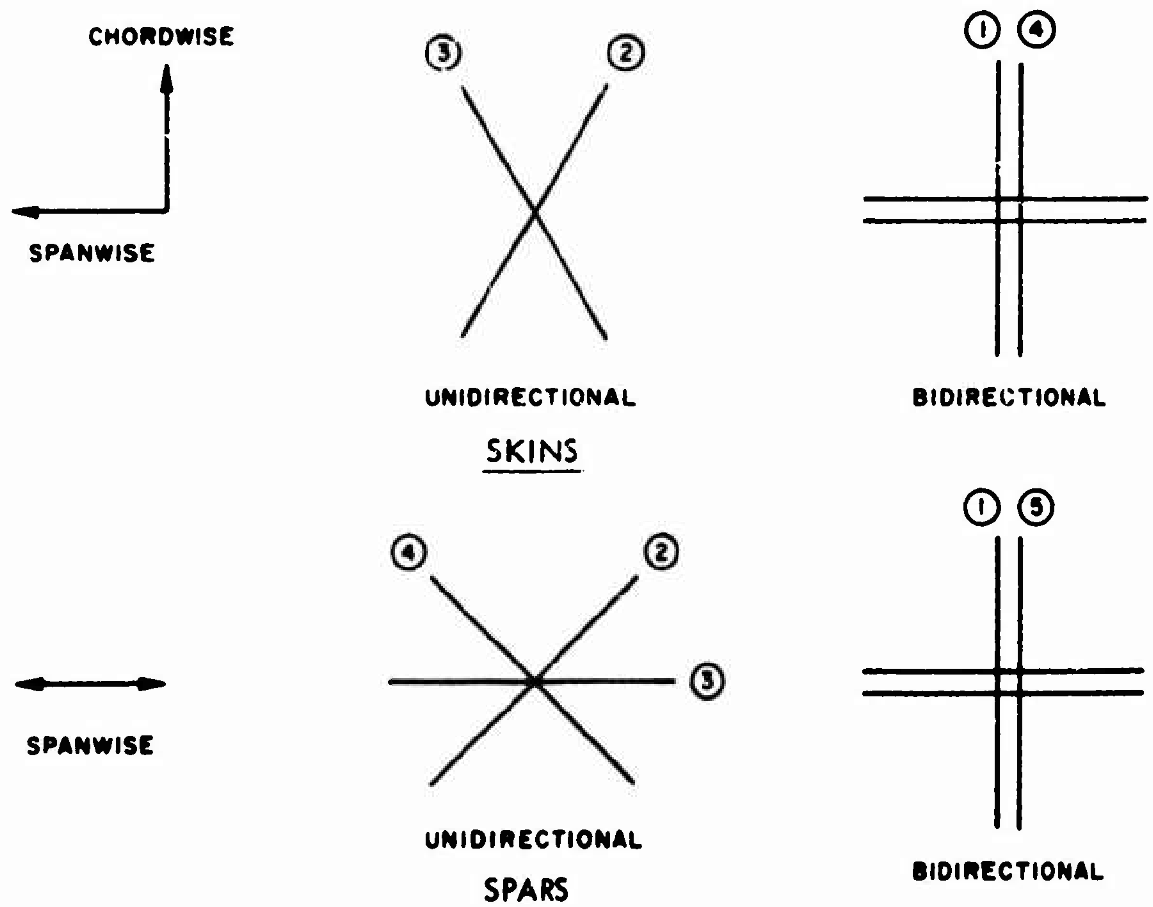

Figure 25. Test Section Ply Orientations.

RIB SUPPORT BOX ANALYSIS

General

The initial design of the rib support box was established using a structural analysis based on properties of the second wing test section. Although the basic section properties used were those of the No. 2 wing section, smaller elements were employed to refine the analysis. This breakdown is shown in Figure 26. The resulting final design was then verified by a final analysis using the actual box section layup configuration.

The basic section properties of the final design were calculated utilizing a GAC computer setup. The program accounts for variability in the elastic properties of the material around the cross section and requires these properties as inputs. For these specimens, derivation of these properties assumed a uniform strain across the laminate and was based on the elastic moduli of the individual plies. The following single-ply properties were used for this analysis:

Material	Young's Modulus		Shear Modulus	Major Poisson's Ratio
	0°	90°		
1581 Cloth	4.24×10^6	4.24×10^6	0.69×10^6	0.120
S Glass Tape	6.63×10^6	2.38×10^6	0.69×10^6	0.250

Resultant calculations produced the following laminate properties:

Location	Young's Modulus		Shear Modulus	Major Poisson's Ratio
	Spanwise	Chordwise		
Skins	4.182×10^6	3.160×10^6	1.181	0.309
Spar Webs	3.998×10^6	3.215×10^6	0.824	0.314
Ribs	2.146×10^6		1.893	0.555

In the spar caps the added plies were considered, and the effect on laminate properties was calculated.

These values for the elastic properties of the skins, spar webs, and ribs were used for conversion of the strain rosette readings to stresses. (Refer to the "data reduction" discussion in this section.)

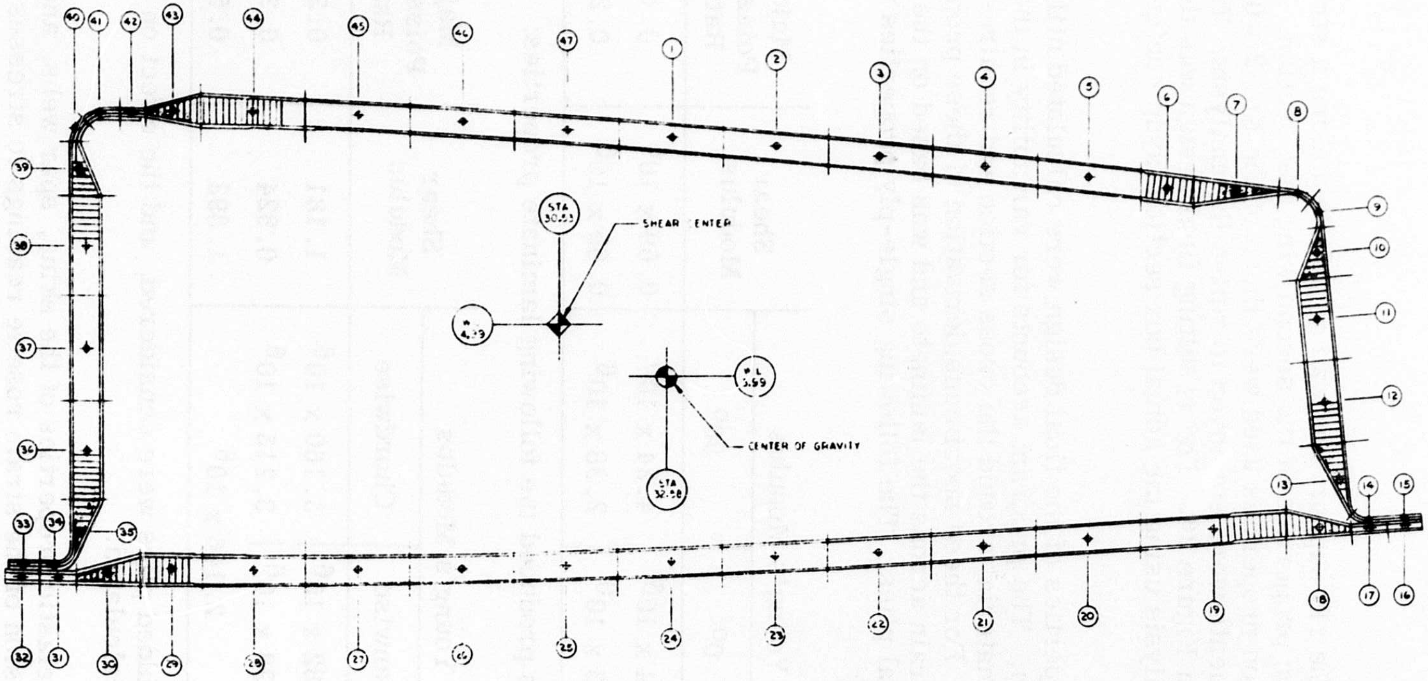

NOTES: UNLESS OTHERWISE SPECIFIED
1. SHEAR FLOW (F) IS IN LBS/INCH.
2. VQ/I FORCES ARE IN LBS/INCH OF SPAN FOR EACH ELEMENT.
3. ALL LOADS ARE FOR A UNIT SHEAR LOAD OF 1000 POUNDS, APPLIED AT THE SHEAR CENTER
4. POSITIVE LOAD POSITION IS UP.

Figure 26. Wing Aft Cell.

The shear flows were determined for vertical and horizontal loads, which were assumed to be applied at the shear center of the box. The shear center was then determined both vertically and horizontally, and the actual torques about the shear center were determined. The location of the shear center and the loading conditions are shown in Figure 27.

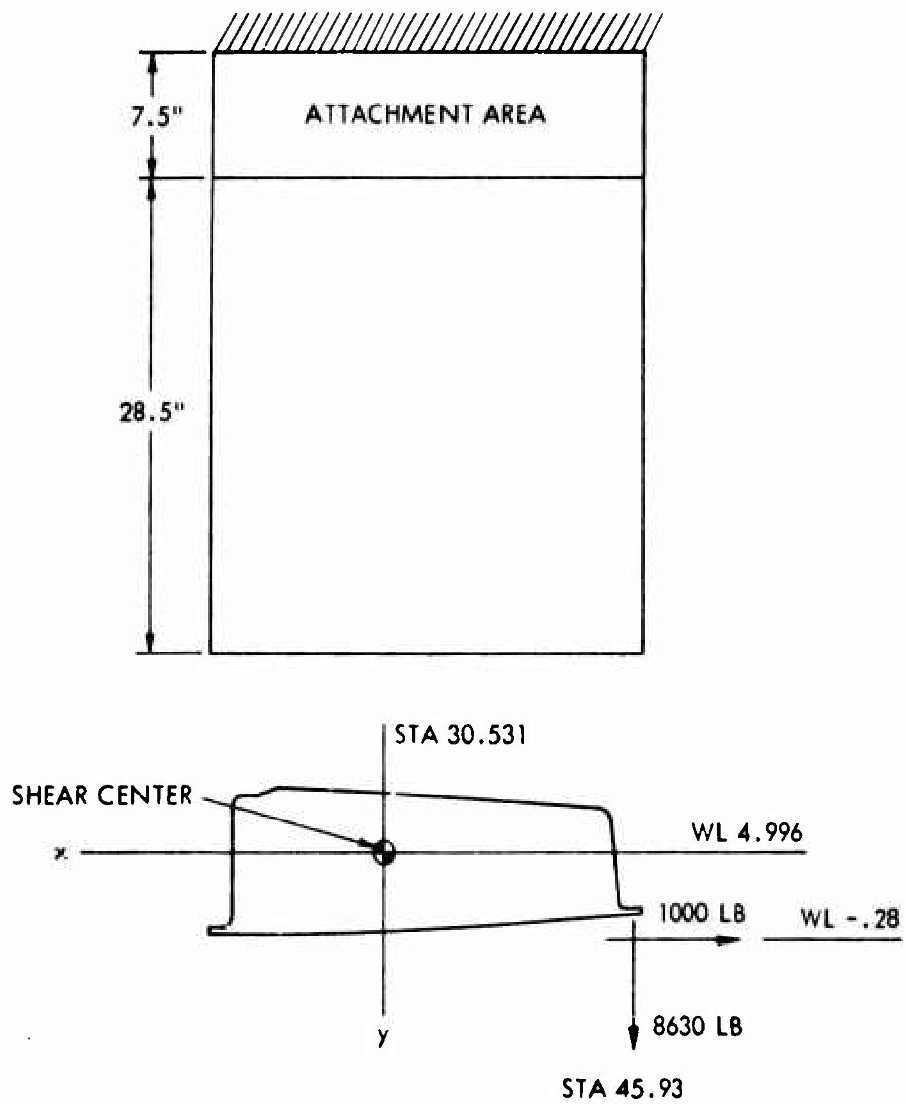

V_y = -8630 LB

V_x = 1000 LB

M_x (AT Z = 28.5) = -233,000 IN.-LB

M_y (AT Z = 28.5) = 27,000 IN.-LB

T = 8630 (45.93 - 30.531) - 1000 (4.996 + 0.28)

= 127,869 IN.-LB

Figure 27. Rib Box Loading Conditions.

The box constants are given below:

I_{x-x} = 98.541 in.^{4}

I_{y-y} = 711.481 in.^{4}

EI_{x-x} = 398.778 x 10^6

EI_{y-y} = 2813.201 x 10^6

G = 1.18 x 10^6 psi

x_{cg} = sta 32.579

y_{cg} = WL 3.991

Cross-sectional area = 7.844 in.^{2}

Torque box area = 187.309 in.^{2}

The final computer-calculated shear flows and bending stresses based on the foregoing loads and box constants are given in Table VII.

The maximum stresses in the wing box are given below:

Compression = 8,729 psi

Tension = 12,720 psi

Shear = 7,795 psi

Structural Analysis

The buckling allowable stress for the bottom skin was determined using the methods given in U. S. Department of Agriculture Report FPL-070.[3] For skins consisting of two plies of 1581 fabric at 0 degrees and two plies of tape at ±30 degrees, d = 0.044 inch. The shear modulus for core aluminum honeycomb (t_c = 0.500 inch) = 25,600 psi.

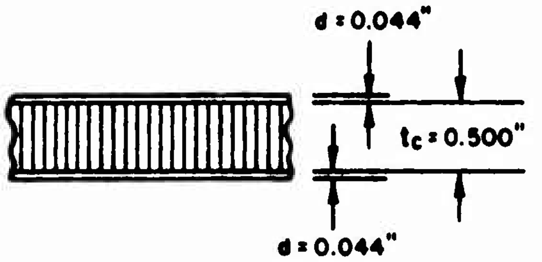

TABLE VII. RIB BOX BENDING AND SHEAR STRESSES							
Element	Bending Stress (psi)	Shear Flow (lb/in.)	Shear Stress (psi)	Element	Bending Stress (psi)	Shear Flow (lb/in.)	Shear Stress (psi)
1	11,124	-380	-4315	25	-8,653	-275	-3126
2	10,637	-451	-5121	26	-8,679	-219	-2484
3	10,126	-518	-5890	27	-8,729	-162	-1840
4	9,567	-583	-6620	28	-8,163	-98	-828
5	8,958	-643	-7306	29	-7,923	-35	-229
6	8,483	-686	-7795	30	-8,031	20	128
7	7,790	-729	-5974	31	-7,974	76	284
8	7,425	-776	-4170	32	-7,960	128	477
9	6,606	-807	-4339	33	-8,358	168	925
10	4,977	-831	-6815	34	-8,372	202	1110
11	2,243	-849	-7585	35	-6,795	246	1354
12	-1,548	-852	-7605	36	-3,040	286	2550
13	-4,856	-831	-6815	37	1,501	291	2600
14	-6,567	-806	-6604	38	6,043	262	2335
15	-6,491	-785	-6439	39	9,546	214	1571
16	-6,548	-758	-3479	40	11,484	168	848
17	-6,620	-722	-3313	41	11,301	117	604
18	-6,437	-680	-4302	42	11,169	68	386
19	-6,938	-612	-4976	43	12,720	17	128
20	-7,666	-549	-6236	44	12,487	-63	-615
21	-7,912	-492	-5591	45	12,264	-149	-1698
22	-8,158	-440	-4996	46	11,925	-228	-2594
23	-8,355	-386	-4384	47	11,561	-305	-3464
24	-8,480	-331	-3761				

The skin properties determined from the computer analysis are given below.

$$E_l = 4.18 \times 10^6 \text{ psi}$$

$$E_t = 3.16 \times 10^6 \text{ psi}$$

$$\mu_{lt} = 0.30$$

$$\mu_{tl} = 0.23$$

$$\sqrt{\frac{E_t}{E_l}} = 0.87$$

The skin bending stiffness per inch is calculated as

$$D = \frac{d\sqrt{E_l E_t}\,(d + t_c)^2}{2\,(1 - \mu_{lt}\mu_{tl})}$$

$$= \frac{0.044\sqrt{4.18(3.16)} \times 10^6\,(0.544)^2}{2\,(1 - 0.30 \times 0.23)}$$

$$= 25,320 \qquad (6)$$

The parameter involving shear stiffness is calculated as

$$U = \frac{G_{cl}\,(d + t_c)^2}{t_c}$$

$$= \frac{25,600\,(0.544)^2}{0.500}$$

$$= 15,120 \qquad (7)$$

The parameter relating shear and bending stiffness is calculated as

$$V' = \frac{\pi^2 D}{b^2 U}$$

$$= \frac{(3.14)^2\,(25,320)}{(23)^2\,(15,120)}$$

$$= 0.031 \qquad (8)$$

The aspect ratio is given as

$$\frac{b}{a} = \frac{23}{28.5} = 0.806 \tag{9}$$

Then from Figure 11 of FPL-070,[3] K = 3.2 for a sandwich panel with orthotropic facings and simply supported edges. Therefore, the allowable buckling load of the panel is

$$N_{cr} = K\frac{\pi^2}{b^2} D$$

$$= 3.2 \frac{(3.14)^2}{(23)^2} 25,320$$

$$= 1513 \text{ lb/in.} \tag{10}$$

and the buckling stress of the panel is

$$\sigma cr = \frac{1513}{0.088} = 17,190 \text{ psi} \tag{11}$$

The margin of safety at the element of maximum compression is

$$MS = \frac{17,190}{8,729} - 1.0 = 0.97 \tag{12}$$

Based on laminate shear tests, the shear strength of the panel is estimated to be

$$F_s = 17,000 \text{ psi} \tag{13}$$

The margin of safety at the element of maximum shear is

$$MS = \frac{17,000}{7,795} - 1.0 = 1.18 \tag{14}$$

For the condition of combined shear and compression, the stress ratios are

$$\text{Element 20} \quad R_b = \frac{7666}{17,190} = 0.466 \tag{15}$$

$$R_s = \frac{6236}{17,000} = 0.366 \tag{16}$$

$$R = R_b + R_s^2 = 0.466 + (0.366)^2 = 0.580 \quad (17)$$

$$MS = \frac{1.00}{0.580} - 1.0 = 0.72 \quad (18)$$

The margin of safety for combined tension and shear stresses is much larger.

For the bonded attachment of the hat section to the bottom sandwich, the maximum shear flow is q = 806 lb/in. The bond strength = 1000 psi. Therefore, the margin of safety is

$$MS = \frac{1000}{806} - 1.0 = 0.24 \quad (19)$$

Rib Analysis

The rib is loaded by the applied loads at its lower aft corner. These loads are reacted by shears from the wing box section as shown in Figure 28. Shear, moment, and axial load curves were developed across the length of the rib, with the following maximum loads resulting:

M = 12,500 in.-lb at Sta 30.0

V = 2390 lb

P = 300

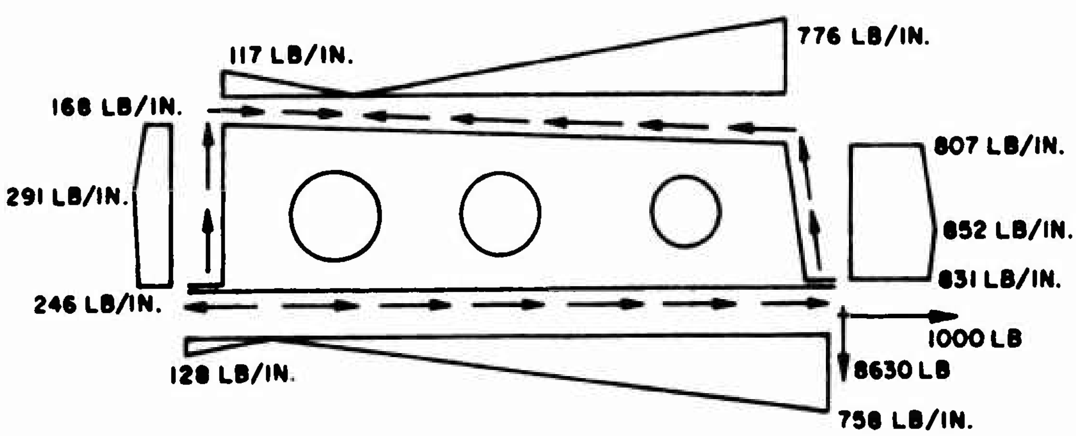

Figure 28. Loads Reacted by Wing Box Section Shears.

Design No. 1 - Solid-Wall Laminate Rib (0.10 Inch)

For 1581 fabric warp parallel to the length of the member, assume flanges resist moment such that

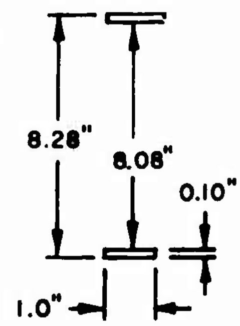

$$p = \frac{M}{8.28} = \frac{12,500}{8.28} = 1510 \text{ lb} \qquad (20)$$

Then

$$f_c = f_t = \frac{1510}{1 \times 0.10} = 15,100 \text{ psi} \qquad (21)$$

and

$$MS = \frac{40,000}{15,100} - 1.0 = 1.65 \qquad (22)$$

For 1581 fabric at 45 degrees, assume a uniform shear in area of web minus area of hole (3.35-inch dia) such that

$$q = \frac{V}{8.08 - 3.35} = \frac{2390}{4.73} = 505 \text{ lb/in.} \qquad (23)$$

Then

$$f_s = \frac{505}{0.10} = 5050 \text{ psi} \qquad (24)$$

and

$$F_s = 30,000 \text{ psi} \qquad (25)$$

The margin of safety is ample.

Attachment of Laminate Rib to Wing

For the top skin to rib attachment (a semiprimary bond), the maximum shear flow is 729 lb/in. with a bond width of 1 inch. Therefore,

$$f_s = \frac{729}{1.0} = 729 \text{ psi} \qquad (26)$$

If we assume an allowable primary bond shear strength of 1500 psi, then

$$MS = \frac{1500}{729} - 1.0 = 1.06 \tag{27}$$

For the forward spar to rib attachment (a secondary bond), the maximum shear flow is 291 lb/in. Therefore,

$$f_s = \frac{291}{1.0} = 291 \text{ psi} \tag{28}$$

If we assume an allowable secondary bond shear strength of 1000 psi, then

$$MS = \frac{1000}{291} - 1.0 = 2.43 \tag{29}$$

For the bottom skin to rib attachment (a secondary bond with screws), the maximum shear flow is 680 lb/in. Therefore,

$$f_s = \frac{680}{1.0} = 680 \text{ psi} \tag{30}$$

and

$$MS = \frac{1000}{680} - 1.0 = 0.47 \tag{31}$$

<u>Design No. 2 - Sandwich Rib (0.050-Inch Skins and 0.500-Inch Core)</u>

Assume caps resist moment such that

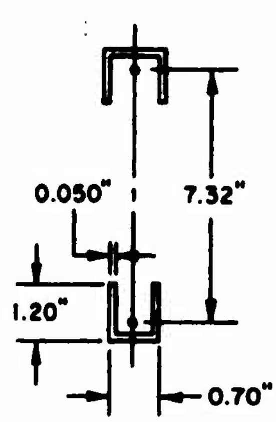

$$p = \frac{M}{7.32} = \frac{12,500}{7.32} = 1708 \text{ lb} \tag{32}$$

Then

$$f_c = \frac{1708}{0.050(3.10)} = 11,000 \text{ psi} \tag{33}$$

and

$$MS = \frac{40,000}{11,000} - 1.0 = 2.64 \tag{34}$$

Assume a uniform shear in area of web minus area of hole such that

$$q = \frac{V}{8.08 - 3.35} = \frac{2390}{4.73} = 505 \text{ lb/in.} \tag{35}$$

Then

$$f_s = \frac{505}{0.10} = 5050 \text{ psi} \tag{36}$$

The margin of safety is ample.

Attachment of Sandwich Rib to Wing

This design utilizes a 0.76-inch-wide bond at the top skin and a 0.70-inch-wide bond at the forward spar and bottom skin.

For the top skin to rib attachment (a secondary bond), the maximum shear flow is 729 lb/in. Therefore,

$$f_s = \frac{729}{0.76} = 959 \text{ psi} \tag{37}$$

and

$$MS = \frac{1000}{959} - 1.0 = 0.04 \tag{38}$$

For the bottom skin to rib attachment (a secondary bond), the maximum shear flow is 680 lb/in. Therefore,

$$f_s = \frac{680}{0.70} = 971 \text{ psi} \tag{39}$$

and

$$MS = \frac{1000}{971} - 1.0 = 0.03 \tag{40}$$

Analysis of Aft Spar/Rib Area

The loads reacted by the aft spar are given in Table VIII.

TABLE VIII. RIB BOX LOADS REACTED BY AFT SPAR						
Element	q (lb/in.)	q_{vert} (lb/in.)	q_{horiz} (lb/in.)	Δs (in.)	V (lb)	H (lb)
8	-776	0	-776	0.70	0	-543
9	-807	-804	-70	0.60	-482	-42
10	-831	-828	-72	0.96	-794	-69
11	-849	-846	-74	1.55	-1311	-115
12	-852	-849	-74	1.55	-1316	-115
13	-831	-828	-72	1.40	-1159	-101
14	-806	-84	-802	0.70	-59	-561
15	-785	-82	-781	0.66	-54	-515
16	-758	-66	755	0.66	-44	498
17	-722	-63	719	0.70	-44	503
18	-680	0	680	1.25	0	850
Totals	-	-	-	-	-5263	-210

The rib loads are calculated as

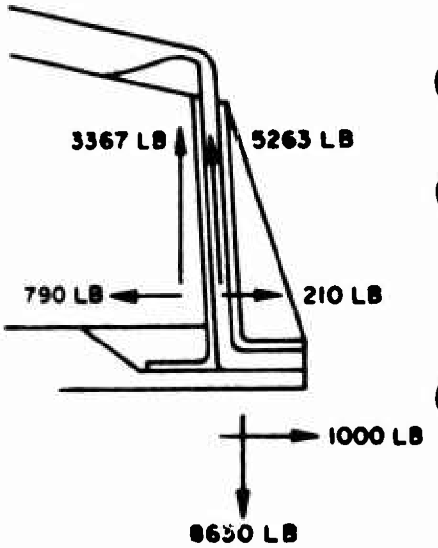

$$V = 8630 - 5263 = 3367 \text{ lb} \tag{41}$$

and

$$H = 1000 - 210 = 790 \text{ lb} \tag{42}$$

The bearing load in the rib (five AN-4 bolts) is given as

$$p = \frac{3367}{5} = 674 \text{ lb/bolt} \tag{43}$$

Therefore,

$$f_{br} = \frac{674}{0.10 \times 0.25} = 27,000 \text{ psi} \tag{44}$$

and

$$MS = \frac{45,000}{27,000} - 1.0 = 0.66 \tag{45}$$

The bearing load in the spar (10 AN-4 bolts) is given as

$$p = \frac{5263}{10} = 526 \text{ lb/bolt} \tag{46}$$

Therefore,

$$f_{br} = \frac{526}{0.162 \times 0.25} = 13,000 \text{ psi} \tag{47}$$

The margin of safety is ample.

Summary

The minimum margin of safety for the solid-wall rib is 0.24 (the bond of the bottom sandwich panel to the top hat sandwich section), indicating a failing load of 10,700 pounds vertical.

The minimum margin of safety for the sandwich-wall rib is 0.03 (bond of rib to wing bottom skin), indicating a failure load of 8890 pounds vertical.

Deflections of the Rib Support Box

Due to the torque of 127,869 in.-lb, the torsional deflection of the 28.5-inch-long test section was calculated to be ϕ = 0.8 degree, and the vertical and horizontal deflections were calculated to be 0.37 and 0.05 inch, respectively.

RIB SUPPORT BOX TESTS

General

The test results and applicable photographs included in this subsection were taken from the Aero Structures Department test summary report.[4]

Workmanship of both boxes was good. All exterior surfaces were smooth, and all bonds appeared to be good. Only one defect was found on both boxes - the width of the lower panel was 1/2 inch shorter than the design dimension. This was due to the misalignment of the forward spar. The same defect was noted in previous specimens and could be corrected by modifying the mold.

The test setup is shown in Figure 29. The box was cantilevered from the strongback and subjected to a single load at the fitting located at the

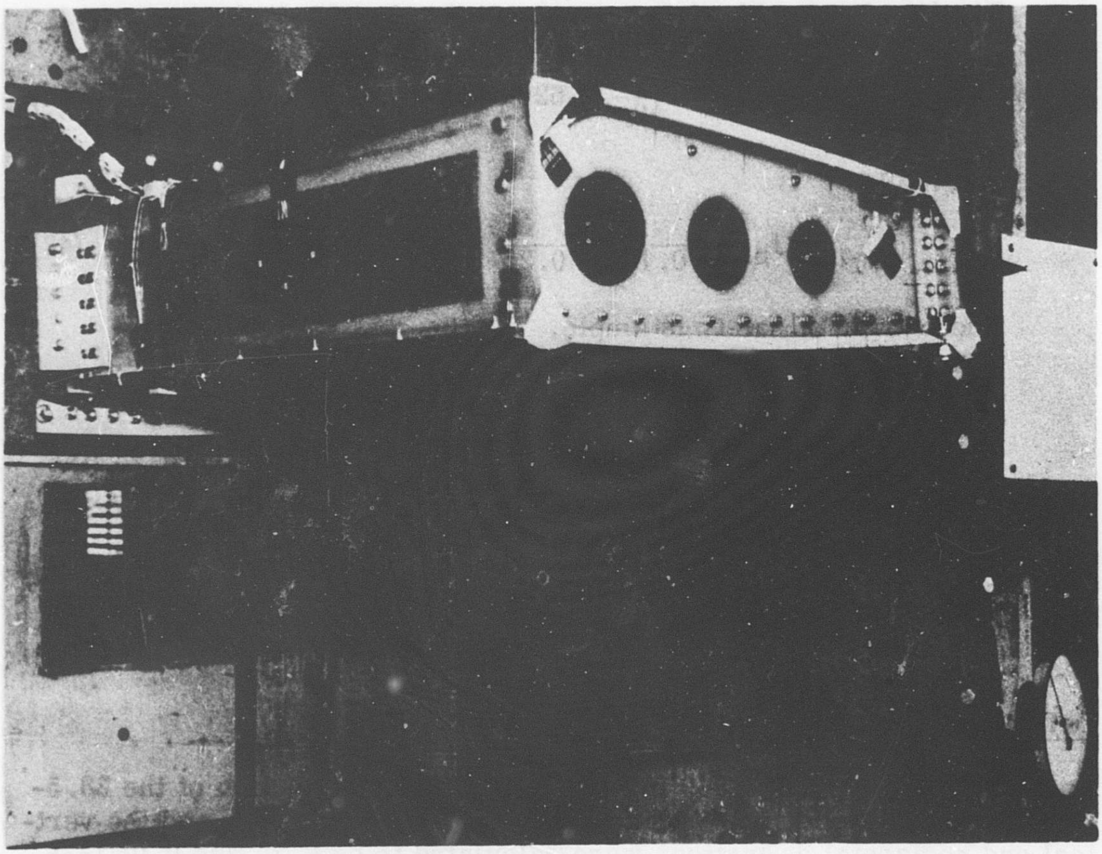

Figure 29. Rib Support Box Test Setup.

intersection of the aft spar and rib. Strain and deflection data were recorded during the tests. The test plan was as follows:

1. Apply load for Condition II (4500 pounds vertical down and 1000 pounds horizontal aft) up to 100 percent DUL; then decrease the load in 20-percent increments.

2. Apply load for Condition I (8630 pounds vertical down and 1000 pounds horizontal aft) up to 100 percent DUL; then decrease the load in 20-percent increments.

3. Apply load for Condition I until failure occurs.

Figures 30, 31, and 32 show the locations of deflection and strain-measuring instrumentation for the two boxes.

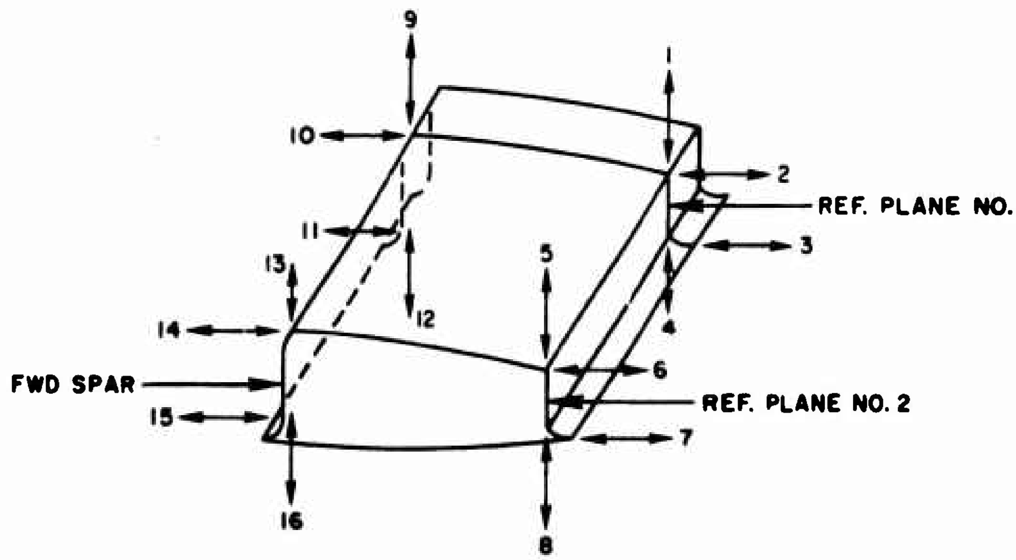

Figure 30. Location of Rib Support Box Deflection Points.

Summary of Tests - Rib Support Box No. 1 (Sandwich Rib)

The load was applied for Condition II to 100 percent DUL and then decreased. No cracking sounds were heard during the test, and no damage was apparent from a visual inspection after the load was removed. The load was next applied for Condition I. No cracking sounds were heard up to 60 percent DUL. As the load was increased to 70 percent DUL, a loud report was heard at 66 percent DUL, and the load dropped to 54 percent DUL. The box was visually examined under load. No damage was apparent. The load was decreased in 20-percent increments. After the load was removed, the box was visually examined; no damage was apparent. The box was again loaded to 100 percent DUL with no audible cracking sounds. The load was removed and the box examined. No damage was apparent. The box was again loaded in Condition I to failing load. No cracking sounds were heard up to 120 percent DUL. A sharp cracking sound was heard at 120 percent DUL. Loading was continued to 160 percent DUL, at which point a loud report was heard. A visual examination showed that the steel plate on the fixed end of the box had been pulled away from the strongback due to a bolt failure. The test was discontinued and the load removed.

The box was removed from the strongback and closely inspected. White areas were observed around each bolt hole along the aft spar flange, indicating some delamination or crazing due to high bearing stresses. The bolts were removed from the holes and found to be slightly bent. The

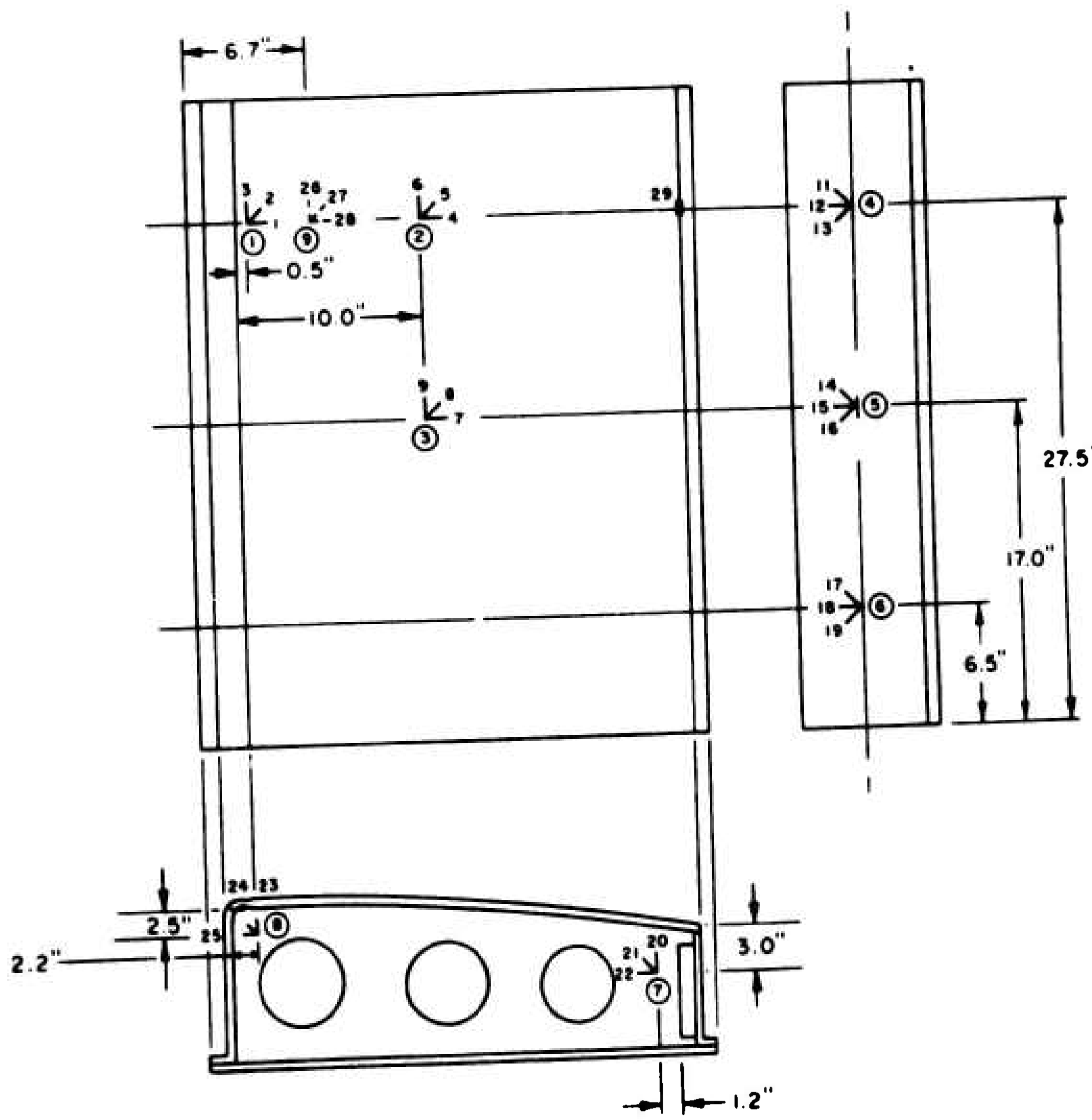

CIRCLED NUMBERS ARE ROSETTE NUMBERS.

Figure 31. Strain Gage Locations for Rib Support Box No. 1 (Sandwich Rib).

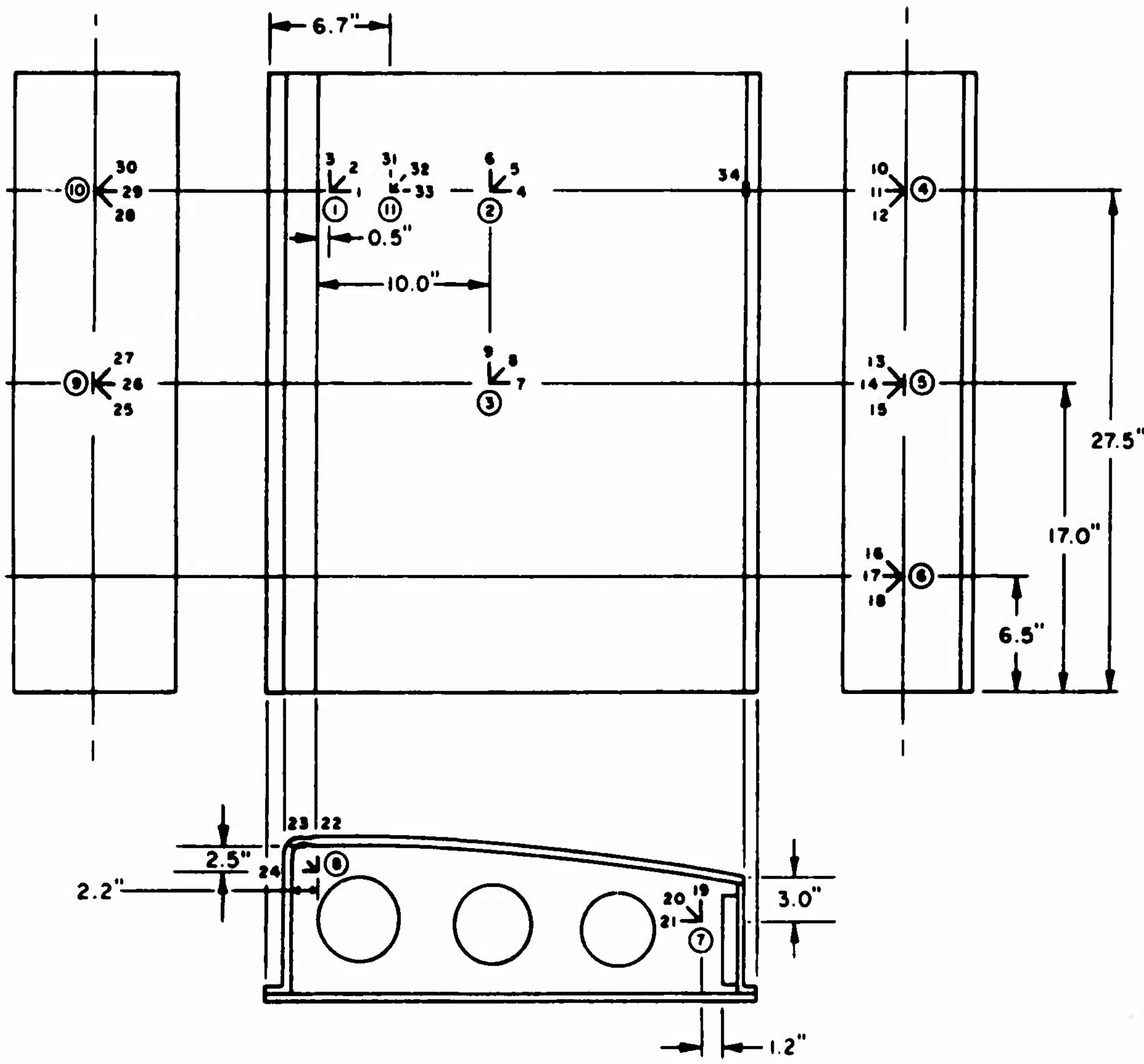

Figure 32. Strain Gage Locations for Rib Support Box No. 2 (Laminate Rib).

flange of the aft spar separated from the solid portion of the lower surface panel upon removal of the bolts. The white areas around the bolts and the separation between the faying surfaces are shown in Figure 33. Also shown in Figure 33 is an apparent delamination of the aft spar web (white area indicated by arrow), which was undetected during the test. An overall view of the failure is shown in Figure 34. From an examination of the failed areas and the deflection data, the bond along the aft spar apparently failed at 66 percent DUL, which is the load at which a loud report was heard; thereafter, the bolts transmitted the shear loads between the surface panel and the aft spar.

Summary of Tests - Rib Support Box No. 2 (Sandwich Rib)

The load was applied for Condition II in 20-percent increments to 100 percent DUL and then decreased. No cracking sounds were heard up to

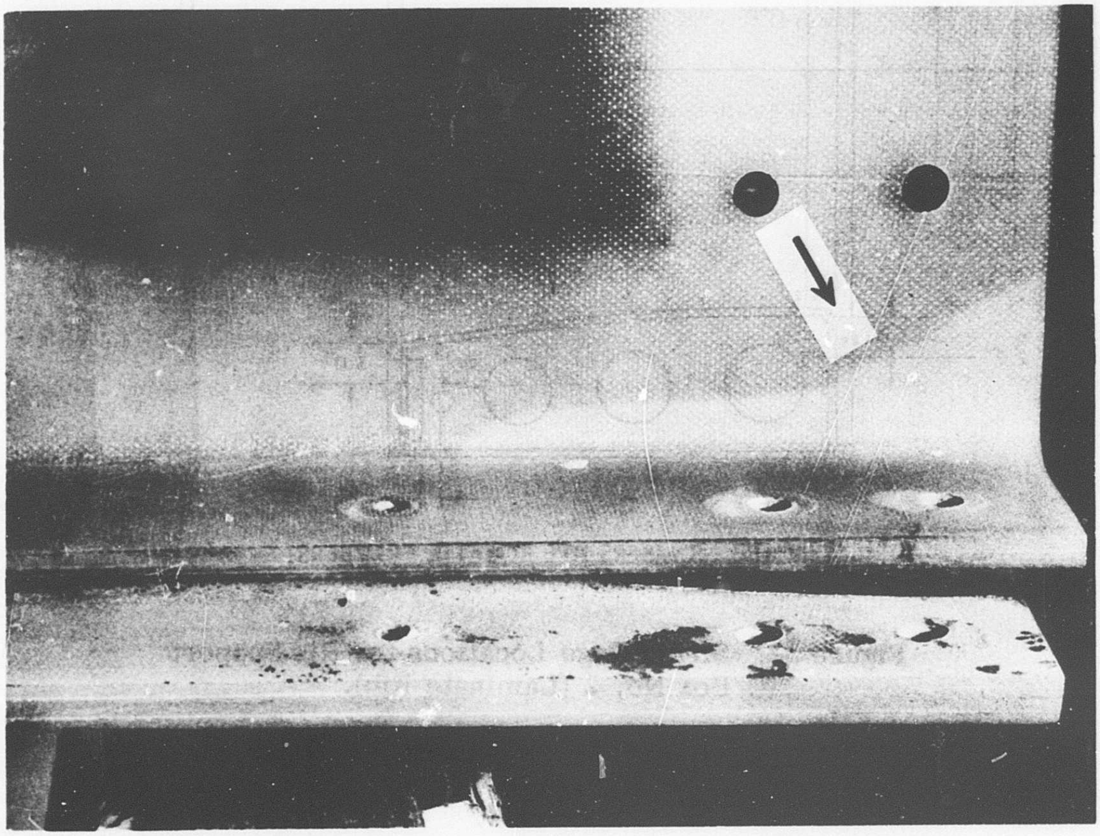

Figure 33. Close-up of Failure of Box No. 1.

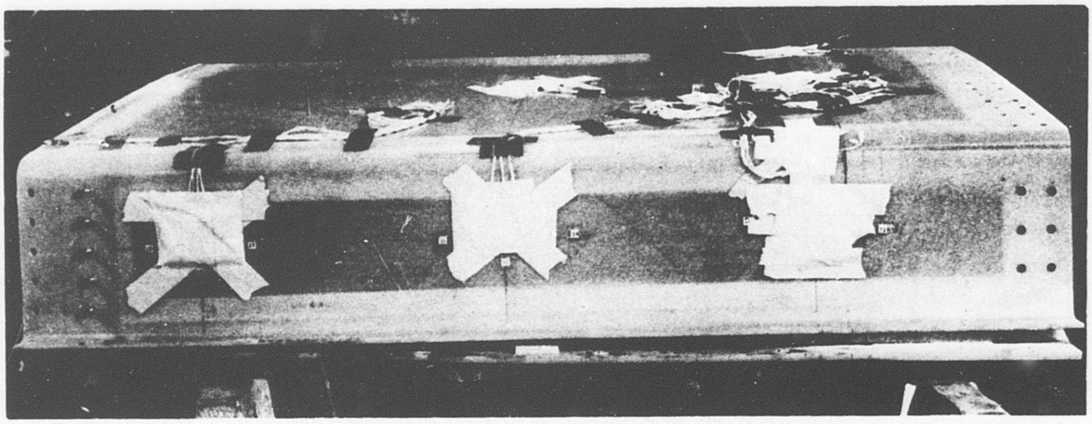

Figure 34. Overall View of Separation Along Aft Spar of Box No. 1.

100 percent DUL. The load was applied for Condition I in 20-percent increments to 100 percent DUL and decreased. Slight cracking sounds were heard above 80 percent DUL. No damage was evident upon inspection. The box was again loaded in 20-percent increments up to 100 percent DUL and then in 10-percent increments above 100 percent DUL. Slight cracking sounds were heard as the load was increased above 110 percent DUL. Failure occurred at 128 percent DUL.

Failure occurred in the bond between the aft spar and the lower surface panel, the same area in which failure occurred in box No. 1. The movement between the aft spar flange and the lower surface panel is shown in Figure 35 by the lines (indicated by arrow), which were initially straight. The photograph shows the box under load just after failure. Failure was not catastrophic since the bolts along the rear spar transferred the shear stresses after failure.

The predicted failing load for box No. 1 was 103 percent DUL, with the minimum margin of safety occurring at the bond between the rib and lower surface panel. The predicted failing load for box No. 2 was 124 percent DUL, with the minimum margin of safety occurring at the bond between the aft spar and lower surface panel. Inspection of the faying surfaces along the aft spar of both boxes indicated that the surfaces were very similar. The areas along both spars were slightly rough, and the adhesive adhered to the faying surfaces randomly as shown in Figure 36, indicating that the surface preparation and adhesion were good.

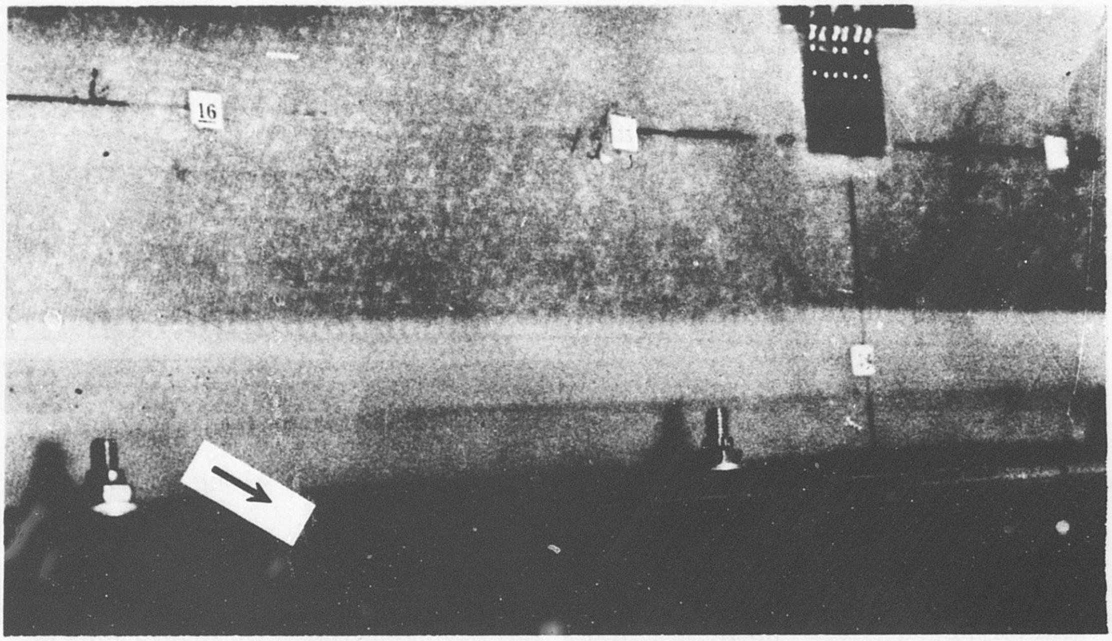

Figure 35. Failure Showing Movement Between Faying Surfaces of Aft Spar Flange and Lower Surface Panel of Box No. 2.

Data Reduction - Rib Support Box No. 1

The configuration and construction details of rib support box No. 1 are discussed in a previous section. The stress analysis and test procedures are also detailed earlier in the report. The strain rosette and deflection gage locations for box No. 1 are shown in Figure 31.

Aft and vertical loads were applied at a point 1.55 inches inboard of the free end of the specimen and 26.05 inches aft of the most forward edge of the lower spar cap flange. This location was approximately 5.28 inches below the calculated shear center and 4.28 inches below the calculated centroid of the box section. Therefore, at the various rosette and strain gage locations, moments and torque on the box cross section are given by the following expressions:

Rosettes 1, 2, 4, and 9 and Gage 29

$$M_x = 25.95\ V_y \qquad M_{xy} = 15.4\ V_y + 5.28\ V_x$$

$$M_y = 25.95\ V_x$$

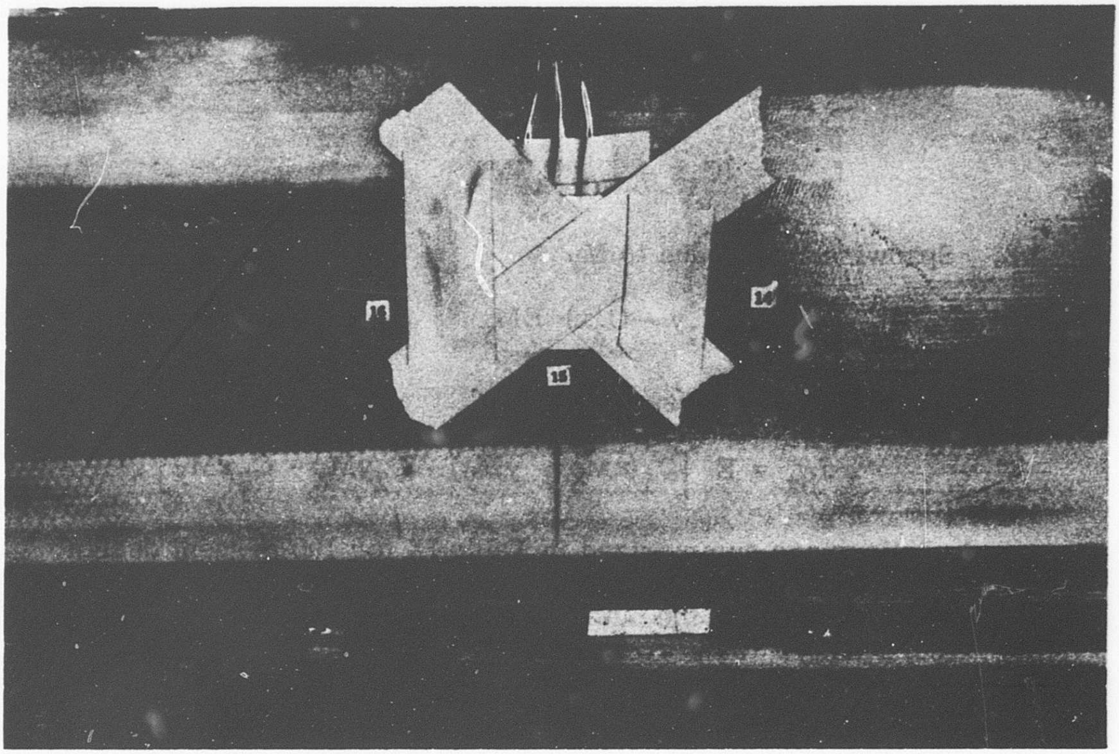

Figure 36. Close-up of Failure Along Aft Spar of Box No. 1.

<u>Rosettes 3 and 5</u>

$$M_x = 15.45\ V_y \qquad M_{xy} = 15.4\ V_y + 5.28\ V_x$$

$$M_y = 15.45\ V_x$$

<u>Rosette 6</u>

$$M_x = 4.95\ V_y \qquad M_{xy} = 15.4\ V_y + 5.28\ V_x$$

$$M_y = 4.95\ V_x$$

where a positive M_x causes compression in the top skin.

The spanwise stresses at the various strain gage locations are as follows:

1. Spanwise Stress due to M_x

$$f_{bx1} = (C_1x - C_2y)\ EM_x$$

2. Spanwise Stress due to M_y

$$f_{bx2} = (C_1y - C_3x)\ EM_y$$

3. Total Spanwise Stress

$$f_{bx} = E\ \left[C_1(xM_x + yM_y) - C_2yM_x - C_3xM_y\right]$$

These calculations are summarized in Table IX for 100 percent design ultimate load under Condition I loading. It should be noted that a single gage (No. 29) is located on the outer surface of the aft upper spar cap. Sample calculations at 100 percent DUL for Condition I at this gage are given below:

$x = 12.131$ in. $y = 3.419$ in. $E = 3.85 \times 10^6$ psi

$Ex = 46.704 \times 10^6$ lb/in. $Ey = 13.163 \times 10^6$ lb/in.

$a = 25.95$ in. $M_x = -223,948$ in.-lb $M_y = 25,950$ in.-lb

Using these values, we can find the bending stress as follows:

$$f_b = (C_1Ex - C_2Ey)\ M_x + (C_1Ey - C_3Ex)M_y$$

$$= 7573 - 437 = 7136 \text{ psi} \tag{48}$$

where C_1, C_2, C_3 are given in Table IX.

Spar stresses as determined by this gage during the Condition I tests are shown in Figure 37.

The equations necessary for converting the strain rosette readings to stresses must consider the non-isotropic characteristics of the material at the different rosette locations. GAC has developed a computer program that performs the data reduction. Values of the elastic properties used in the program are given on page 49. Table X summarizes results

TABLE IX. CALCULATION OF THEORETICAL SPANWISE BENDING STRESSES AT THE VARIOUS ROSETTE LOCATIONS

Rosette No.	x (in.)	y (in.)	E (psi x 10^6)	Ex (lb/in. x 10^6)	Ey (lb/in. x 10^6)	a (in.)	M_x (in.-lb x 10^4)	f_{bx1} (psi)	M_y (in.-lb x 10^4)	f_{bx2} (psi)	Total f_{bx} (psi)
1	-8.40	+5.07	4.1938	-35.23	21.26	25.95	-22.3948	11,808	2.595	315.8	12,124
2	+1.10	+4.42	4.1823	4.6	18.5	25.95	-22.3948	10,410	2.595	-50.7	10,359
3	+1.10	+4.42	4.1823	4.6	18.5	15.45	-13.3333	6,198	1.545	-30.2	6,168
4	+12.65	+0.29	3.9976	50.57	1.16	25.95	-22.3948	845	2.595	-467.4	378
5	+12.65	+0.29	3.9976	50.57	1.16	15.45	-13.3333	503	1.545	-278.3	225
6	+12.65	+0.29	3.9976	50.57	1.16	4.95	-3.8835	147	0.495	-89.2	58
9*	-6.02	-3.63	4.1823	-25.2	-15.2	25.95	-22.3948	-8,634	2.595	239.4	-8,395

V_y = -8630 lb　　V_x = 1000 lb　　a = distance from loading plane to station of rosette location

M_x = -8630a　　M_y = 1000a

$C_2 = 25.085 \times 10^{-10}$　　$C_3 = 3.558 \times 10^{-10}$

$C_1 = -0.171 \times 10^{-10}$

$f_{bx} = (C_1 Ex - C_2 Ey) M_x$　　$f_{by} = (C_1 Ey - C_3 Ex) M_y$

*Rosette No. 11 was located at this position on box No. 2.

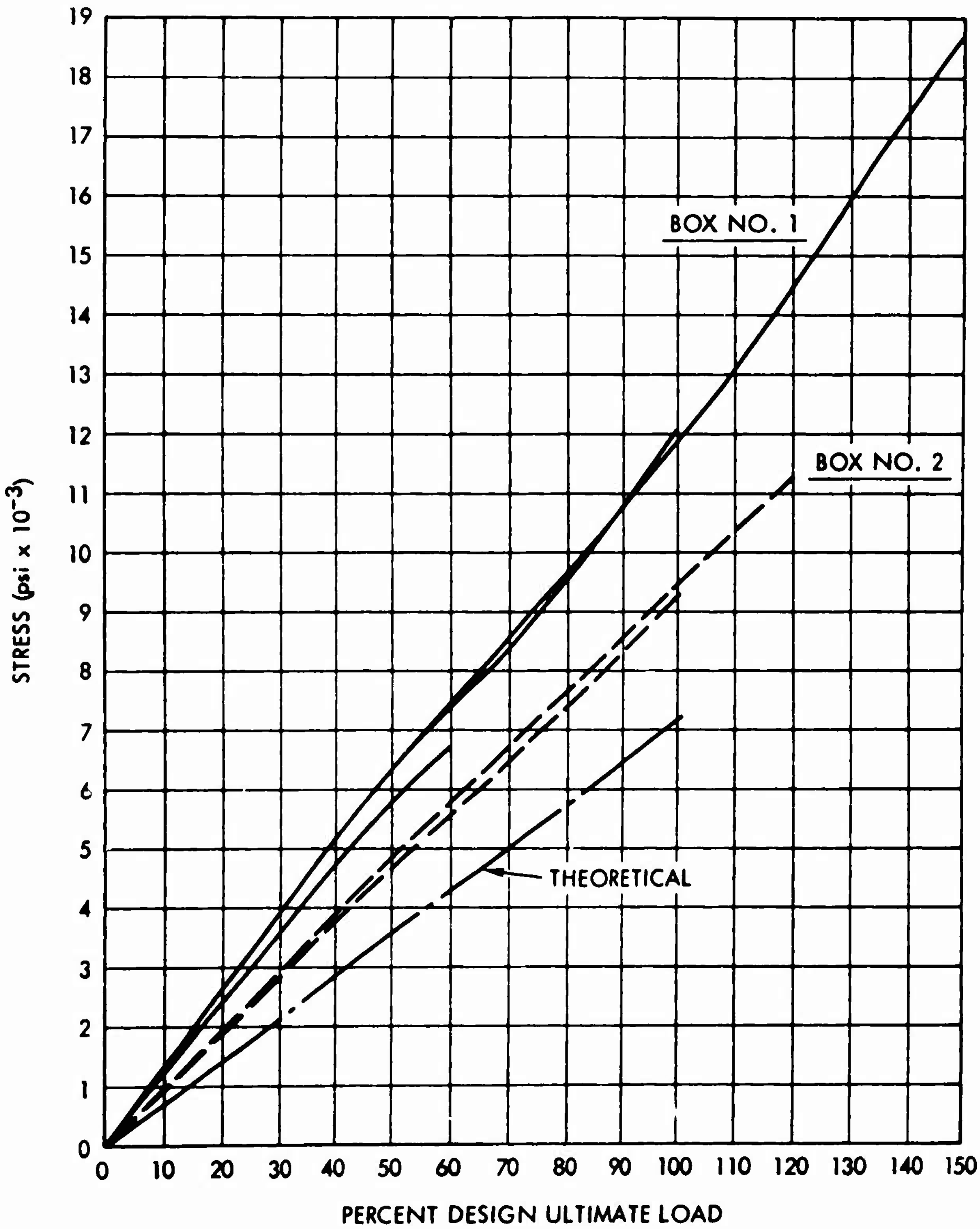

Figure 37. Stresses in Upper Aft Spar Cap of Boxes No. 1 and 2 Under Condition I Loading.

TABLE X. EXPERIMENTAL BENDING AND SHEAR STRESSES IN BOX NO. 1 AT 100 PERCENT DUL FOR CONDITION I LOADING

Rosette No.	100% DUL During 100% DUL Test					100% DUL During Failing Load Test				
	ϵ_n (μin./in.)	ϵ_{n+1} (μin./in.)	ϵ_{n+2} (μin./in.)	f (psi)	f_s (psi)	ϵ_n (μin./in.)	ϵ_{n+1} (μin./in.)	ϵ_{n+2} (μin./in.)	f (psi)	f_s (psi)
1	-257	-377	2084	9123	-3049	-236	-341	2114	9280	-3024
2	537	-124	1513	7384	-2714	569	-100	1543	7553	-2731
3	-345	-982	1170	4911	-3294	-333	-990	1178	4959	-3337
4	3226	-569	-2866	3410	5018	3176	-577	-2836	3349	4952
5	3397	-24	-3046	1602	5307	3317	-28	-3026	1354	5225
6	3236	-16	-2856	1702	5018	3206	-48	-2866	1632	5001
7	160	1535	-216	124*	5917	208	1475	-309	113*	5775
8	-693	-60	-778	-3487*	2557	-693	-60	-798	-3519*	2595
9	-1559	-208	40	-6984	1303	-1962	-100	-4	-8847	2086

* These are rib bending stresses parallel to chord direction.

of the calculations for spanwise and shear stresses at 100 percent DUL during both the 100 percent DUL test and the failing load test for Condition I.

The skin spanwise stresses obtained by the data reduction are shown in Figures 38 through 41 for box No. 1 under Condition I loading. Also shown in these graphs are the stresses determined in the stress analysis. It should be noted that rosettes No. 2 and 3, with only a station variation in location, recorded stresses very close to those predicted during the 66 percent DUL test, whereas both rosettes No. 1 and 9, which were closer to the forward edge than No. 2 and 3, recorded stresses lower than predicted during this test. This was also true for Condition II loading, shown in Figure 42.

Testing subsequent to the 66 percent DUL Condition I tests produced lower spanwise stresses at rosettes No. 2 and 3 on the tension skin but did not appear to significantly affect those at rosettes No. 1 and 9, except to indicate a slight increase in values.

Skin shear stresses as determined by data reduction are compared with those obtained by the stress analysis in Tables XI and XII and are shown graphically in Figure 43. Very poor agreement of shear stress was obtained at all skin strain rosettes and particularly at rosette No. 1, where recorded strains were four times those predicted during the 66 percent DUL test and almost nine times greater than predicted during the 100 percent DUL and failing load test.

Aft spar shear stresses are shown in Figure 44 and compared with calculated values for Condition I loading. Calculated spar stresses were much higher than the values obtained from the tests.

During the first loading of box No. 1 with the Condition I loads, a loud report was heard at 66 percent DUL and the load dropped. Since no damage was apparent under load or after removal of the load, the loading was repeated up to 100 percent DUL with no recurrence of audible sounds. Although the reason for the loud report at 66 percent DUL during the first Condition I loading is not known, the strain rosettes indicate that some structural change resulted. For example, in this first Condition I test, the 45-degree gage in rosette No. 1 (gage No. 2) recorded tensile strains during loading and compressive strains during unloading. This gage then recorded compressive strains during subsequent loadings. Rosette No. 2 also behaved much differently after the first Condition I loading. Strain readings for these two rosettes are given in Table XIII.

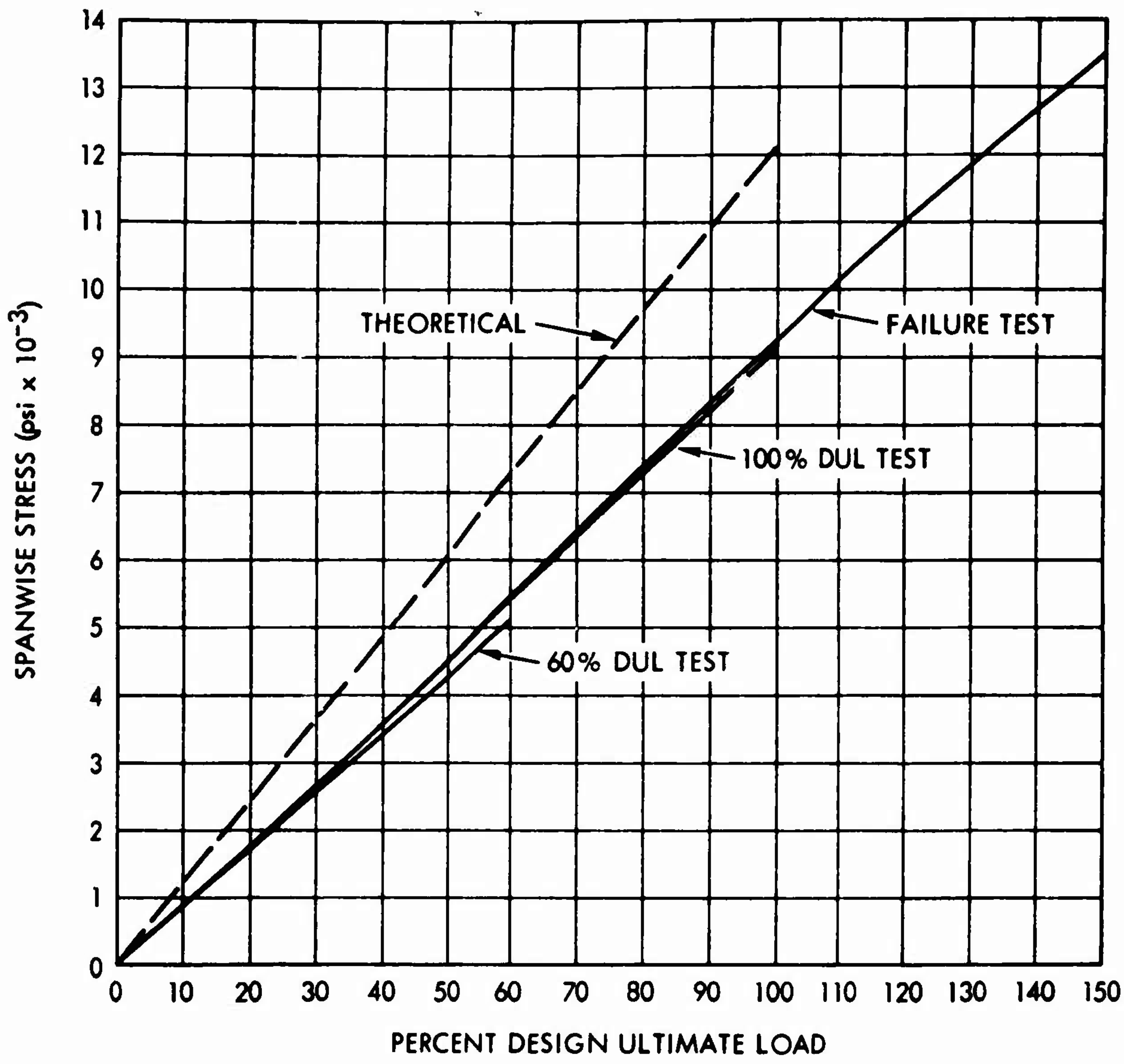

Figure 38. Spanwise Stresses at Rosette No. 1 in Box No. 1 Under Condition I Loading.

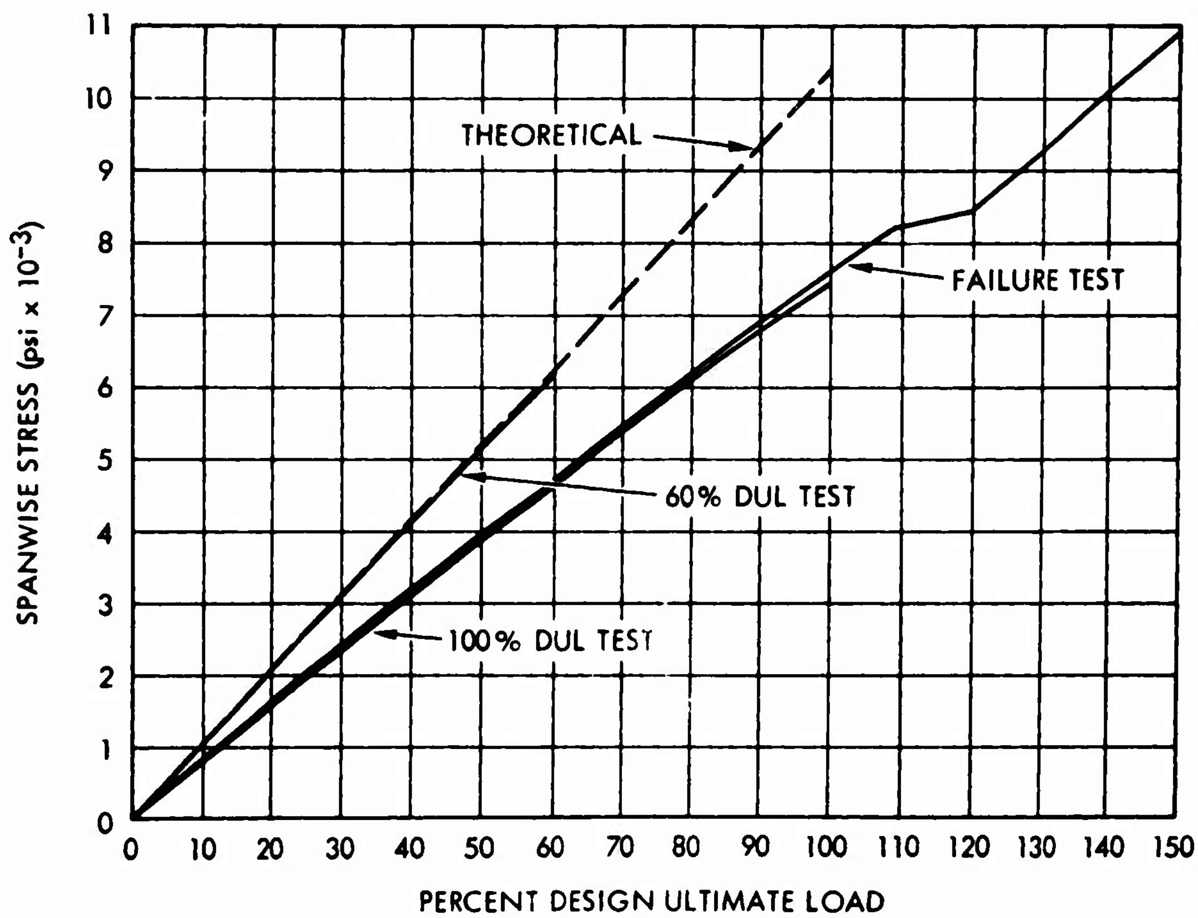

Figure 39. Spanwise Stresses at Rosette No. 2 in Box No. 1 Under Condition I Loading.

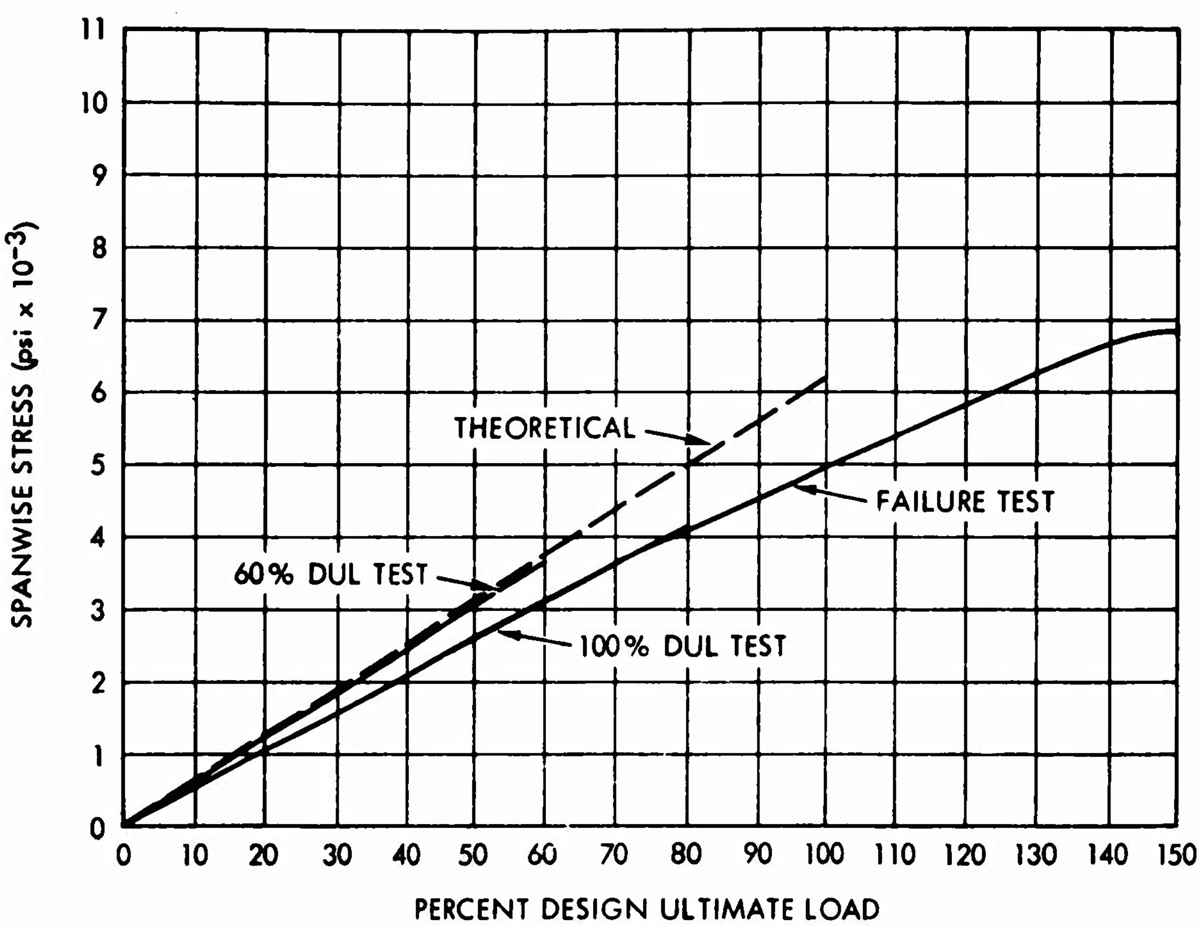

Figure 40. Spanwise Stresses at Rosette No. 3 in Box No. 1 Under Condition I Loading.

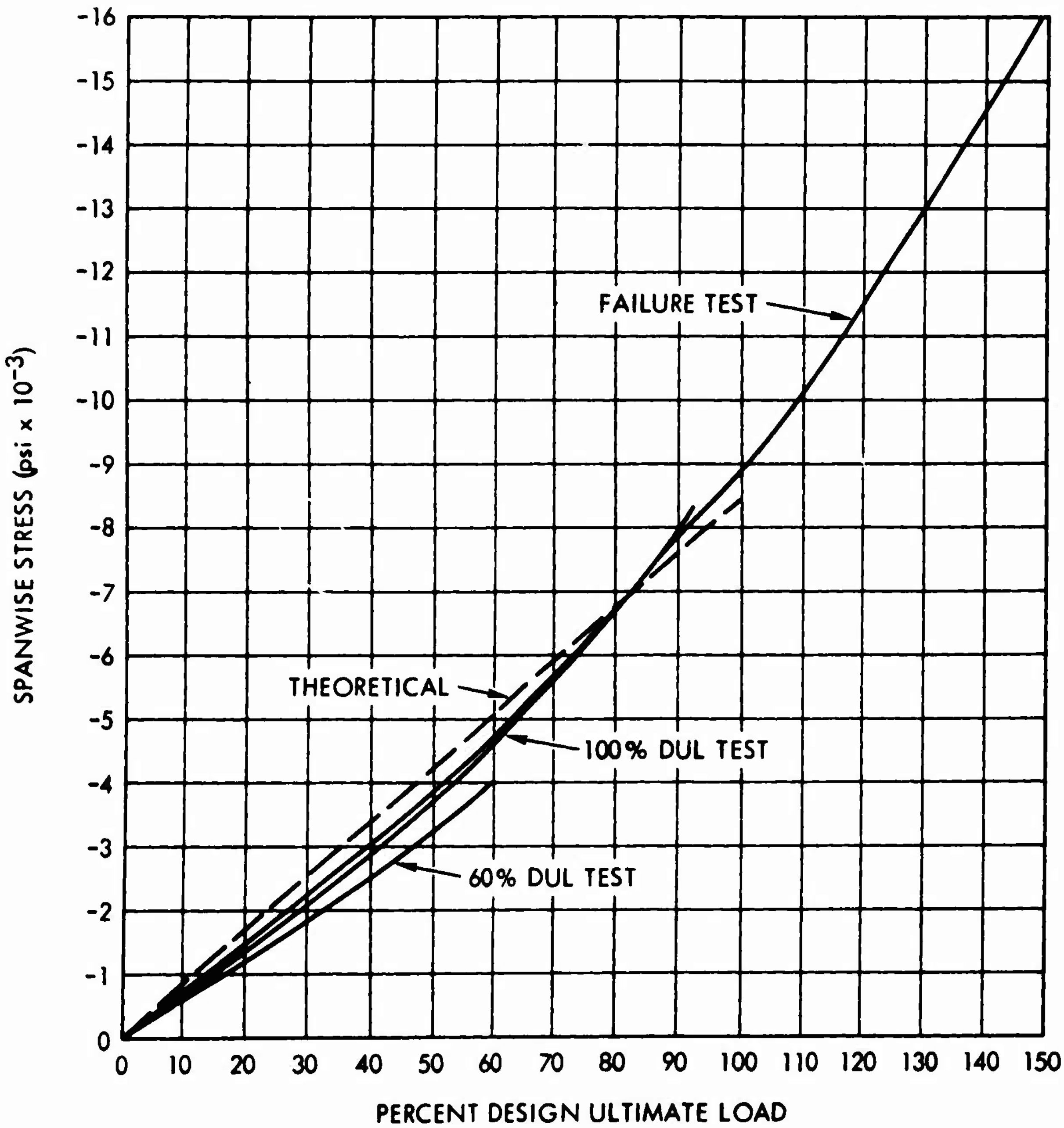

Figure 41. Spanwise Stresses at Rosette No. 9 in Box No. 1 Under Condition I Loading.

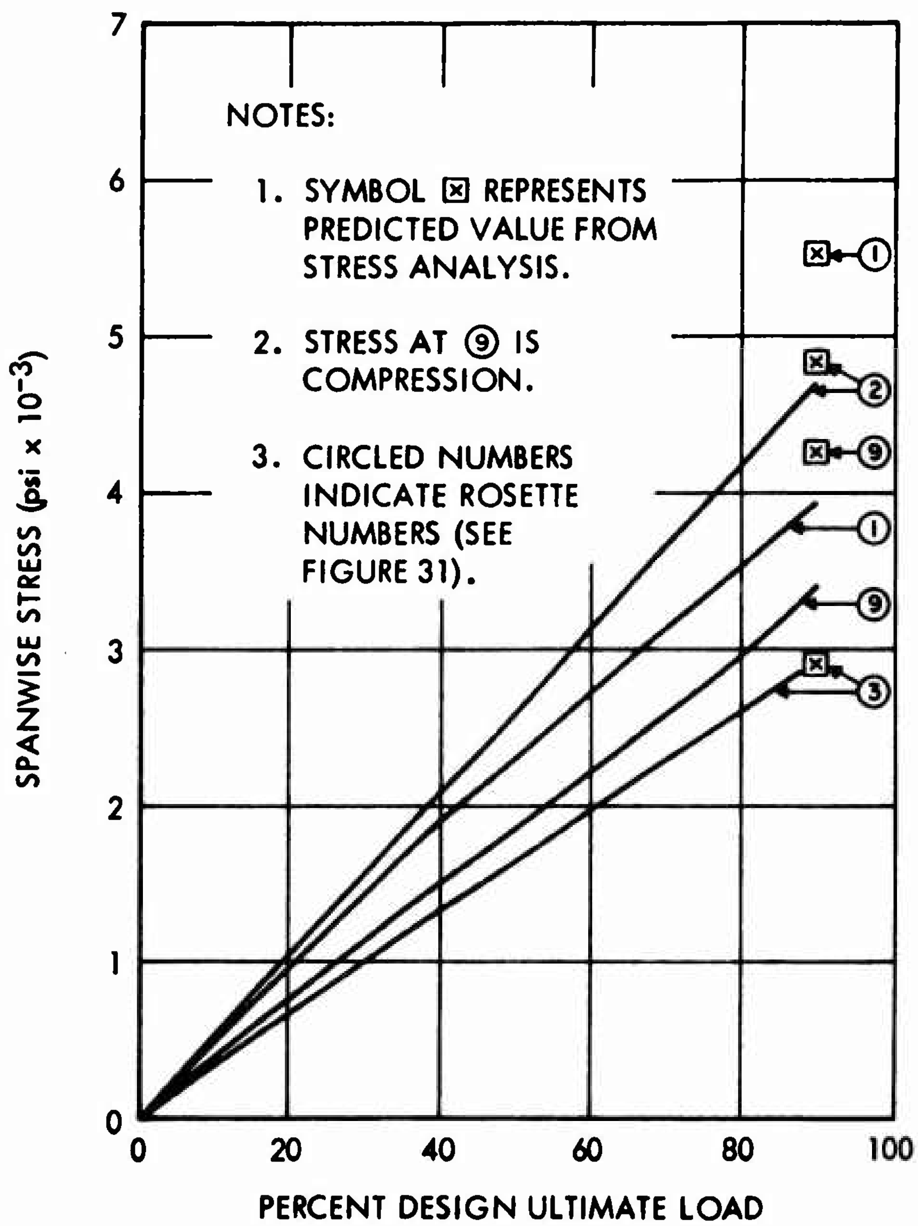

Figure 42. Spanwise Stresses in Skins of Box No. 1 Under Condition II Loading.

TABLE XI. COMPARISON OF EXPERIMENTAL AND THEORETICAL SHEAR STRESSES IN SKINS OF BOX NO. 1 AT ROSETTES NO. 1 AND 9 UNDER CONDITION I LOADING

Applied Load in Percent DUL	Rosette No. 1 (Tension Skin)				Rosette No. 9* (Compression Skin)			
	Stress Analysis (psi)	Experimental Stress (psi)			Stress Analysis (psi)	Experimental Stress (psi)		
		60% DUL Test	100% DUL Test	Failure Load Test		60% DUL Test	100% DUL Test	Failure Load Test
10	34	146	300	291	184	302	255	293
20	67	301	600	622	368	549	459	535
30	100	448	906	913	552	852	715	828
40	134	576	1181	1226	736	1145	998	1093
50	168	673	1465	1493	920	1386	1288	1377
60	201	813	1741	1795	1104	1533	1476	1547
70	234	-	1969	2108	1288	-	1585	1647
80	268	-	2326	2385	1472	-	1695	1804
90	302	-	2627	2729	1656	-	1785	1981
100	335	-	3049	3024	1840	-	1303	2086
110	368	-	-	3350	2024	-	-	2119
120	402	-	-	3763	2208	-	-	2097
130	436	-	-	4120	2392	-	-	2077
140	469	-	-	4528	2576	-	-	2020
150	502	-	-	4927	2760	-	--	1924

*This rosette number becomes 11 for box No. 2.

TABLE XII. COMPARISON OF EXPERIMENTAL AND THEORETICAL SHEAR STRESSES IN TOP SKIN OF BOX NO. 1 AT ROSETTES NO. 2 AND 3 UNDER CONDITION I LOADING

Applied Load in Percent DUL	Shear Analysis (psi)	Shear Stress (in psi) From Data Reduction					
		60% DUL Test Rosette No.		100% DUL Test Rosette No.		Failure Test Rosette No.	
		2	3	2	3	2	3
10	472	241	293	260	321	265	340
20	944	500	597	523	619	542	633
30	1415	741	889	783	944	807	977
40	1887	990	1204	1038	1260	1068	1298
50	2359	1278	1520	1315	1596	1308	1624
60	2830	1508	1846	1577	1922	1615	1979
70	3303	-	-	1846	2254	1885	2301
80	3774	-	-	2119	2628	2162	2647
90	4246	-	-	2384	2945	2464	3011
100	4718	-	-	2714	3294	2731	3337
110	5190	-	-	-	-	2996	3659
120	5662	-	-	-	-	3298	4037
130	6133	-	-	-	-	3573	4380
140	6705	-	-	-	-	3880	4720
150	7077	-	-	-	-	4165	4985

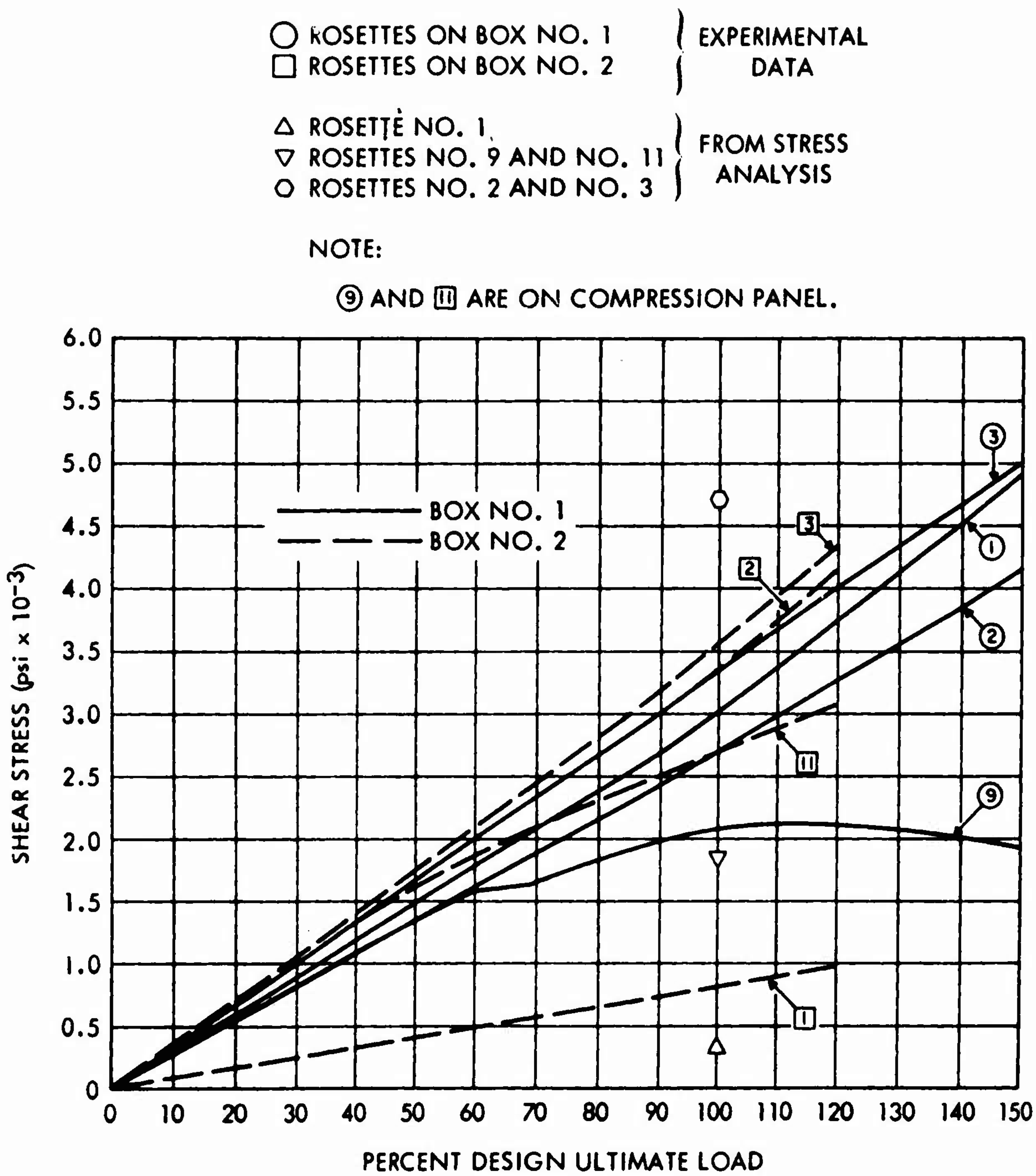

Figure 43. Comparison of Skin Shear Stresses in Boxes No. 1 and 2 During Failure Tests Under Condition I Loading.

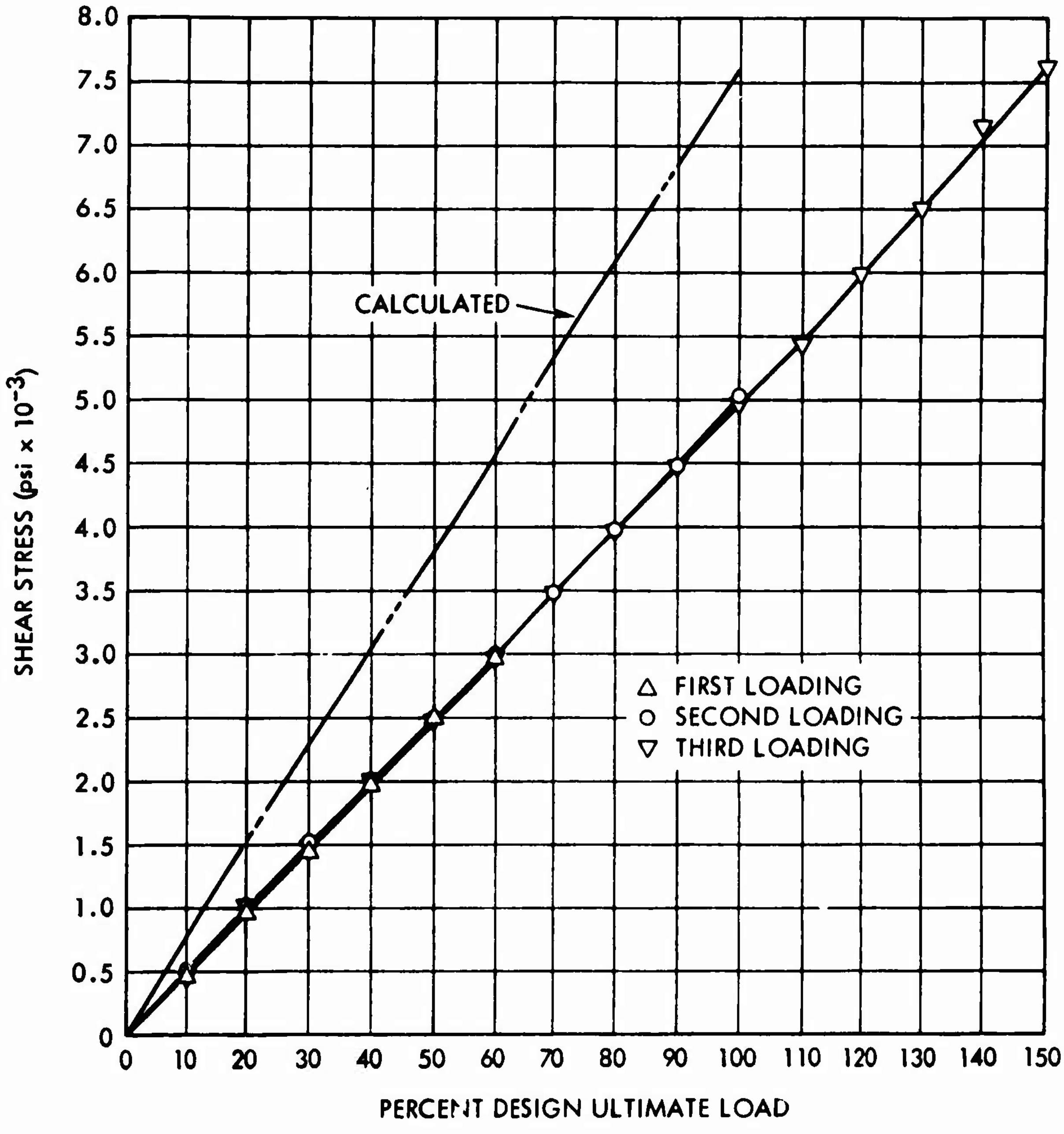

Figure 44. Shear Stresses in Aft Spar of Box No. 1 Under Condition I Loading.

TABLE XIII. COMPARISON OF RECORDED STRAINS AT ROSETTES NO. 1 AND 2 IN BOX NO. 1 DURING FIRST AND SECOND APPLICATION OF CONDITION I TEST LOADS

Applied Load in Percent DUL	Strain at Rosette No. 1 (μin./in.)												Strain at Rosette No. 2 (μin./in.)											
	ϵ_1				ϵ_2				ϵ_3				ϵ_6				ϵ_5				ϵ_4			
	A		B		A		B		A		B		A		B		A		B		A		B	
	L	U	L	U	L	U	L	U	L	U	L	U	L	U	L	U	L	U	L	U	L	U	L	U
10	-28	-	-12	-	24	-	-28	-	200	-	210	-	0	-	60	-	8	-	0	-	220	-	160	-
20	-56	-	-32	-60	40	-	-72	-116	391	-	401	401	4	-	132	100	16	-	0	-36	451	-	311	321
30	-84	-76	-44	-	64	-116	-100	-	591	571	611	-	4	200	192	-	24	-16	0	-	671	371	471	-
40	-120	-	-68	-108	92		-128	-184	792	-	812	832	0	-	248	224	32	-	0	-48	902	-	631	631
50	-156	-120	-96	-	128	-172	-152	-	982	982	1032	-	-16	325	313	-	32	-24	-4	-	1162	671	792	-
60	-188	-	-120	-152	148	-	-176	-253	1172	-	1242	1242	-16	-	361	337	40	-	-16	-72	1373	-	942	932
70	-	-	-152	-	-	-	-188	-	-	-	1443	-	-	-	393	-	-	-	-24	-	-	-	1122	-
80	-	-	-192	-208	-	-	-244	-321	-	-	1673	1673	-	-	433	445	-	-	-44	-100	-	-	1273	1222
90	-	-	-220	-	-	-	-265	-	-	-	1874	-	-	-	469	-	-	-	-68	-	-	-	1413	-
100	-	-	-257	-	-	-	-377	-	-	-	2084	-	-	-	537	-	-	-	-124	-	-	-	1513	-

A - Strains recorded during first application of Condition I test loads.

B - Strains recorded during second application of Condition I test loads.

L - Loading applied.

U - Loading removed.

ROSETTE NO. 1

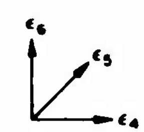

ROSETTE NO. 2

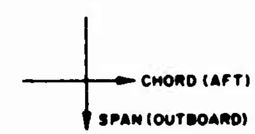

Rosettes No. 7 and 8 were located in the upper aft and forward corners, respectively, of the sandwich rib at the loaded end of the specimen. The shear stresses at these two rosette locations are plotted in Figure 45 along with the shear stress determined by the stress analysis.

Data Reduction - Rib Support Box No. 2

Rib support box No. 2 was identical with box No. 1 except that the closing rib for box No. 2 was a solid laminate. Two additional rosettes were added to this specimen on the forward spar, as shown in Figure 32. Locations for the other rosettes were the same as on box No. 1. Therefore, the calculated stresses given in Table IX also apply to specimen No. 2. A comparison of measured skin spanwise stresses and those from the stress analysis is plotted in Figures 46, 47, and 48. As with box No. 1 during the first loading, rosettes No. 2 and 3 show the best agreement with calculated stresses from the stress analysis.

Skin shear stresses at the three rosette locations are compared with the stress analysis in Tables XIV and XV and Figure 43. Aft spar web shear stresses are compared with those determined from the stress analysis in Figure 49, and the forward spar web shear stresses are plotted in Figure 50. As with box No. 1, poor agreement was obtained for skin and spar web shear stresses.

The rib shear stresses are shown in Figure 51. Agreement with calculations was not as good as with the sandwich rib of box No. 1. Perhaps it should be noted here that rosette No. 7 gave comparable results on both the sandwich and the laminate rib, whereas the readings from rosette No. 8 (near the forward upper corner) were significantly different.

A single gage (No. 34) was located on the outer surface of the upper aft spar cap as shown in Figure 32. Spar stresses determined by this gage are plotted in Figure 37.

Summary of Data Reduction From Strain Gages

In general, very poor agreement between experimental and calculated stresses was obtained, particularly with respect to shear stresses. The rosettes (No. 2 and 3) on the upper skin at approximately 13.5 inches aft of the forward edge agreed best with the predicted values of spanwise stress for both specimens, but shear stresses at these rosettes were in significant disagreement with calculations.

A part of the discrepancy for box No. 1 is apparently due to some unknown occurrence during the first application of Condition I loads, as evidenced

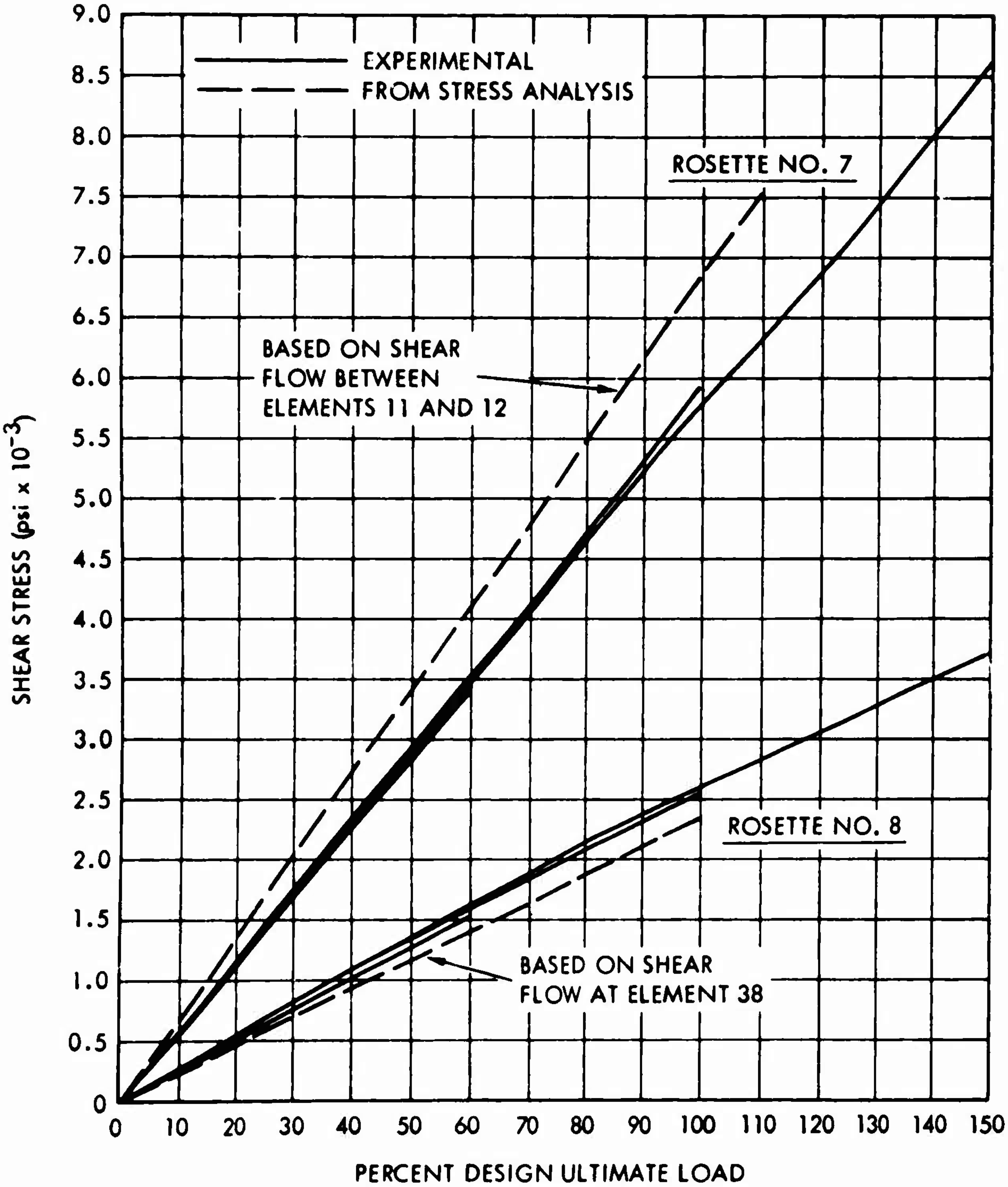

Figure 45. Comparison of Measured and Calculated Shear Stresses in Sandwich Rib of Box No. 1 Under Condition I Loading.

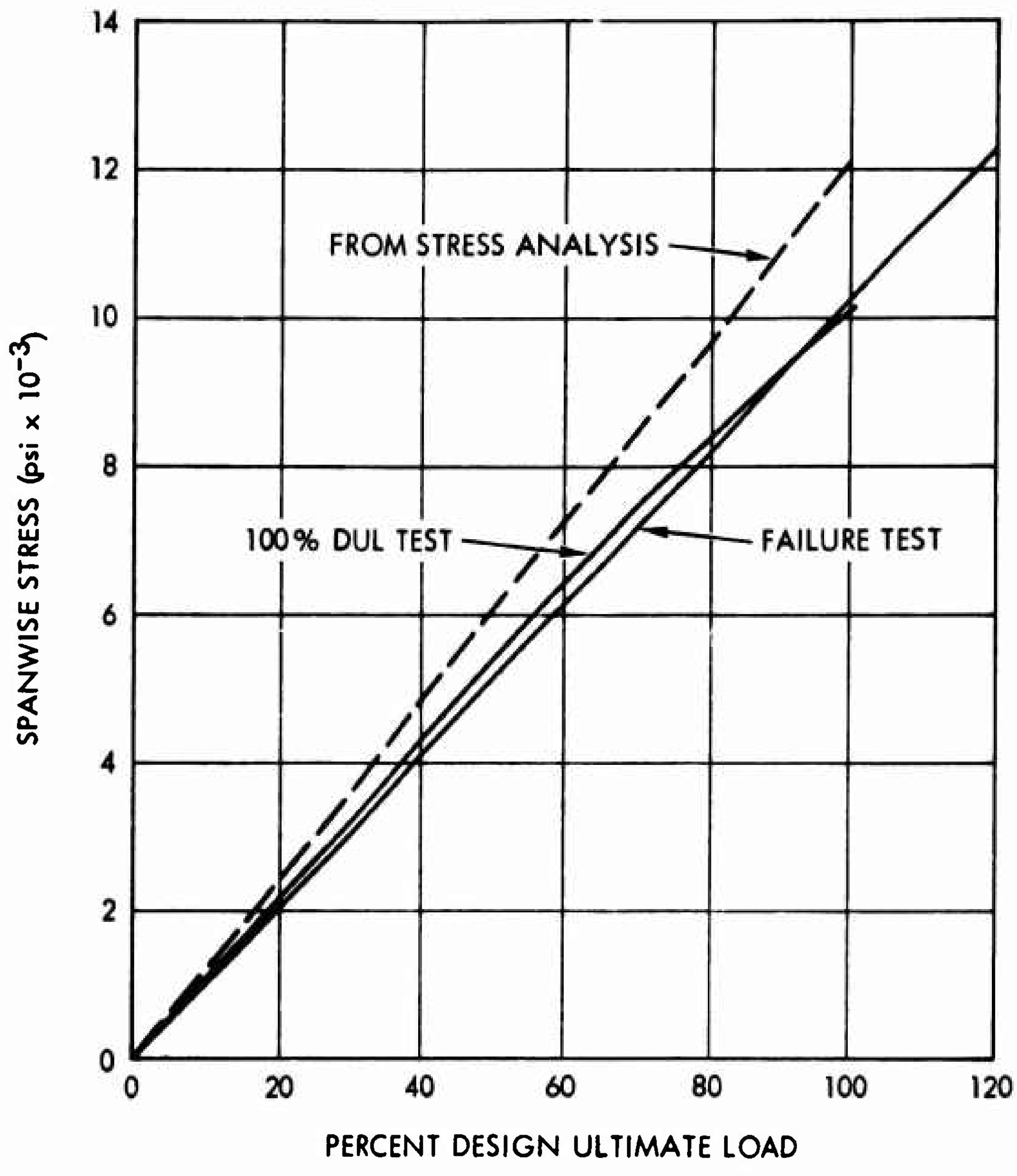

Figure 46. Spanwise Stresses at Rosette No. 1 in Box No. 2 Under Condition I Loading.

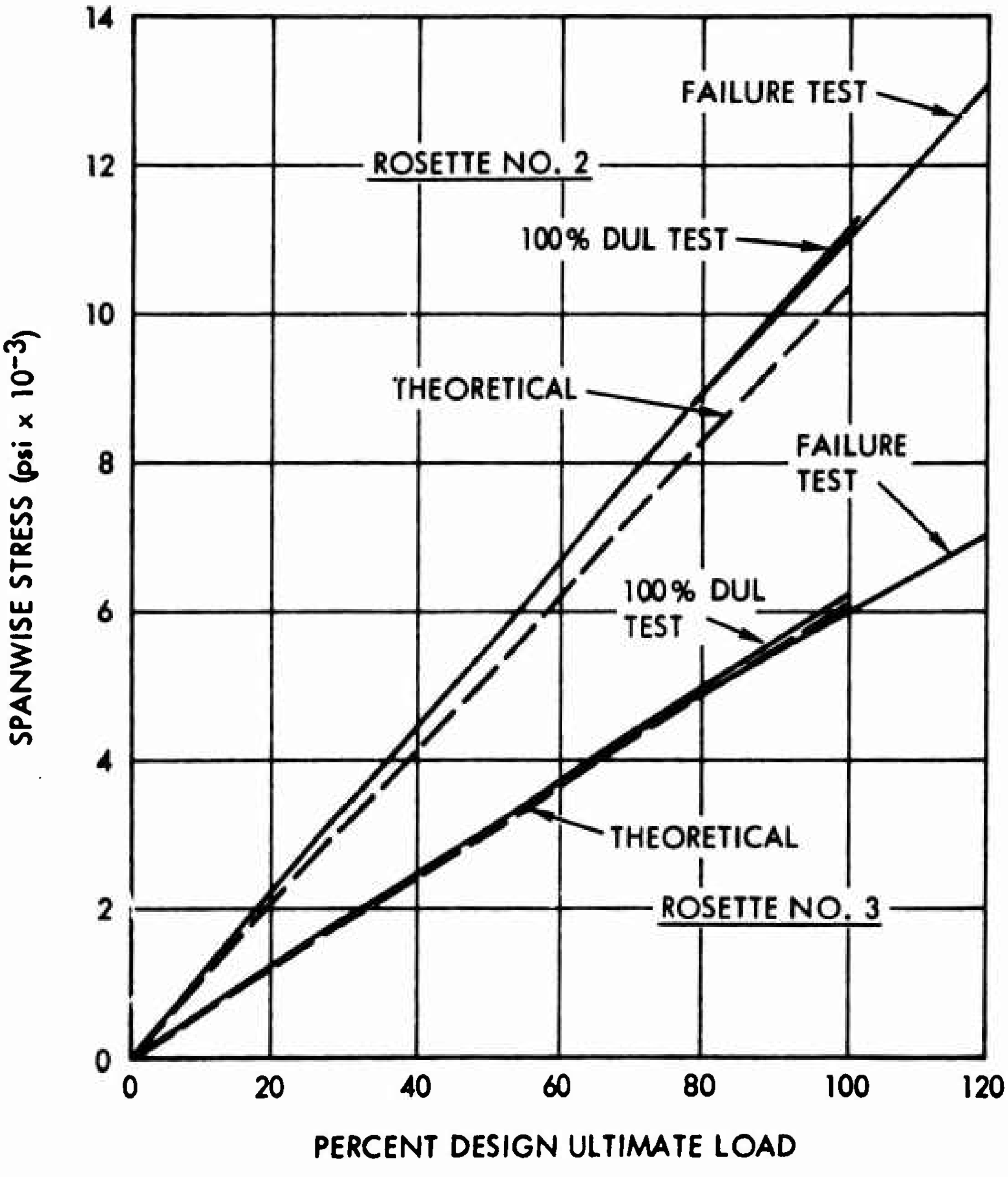

Figure 47. Spanwise Stresses at Rosettes No. 2 and 3 in Box No. 2 Under Condition I Loading.

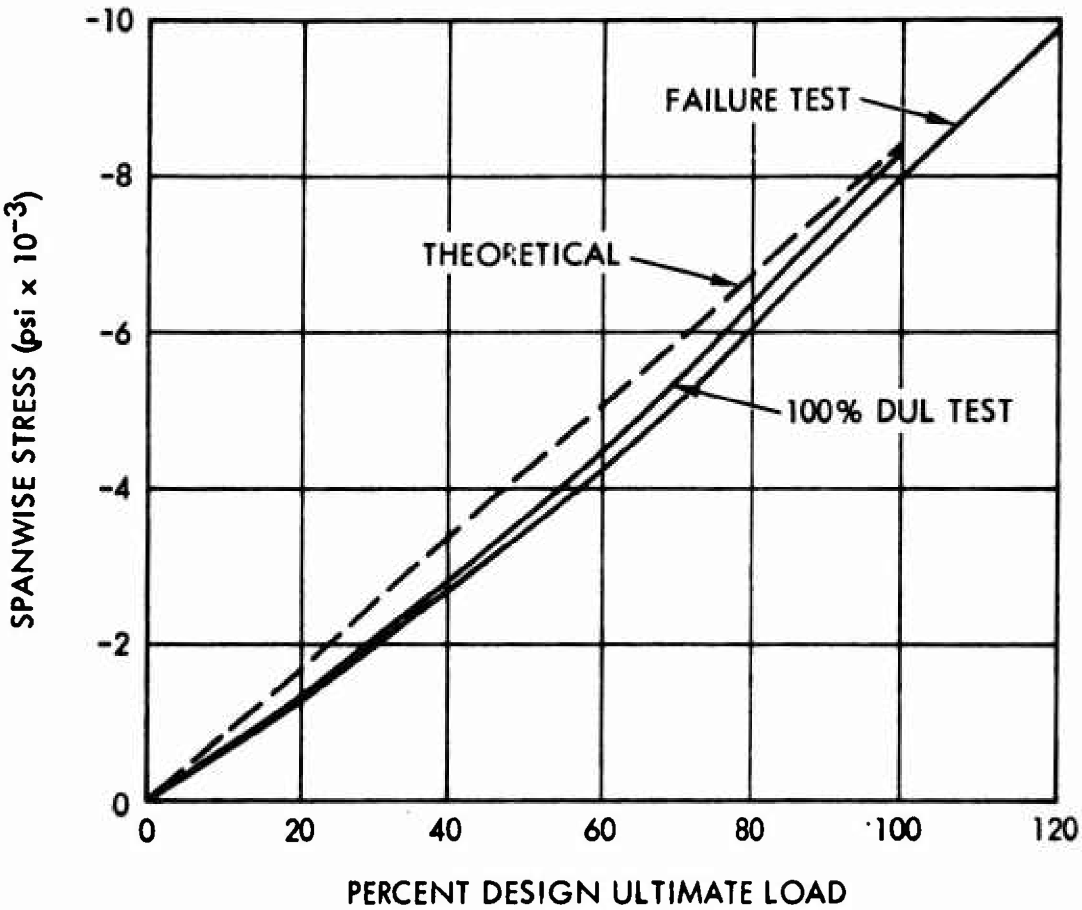

Figure 48. Spanwise Stresses at Rosette No. 11 in Box No. 2 Under Condition I Loading.

TABLE XIV. COMPARISON OF EXPERIMENTAL AND THEORETICAL SHEAR STRESSES IN SKINS OF BOX NO. 2 AT ROSETTES NO. 1 AND 11 UNDER CONDITION I LOADING

Applied Load in Percent DUL	Stress (in psi) at Rosette No. 1 (Tension)			Stress (in psi) at Rosette No. 11 (Compression)		
	Stress Analysis	100% DUL Test	Failure Test	Stress Analysis	100% DUL Test	Failure Test
10	34	85	78	184	317	305
20	67	184	131	368	625	677
40	134	351	286	736	1258	1286
60	201	452	461	1104	1784	1814
80	268	617	634	1472	2248	2293
100	335	871	815	1840	2636	2697
110	368	-	912	2024	-	2925
120	402	-	986	2208	-	3081

TABLE XV. COMPARISON OF EXPERIMENTAL AND THEORETICAL SHEAR STRESSES IN TOP SKIN OF BOX NO. 2 AT ROSETTES NO. 2 AND 3 UNDER CONDITION I LOADING

Applied Load in Percent DUL	Stress Analysis (psi)	Experimental Stress (psi)			
		100% DUL Test Rosette No.		Failure Test Rosette No.	
		2	3	2	3
10	472	318	361	308	335
20	944	622	684	638	691
40	1887	1257	1409	1256	1364
60	2830	1915	2127	1940	2069
80	3774	2665	2867	2659	2820
100	4718	3311	3600	3388	3548
110	5190	-	-	3749	3957
120	5662	-	-	4147	4342

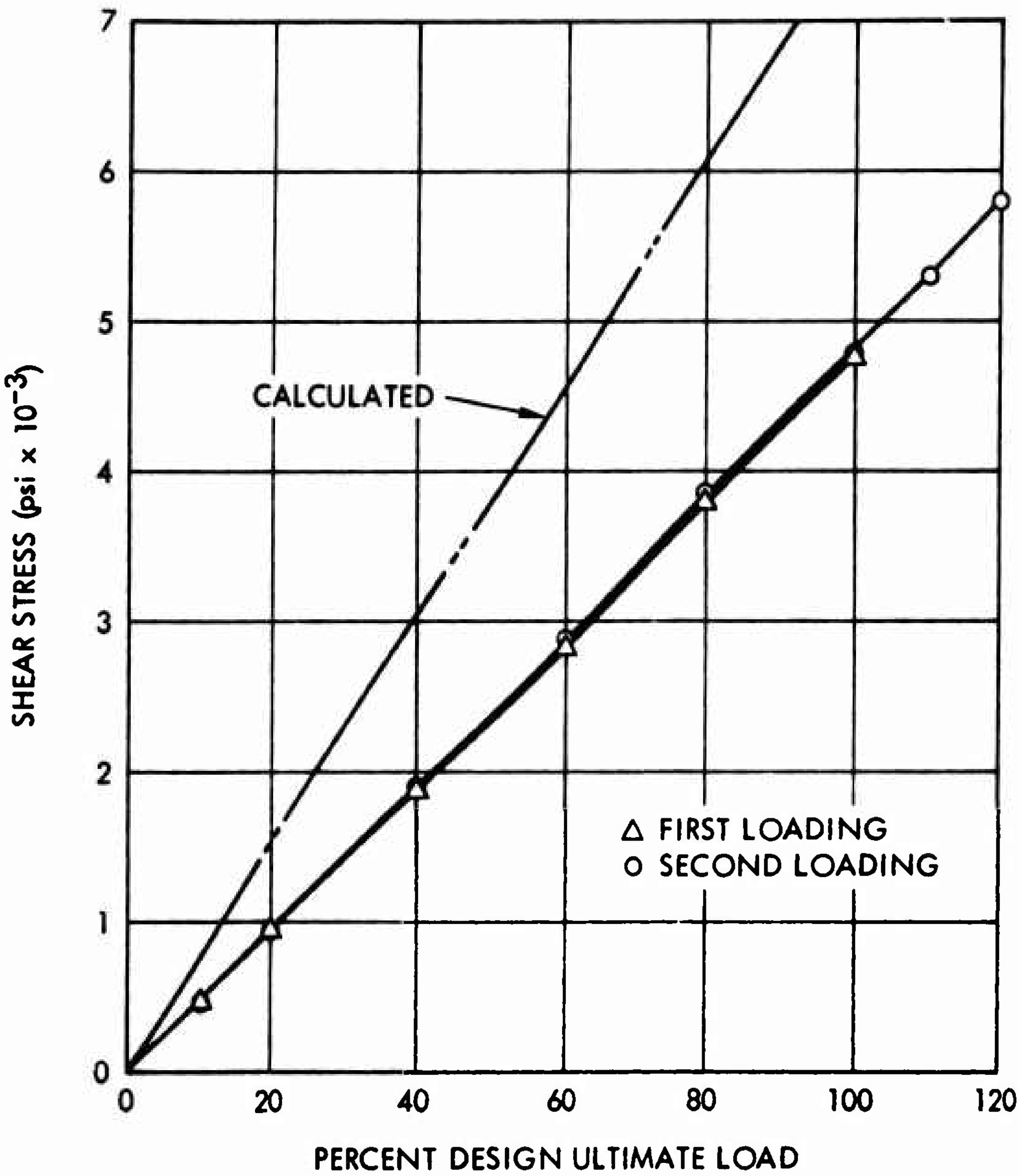

Figure 49. Shear Stresses in Aft Spar of Box No. 2 Under Condition I Loading.

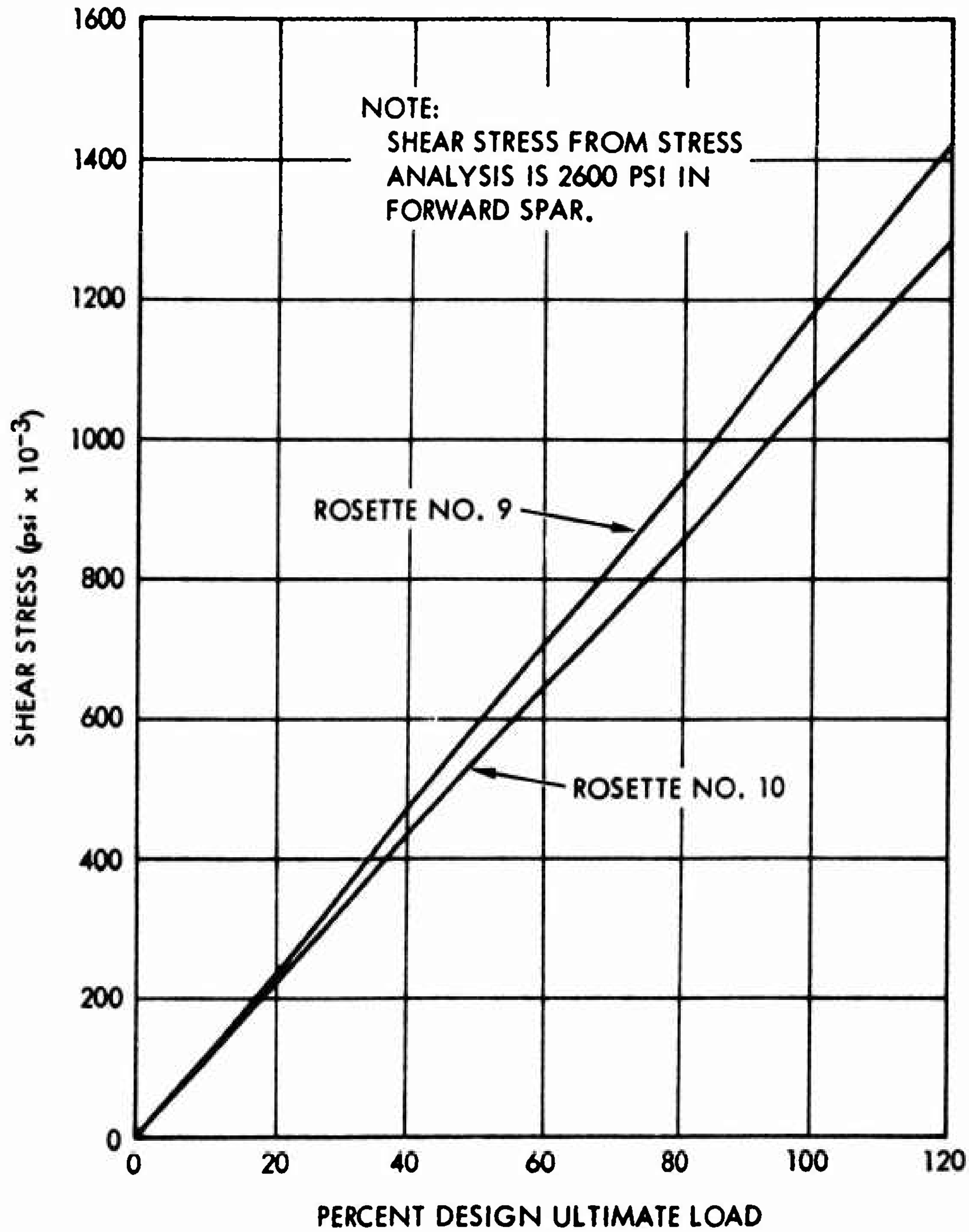

Figure 50. Shear Stresses in Forward Spar of Box No. 2 Under Condition 1 Loading.

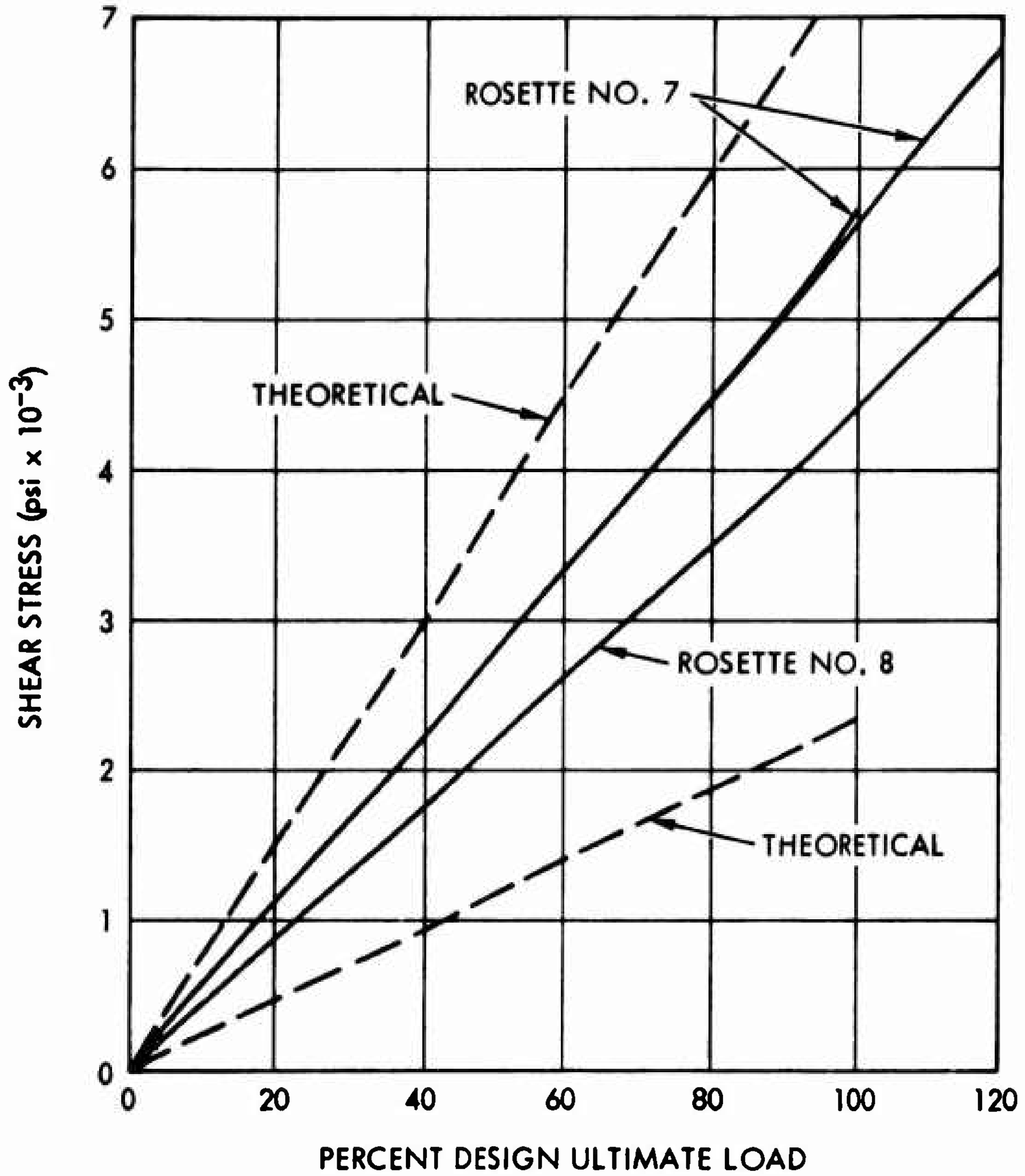

Figure 51. Shear Stresses in Laminate Rib of Box No. 2 Under Condition I Loading.

by the loud report heard at 66 percent DUL. However, it cannot account for the majority of the deviations.

A second possibility is a difference between the values for elastic constants used in the data reduction and actual values of the laminates. However, because of the large disagreement between test and predictions, it seems very unlikely that there can be this much difference between actual values and those used in the data reduction.

A third, and perhaps the most probable, reason for the discrepancy is shear lag effects resulting from the relatively large width-to-length ratio of the specimen and the distribution of structural material.

The behavior of the strain rosette on the lower (compression) skin indicated nonlinear behavior beginning at very low strain levels and was noticeable in both boxes. The two torque boxes behaved differently in the way the chordwise stress increased. This difference, indicated in Figure 52, may have resulted from whatever caused the loud report during the first Condition I loading on box No. 1. The subsequent 100 percent DUL test on this specimen shows a slight increase in spanwise stress, but a well-behaved increasing chordwise stress all the way to 100 percent DUL. However, in the failing load test, deviation of the chordwise stress commenced at about the load level that ended the first Condition I test loading.

Comparison of Deflection Data

A comparison of the measured and calculated deflections and rotations of the two boxes is given in Table XVI for Condition I at 100 percent DUL during the failing load test.

TABLE XVI. COMPARISON OF EXPERIMENTAL AND THEORETICAL DISPLACEMENT

Vertical Deflection, inches	
Calculated	0.37
Experimental	
Box No. 1	1.04
Box No. 2	0.55
Twist Angle, degrees	
Calculated	0.80
Experimental	
Box No. 1	0.47
Box No. 2	0.60

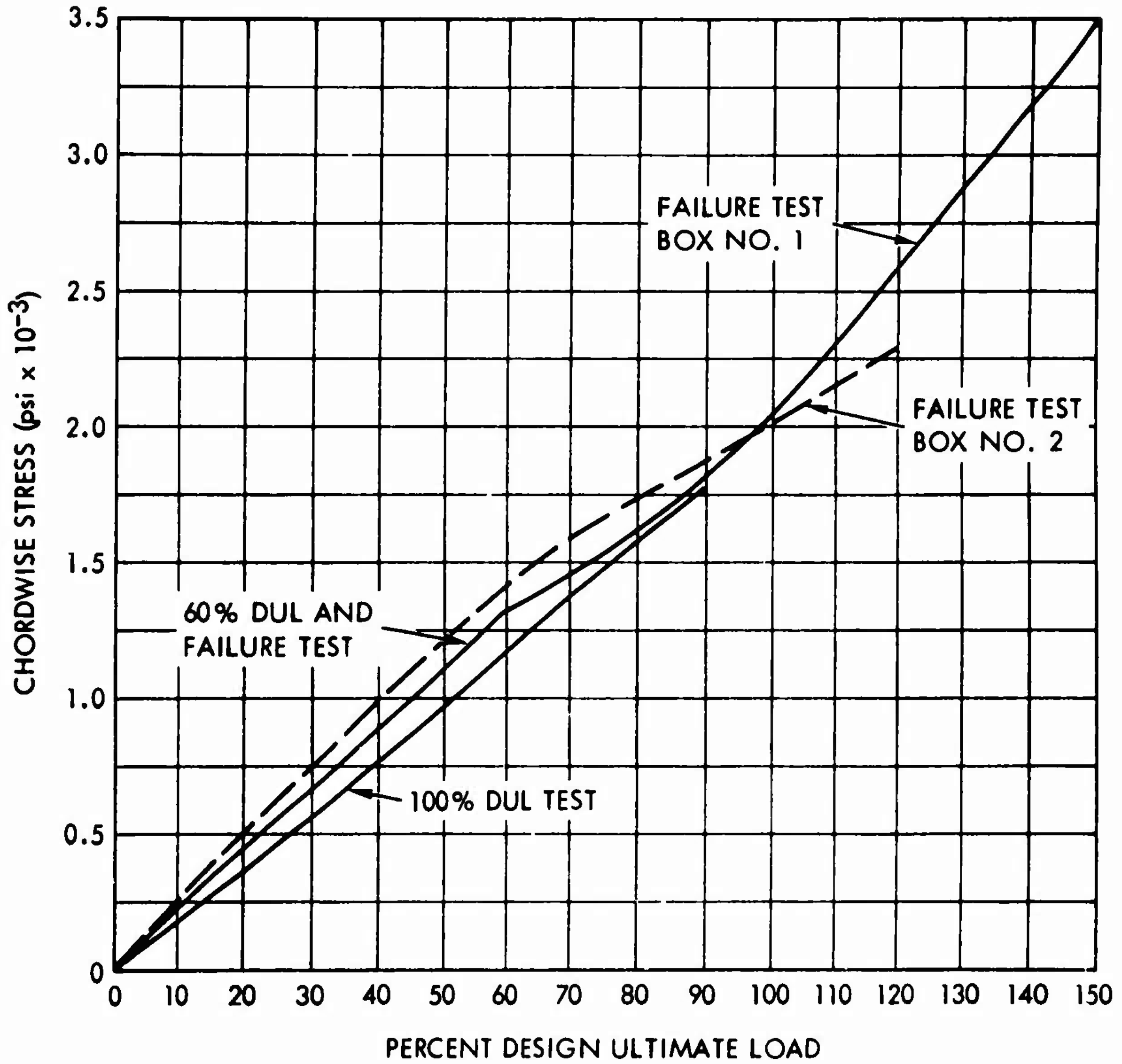

Figure 52. Chordwise Stresses in Lower Skin Under Condition I Loading.

Vertical deflections of the lower spar caps are plotted in Figures 53 and 54. The differences in deflections of the two lower spar caps between the first and third loadings shown in Figure 53 indicate a significant softening of the structure as a result of the unexplained structural change that occurred at the 66 percent DUL level of the first Condition I loading.

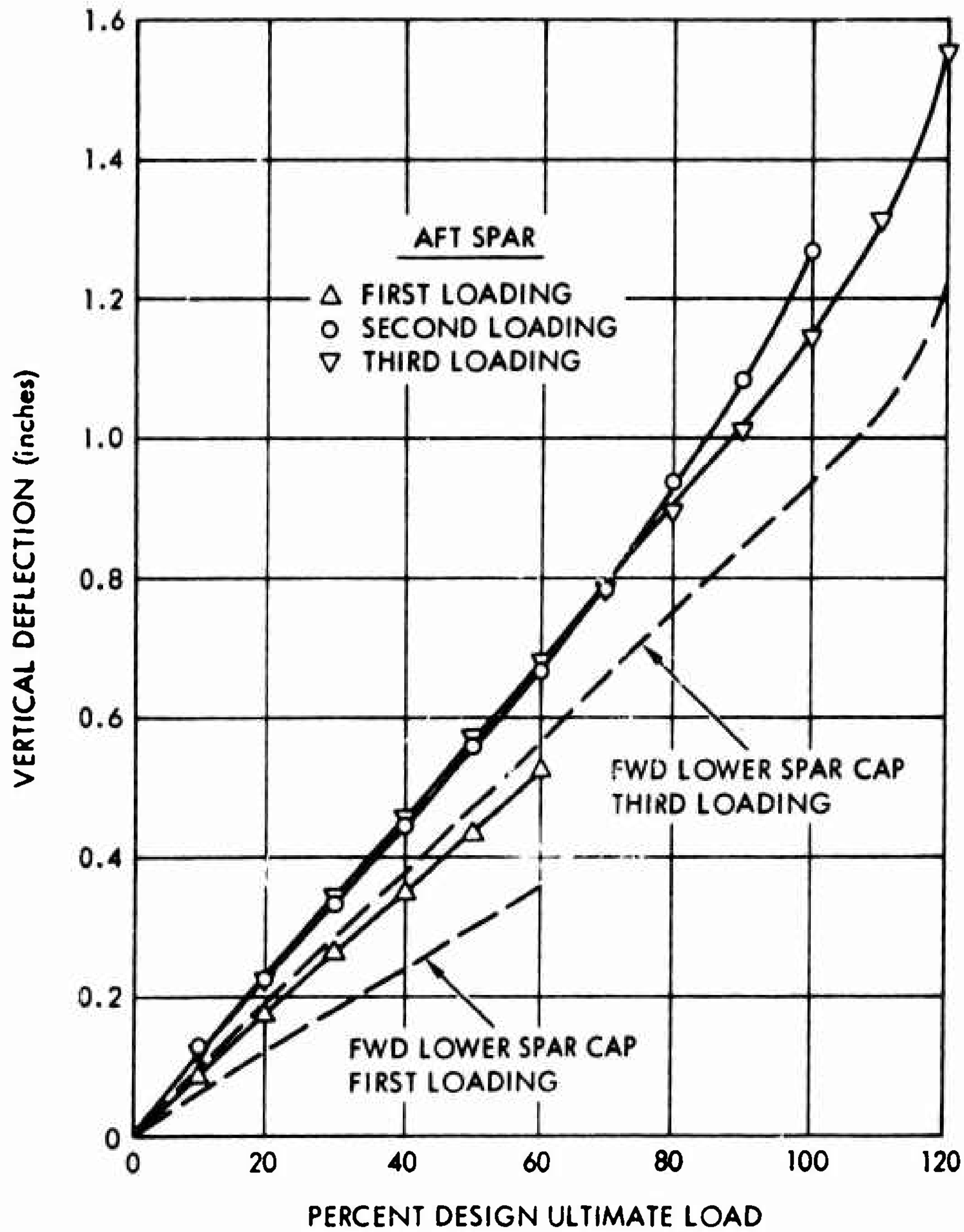

Figure 53. Vertical Deflections of Lower Spar Caps for Box No. 1 Under Condition I Loading.

As with the stresses, the comparison showed poor agreement between calculated and measured displacements. The large deflection of box No. 1 must have been caused by whatever damage was done at 66 percent DUL in the Condition I testing. Although the horizontal deflections were measured, they were too small to permit a realistic comparison with calculations.

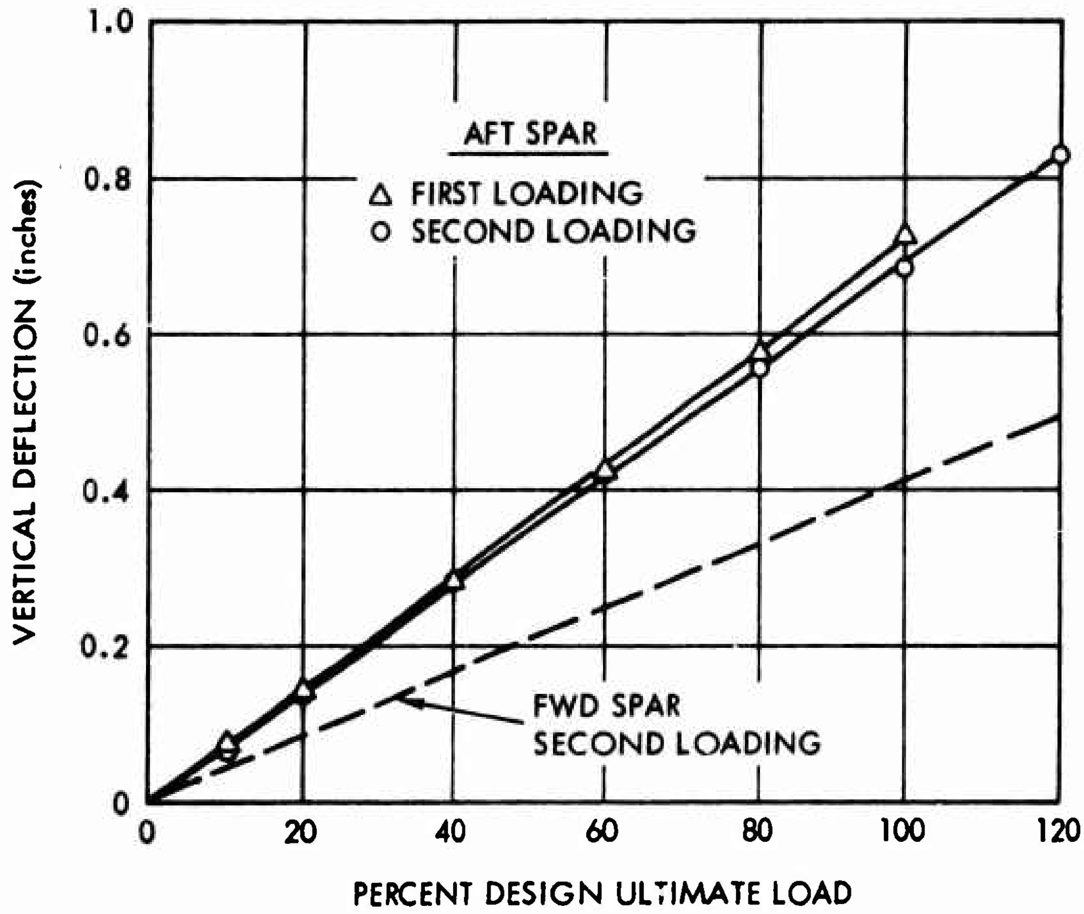

Figure 54. Vertical Deflections of Lower Spar Caps for Box No. 2 Under Condition I Loading.

STRUCTURAL ANALYSIS FOR THE NO. 3 WING

GENERAL

The overall structure for wing No. 3 was similar to the first two structures. It consisted of a two-cell box beam of integral cap sections and sandwich construction. The two-cell box was 48 inches wide and [illegible] inches long. The part was designed to perform under the loading spectrum of a known metal aircraft structure, the T2B outer wing panel. The T2B wing section, which has been under study as a filament-wound wing at North American Rockwell Corporation,[5] is subjected to a root section shear of 13,300 pounds (limit) and a bending moment of 575,000 in.-lb (limit). For the maximum torque condition for the T2B, there is a moment of 400,000 in.-lb (limit). Therefore, the following ultimate design conditions were established for the root section:

Condition I	Condition II
$T = 500,000$ in.-lb	$T = 0$
$M = 600,000$ in.-lb	$M = 862,500$ in.-lb
$V_y = 15,600$ lb	$V_y = 20,200$ lb

Because of the previously established test setup, test loads were again applied as concentrated loads at the wing section tip. Therefore, to achieve the established bending moments for the wing section tests, the following modified test load conditions existed at the design section (wing station 68.00):

Test Condition I	Test Condition II
$T = 500,000$ in.-lb	$T = 0$
$V_y = 8824$ lb	$V_y = 12,684$ lb
$M_x = 600,000$ in.-lb at $x = 68$	$M_x = 862,500$ in.-lb at $x = 68$

A detailed analysis has been made for these loads for comparison with the test results.

REVIEW OF FAILURES - WINGS NO. 1 AND 2

To supplement the analysis of the No. 3 wing, the following recap is made of the performance of wings No. 1 and 2.

Wing test section No. 1 failed at 80 percent DUL; however, buckling was initiated at 40 percent DUL. The buckling allowable stress for this wing was determined using the methods given in U.S. Department of Agriculture Report FPL-070.[3] The calculations are given below.

The skin bending stiffness per inch is calculated as

$$D = \frac{d\sqrt{E_l E_t}\ \ (d + t_c)^2}{2\ (1 - \mu_{lt}\,\mu_{tl})}$$

$$= \frac{0.030\ \sqrt{3.1 \times 3.3} \times 10^6\ (0.530)^2}{2\ (0.94)}$$

$$= 14,580 \tag{49}$$

where $d = 0.030$ in.

$t_c = 0.500$ in.

$E_l = 3.3 \times 10^6$ psi

$E_t = 3.1 \times 10^6$ psi

$\sqrt{\dfrac{E_t}{E_l}} = 0.97$

$\mu_{lt} = 0.25$

$\mu_{tl} = 0.25$

The parameter involving shear stiffness is calculated as

$$U = \frac{G_{cl}\ (d + t_c)^2}{t_c}$$

$$= \frac{25,600\ (0.530)^2}{0.500}$$

$$= 14,400 \tag{50}$$

where $G_{cl} = 25,600$ psi.

The parameter relating shear and bending stiffness is calculated as

$$V' = \frac{\pi^2 D}{b^2 U}$$

$$= \frac{(3.14)^2\ 14,580}{(23)^2\ (14,400)}$$

$$= 0.0189 \tag{51}$$

The aspect ratio is given as

$$\frac{b}{a} = \frac{23}{84} = 0.274 \tag{52}$$

Then from Figure 11 of FPL-070,[3] K = 3.2 for a sandwich panel with orthotropic facings and simply supported edges. Therefore, the allowable buckling load of the wing is

$$N_{cr} = K \frac{\pi^2}{b^2} D$$

$$= 3.2\ \frac{(3.14)^2}{(23)^2}\ (14,580)$$

$$= 870 \text{ lb/in.} \tag{53}$$

and the buckling stress of the wing is

$$\sigma = \frac{870}{0.060} = 14,500 \text{ psi} \tag{54}$$

The calculated maximum compressive stress in the aft cell at 100 percent DUL was 37,600 psi (from Table II of USAAVLABS Technical Report 68-66[1]). Therefore, the stress at the time of buckling was (see page 98)

$$37,600 \text{ psi} \times 0.40 = 15,000 \text{ psi} \tag{55}$$

After the aft box upper skin buckled, the moment of inertia of the wing was reduced from the original 138.59 in.^{4} to 126.43 in.^{4}. Therefore, the stresses at failure (80 percent DUL) were as follows:

$$\sigma_c = 40,000 \times 0.80 \times \frac{138.59}{126.43} = 35,000 \text{ psi} \tag{56}$$

$$\sigma_t = 36,700 \times 0.80 \times \frac{138.59}{126.43} = 32,200 \text{ psi} \tag{57}$$

Although failure occurred on the compression side, the lower or tension side spar cap also showed signs of failure (whitening).

Wing No. 2 failed at 80 percent DUL in tension at the lower spar cap. The calculated stress at 100 percent DUL was 39,614 psi (from Table XXII of USAAVLABS Technical Report 68-66[1]). Therefore, the stress at failure was

$$\sigma_t = 39,614 \times 0.80 = 31,700 \text{ psi} \tag{58}$$

The calculated compressive stress in the aft box at failure was

$$\sigma_c = 31,414 \times 0.80 = 25,160 \text{ psi} \tag{59}$$

The buckling allowable stress for the stiffened aft box was determined using the methods given in U. S. Department of Agriculture Report FPL-070.[3] The calculations are given below.

The skin stiffness per inch is calculated as

$$D = \frac{d\sqrt{E_l E_t}\,(d + t_c)^2}{2(1 - \mu_{lt}\mu_{tl})}$$

$$= \frac{0.050\sqrt{3.1 \times 3.3} \times 10^6\ (0.550)^2}{2(0.94)}$$

$$= 26,200 \tag{60}$$

where $d = 0.050$ in.

$t_c = 0.500$ in.

$E_l = 3.3 \times 10^6$ psi

$E_t = 3.10 \times 10^6$ psi

$$\sqrt{\frac{E_t}{E_l}} = 0.97$$

$$\mu_{lt} = 0.25$$

$$\mu_{tl} = 0.25$$

The parameter involving shear stiffness is calculated as

$$U = \frac{G_{cl}\ (d + t_c)^2}{t_c}$$

$$= \frac{25,600\ (0.550)^2}{0.500}$$

$$= 15,500 \tag{61}$$

where $G_{cl} = 25,600$ psi.

The parameter relating shear and bending stiffness is calculated as

$$V' = \frac{\pi^2 D}{b^2 U}$$

$$= \frac{(3.14)^2\ 26,200}{(23)^2\ 15,500}$$

$$= 0.0314 \tag{62}$$

The aspect ratio is given as

$$\frac{a}{b} = \frac{9.0}{23} = 0.39 \tag{63}$$

Then from Figure 11 of FPL-070,[3] K = 6.3 for a sandwich panel with orthotropic facings and simply supported edges. Therefore, the allowable buckling load of the aft box is

$$N_{cr} = K \frac{\pi^2}{b^2} D$$

$$= 6.3 \frac{(3.14)^2}{(23)^2} 26,200$$

$$= 3080 \text{ lb/in.} \tag{64}$$

and the buckling stress of the aft box is

$$\sigma_c = \frac{3080}{0.100} = 30,800 \text{ psi} \tag{65}$$

This value indicates no buckling of the aft box.

The results of the tests of these two wings indicate that the buckling stress as calculated by the methods given in FPL-070[3] is accurate and that the spar cap at the location of bolt holes is good for approximately 32,000-psi tensile stress. The latter was verified by coupon testing.

THIRD WING DESIGN

The third wing incorporated the higher strength and stiffness of S glass fabric and tape. The upper skin of the wing, which was in compression, required a balanced modulus for good buckling characteristics, shear strength, and stiffness. The bottom skin, which was in tension, required good axial strength and shear resistance. With these requirements in mind, the upper surface sandwich was designed with skins consisting of two plies of 1581 fabric (warp direction parallel to the wing span) and two plies of tape (filament direction at ±30 degrees to the wing span) with an aluminum honeycomb core 0.75 inch thick. The lower surface was made with skins of two plies of tape (filament direction parallel to the wing span) and two plies of 1581 fabric (warp direction at ±45 degrees to the wing span) with a core 0.375 inch thick. The spars had sandwich skins made up of two plies of 1581 fabric (warp parallel to the wing span), one ply of tape (filament direction parallel to the wing span), and two plies of 1581 fabric (warp direction at ±45 degrees to the wing span).

An error in fabrication of the upper forward panel of the No. 3 wing resulted in the tapes being oriented at ±60 degrees to the wing span rather than the ±30 degrees specified on the part drawing.

The structure was reanalyzed based on the material orientation as fabricated. Based on this reanalysis, the minimum margin of safety remained unchanged.

The weight of the completed wing section exclusive of instrumentation was 155.5 pounds.

The above materials and orientations result in a wing with the following section properties:

Area of skin = 12.876 $in.^2$ Shear center at sta 23.636

I_{x-x} = 165.072 $in.^4$ EI_{x-x} = 638.411 $lb\text{-}in.^2$

I_{y-y} = 2415.970 $in.^4$ EI_{y-y} = 9456.551 $lb\text{-}in.^2$

Figure 55 is a cross-sectional view of the No. 3 test article, showing the element breakdown. The stresses in each element were determined from the computer analysis. These stresses are given in Table XVII.

TABLE XVII. SUMMARY OF SHEAR AND BENDING STRESSES

Element	Condition I Stresses		Condition II Stresses	
	Shear (psi)	Bending (psi)	Shear (psi)	Bending (psi)
1	2,030	-14,416	837	-20,723
2	4,815	-14,243	913	-20,475
3	5,495	-13,840	547	-19,894
4	7,420	-13,870	160	-19,939
5	8,880	-13,772	455	-19,797
6	9,280	-13,614	1,034	-19,571
7	9,675	-13,250	1,602	-19,047
8	10,040	-12,707	2,136	-18,266
9	10,410	-11,631	2,659	-16,719
10	10,730	-10,138	3,136	-14,573
11	11,000	-8,382	3,511	-12,049
12	9,160	-5,886	3,153	-8,461

TABLE XVII - Continued				
Element	Condition I Stresses		Condition II Stresses	
	Shear (psi)	Bending (psi)	Shear (psi)	Bending (psi)
13	6,210	-1,352	2,244	-1,943
14	6,150	5,019	2,156	7,215
15	9,105	9,179	2,874	13,195
16	10,670	10,555	3,037	15,173
17	10,420	11,608	2,678	16,686
18	10,070	12,764	2,172	18,348
19	9,560	13,711	1,600	19,710
20	9,245	14,533	1,000	20,891
21	8,820	15,146	376	21,773
22	8,360	15,760	278	22,655
23	5,740	15,246	766	21,916
24	4,655	15,726	1,156	22,607
25	3,900	14,680	1,571	21,103
26	7,090	15,873	2,364	22,817
27	7,595	15,581	2,202	22,397
28	9,200	15,390	2,214	22,123
29	9,760	16,136	1,764	23,195
30	9,290	15,872	1,094	22,817
31	8,830	15,651	425	22,499
32	8,385	15,179	229	21,820
33	7,930	14,791	865	21,262
34	7,510	14,279	1,470	20,526
35	7,100	13,682	2,058	19,668
36	6,710	13,085	2,629	18,810
37	4,840	11,743	2,607	16,881
38	3,660	11,017	2,562	15,837

TABLE XVII - Continued				
Element	Condition I Stresses		Condition II Stresses	
	Shear (psi)	Bending (psi)	Shear (psi)	Bending (psi)
39	2, 144	10, 543	1, 865	15, 156
40	3, 470	10, 051	3, 720	14, 448
41a	3, 910	3, 826	4, 753	5, 500
41b	3, 840	-5, 618	4, 566	-8, 077
42	2, 530	-12, 074	2, 460	-17, 357
43	4, 460	-12, 931	3, 493	-18, 589
44	5, 770	-13, 819	3, 968	-19, 865
45	6, 080	-14, 184	3, 527	-20, 389
46	6, 510	-14, 998	2, 907	-21, 560
47	6, 960	-15, 734	2, 270	-22, 617
48	7, 425	-16, 391	1, 584	-23, 561
49	7, 920	-17, 008	886	-24, 449
50	8, 440	-17, 547	147	-25, 224
51	8, 955	-17, 771	604	-25, 546
52	9, 455	-17, 956	1, 339	-25, 811
53	8, 655	-18, 144	1, 874	-26, 082
54	7, 860	-17, 912	2, 168	-25, 748
55	1, 660	-15, 584	2, 395	-22, 402
56a	5, 350	-7, 365	7, 710	-10, 587
56b	4, 945	6, 174	7, 134	8, 876
57	2, 740	14, 883	3, 960	21, 395

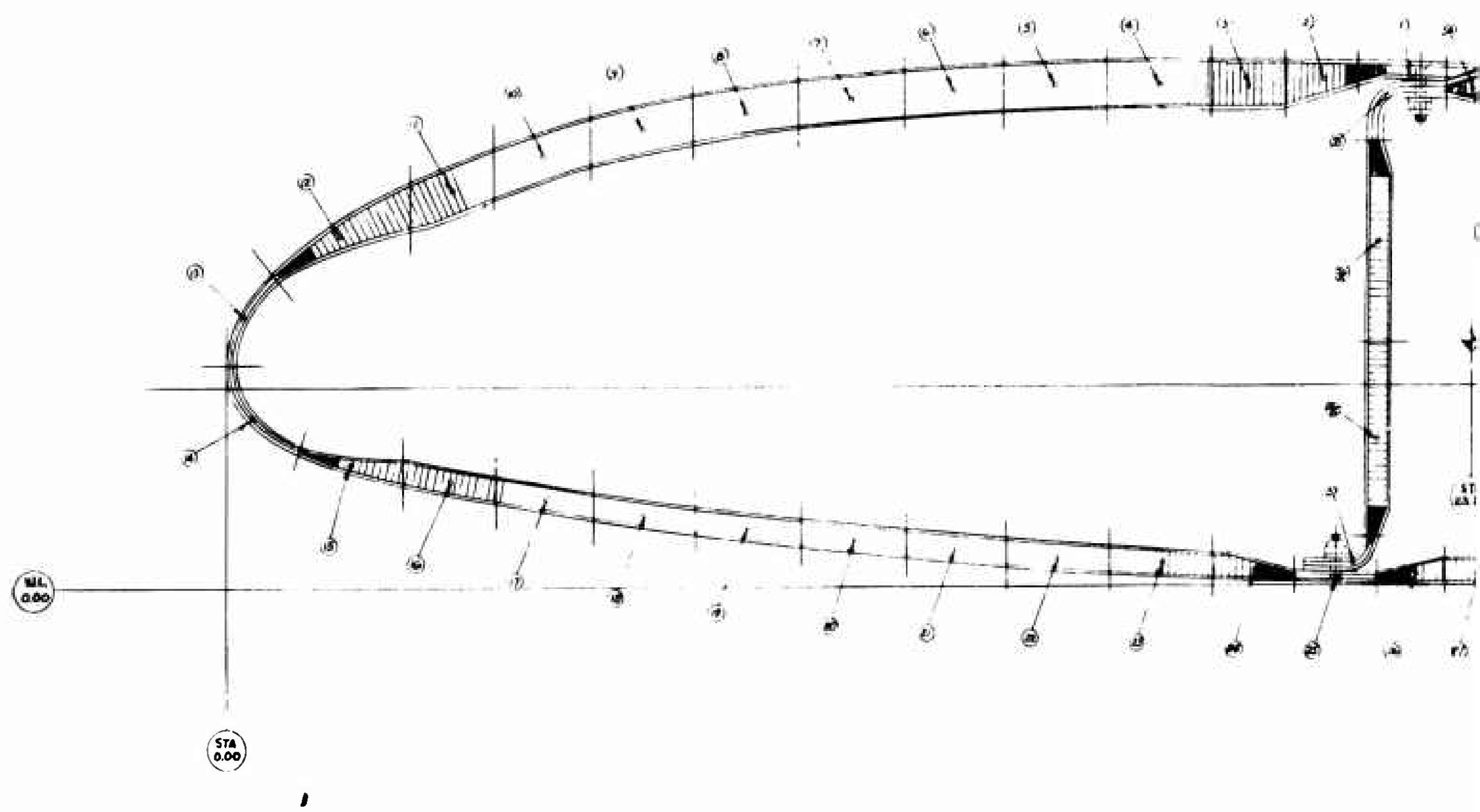

Figure 55. Test Section Layout for Stress Analysis of No. 3 Wing.

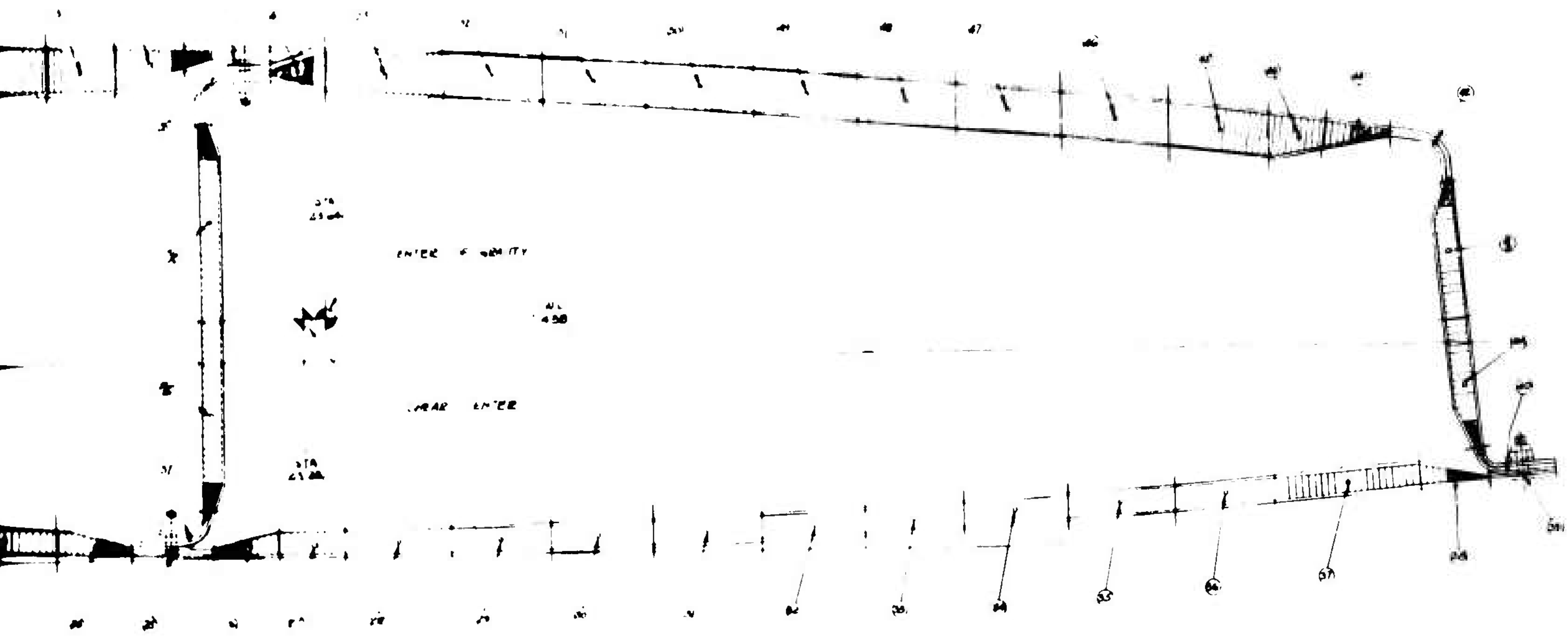

To increase the resistance to buckling, the thira wing had a rib located as shown in Figure 56.

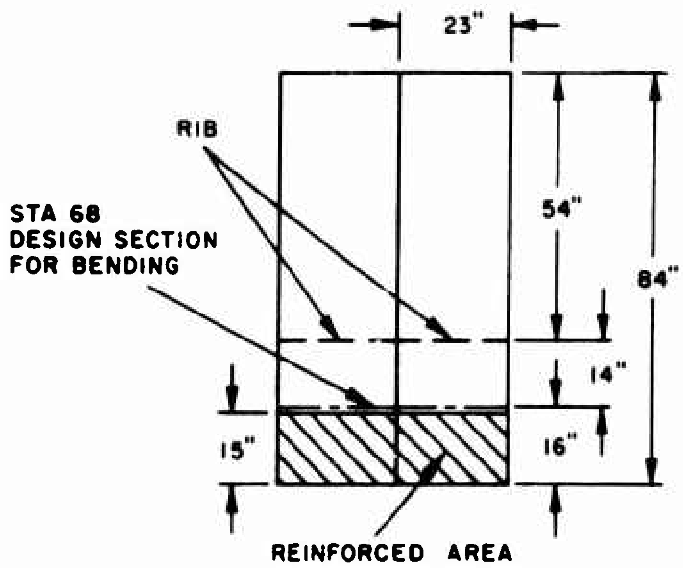

Figure 56. Rib Location.

The buckling allowable stress of the resulting small panel was determined using the methods given in FPL-070.[3] The calculations are given below

The skin stiffness per inch is calculated as

$$D = \frac{d\sqrt{E_l E_t}\,(d + t_c)^2}{2(1 - \mu_{lt}\,\mu_{tl})}$$

$$= \frac{0.044\ \sqrt{4.07\ (3.16) \times 10^6}\ (0.794)^2}{2\ (1 - 0.30 \times 0.23)}$$

$$= 53,300 \qquad (66)$$

where $d = 0.044$ in.

$t_c = 0.750$ in.

$E_l = 4.07 \times 10^6$ psi

$E_t = 3.16 \times 10^6$ psi

$$\sqrt{\frac{E_t}{E_l}} = 0.88$$

$$\mu_{lt} = 0.30$$

$$\mu_{tl} = 0.23$$

The parameter involving shear stiffness is calculated as

$$U = \frac{G_{cl}\,(d + t_c)^2}{t_c}$$

$$= \frac{25,600\ (0.794)^2}{0.750}$$

$$= 21,460 \tag{67}$$

where $G_{cl} = 25,600$ psi.

The parameter relating shear and bending stiffness is calculated as

$$V' = \frac{\pi D}{b^2 U}$$

$$= \frac{(3.14)^2\ 53,300}{(23)^2\ (21,460)}$$

$$= 0.046 \tag{68}$$

The aspect ratio is given as

$$\frac{a}{b} = \frac{14}{23} = 0.61 \tag{69}$$

Then from Figures 11 and 29 of FPL-070,[3] K = 4.0. Therefore, the allowable buckling load of the small panel is

$$N_{cr} = K \frac{\pi^2}{b^2} D$$

$$= 4.0 \frac{(3.14)^2}{(23)^2} 53,300$$

$$= 3980 \text{ lb/in.} \tag{70}$$

and the buckling stress of the panel is

$$\sigma_{cr} = \frac{3980}{0.088} = 45,250 \text{ psi} \tag{71}$$

The maximum compressive stress for Condition II is

$$\sigma = 26,082 \text{ psi (from Table XVII, element 53)}$$

Therefore, the margin of safety for the small panel is

$$MS = \frac{45,250}{26,082} -1.0 = 0.73 \tag{72}$$

For the large panel, $a = 54$, $b/a = 0.426$, and $K = 3.1$. Therefore, the allowable buckling load of the large panel is

$$N_{cr} = K \frac{\pi^2}{b^2} D$$

$$= 3.1 \frac{(3.14)^2}{(23)^2} 53,300$$

$$= 3084 \text{ lb/in.} \tag{73}$$

and the buckling stress of the panel is

$$\sigma_{cr} = \frac{3084}{0.088} = 35,040 \text{ psi} \tag{74}$$

The maximum compressive stress for the large panel is

$$\sigma = 26,082 \times \frac{54}{68} = 20,700 \text{ psi} \tag{75}$$

Therefore, the margin of safety is

$$MS = \frac{35,040}{20,700} - 1.0 = 0.59 \tag{76}$$

The maximum tensile stress in the spar cap is 21, 103 psi. Based on an allowable of 32, 000 psi, the margin of safety is

$$MS = \frac{32,000}{21,103} - 1.0 = 0.51 \tag{77}$$

The maximum bond shear stress at the spar/skin attachment is 784 lb/in. Therefore, the margin of safety is

$$MS = \frac{1000}{784} - 1.0 = 0.27 \tag{78}$$

The maximum skin loads calculated for the No. 3 wing test conditions are given in Table XVIII.

TABLE XVIII. MAXIMUM SKIN LOADS

Element	Thickness (in.)	Load Condition	Bending Stress (psi)	Normal Load (lb/in.)	Shear Stress (psi)	Shear Load (lb/in.)
UPPER SKIN						
53	0.044	II	-26,082	-1148	1,874	96
52	0.044	I	-17,956	-790	9,455	417
11	0.044	I	-8,382	-403	11,000	484
LOWER SKIN						
26	0.044	II	22,817	1003	2,364	163
16	0.044	I	10,555	465	10,670	470
SPAR						
56a	0.052	II	-10,587	-550	7,710	410
56b	0.052	II	8,873	461	7,134	403

The stresses in the individual plies for these conditions were calculated by using the GAC computer program for the analysis of orthotropic laminates. These stresses are shown in Figure 57.

The maximum stresses calculated for the individual plies are compared with the actual test values in Table XIX. The minimum margins for the test loads are therefore

Bond shear stress at spar/skin attachment (Condition I)	0.27
Transverse tension in 901 tape (Condition I).	0.99
Tension stress in spar cap (Condition II)	0.51
Shear in 901 tape (Condition I).	0.35
Shear in 1581 cloth (Condition I)	1.34

TABLE XIX. COMPARISON OF CALCULATED MAXIMUM PLY STRESSES AND SMALL SPECIMEN TEST VALUES

Material	Stress Condition	Calculated Stress (psi)	Average Test Value (psi)	Margin of Safety
1581 Cloth	Longitudinal tension	9, 182	91, 800	Ample
	Longitudinal compression	27, 705	73, 200	1. 64
	Transverse tension	18, 918	76, 900	Ample
	Transverse compression	4, 209	66, 000	Ample
	Shear	6, 682	15, 600	1. 34
901 Tape	Longitudinal tension	33, 443	260, 500	Ample
	Longitudinal compression	38, 861	102, 600	1. 64
	Transverse tension	4, 422	8, 800	0. 99
	Transverse compression	13, 016	26, 800	1. 06
	Shear	6, 645	9, 000	0. 35

LOWER SKIN - LOAD CONDITION II

$E_{11} = 4.45 \times 10^6$ PSI $\quad E_{22} = 4.49 \times 10^6$ PSI $\quad G = 1.29 \times 10^6$ PSI $\quad \mu_{12} = 0.420 \quad \mu_{21} = 0.235$

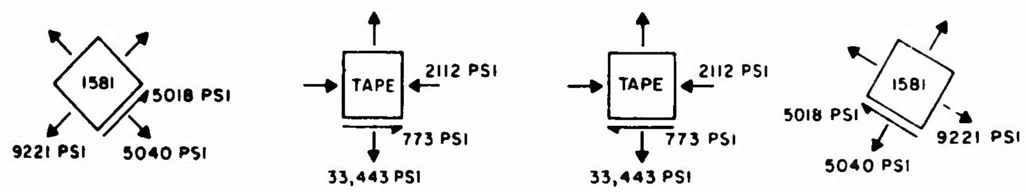

SPAR - LOAD CONDITION II AT ELEMENT 56a

$E_{11} = 4.02 \times 10^6$ PSI $\quad E_{22} = 3.19 \times 10^6$ PSI $\quad G = 1.17 \times 10^6$ PSI $\quad \mu_{12} = 0.295 \quad \mu_{21} = 0.234$

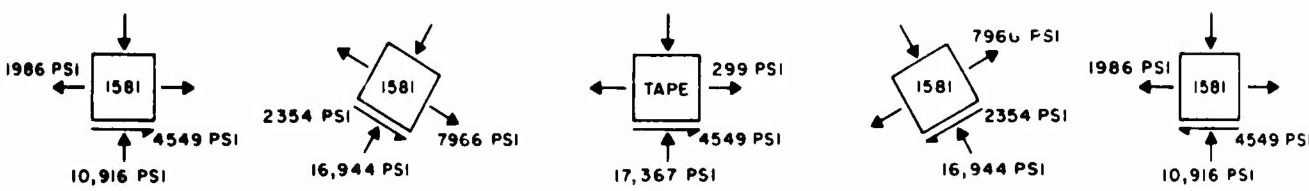

UPPER SKIN - LOAD CONDITION I AT ELEMENT 11

$E_{11} = 4.07 \times 10^6$ PSI $\quad E_{22} = 3.16 \times 10^6$ PSI $\quad G = 1.16 \times 10^6$ PSI $\quad \mu_{12} = 0.300 \quad \mu_{21} = 0.233$

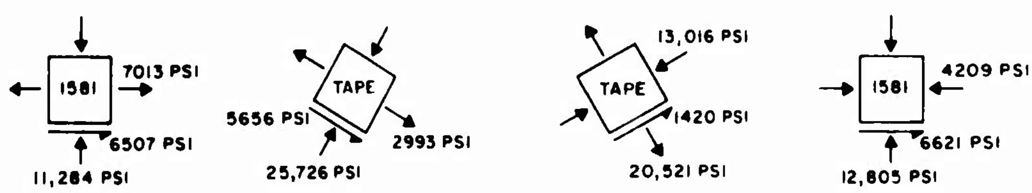

UPPER SKIN - LOAD CONDITION I AT ELEMENT 52

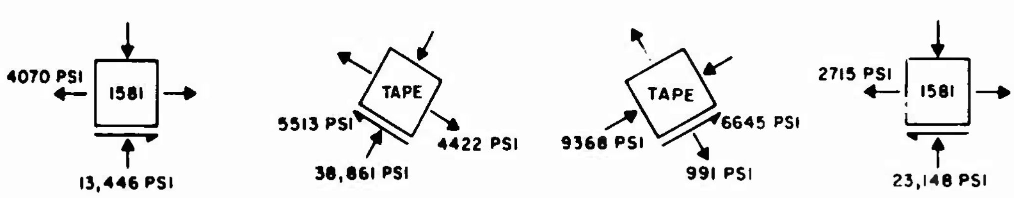

Figure 57. Calculated Stresses in Individual Plies of No. 3 Wing.

LOWER SKIN - LOAD CONDITION I

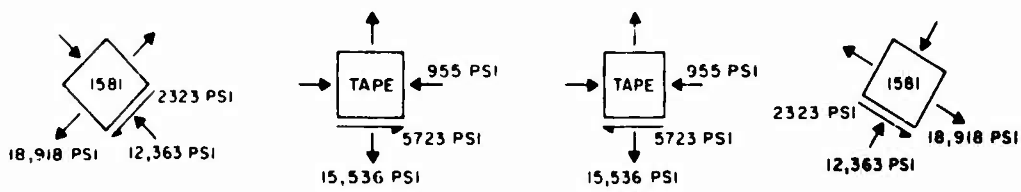

SPAR - LOAD CONDITION II AT ELEMENT 56b

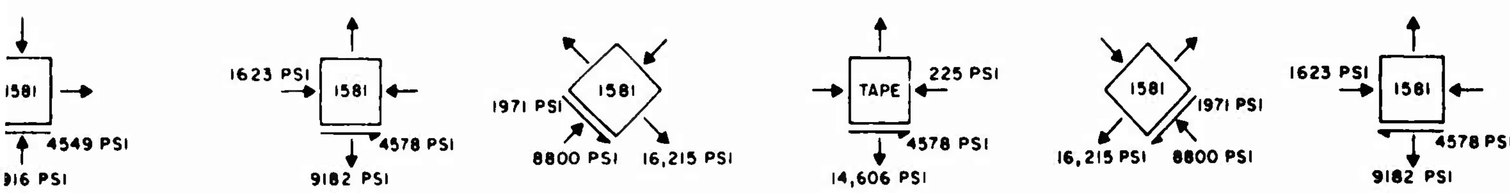

UPPER SKIN - LOAD CONDITION II

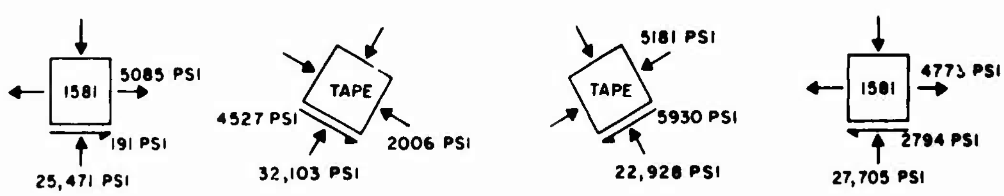

VERTICAL DEFLECTION

The vertical deflection of the wing was calculated for both test Conditions I and II. For test Condition II, the deflection is a combination of bending and shear deflection for a cantilever beam with a concentrated load and is equal to

$$y = \frac{P}{6EI}(x^3 - 3L^2x + 2L^3) + \frac{V(L - x)}{AG} \tag{79}$$

where $P = V = 12,684$ lb

$EI_{x-x} = 638,411,000$

$L = 84$ in.

$A = 12.876$ in.^{2}

$G = 1,330,000$ psi

At the end of the wing, $x = 0$; therefore,

$$y = \frac{12,684}{6(638,411,000)}[2(84)^3] + \frac{12,684(84)}{12.876(1,330,000)}$$

$$= 3.92 + 0.06 = 3.98 \text{ in.} \tag{80}$$

This calculation assumes a constant stiffness over the entire span length, and in reality the stiffness in the attachment area ($x = 68$ to $x = 84$) has been greatly increased. Therefore, a more accurate deflection calculation is obtained by eliminating the deflection of the area:

$$y = 3.98 - 0.20 = 3.78 \text{ in.} \tag{81}$$

The maximum vertical deflection for the bending and torsion condition would include a bending and shear deflection plus a deflection due to twist. The bending and shear deflection is directly proportional to the end load. For Condition I, therefore,

$$y_b = 3.78 \times \frac{8,824}{12,684} = 2.64 \text{ in.} \tag{82}$$

The angle of twist (ϕ) can be determined from the calculated shear flows (q lb/in.) and the parameters of the cell section as follows:

$$\phi = \frac{q_a\left(\frac{\Delta s}{t}\right)_a - q_b\left(\frac{\Delta s}{t}\right)_{ab}}{2A_a}\left(\frac{L}{G}\right)$$

$$= \frac{753(539) - 751(81.19)}{2(148.78)} \frac{84}{1,330,000}$$

$$= 0.0731 \text{ radian or } 4.19 \text{ degrees} \tag{83}$$

Then the maximum torsional deflection is

$$y_t = \tan 4.19\,(23.6) = 1.73 \text{ in. (leading edge)} \tag{84}$$

This calculation again assumes a constant section. A more accurate calculation is obtained by assuming twice the torsional stiffness in the attachment area:

$$y_t = 1.57 \text{ in.} \tag{85}$$

The maximum deflection of the leading edge is therefore

$$y = 2.64 + 1.57 = 4.21 \text{ in.} \tag{86}$$

TEST RESULTS AND DATA REDUCTION FOR THE NO. 3 WING

GENERAL

Tests of the No. 3 wing section were performed in the following sequence:

1. Cantilevered end shear to determine location of section shear center.
2. Cantilevered vibration scan to determine first mode bending frequency.
3. Condition II loading (862,500 in.-lb maximum moment in test section with 12,684-pound end shear).
4. Condition I loading (600,000 in.-lb maximum moment plus 500,000 in.-lb maximum torque in test section with 8824-pound end shear).

During the bending tests, the upper skin was in compression. For combined loading, torque was applied clockwise to the free end of the specimen; i.e., the leading edge was raised with respect to the trailing edge with a positive torque.

Instrumentation for the structural load tests consisted of the same types of strain gages, strain rosettes, and deflection potentiometers as used in the tests of the No. 1 and No. 2 wing sections. (Refer to USAAVLABS Technical Report 68-66[1] and Naval Air Development Center Report No. NADC-ST-6903.[6]) Strain gage and rosette locations are shown in Figure 58, and wing section deflection points are shown in Figure 59.

Data from all strain gages and rosettes were converted to stresses by using the same elastic constants as applied in the stress analysis discussed in the previous section. These values at the strain rosette locations are given in Table XX. For the single gages on the skin surfaces and the spar caps, the elastic constants used in the data reduction are given in Appendix II, which consists of tabular summary pages comparing the experimental stresses with those determined in the stress analysis.

SHEAR CENTER STATION LOCATION

The shear center station location was determined by separately applying vertical loads to the free end of the cantilevered specimen at two locations, recording leading edge and trailing edge displacements for both

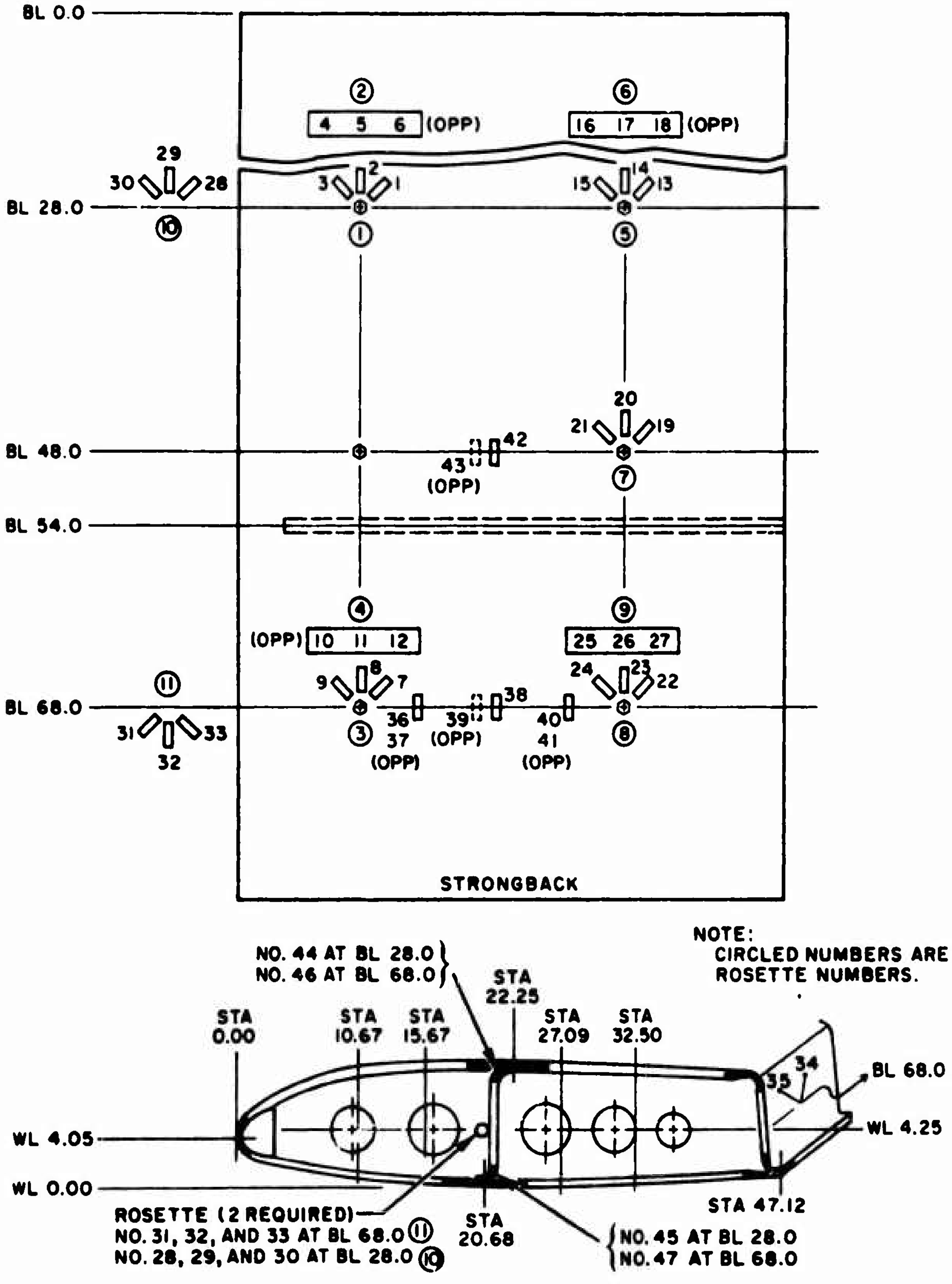

Figure 58. Strain Gage and Rosette Locations on No. 3 Wing Section.

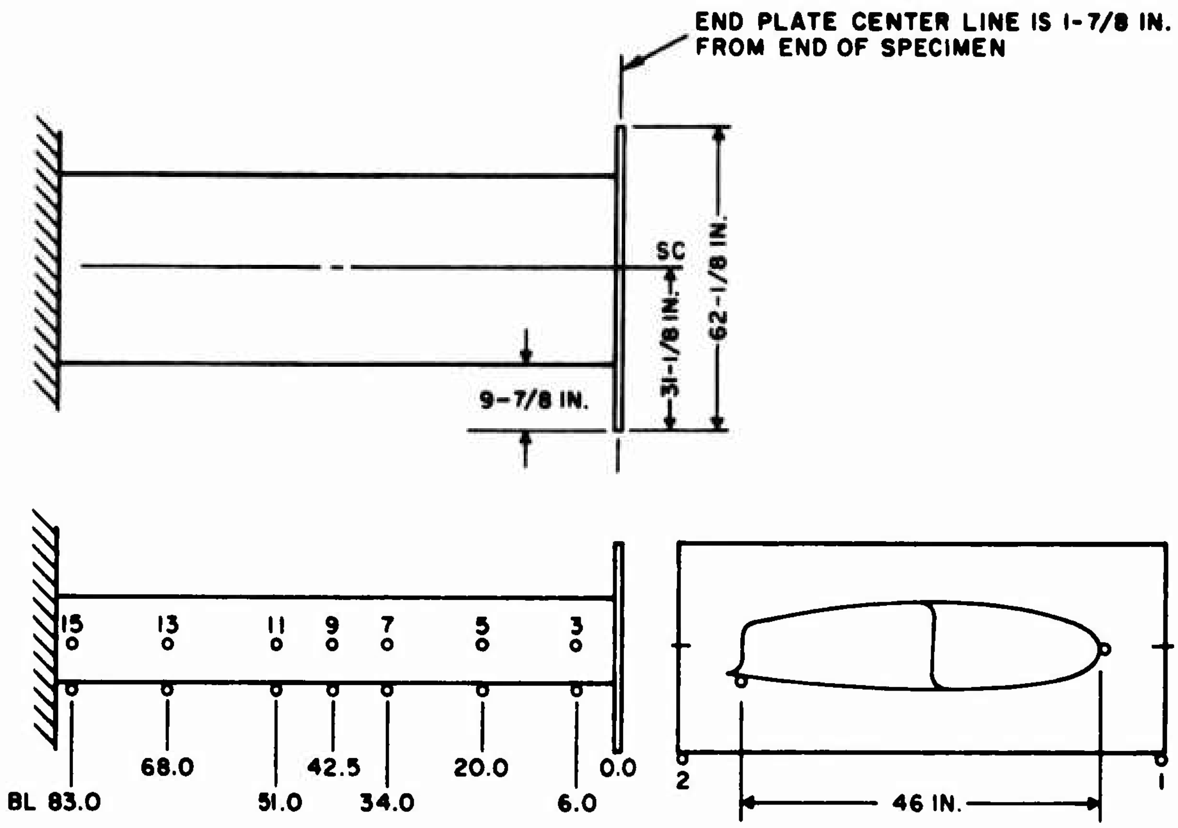

Figure 59. Wing Section Deflection Points.

TABLE XX. ELASTIC CONSTANTS AT ROSETTE LOCATIONS					
Location	E_x (psi)	E_y (psi)	G_{xy} (psi)	μ_{xy}	μ_{yx}
Forward cell/ upper skin	3.17×10^6	4.06×10^6	1.16×10^6	0.234	0.299
Lower skin/ both cells	4.45×10^6	2.49×10^6	1.29×10^6	0.420	0.235
Aft cell/ upper skin	4.06×10^6	3.17×10^6	1.16×10^6	0.299	0.234
Main and aft spar webs	4.02×10^6	3.19×10^6	1.17×10^6	0.295	0.234

cases in order to find the angle of twist, and then solving for the point at which the vertical load would produce no rotation. This is the same test procedure as defined in USAAVLABS Technical Report 68-66[1] and Naval Air Development Center Report No. NADC-ST-6903.[6]

The following equation was used to make the necessary calculations:

$$e = \ell \left[\frac{\delta_{71} - \delta_{81}}{(\delta_{72} - \delta_{71}) - (\delta_{82} - \delta_{81})}\right] \tag{87}$$

where e = station distance between the shear center and the first application point

ℓ = station distance between successive points of vertical load application = 10

δ_7 = leading edge displacement

δ_8 = trailing edge displacement

1 = subscript denoting first load

2 = subscript denoting second load

The applied loads and resultant displacements are given in Table XXI. The reference point for locating the two load application points was the shear center as determined by the stress analysis in the previous section. Also, the first load point was taken 8.0 inches aft of this reference point, and the second load point was 18.0 inches aft of the reference point. Therefore, the value of ℓ in Equation (87) is 10.0 inches.

Substitution of the data from Table XXI with the 1600-pound shear load gives a shear center location 1.5 inches aft of the location determined by the stress analysis in the previous section.

FORCED VIBRATION TESTS

A vibration scan was performed with a portable speaker to determine dynamic response characteristics. As in the shear center tests, the wing specimen was cantilevered from the strongback. The frequencies at which resonances occurred were noted, and these particular frequencies were repeated to obtain accelerometer traces for defining mode shape. Accelerometer locations are shown in Figure 60.

The first-mode bending frequency was determined to be approximately 23 Hz, and the first-mode torsional frequency was found at approximately

TABLE XXI. RESULTS OF SHEAR CENTER STATION DETERMINATION TESTS				
Shear Load, V (lb)	Load Point	Leading Edge Deflection, δ_7 (in.)	Trailing Edge Deflection, δ_8 (in.)	$\delta_7 - \delta_8$ (in.)
400	1	0.050	0.040	0.010
800	1	0.098	0.078	0.020
1200	1	0.148	0.120	0.028
1600	1	0.202	0.164	0.038
400	1	0.048	0.040	0.008
800	1	0.094	0.076	0.018
1200	1	0.146	0.118	0.028
1600	1	0.198	0.162	0.036
400	2	0.056	0.036	0.020
800	2	0.110	0.070	0.040
1200	2	0.168	0.108	0.060
1600	2	0.234	0.156	0.078
400	2	0.054	0.036	0.018
800	2	0.108	0.070	0.038
1200	2	0.164	0.108	0.056
1600	2	0.220	0.146	0.074

44.2 Hz. Additional mixed modes were found at 87.8, 121.3, 193.6, 248, 375, and 475 Hz, but mode shapes are difficult to visualize at the higher frequencies. Therefore, Table XXII was prepared to show motion at the various accelerometer locations as an indication of mode shape.

STRUCTURAL LOAD TESTS

Two structural loading conditions were applied to the No. 3 wing specimen. Since the minimum margin of safety (+0.27) was analytically determined to occur in the combined bending and torsion loading, Condition II, which applies bending and vertical shear only, was applied first. The testing sequence was as follows:

1. 50 percent DUL bending (Condition II)

2. 50 percent DUL combined bending and torsion (Condition I)

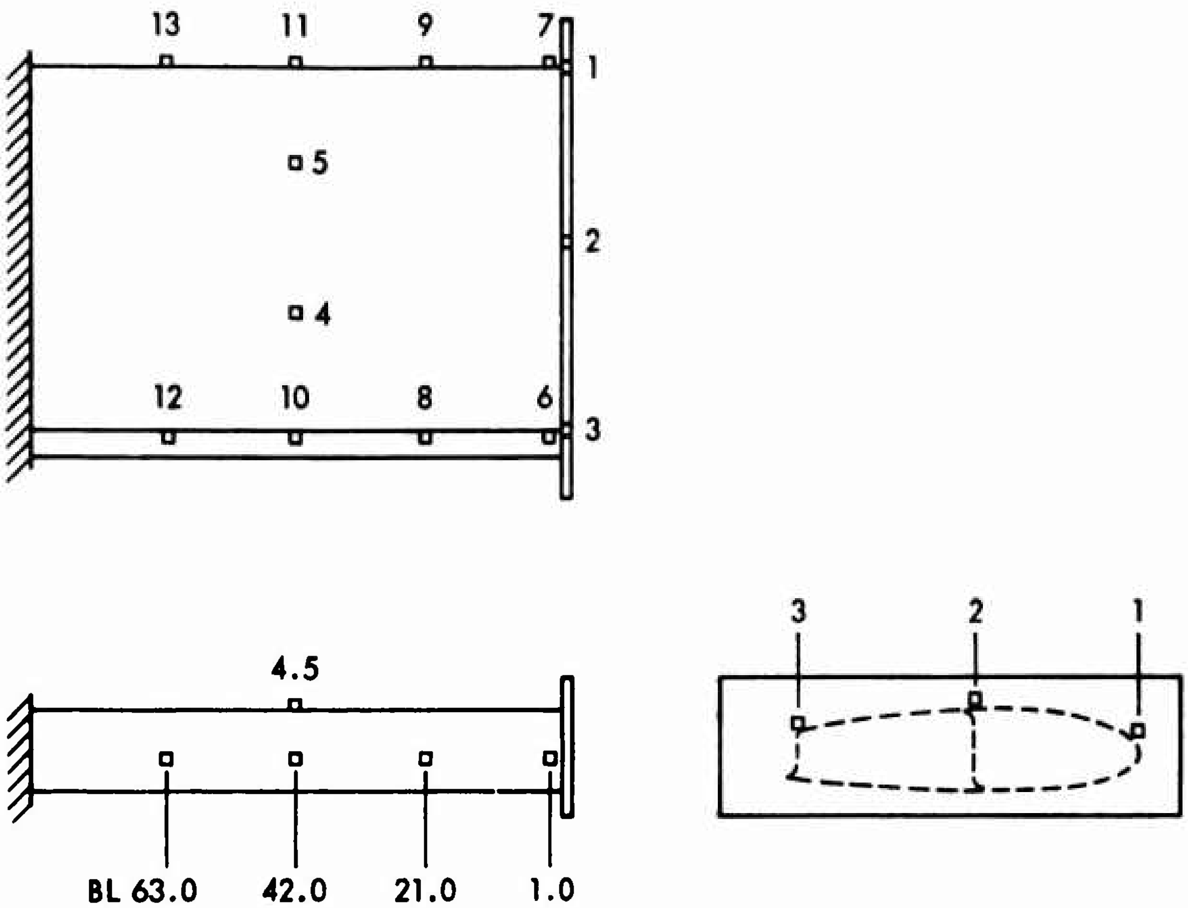

Figure 60. Location of Vibration Survey Accelerometers on No. 3 Wing Section.

3. 100 percent DUL (Condition II)

4. 100 percent DUL (Condition I)

5. 150 percent DUL (Condition I)

6. 200 percent DUL (Condition I)

Considering first the bending condition (Condition II), end shear was applied in 10-percent increments, and strain gage and deflection gage readings were recorded to the full 100 percent DUL at each increment. Readings were also taken during removal of the load at 10-percent increments during the first loading test and at 20-percent increments during the 100 percent DUL test for Condition II loads. The wing specimen at 100 percent DUL in bending is shown in Figure 61.

TABLE XXII. DYNAMIC RESPONSE DUE TO SPEAKER EXCITATION OF NO. 3 WING SECTION*

Freq (Hz)	Accelerometer Locations (See Figure 60)												
	BL 0.0			BL 1.0		BL 21.0		BL 42.0				BL 63.0	
	LE 1	CS 2	TE 3	LE 7	TE 6	LE 9	TE 8	LE 11	FP 5	RP 4	TE 10	LE 13	TE 12
23	+1.00	+0.605	+0.417	+0.663	+0.479	+0.375	+0.417	+0.250	+0.216	+0.187	+0.333	+0.125	0
44.2	+1.00	0	-0.75	+0.55	-0.78	+0.31	-0.63	+0.16	-0.17	0	-0.41	-	-
87.8	+1.00	-0.80	+0.64	+0.40	+0.65	+0.30	+0.45	0	-0.12	-0.12	+0.18	-0.13	0
121.3	-0.42	-0.15	+0.38	+0.10	+0.21	+0.87	-0.36	+1.00	-0.45	+0.48	-0.65	+0.34	-0.15
193.6	+1.00	+0.15	**	+0.51	-0.16	-0.39	-0.13	-0.30	+0.67	-0.52	-0.24	0	-0.22
248	0	+	+	-	+	-	-	-	-	+	+	+	+
375	+	-	**	-	+	-	-	+	+	+	-	-	+
475	+	+	**	+	+	-	-	0	-	+	0	0	0

*Normalized largest recorded displacement where measurable.

**Too much noise on trace to compare with adjacent accelerometer readings.

Note: LE - Leading Edge. CS - Center Spar. TE - Trailing Edge. FP - Forward Panel.

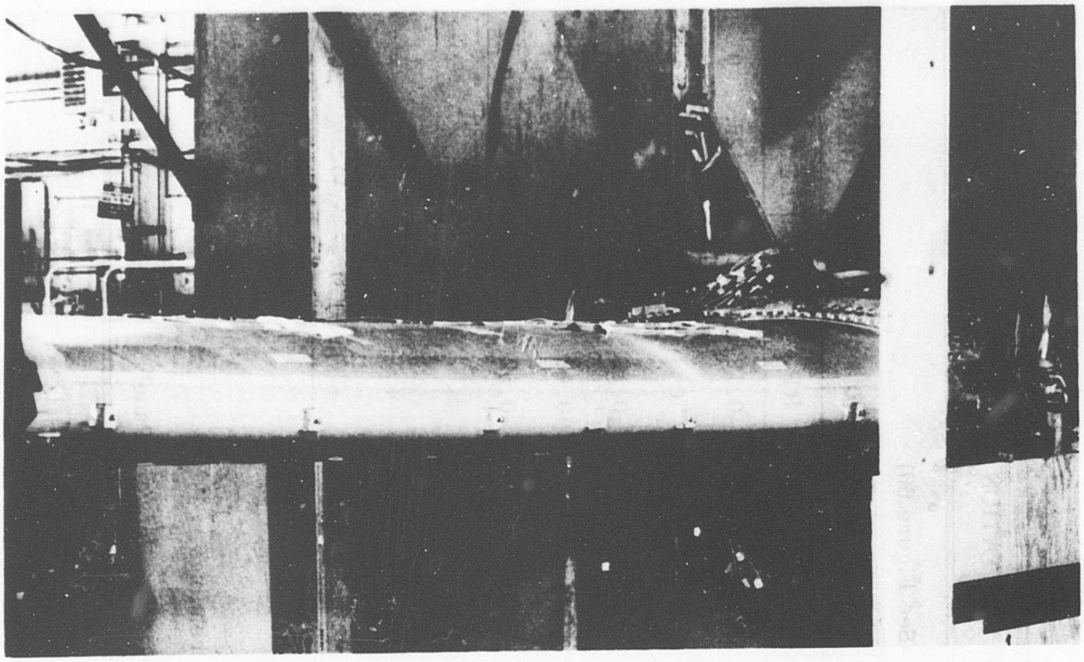

Figure 61. No. 3 Wing Section - Bending Condition: Leading Edge Deflection at 100 Percent DUL.

The rosettes that recorded the highest spanwise compression and tension stresses were No. 8 (upper skin of aft cell) and No. 9 (lower skin of aft cell), respectively, both at BL 68.0. Readings from these gages are plotted in Figure 62 to show the nature of the stress buildup at both points and the comparison of test data with the stress analysis at these two locations.

Rosettes No. 3 and 4, also at BL 68.0, are plotted in Figure 63. All four gages appear to be somewhat nonlinear, with the greatest deviation from a straight line load/stress relationship occurring after about 70 percent DUL.

A comparison of calculated and experimental spanwise stresses at all rosette and strain gage locations is shown in Figure 64 at 100 percent DUL under Condition II loading. A tabular comparison of experimental and calculated spanwise stresses under Condition II loading is given in Tables XXV through XLVII in Appendix II. The greatest difference between test data and analysis is shown to be on the lower skin at the main spar. This particular gage was on the line of bolts connecting the forward and aft cells and would therefore indicate a loss in effective section due to the bolt holes on the tension side of the skin. The gage on the skin at the main spar on the compression side shows no loss in section, but rather indicates a fully effective section, which would be expected.

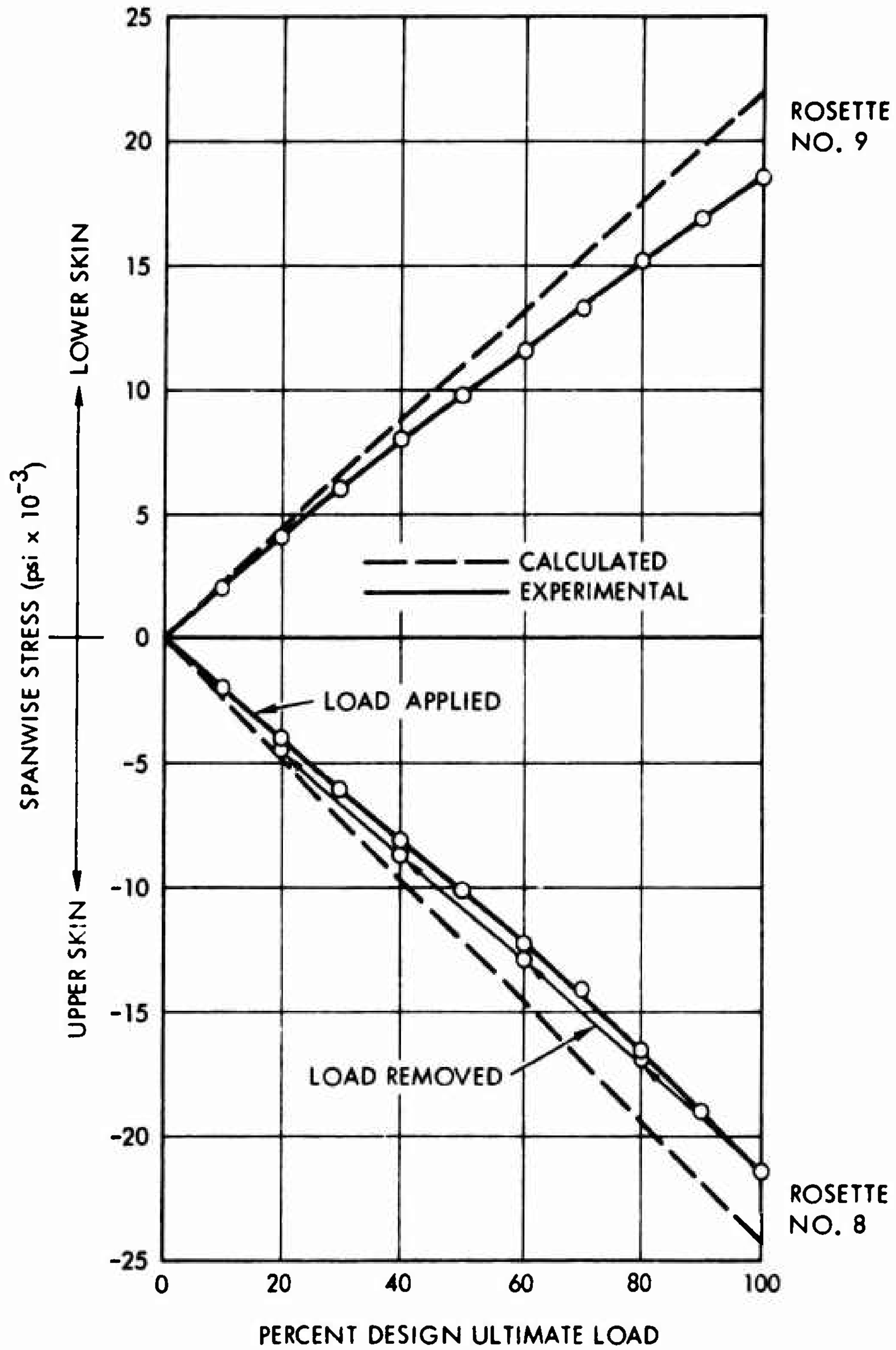

Figure 62. Comparison of Experimental and Calculated Spanwise Stresses in Aft Cell at BL 68.0 Under Condition II Loading.

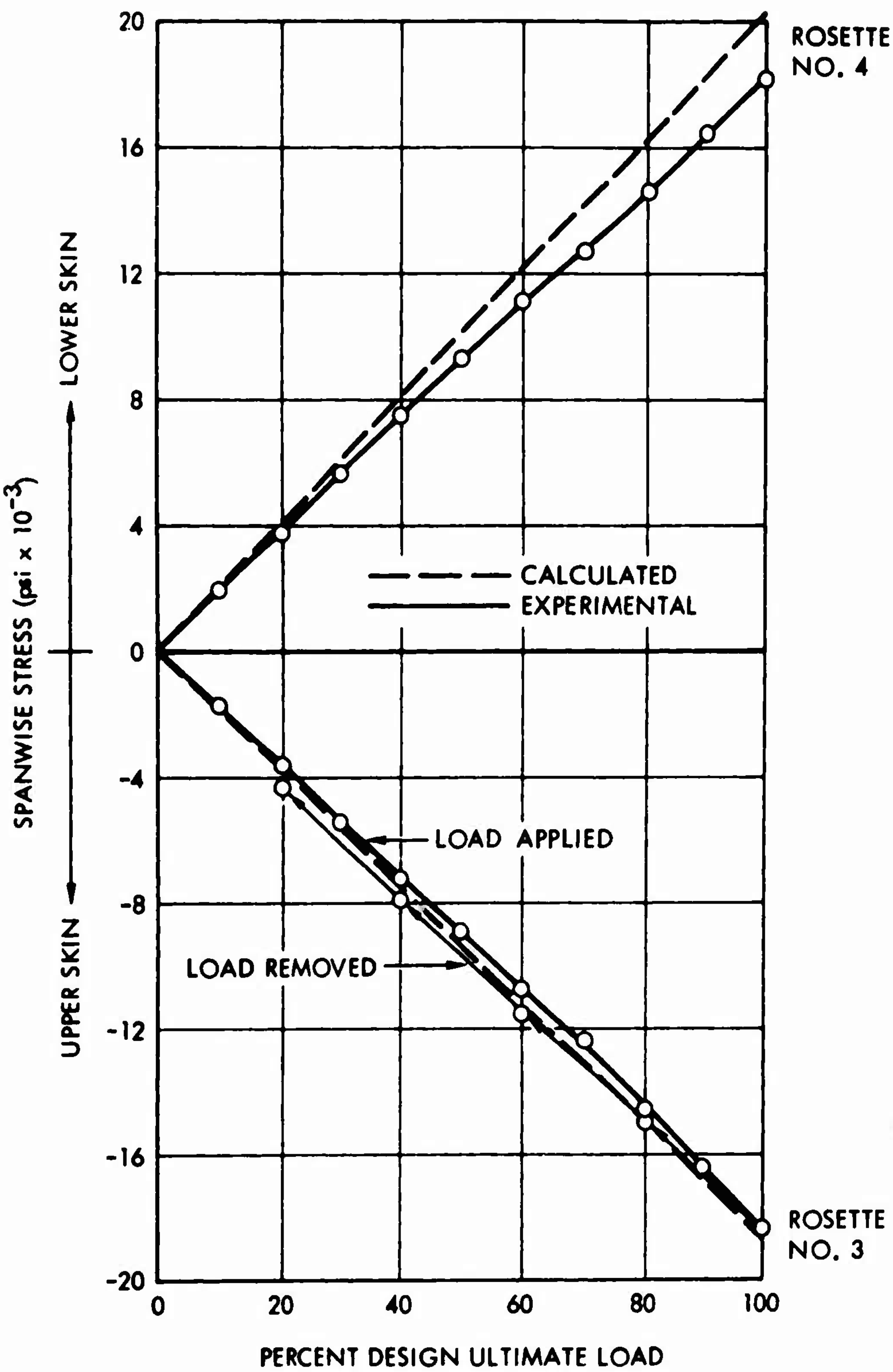

Figure 63. Comparison of Experimental and Calculated Spanwise Stresses in Forward Cell at BL 68.0 Under Condition II Loading.

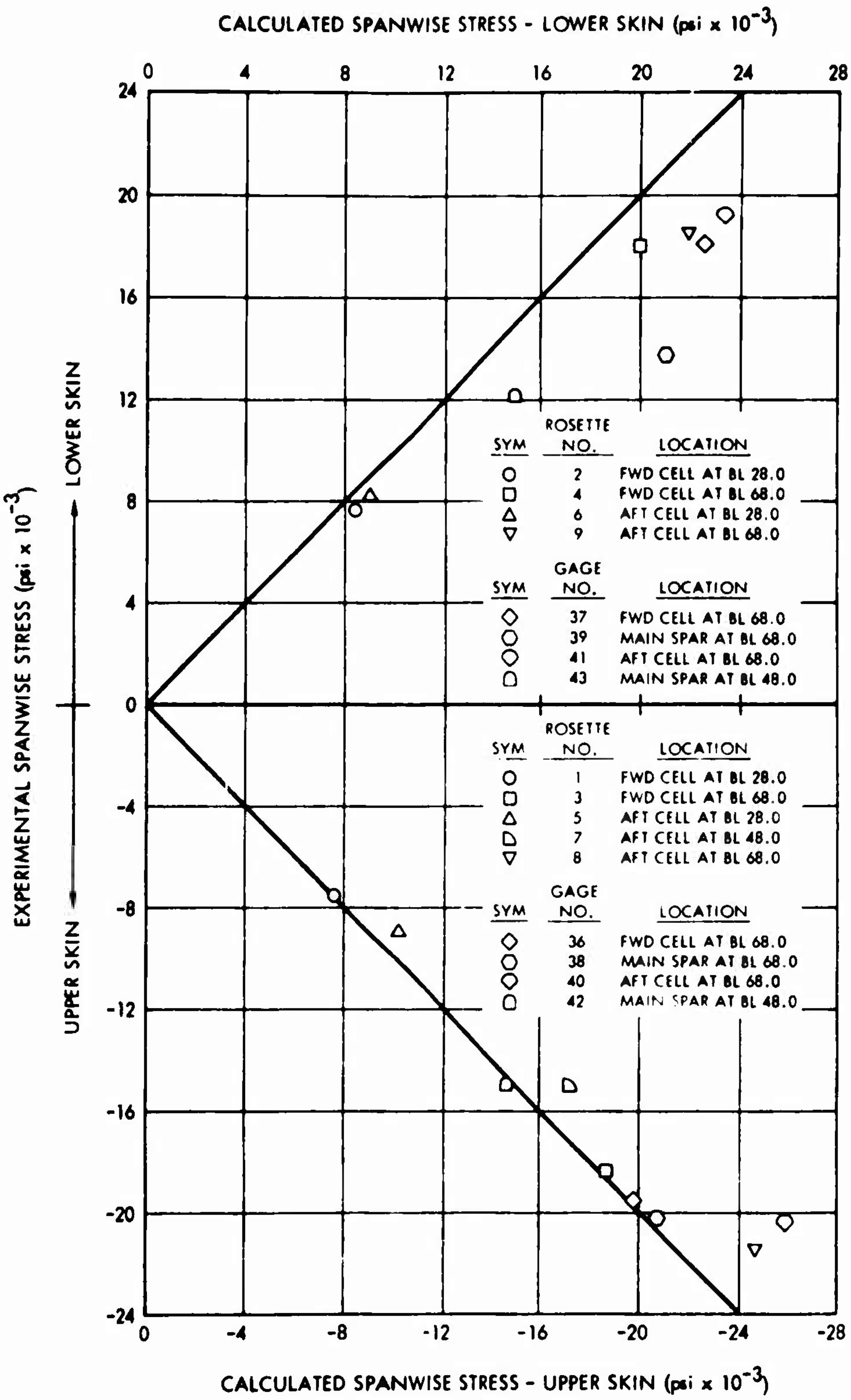

Figure 64. Comparison of Experimental and Calculated Spanwise Stresses Under Condition II Loading at 100 Percent DUL.

In all cases of spanwise stress, the test data are lower than the stress levels calculated from the analysis. The greatest differences occur at the higher stress levels and on the bolt line on the tension side. The location of these points suggests that actual elastic modulus of the wing skin material is higher than calculated in all areas except the upper skin of the forward cell, where the layup is $0^\circ/+60^\circ/-60^\circ/0^\circ$ and where the experimental data are very close to the calculated values.

A tabular comparison of experimental and calculated shear stresses under Condition II loading is given in Tables XLVIII through LIX in Appendix II. Comparisons at 100 percent DUL are shown in Figure 65. In addition, the variation in shear stress with increasing load at the various skin rosettes is plotted in Figures 66, 67, and 68. The forward cell data at BL 68.0 are very erratic and may be affected by the proximity of the reinforcement and rib, although such an effect is not evident to the same degree in the aft cell test data at the same butt line. Neither does the main spar shear data at BL 68.0 in Figure 68 show any trends in shear stress similar to those of the forward cell upper and lower skins.

An additional observation from the test data in both the spanwise and shear stress results is an apparent discontinuity in the rate of stress increase with the application of load between 70 and 80 percent DUL. The same discontinuity is not noticeable in the specimen deflections shown in Figure 69.

Condition I loads (bending plus torsion) were applied in the following sequence:

1. 50 percent DUL in 10-percent increments, and removed in 10-percent increments

2. 100 percent DUL in 20-percent increments to 60 percent DUL, 20-percent increments to 100 percent DUL, and removed in 20-percent increments

3. 150 percent DUL in 20-percent increments to 100 percent DUL, 10-percent increments to 150 percent DUL, and removed in 20-percent increments

4. 200 percent DUL in 20-percent increments to 120 percent DUL, 10-percent increments to 200 percent DUL, and removed in 40-percent increments

The specimen under load at 100, 150, and 200 percent of the Condition I design ultimate load is shown in Figures 70, 71, and 72.

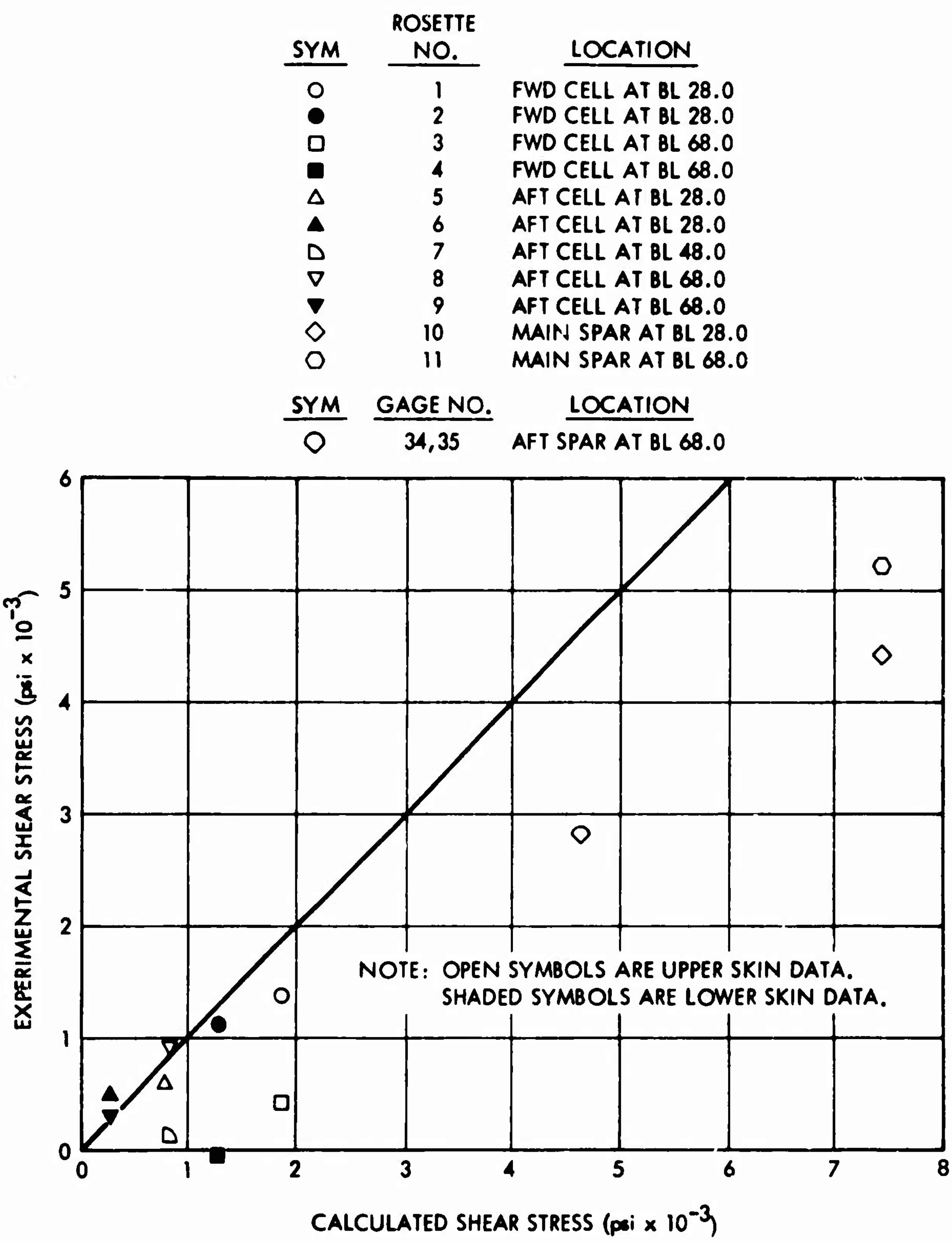

Figure 65. Comparison of Experimental and Calculated Shear Stresses Under Condition II Loading at 100 Percent DUL.

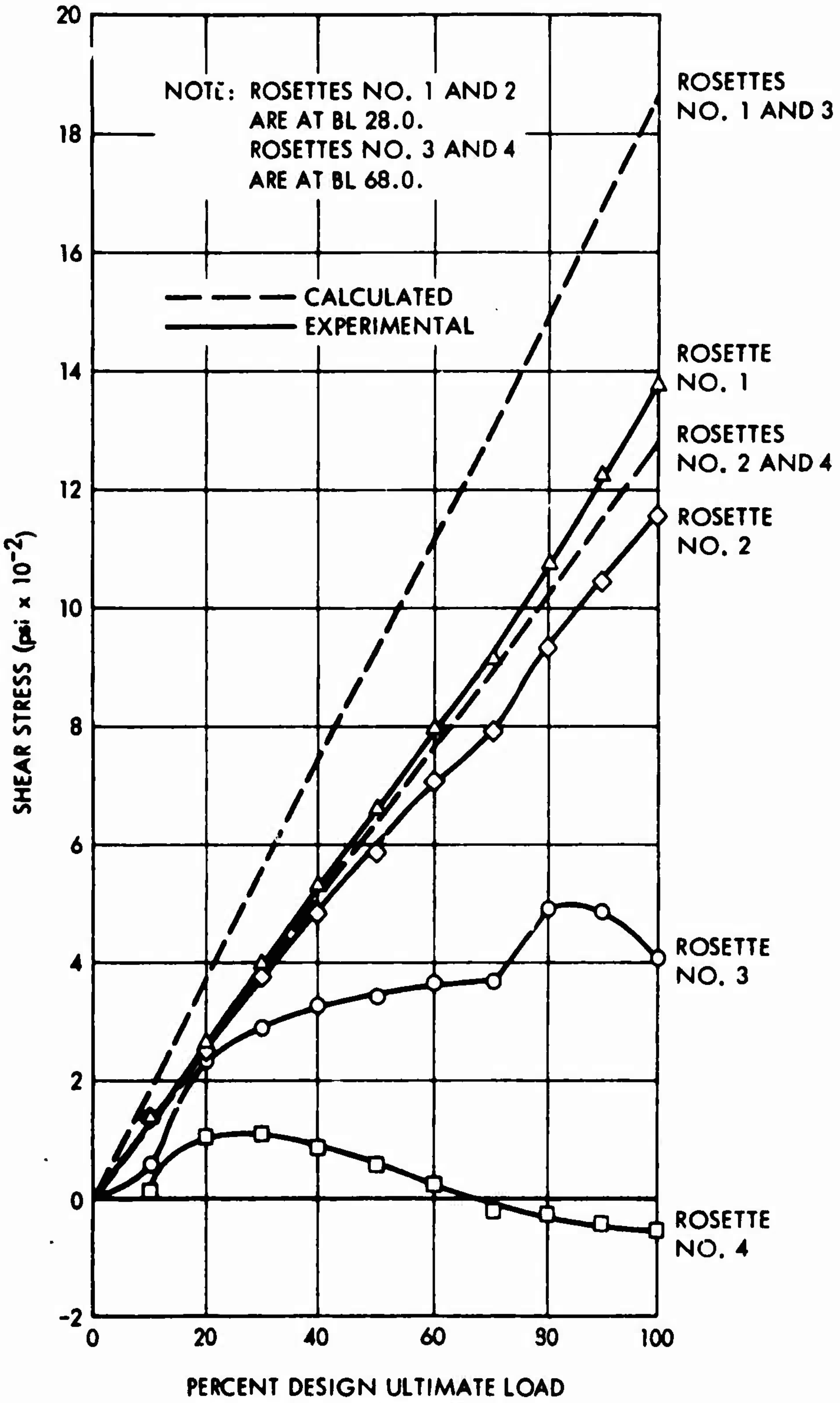

Figure 66. Comparison of Experimental and Calculated Shear Stresses in Forward Cell at BL 28.0 and 68.0 Under Condition II Loading.

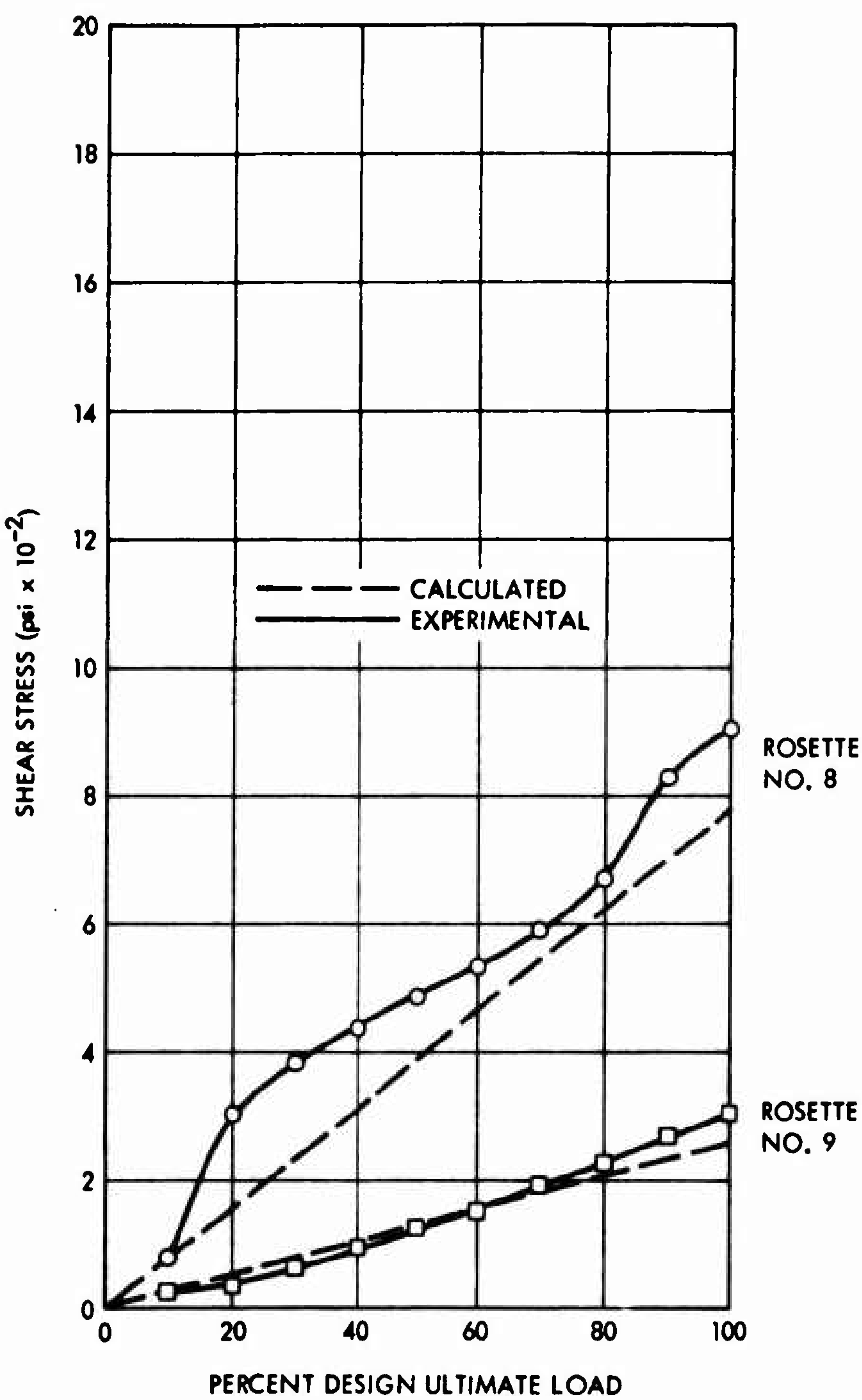

Figure 67. Comparison of Experimental and Calculated Shear Stresses in Aft Cell at BL 68.0 Under Condition II Loading.

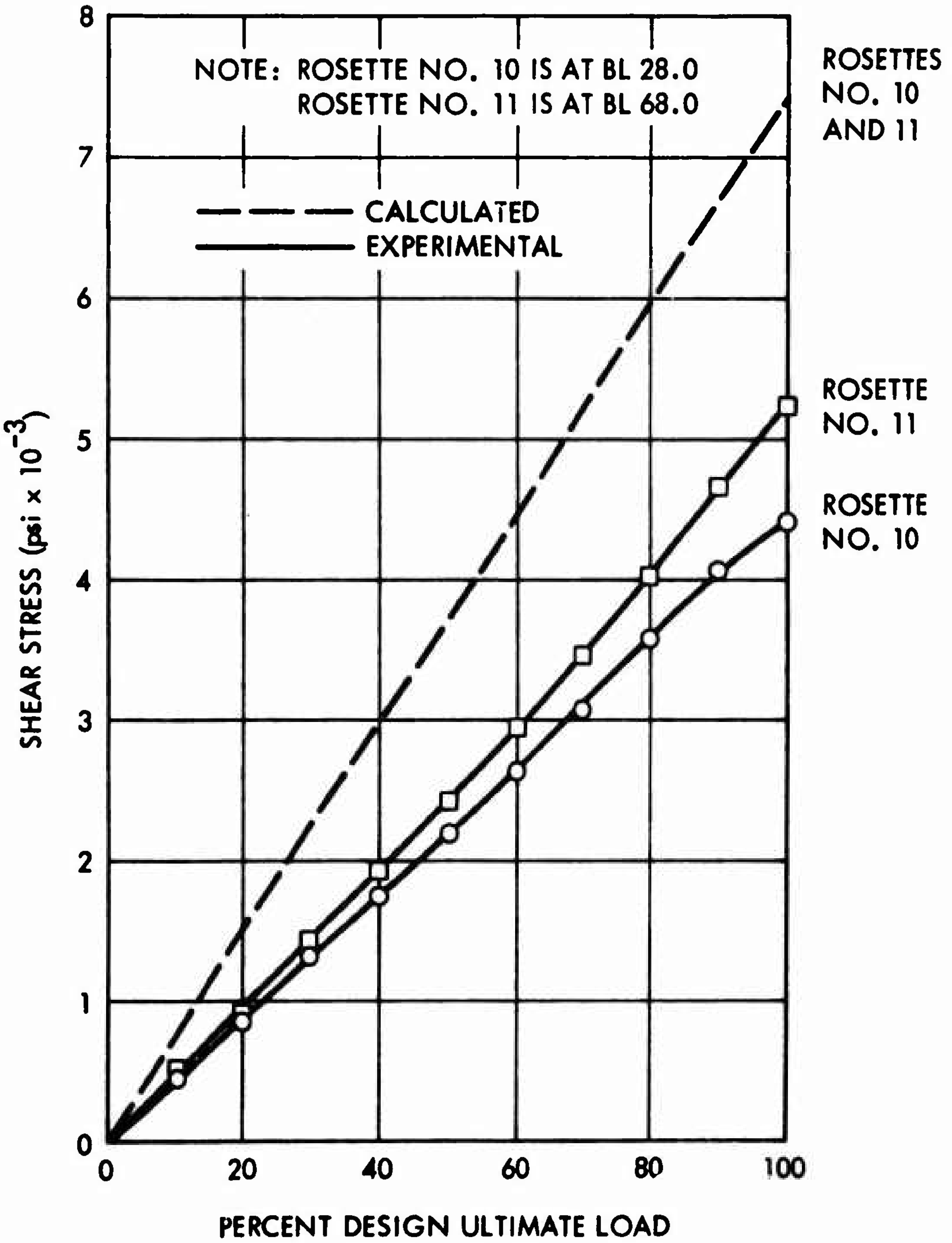

Figure 68. Comparison of Experimental and Calculated Shear Stresses in Main Spar Under Condition II Loading.

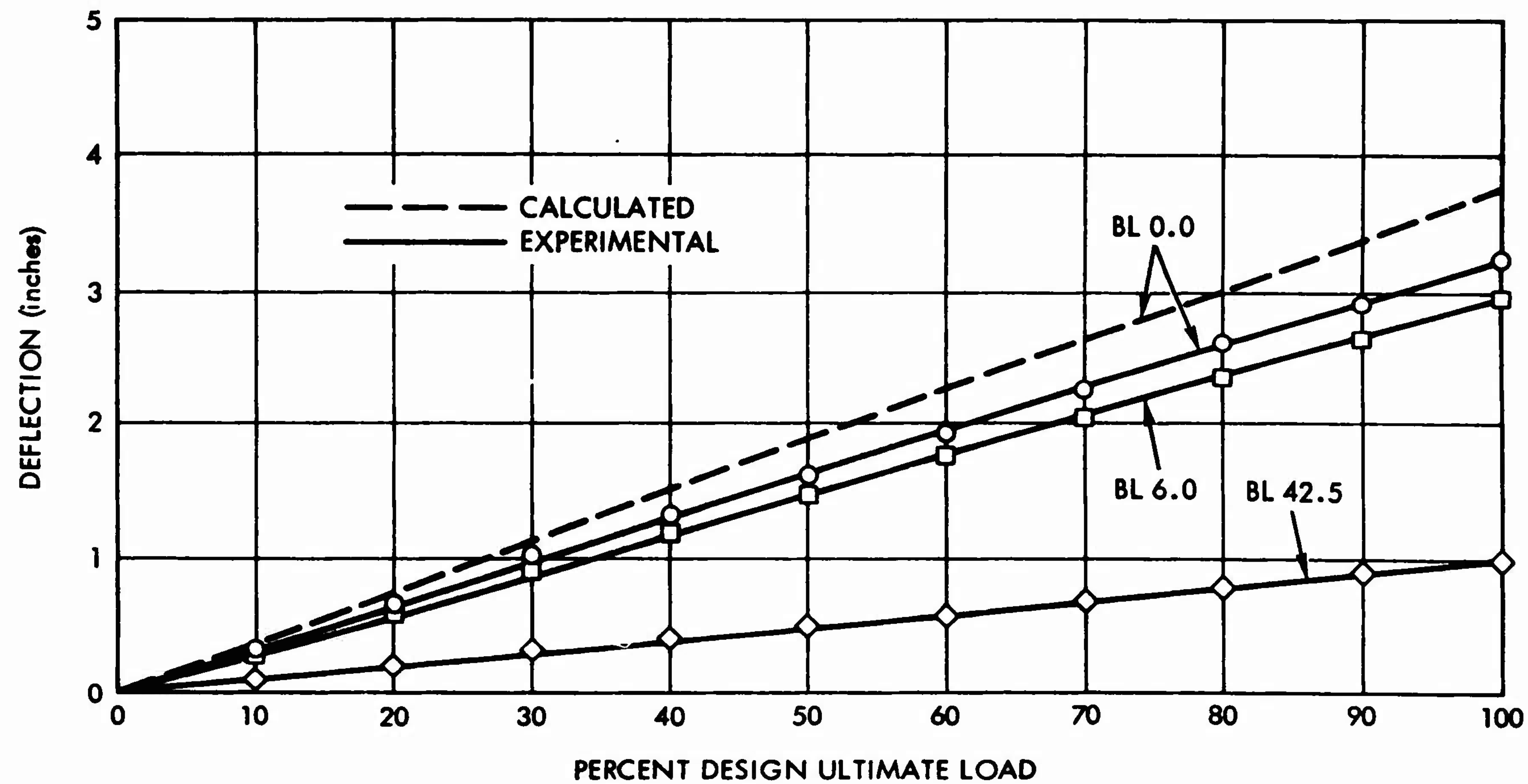

Figure 69. Specimen Deflections Resulting From Condition II Loading.

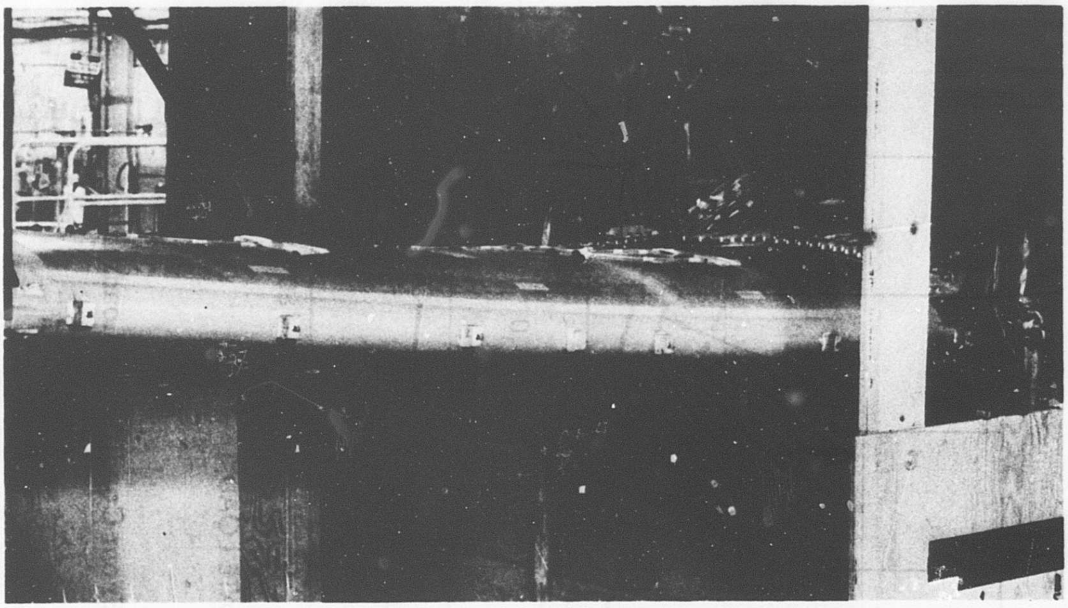

Figure 70. No. 3 Wing Section - Combined Condition: Leading Edge Deflection at 100 Percent DUL.

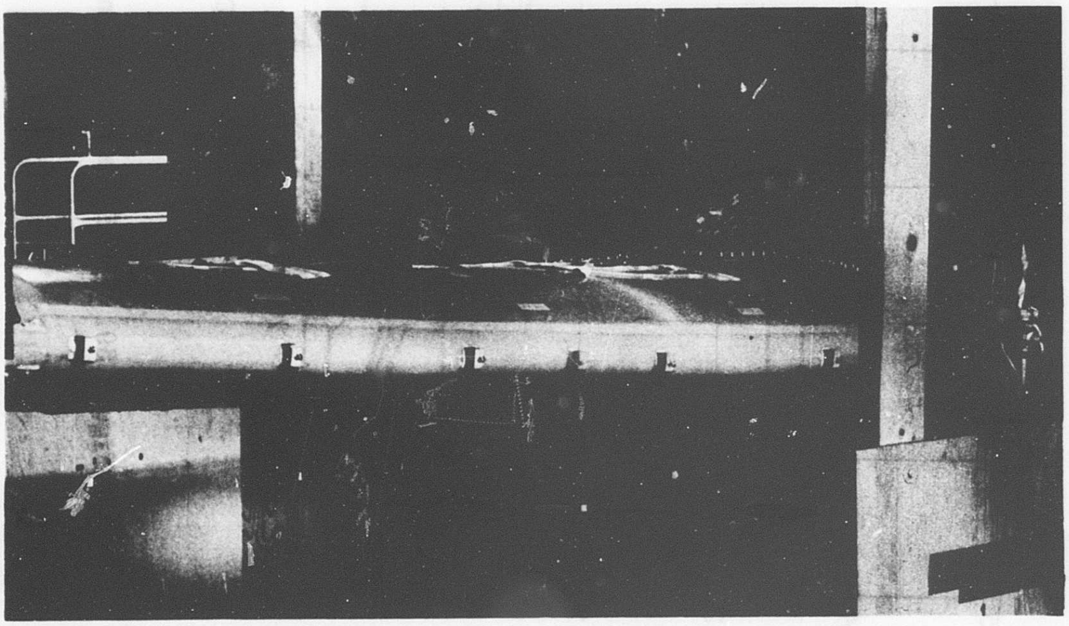

Figure 71. No. 3 Wing Section - Combined Condition: Leading Edge Deflection at 150 Percent DUL.

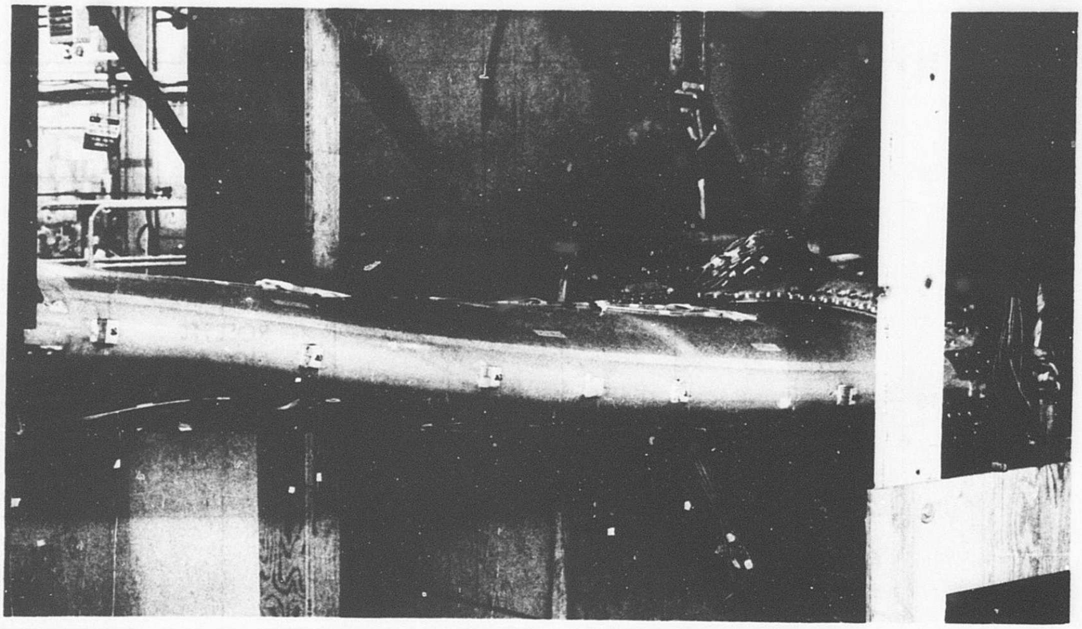

Figure 72. No. 3 Wing Section - Combined Condition: Leading Edge Deflection at 200 Percent DUL.

A tabular comparison of experimental and calculated spanwise stresses under Condition I loading is given in Tables XXV through XLVII in Appendix II. A similar comparison of shear stresses is given in Tables XLVIII through LIX in Appendix II.

For Condition I loading, the highest measured spanwise stresses were in the forward cell at BL 68.0 at rosettes No. 3 and 4. These are plotted in Figure 73 to show the relationship of stress to the applied load. Figure 73 indicates the onset of nonlinearity at about 100 percent DUL on the tension skin and at about 80 percent DUL on the compression skin.

The highest skin shear stresses were at rosette No. 2 on the lower skin of the forward cell at BL 28.0. The shear data from this rosette are plotted in Figure 74 and compared with the calculated shear stress. Shear stress in the main spar web is plotted in Figure 75.

As in Condition II, the spanwise stresses in the upper skin of the forward cell agree best with stresses calculated in the analysis. The exception is at BL 68.0 at rosette No. 3 and gage No. 36, where the measured stresses exceeded the calculated stresses as shown in Figure 73. A tabular comparison is given in Table XXXVI in Appendix II. In addition, as shown in Figure 76, all measured spanwise stresses on the lower skin of the

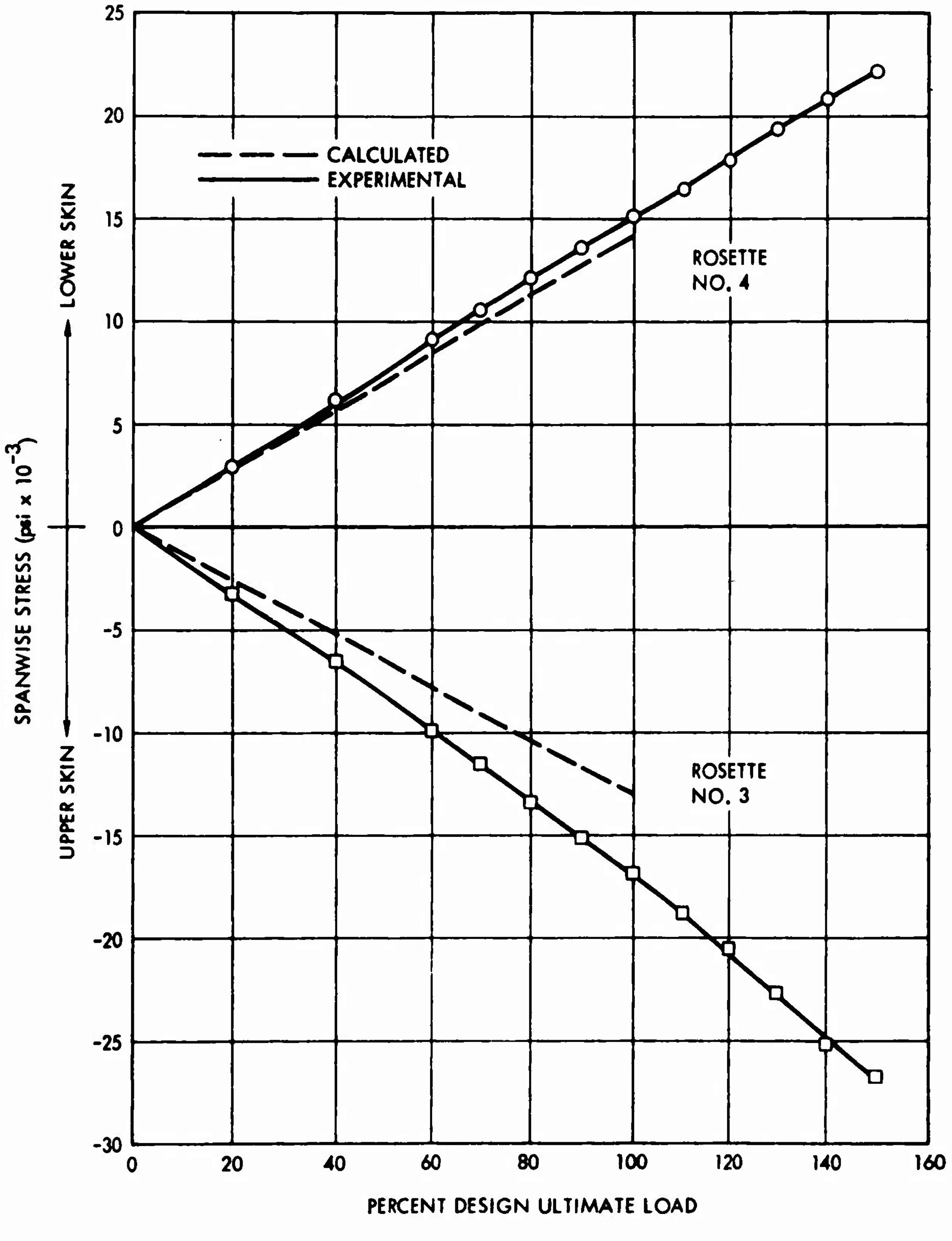

Figure 73. Comparison of Experimental and Calculated Spanwise Stresses in Forward Cell at BL 68.0 Under Condition I Loading.

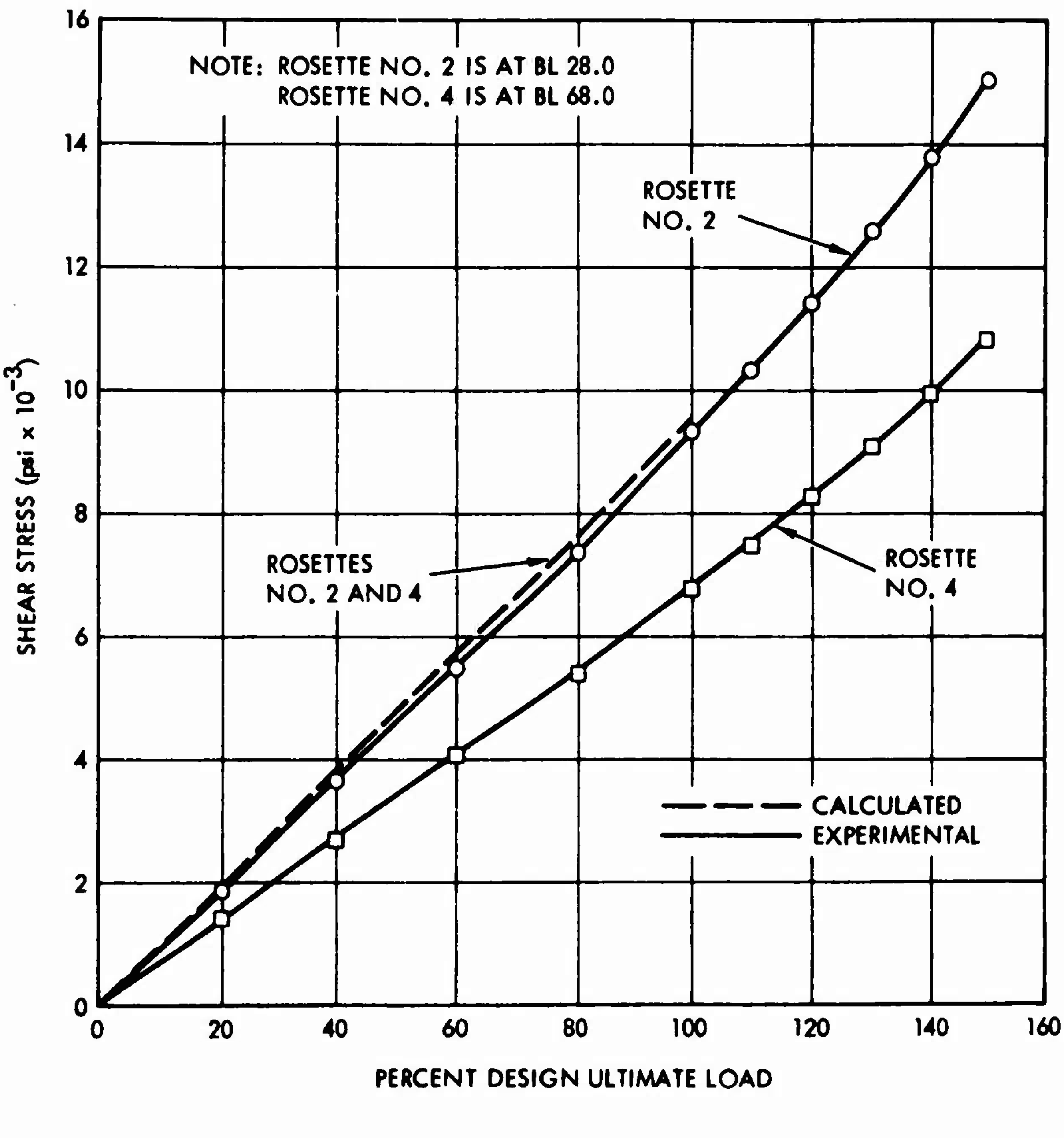

Figure 74. Comparison of Experimental and Calculated Shear Stresses in Lower Skin of Forward Cell at BL 28. 0 and 68. 0 Under Condition I Loading.

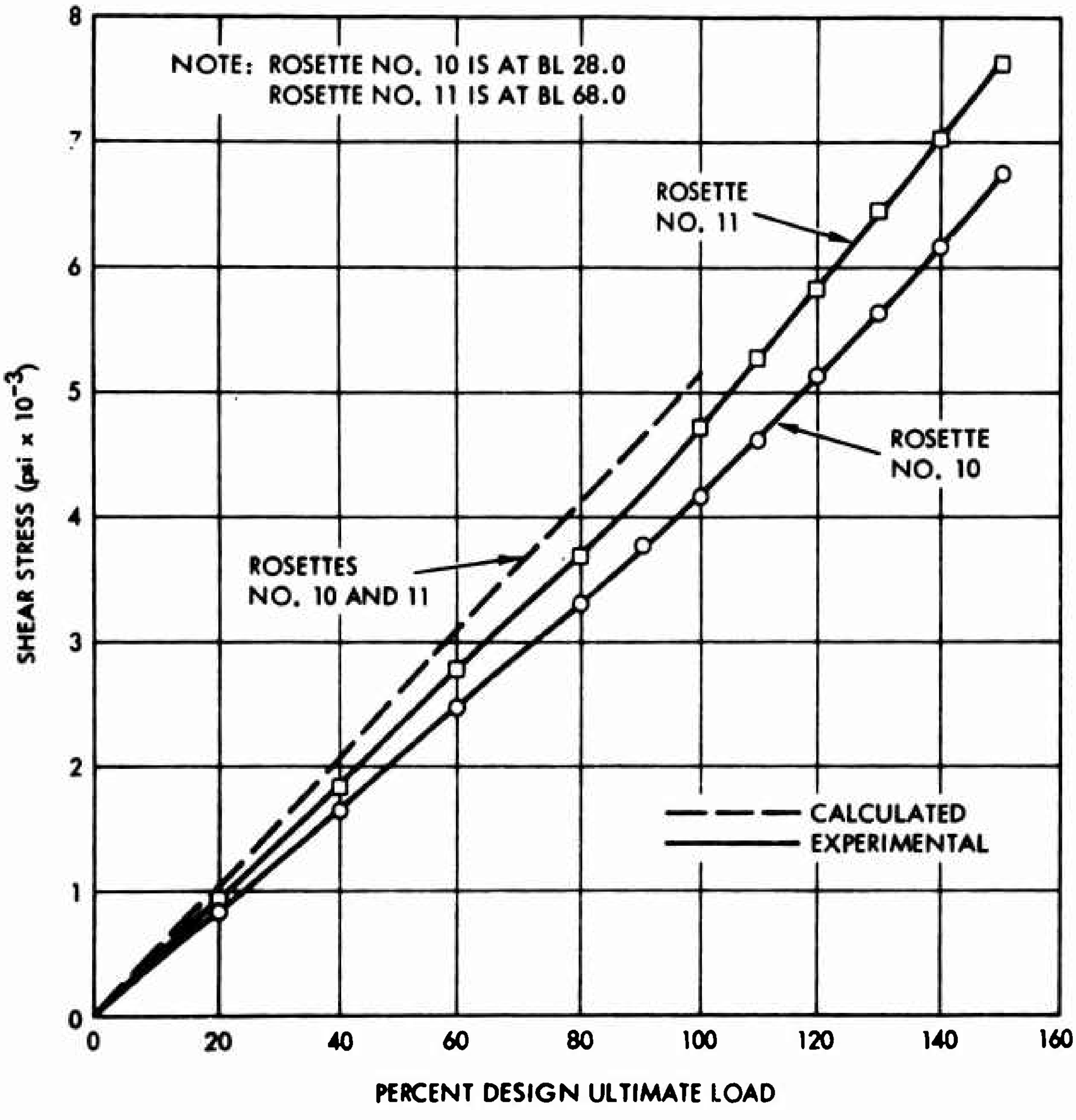

Figure 75. Comparison of Experimental and Calculated Shear Stresses in Main Spar at BL 28.0 and 68.0 Under Condition I Loading.

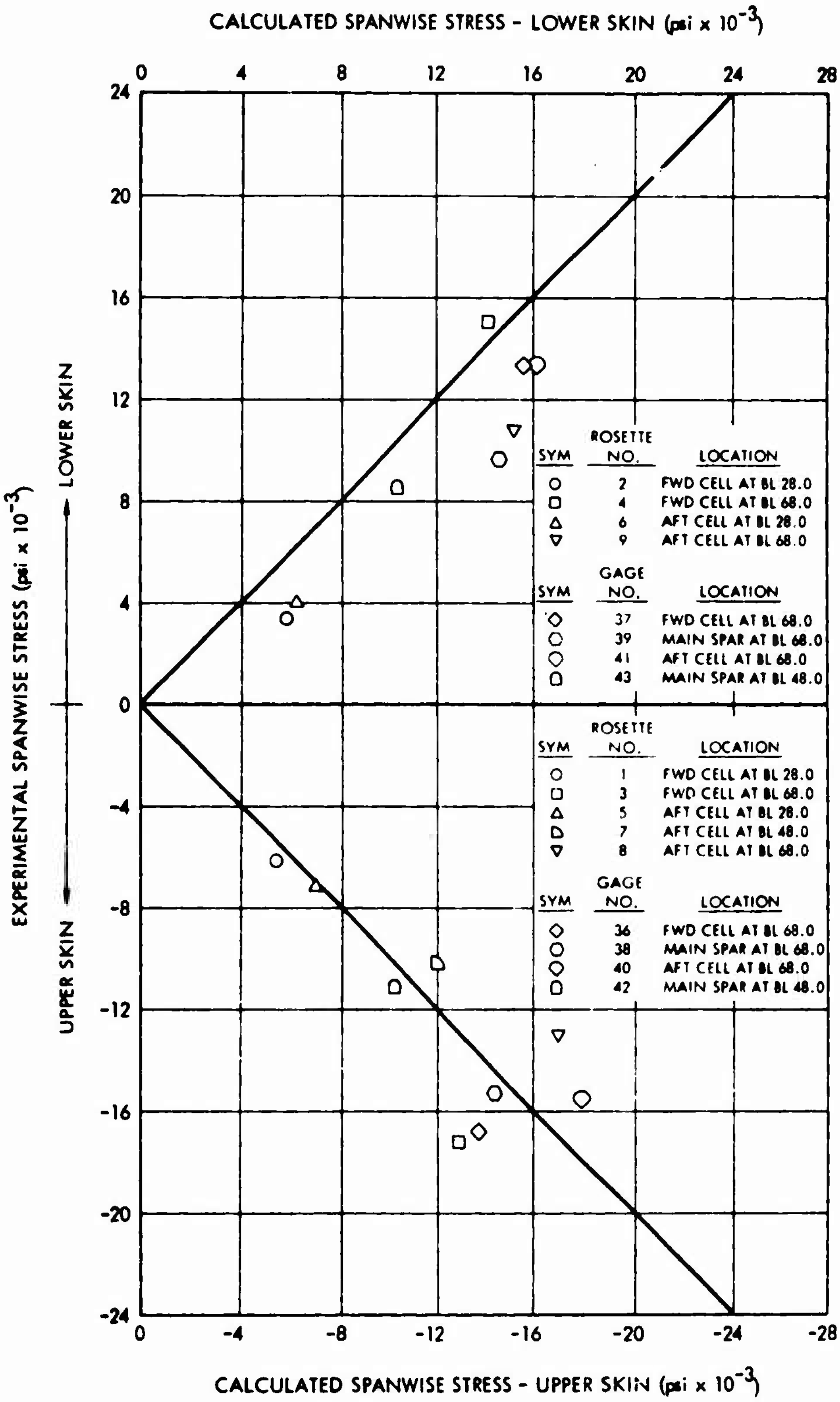

Figure 76. Comparison of Experimental and Calculated Spanwise Stresses Under Condition I Loading at 100 Percent DUL.

forward cell were higher than calculated. At all other points, except at rosette No. 4 on the lower skin of the forward cell, stresses derived from the test were less than calculated at 100 percent DUL. Shear stresses for Condition I loading were less erratic than for Condition II, but still did not compare favorably with test data except on the lower skin at BL 28.0 and on the main and aft spars at BL 68.0 (see Figure 77).

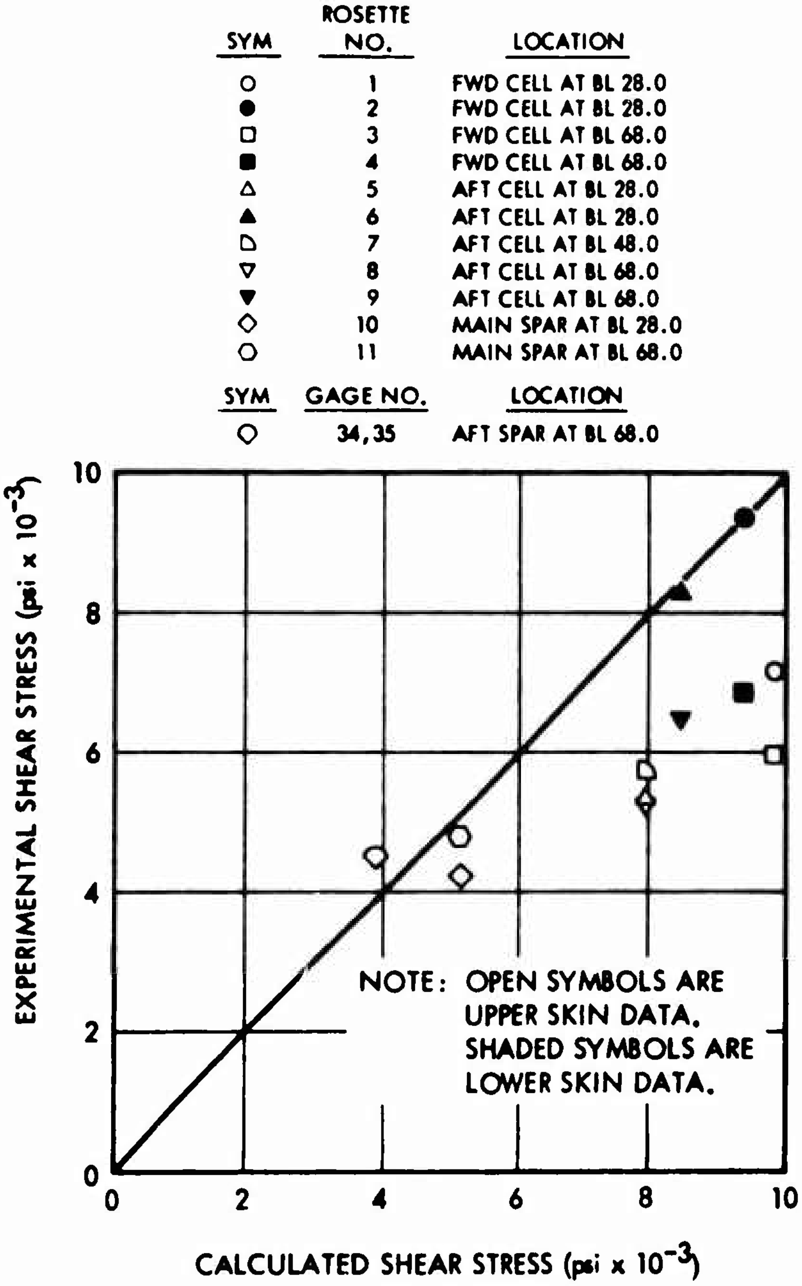

Figure 77. Comparison of Experimental and Calculated Shear Stresses Under Condition I Loading at 100 Percent DUL.

Nonlinearity of spanwise and shear stresses becomes evident at a load level between 80 and 100 percent DUL on all gages and rosettes. Rosettes No. 2 and 4 on the bottom skin at BL 28.0 show a drop in stress level with increasing load beyond 120 percent DUL in the forward cell and 130 percent DUL in the aft cell. Since all gages give this indication of nonlinearity, the structure must have sustained some structural damage below 100 percent DUL, but only to the point that structural stiffness had been affected. This change in stiffness is also apparent in the deflection curves plotted in Figure 78.

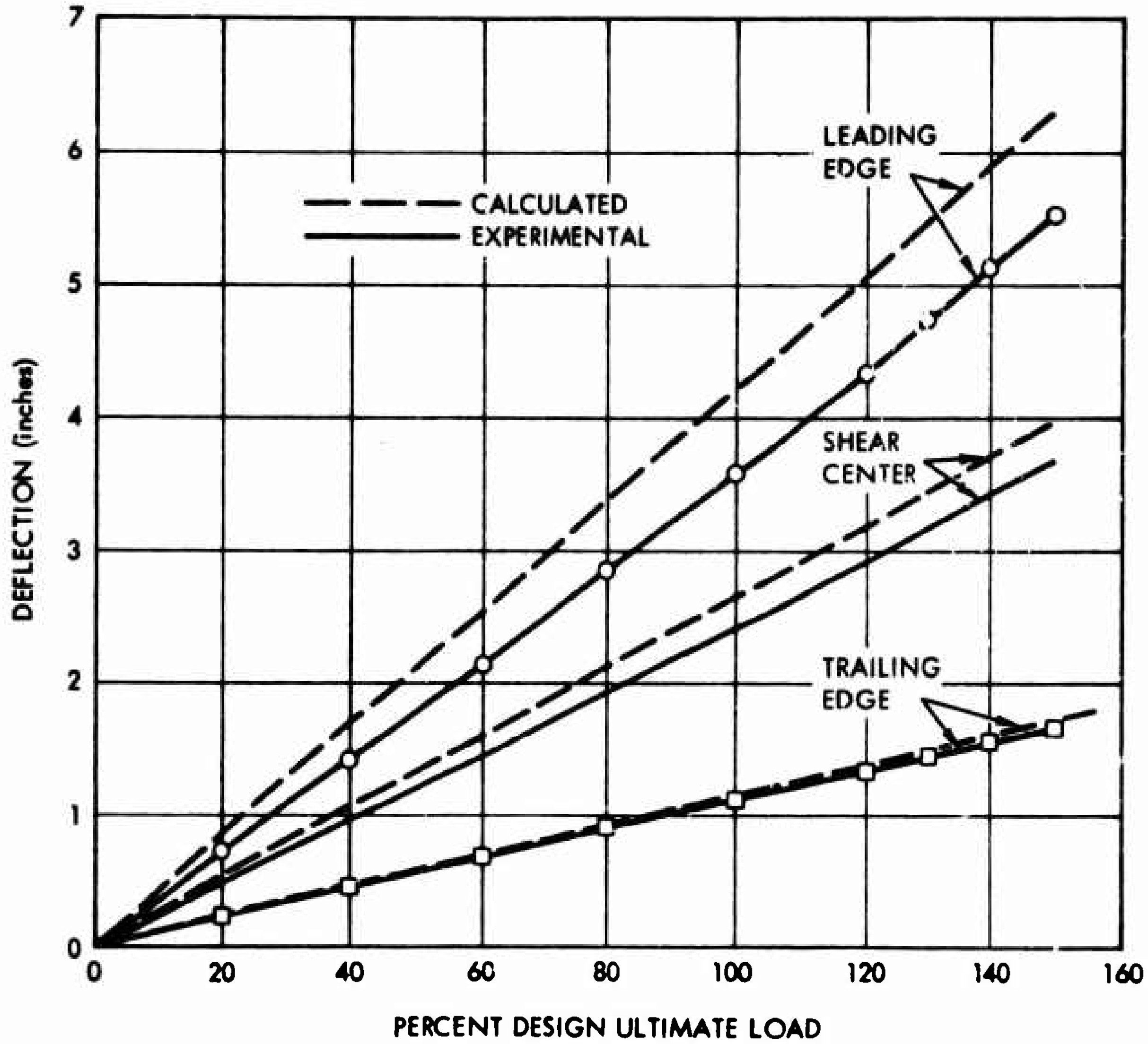

Figure 78. Comparison of Experimental and Calculated Deflection and Twist Data.

Tables XXIII and XXIV are included to show the specimen rotations at various stations along the span during the 100 and 150 percent DUL tests in combined bending and torsion.

TABLE XXIII. MEASURED TWIST ANGLES - CONDITION I LOADING TO 100 PERCENT DUL

Applied Load in Percent DUL	Twist Angle (degrees)							
	Sta 0.0	Sta 6.0	Sta 20.0	Sta 34.0	Sta 42.5	Sta 51.0	Sta 68.0	Sta 83.0
20	0.60	0.55	0.45	0.32	0.25	0.17	0.06	0.00
40	1.18	1.08	0.89	0.64	0.50	0.35	0.12	0.01
60	1.78	1.62	1.34	0.95	0.75	0.53	0.18	0.01
70	2.07	1.91	1.56	1.12	0.87	0.62	0.21	0.02
80	2.40	2.21	1.80	1.29	1.00	0.70	0.24	0.02
90	2.75	2.16	2.05	1.48	1.14	0.81	0.27	0.03
100	3.08	2.84	2.30	1.66	1.28	0.91	0.30	0.03

TABLE XXIV. MEASURED TWIST ANGLES - CONDITION I LOADING TO 150 PERCENT DUL

Applied Load in Percent DUL	Twist Angle (degrees)							
	Sta 0.0	Sta 6.0	Sta 20.0	Sta 34.0	Sta 42.5	Sta 51.0	Sta 68.0	Sta 83.0
20	0.62	0.58	0.47	0.33	0.27	0.19	0.06	0.01
40	1.18	1.12	0.93	0.66	0.52	0.38	0.13	0.01
60	1.80	1.70	1.40	0.99	0.79	0.57	0.19	0.02
80	2.43	2.29	1.87	1.33	1.04	0.76	0.25	0.02
100	3.08	2.90	2.35	1.68	1.30	0.94	0.31	0.03
120	3.75	3.53	2.85	2.04	1.57	1.14	0.37	0.04
130	4.11	3.87	3.11	2.25	1.71	1.24	0.40	0.04
140	4.45	4.20	3.36	2.41	1.84	1.34	0.44	0.05
150	4.84	4.57	3.66	2.60	1.98	1.45	0.47	0.05

CONCLUSIONS AND RECOMMENDATIONS

WING TEST SPECIMEN FABRICATION

Concepts for design and fabrication of the third wing were modifications of those used on the first two wings. The techniques of integrally molding sandwich skin, honeycomb core, spar caps, and shear webs into two large moldings were followed. Refinements were made by substituting unidirectional tapes combined with bidirectional woven fabrics for the previous all-bidirectional fabric layups in the surface panels and spar webs. Additional refinements were made in the surface panels and spar webs to accommodate the attachment of the sandwich rib.

The molding processes again proved their repeatability and reliability by producing parts of exceptional quality.

A departure from the previous designs was taken in the method of attachment of the main components. The third wing contained continuous bonded joints in the spar cap attachment areas rather than the all-bolted joints of the No. 1 and No. 2 wings. Uniform bond lines were obtained by matching mating surfaces. A room-temperature-vulcanizing silicone elastomer was placed between sheets of release film and inserted in the areas of the bond lines. The parts were mated without adhesive, and clamping pressures were applied. The RTV silicone was allowed to set up, and the parts were disassembled. Apparent bond line thicknesses were obtained by measuring the thicknesses of the elastomer. The mating spar cap surfaces were reworked to minimize bond line thickness variations, and the parts were again mated and checked. It is felt that this procedure contributed to the bonded assembly strength displayed by the test specimen.

The dimensional problems associated with part springback from the tooling were again experienced. Springback should be anticipated and allowed for in tool design.

TEST DATA AND DESIGN ANALYSIS CORRELATION

The two rib support boxes failed at load levels reasonably close to the predicted values. However, in the one case, there is a suggestion that preliminary failure - perhaps of a bond line - occurred at a lower load, but catastrophic failure was prevented by the redundancy of hat to skin attachments, i. e., the combination of adhesive and bolts. In both of these boxes, poor correlation was achieved between calculated and measured shear stresses, where the measured shear stresses are actually calculated by conversion of strain measurements to stress values by the use of material properties. Nevertheless, both methods of rib construction and attachment proved feasible and structurally adequate.

Some of the results of the full wing cross-sectional specimen test were encouraging and some were disappointing.

With respect to deflections, measurements indicate that the section is stiffer in bending and torsion than calculated. For example, in the bending test, measured tip deflection was only 86.5 percent of the predicted value. This corresponds to a stiffness 16 percent greater than that calculated. Similarly, at 100 percent DUL in torsion and bending, an angle of twist at the tip of 4.19 degrees was calculated, whereas an angle of 3.08 degrees was measured. Based on this comparison, the torsional stiffness is almost 36 percent greater than calculated.

However, comparing torsional stiffness at various stations gives better agreement with calculations. For example, the torsional stiffness indicated by the differences in readings between stations 20.0 and 51.0 is approximately 11,200,000 lb-in.^{2} per degree of twist, whereas the value effectively calculated for the section is 10,030,000 lb-in.^{2} per degree of twist. The larger discrepancy at the tip is probably due to the fact that the reinforcements were neglected in the twist angle calculations.

Therefore, reasonable agreement was obtained between the calculated and measured section stiffnesses in bending and torsion, although a better comparison with the measured bending stiffness would have been preferred.

The strain gage showing the measured stress higher than calculated by the largest amount was rosette No. 3 (upper skin of forward cell at BL 68.0) during the Condition I (bending plus torsion) test. During this test, the gages indicated a stress of -17,270 psi rather than the -13,000 psi calculated. However, during the Condition II (bending only) test, this same rosette indicated a stress of -18,380 psi as compared with a calculated stress of -18,650 psi, which is less than a 2-percent difference.

A similar occurrence is noted at other rosette locations. During the Condition I test, greater disagreement between measured and calculated spanwise stresses occurs than during the Condition II test and at lower stress levels. This suggests that (1) some change took place in the structure during the Condition II test that altered the elastic behavior of the skins, or (2) the presence of higher skin shear stresses due to torque during the Condition I loading had the same effect.

In general, there appeared to be better agreement between experimental and calculated stresses on the compression skin. On the tension side, all rosettes gave lower spanwise stresses than calculated during both the Condition I and Condition II tests.

Skin shear stresses were in very poor agreement with predicted values, and in some areas were totally erratic in response to load application. Although more well-behaved, spar web shear stresses also fell short of calculations.

By far the most difficult strain readings to understand are the single gages on the upper and lower spar caps of the main spar. These readings, given in Tables XLIV through XLVII in Appendix II, are compared with calculated stresses from the section analysis. Not only are absolute values of the stresses less than calculated, but tensile strains recorded on the compression surface and compression strains recorded on the tension side of the wing are questionable and were not used in any other data reduction.

The minimum margin of safety determined for the wing is 0. 27 and is based on shear failure in the bond between the hat section and the lower skin. The allowable shear stress was conservatively taken as 1000 psi, although adhesive tests have shown values of 2300 psi. Therefore, at the higher strength, failure would occur at 293 percent of DUL.

The second lowest margin of safety is +0. 35. This value is based on a shear stress of 6645 psi in the unidirectional tapes in the upper skin of the aft cell at element No. 52 and is caused by the combined bending and torque loading. The strain rosette closest to this element is No. 8, which is located between elements No. 53 and No. 54, where the calculated skin shear stress is 7990 psi. Measured shear stress was 5200 psi. Also, the measured axial stress was -13, 000 psi compared with -17, 100 psi calculated. Based on the measured strains, the tape shear stress was 3328 psi rather than 6645 psi, so that the margin of safety was +1. 70 rather than +0. 35.

Stresses in the spar caps were also evidently much lower than calculated based on the readings of the single gages and would invalidate the +0. 51 margin of safety based on spar tension failure.

The remaining two margins of safety, which predict failure prior to 200 percent DUL, are based on stability calculations for the upper skin. From Figures 64 and 76 it is noted that compressive stresses in the aft cell - where buckling is predicted - are less than calculated. The same is true for the shear stresses shown in Figures 65 and 77.

In addition to the general discrepancy between measured and calculated stresses, the nonlinear response of the strain gages indicates a redistribution of stresses that would permit alleviation of high stress areas and subsequent increase in the failing load. Both factors contributed to the capability of the wing to survive the 200-percent-DUL condition.

One of the most perplexing results of the testing is the discrepancy in spanwise stress levels at certain rosette locations during the two different loading conditions but at the same value of bending moment. For example, to compare actual applied moments rather than percent design ultimate load, bending stresses at 100 percent DUL for Condition I can be compared approximately with 70 percent DUL for Condition II. These values correspond to a moment of 600, 000 in. -lb for Condition I and a moment of 603, 750 in. -lb for Condition II. In general, compression stresses are higher for Condition I than for Condition II, whereas tensile stresses tend to behave in the opposite way. This would suggest a shift and rotation in the neutral axis position between the two tests. A further indication that this happened can be seen by an examination of the readings recorded from the strain rosettes on the main spar web.

On the basis of these tests, it can be concluded that laminated composite elastic properties can be determined with a reasonable degree of accuracy from the combination of composite theory and the application of small specimen unidirectional test results. As with the previous specimens, the most questionable correlation relates to panel shear properties. Since sandwich construction was used, the layer of filleting resin between the skins and the core may have had some influence on the effective skin thickness and, consequently, the recorded stresses and section stiffnesses in shear.

If the spar cap stresses as recorded are correct, the method of analysis was apparently inadequate in this area and needs refinement. This is true even if only the signs are incorrect, since the areas are not as effective as assumed. In any event, for this type of construction a more detailed analysis of these areas is recommended.

REFERENCES CITED

1. Bauch, Fred E., Nordlie, Robert W., and Lair, Robert C., FABRICATION AND TESTING OF THE COMPOSITE MATERIALS AIRCRAFT WING SECTION, Goodyear Aerospace Corporation, Akron, Ohio; USAAVLABS Technical Report 68-66, U. S. Army Aviation Materiel Laboratories, Fort Eustis, Virginia, September 1968.

2. PROPOSAL FOR COMPOSITE MATERIALS AIRCRAFT WING SECTION FABRICATION AND TEST, Goodyear Aerospace Corporation, Akron, Ohio, GAP-3417S/9, 21 March 1967.

3. BUCKLING COEFFICIENTS FOR SIMPLY SUPPORTED AND CLAMPED FLAT, RECTANGULAR SANDWICH PANELS UNDER EDGEWISE COMPRESSION, Forest Products Laboratory, Forest Service, U. S. Department of Agriculture, FPL-070, December 1964.

4. SUMMARY REPORT ON STATIC TESTS OF GAC RIB-SUPPORT BOXES, Naval Air Development Center, Aero Structures Department, Johnsville, Warminister, Pennsylvania.

5. MANUFACTURING METHODS FOR PLASTIC AIRFRAME STRUCTURES BY FILAMENT WINDING, AFML-TR-68-378, Air Force Materials Laboratory, Air Force Systems Command, Wright-Patterson Air Force Base, Ohio, March 1969.

6. Bauch, Fred E., Nordlie, Robert W., and Lair, Robert C., APPLICATION OF COMPOSITE MATERIALS TO AN AIRCRAFT WING SECTION, Goodyear Aerospace Corporation, Akron, Ohio; NADC-ST-6903, Naval Air Development Center, Johnsville, Warminister, Pennsylvania, November 1969.

7. PROCESS SPECIFICATION, MANUFACTURE OF POSITIVE PRESSURE MOLDED PREIMPREGNATED EPOXY GLASS CLOTH AND TAPE FACED METAL HONEYCOMB CORE STRUCTURAL SANDWICH, Goodyear Aerospace Corporation, Akron, Ohio, GER-14321, 15 August 1969.

APPENDIX I
PROCESS SPECIFICATION FOR THE MANUFACTURE OF POSITIVE PRESSURE MOLDED PREIMPREGNATED EPOXY GLASS CLOTH AND TAPE FACED METAL HONEYCOMB CORE STRUCTURAL SANDWICH*

TABLE OF CONTENTS

*The process specification in this appendix is presented in the same format as the GAC specification.[7]

1. SCOPE

1.1 This specification establishes the materials and processing for structural parts fabricated by a multistage sandwich process.

2. REFERENCE DOCUMENTS

2.1 Military

MIL-A-5090	Adhesive, Airframe Structural, Metal to Metal
MIL-C-7438	Core Material; Aluminum Honeycomb
MIL-P-25421	Plastic Materials, Glass Fiber Base - Epoxy Resin, Low-Pressure Laminated
MIL-R-9300	Resin Epoxy, Low-Pressure Laminating
MIL-STD-401	Sandwich Construction and Core Materials; General Test Method

2.2 Goodyear Aerospace Corporation (GAC)

CL1	Cleaning
M69	Screw Thread Inserts

3. GENERAL REQUIREMENTS

3.1 Materials

3.1.1 The materials listed below are incorporated into the part during fabrication and shall be certified to meet the requirements stated herein.

	Materials	Sources
3.1.1.1	Epoxy Prepreg E293-1581-s/901 Resin Content - Dry - 36 ± 2% Gel Time 50 - 90 sec at 325°F Volatiles 2 - 4% at 325°F Flow 13 - 18% at 325°F and 60 psi	Cordo Div. of Ferro Corp. Norwalk, Conn.

	Materials	Sources
3.1.1.2	Epoxy Prepreg Tape - E293-s/901 Resin Content - Dry 33 ±2% Gel Time 50 - 90 sec at 325°F Volatiles 2 - 4% at 325°F Flow 13 - 18% at 325°F and 60 psi	Cordo Div. of Ferro Corp. Norwalk, Conn.
3.1.1.3	Liquid Epoxy Resin DER 332	Dow Chemical Co. Midland, Mich.
3.1.1.4	Curing Agent A	Shell Chemical Co. Pittsburg, Calif.
3.1.1.5	Adhesive, Bondmaster M602-1, M602-2	Pittsburgh Plate Glass Co. Adhesive Products Div. Pittsburgh, Pa.
3.1.1.6	Glass Microballoon Spheres IG101	Sohio Chemical Co. Microballoons Spheres Div. Midland Bldg. Cleveland, Ohio
3.1.1.7	Aluminum Honeycomb 1/8-0.001-5052H39	Hexcell Products, Inc. Havre de Grace, Md.
3.1.1.8	Diethanolamine	Union Carbide Corp. New York, New York
3.1.1.9	Cab-O-Sil	Cabot Corp. Boston, Mass.
3.1.1.10	Glacial Acetic Acid	E.I. DuPont de Nemours & Co. Wilmington, Del.
3.1.1.11	Epon 921 Adhesive	Shell Chemical Co. Pittsburg, Calif.

3.1.2 The materials listed below are not incorporated into the product. Certification of these materials is not required.

	Materials	Sources
3.1.2.1	Vacuum Bag Material PVA (Polyvinyl Alcohol) Film	Reynolds Company Grottoes, Virginia
3.1.2.2	Parting Agents	
	Teflon FEP Fluorocarbon Film	E. I. DuPont de Nemours Co. Film Dept. Wilmington, Del.
	Release Agent Ramm 225 Release Agent Ramm 334	Dacco Inc. Cleveland, Ohio
3.1.2.3	Surface Bleeder - Glass Cloth 128	Open
3.1.2.4	Edge Bleeder - Glass Cloth TG30	Open
3.1.2.5	Peel Ply - Dacron Fabric 15,004	Stern & Stern Textiles Inc. Hornell, N. Y.
3.1.2.6	Sealing Compound, Presstite 587	Interchemical Co. Presstite Div. St. Louis, Mo.
3.1.2.7	MEK (Methylethyl ketone)	Open
3.1.2.8	Acetone	Open
3.1.2.9	Naphtha	Open
3.1.2.10	Gloves, white, lightweight, knitted	Open
3.1.2.11	Thermocouple Wire, Iron-Constantan 12432P 30 gauge or finer	Open

3.2 Storage and Handling of Materials

3.2.1 The preimpregnated (prepreg) material is fully catalyzed and ready for use. It shall be packaged with an interlayer of polyethylene film or equivalent, and the fabric roll or tape sheets shall be wrapped in a cover of laminated Kraft paper, polyethylene film, and aluminum foil. The fabric prepreg shall be suspended horizontally by its core. The tape prepreg sheets shall be firmly secured to the base of a flat wood carton. After removal from refrigeration, the material shall be brought to room temperature before its protective wrapping is removed.

3.2.2 Honeycomb shall be stored in clean, dry areas and shall not be contaminated by moisture, dirt, or other substances. After vapor degreasing and prior to priming, it shall be handled only by persons wearing white gloves.

3.3 Facilities Control

3.3.1 Autoclave - A heated air, circulating autoclave shall be used to provide the temperature and pressures required by Section 5.6.1 of this specification.

3.3.2 Oven - An air circulating oven shall be used to provide the temperature required by Sections 4.1.3.4, 4.1.3.5, 4.1.4.5, 5.3.8, and 5.3.13 of this specification.

3.3.3 Layup Area - All prepreg layups shall be accomplished in a temperature- and humidity-controlled room.

Limits - Temperature $75^{\circ} \pm 5^{\circ}F$
Relative Humidity 55% (Max)

3.4 Tools

3.4.1 The parts shall be fabricated so that the aerodynamic skin is adjacent to the mold surface.

3.4.2 The mold surface shall be nonporous and shall be free of cracks, pits, and any other irregularities which would affect the quality of the part.

3.4.3 Plastic molds are suitable for fabrication of parts to this specification. The material on the mold surface should be completely nonreactive with the resin used in the part. The mold should be unaffected by the conditions of the cure.

3.4.4 In-Process Control Forms - A GAC process control form outlining the fabrication steps and materials used must be prepared for each item produced to this specification.

4. PREPARATION OF MATERIALS

4.1 Honeycomb Materials

4.1.1 In cases where core forming is required, this forming shall be accomplished prior to the core priming operation.

4.1.2 Prior to priming, all honeycomb core material shall be vapor-degreased. The core shall receive its first primer coat within 24 hours after it has been vapor-degreased.

4.1.3 Core Priming

4.1.3.1 Mix Resin M602

Part I 100 pbv
Part II 80 pbv

(Continue to stir batch while using to assure good mixture.)

4.1.3.2 Roller coat each piece 3 times, each side. Each coat is to be applied with roller strokes at approximately 120° to previous stroke (allow approximately 30 minutes between coats).

4.1.3.3 After last coat - air dry

1 hr (min)
72 hr (max)

4.1.3.4 Oven dry 1 hr at 200° - $225^{\circ}F$.

4.1.3.5 Cure 45 - 50 minutes at 325° ±50°F.

4.1.3.6 Cover each cured piece with a protective film and store in a clean, dry area.

4.1.4 Core Stabilization

4.1.4.1 Trim primed honeycomb to drawing dimensions.

4.1.4.2 Mix resin

Epoxy Resin DER 332	64.6	pbw
Glass Microballoons IG101	27.6	pbw
Cab-O-Sil	3.0	pbw
Glacial Acetic Acid	0.44	pbw
Diethanolamine	0.76	pbw
Curing Agent A	4.5	pbw

4.1.4.3 Fill honeycomb edges to drawing dimensions with above resin mix.

4.1.4.4 Cure 8 hours minimum at room temperature.

4.1.4.5 Oven cure 2 hours at 250° ±10°F.

4.1.4.6 Cool to below 125°F, remove flash, and clean up part.

4.1.4.7 Cover each stabilized piece with a protective film and store in a clean, dry area.

4.2 Preparation of Mold

4.2.1 Parting agents (mold release) per Section 3.1.2.2 shall be applied to the tool surface and allowed to dry.

5. FABRICATION PROCEDURE

5.1 Layup Procedure - Surface Panels, Spars, and Spar Caps (warp direction for all fabric plies and filament direction for all tape plies shall be specified on the part drawing).

5.1.1 The prepreg material per Sections 3.1.1.1 (E293-1581) and 3.1.1.2 (E293 Tape) shall be carefully positioned in the mold.

5.1.2 Position the necessary number of E293-1581 plies to obtain doubler thicknesses consistent with drawing requirements. There must be no cutting of doubler plies directly over other plies of the layup. Any evidence of this practice shall be cause for immediate rejection of the part.

5.1.3 Cover the entire layup with FEP film.

5.1.4 Apply surface bleeder in accordance with Section 5.4.1.

5.1.5 Apply edge bleeder in accordance with Section 5.4.2

5.1.6 Bag layup, 3-mil PVA, and apply vacuum pressure.

5.1.7 Allow layup to remain under vacuum pressure at room temperature for 12 hours (min).

5.1.8 Remove vacuum, bag, bleeder, and FEP film.

5.1.9 Locate honeycomb core material on skin and doubler layups.

5.1.10 Cover exposed honeycomb surfaces with FEP film.

5.1.11 Trim prepreg material per Section 3.1.1.1 (E293-1581) to drawing dimensions for layup in cap strip and edge band areas.

5.1.12 Carefully position the necessary number of plies of E293-1581 material to obtain the required cap strip and edge band thickness for this operation.

5.1.13 Cover all exposed prepreg with a peel ply of Dacron cloth.

5.1.14 Cover peel ply with FEP film.

5.1.15 Apply surface bleeder in accordance with Section 5.4.1.

5.1.16 Apply edge bleeder in accordance with Section 5.4.2

5.1.17 Install thermocouple wire into edge of part outside of part-net-trim line.

5.1.18 Bag part (6 mil PVA), and apply pressure per Section 5.5.1.

5.1.19 Cure part per Section 5.6.1.

5.1.20 Remove bag, bleeder, FEP film, and peel plies.

5.1.21 Locate vent positions per process card, and drill 3/32-in.-dia holes through the honeycomb stabilizing syntactic foam into honeycomb panel to facilitate venting.

5.1.22 Trim prepreg material per Section 3.1.1.1 (E293-1581) to drawing dimensions for layup in cap strip and edge band areas.

5.1.23 Carefully position the necessary number of plies of E293-1581 material to bring cap strips and edge bands to final thickness.

5.1.24 Layup inner skin plies of prepreg material per Sections 3.1.1.1 (E293-1581) and 3.1.1.2 (E293 Tape) over honeycomb, cap strips, and edge band areas.

5.1.25 Position the necessary number of E293-1581 plies to obtain doubler thicknesses consistent with drawing requirements.

5.1.26 Position the necessary number of E293-1581 plies to obtain edge reinforcement thicknesses consistent with drawing requirements.

5.1.27 Cover cap strip areas and rib attachment doublers with a peel ply of Dacron.

5.1.28 Cover entire assembly with perforated FEP film.

5.1.29 Apply surface bleeder in accordance with Section 5.4.1.

5.1.30 Apply edge bleeder in accordance with Section 5.4.2.

5.1.31 Install thermocouple wire into edge of part outside of part-net-trim line.

5.1.32 Bag part (6-mil PVA), and apply pressure per Section 5.5.1.

5.1.33 Cure part per Section 5.6.1.

5.1.34 Remove bag, bleeder FEP film, and peel ply.

5.1.35 Remove part from mold.

5.1.36 Abrade mold surface of part which is to receive secondary edge reinforcement layup.

5.1.37 Mask areas of part which do not receive above layups to protect against excess resin flow.

5.1.38 Position the necessary number of E293-1581 plies to obtain an edge reinforcement thickness consistent with drawing requirements.

5.1.39 Cover layup with FEP film.

5.1.40 Apply surface bleeder in accordance with Section 5.4.1.

5.1.41 Apply edge bleeder in accordance with Section 5.4.2.

5.1.42 Install thermocouple wire into edge of part outside of part-net-trim line.

5.1.43 Bag part (6-mil PVA), and apply pressure per Section 5.5.1.

5.1.44 Cure part per Section 5.6.1.

5.1.45 Remove bag, bleeder, and FEP film, and clean up part.

5.2 Layup Procedure - Rib (warp direction for all plies shall be specified on the part drawing).

5.2.1 The prepreg material per Section 3.1.1.1 (E293-1581) shall be carefully positioned on the layup plate to make the rib outer (mold side) skin.

5.2.2 Locate honeycomb core material on skin layup.

5.2.3 Lay up inner (bag side) skin plies of prepreg material per Section 3.1.1.1 (E293-1581) over honeycomb.

5.2.4 Position the necessary numbers of E293-1581 plies to obtain doubler thicknesses consistent with drawing requirements.

5.2.5 Cover doubler plies with a peel ply of Dacron cloth.

5.2.6 Cover the entire assembly with perforated FEP film.

5.2.7 Apply surface bleeder in accordance with Section 5.4.1.

5.2.8 Apply edge bleeder in accordance with Section 5.4.2.

5.2.9 Install thermocouple wire into edge of part outside of part-net-trim line.

5.2.10 Bag part (6 mil PVA), and apply pressure per Section 5.5.1.

5.2.11 Cure part per Section 5.6.1.

5.2.12 Remove bag, bleeder, FEP film, and Dacron peel ply.

5.2.13 Abrade mold surface of part which is to receive secondary doubler layup.

5.2.14 Mask areas of part which do not receive above layups to protect against excess resin flow.

5.2.15 Locate vent positions per process card, and drill 3/32-in.-dia holes through the honeycomb stabilizing syntactic foam into honeycomb panel to facilitate venting.

5.2.16 Position the necessary number of E293-1581 plies to obtain doubler thicknesses consistent with drawing requirements.

5.2.17 Cover doubler plies with a peel ply of Dacron cloth.

5.2.18 Cover peel ply with FEP film.

5.2.19 Apply surface bleeder in accordance with Section 5.4.1.

5.2.20 Apply edge bleeder in accordance with Section 5.4.2.

5.2.21 Install thermocouple wire into edge of part outside of part-net-trim line.

5.2.22 Bag part (6 mil PVA), and apply pressure per Section 5.5.1.

5.2.23 Cure part per Section 5.6.1.

5.2.24 Remove bag, FEP film, and peel ply.

5.2.25 Trim rib assembly to fit wing inside contours with 0.090 inch clearance.

5.2.26 Mask areas of part which do not receive secondary edge reinforcement layups to protect against excess resin flow.

5.2.27 Position the necessary number of E293-1581 plies to obtain an edge cap reinforcement thickness consistent with drawing requirements.

5.2.28 Cover edge cap layup with a peel ply of Dacron cloth.

5.2.29 Cover layup with FEP film.

5.2.30 Apply surface bleeder in accordance with Section 5.4.1.

5.2.31 Apply edge bleeder in accordance with Section 5.4.2.

5.2.32 Install thermocouple wire into edge of part outside of part-net-trim line.

5.2.33 Bag part (6-mil PVA), and apply pressure per Section 5.5.1.

5.2.34 Cure part per Section 5.6.1.

5.2.35 Remove bag, bleeder, FEP film, and peel ply, and clean up part.

5.3 <u>Assembly Procedure</u>

5.3.1 Trim part in accordance with Section 5.7.1 to final trim dimensions.

5.3.2 Assemble parts and match drill in accordance with drawing requirements and the requirements of Section 5.7.2.

5.3.3 Disassemble parts

5.3.4 Mix Resin - Epoxy Adhesive Epon 921, Part A, 100 pbw
Part B, 25 pbw.

5.3.5 Apply above resin mix to mating surfaces of cap strips (upper forward spar cap, lower forward spar cap, and lower aft spar cap).

5.3.6 Assemble leading edge part (upper forward panel and lower panels) to hat part (forward spar, upper aft panel, and aft spar).

5.3.7 Install clamping screws at cap strips.

5.3.8 Oven cure 2-1/2 hours at $140^{\circ} \pm 10^{\circ}$F.

5.3.9 Install aft and forward cell rib assemblies.

5.3.10 Install forward rib to forward spar attachment angles.

5.3.11 Mix resin per Section 5.3.4.

5.3.12 Inject resin mix into 0.040-inch clearance spaces between ribs and spar webs and between ribs and surface panels.

5.3.13 Oven cure 2-1/2 hours at $140^{\circ} \pm 10^{\circ}$F.

5.4 <u>Application of Bleeders</u>

5.4.1 <u>Surface Bleeder</u>

5.4.1.1 Place 128 glass cloth bleeder as required over FEP film. The bleeder shall be tailored as required to make intimate contact with the layup. No bridging is to be tolerated, and the glass bleeder should extend sufficiently beyond the edge of the part to contact the edge bleeder, which serves as the direct connection to the vacuum line.

5.4.2 Edge Bleeder

5.4.2.1 Edge bleeder may be made from rolled strips of TG30 glass fabric.

5.4.2.2. Place edge bleeder around the edge of the layup. Edge bleeders shall not be in direct contact with the layup; rather, they shall be separated by a layer of FEP film.

5.5 Application of Pressure

5.5.1 Vacuum Pressure

5.5.1.1 Vacuum pressure is applied to the part by the use of a bag or diaphragm made using polyvinyl alcohol.

5.5.1.2 A sealing compound per Section 3.1.2.6 shall be used to effect a seal between the prepared form and the diaphragm.

5.5.1.3 Slowly apply full plant vacuum (22 inches of mercury, minimum) to the interior of the vacuum bag. As the air is evacuated, make the bag conform to the shape of the part and keep wrinkles to a minimum. Wrinkling of the surface bleeder under the bag shall not be allowed.

5.5.1.4 There shall be no bridging of the fabric of the part, the bleeder cloth, or the bag material. Elimination of bridging can best be accomplished by performing a squeegee operation employing a Teflon paddle having generously radiused edges. If any holes develop in the bag, they must be sealed immediately with cellulose tape.

5.6 Cure

5.6.1 Autoclave Cure

5.6.1.1 All temperatures referred to are part temperatures as taken by a thermocouple imbedded in the part.

5.6.1.2 Place the assembly, while under vacuum pressure, in the autoclave and apply 50 ±5 psi positive pressure into the autoclave cavity. When the autoclave pressure reaches 15 ±5 psi, vent the vacuum to atmosphere.

5.6.1.3 Heat the part to $160^{\circ} \pm 10^{\circ}F$ at the rate of 2° - $4^{\circ}F$ per minute and hold for 30 minutes ±5 minutes.

5.6.1.4 Heat from 160° to $250^{\circ} \pm 10^{\circ}F$ at a rate not to exceed 2° per minute and hold for a minimum of 30 minutes.

5.6.1.5 Heat from 250° to $290^{\circ} \pm 10^{\circ}F$ at a rate not to exceed 1° per minute, and cure for a minimum of 2 hours.

5.6.1.6 Apply full plant vacuum and depressurize autoclave.

5.6.1.7 Remove part from autoclave.

5.6.1.8 Cool under vacuum until part is $125^{\circ}F$ or less.

5.7 <u>Finishing</u>

5.7.1 Trimming shall be accomplished in such a manner that delamination and scorching of the part edges do not occur.

5.7.2 Drilling and countersinking shall be accomplished with carbide-tipped drills, or equivalent, and the material shall be properly clamped to minimize delamination around drilled holes.

6. QUALITY CONTROL

6.1 The prepreg shall be tested for compliance with MIL-P 25421. The resin shall be approved under MIL-R-9300, and the honeycomb shall be purchased to MIL-C-7438.

6.2 Temperature checks shall be run on curing ovens periodically to establish and maintain satisfactory operation. The autoclave shall also be checked for proper operating conditions.

6.3 A quality control check shall be run biweekly on all prepreg skin material. This shall be in the form of a gel time check. Gel time must not exceed 1 minute 30 seconds when run at 60 psi and at 325°F. Skin layup date, roll number and batch number, gel time, and gel time check date shall be entered on the process control card for each skin layup of each part.

6.4 Autoclave temperature and pressure shall be recorded for each autoclave cure. Part temperatures shall be recorded for each autoclave cure to verify compliance with Section 5.6.1.

6.5 A running recording shall be kept of the temperature and relative humidity of the part layup room. The record must confirm that the conditions as set forth in Section 3.3.3 are met.

APPENDIX II
COMPARISON OF EXPERIMENTAL AND CALCULATED SPANWISE AND SHEAR STRESSES

This appendix presents a tabular comparison of experimental and calculated spanwise and shear stresses. Data are given for both Condition I (bending plus torsion) and Condition II (bending only) loading. Spanwise stress data for both loading conditions are given in Tables XXV through XLVII. Shear stress data for both loading conditions are given in Tables XLVIII through LIX.

TABLE XXV. COMPARISON OF EXPERIMENTAL AND CALCULATED SPANWISE STRESSES AT ROSETTE NO. 1 (UPPER SKIN OF FORWARD CELL AT BL 28.0)

Percent DUL	Condition II Stresses (psi)			Condition I Stresses (psi)				
	Test Results		Stress Analysis	Test Results				Stress Analysis
	Run No. 1	Run No. 2		Run No. 1	Run No. 2	Run No. 3	Run No. 4	
10	-766	-756	-768	-525	-	-	-	-535
20	-2135	-1479	-1536	-1152	-1183	-1203	-1,251	-1,070
30	-2904	-2234	-2304	-1675	-	-	-	-1,605
40	-3603	-2965	-3072	-2248	-2362	-2294	-2,383	-2,140
50	-4343	-3669	-3840	-2858	-	-	-	-2,675
60	-	-4402	-4608	-	-3545	-3498	-3,634	-3,210
70	-	-5039	-5376	-	-4191	-	-	-3,745
80	-	-5864	-6144	-	-4827	-4742	-4,900	-4,280
90	-	-6811	-6912	-	-5495	-	-	-4,815
100	-	-7531	-7680	-	-6153	-6011	-6,209	-5,350
110	-	-	-	-	-	-6688	-	-5,885
120	-	-	-	-	-	-7412	-7,610	-6,420
130	-	-	-	-	-	-8178	-8,376	-6,955
140	-	-	-	-	-	-8895	-9,072	-7,490
150	-	-	-	-	-	-	-9,809	-8,025
160	-	-	-	-	-	-	-10,600	-8,560
170	-	-	-	-	-	-	-11,488	-9,095
180	-	-	-	-	-	-	-12,664	-9.630
190	-	-	-	-	-	-	-13,832	-10,165
200	-	-	-	-	-	-	-15,371	-10,700

TABLE XXVI. COMPARISON OF EXPERIMENTAL AND CALCULATED SPANWISE STRESSES AT ROSETTE NO. 2 (LOWER SKIN OF FORWARD CELL AT BL 28.0)

Percent DUL	Condition II Stresses (psi)			Condition I Stresses (psi)				
	Test Results		Stress Analysis	Test Results				Stress Analysis
	Run No. 1	Run No. 2		Run No. 1	Run No. 2	Run No. 3	Run No. 4	
10	787	791	837	481	-	-	-	583
20	1971	1561	1674	809	818	785	676	1,166
30	2759	2353	2511	1294	-	-	-	1,749
40	3583	3149	3348	1747	1725	1695	1,526	2,332
50	4319	3914	4185	2197	-	-	-	2,915
60	-	4685	5022	-	2543	2479	2,202	3,498
70	-	5313	5859	-	2942	-	-	4,081
80	-	6198	6696	-	3298	3052	2,837	4,664
90	-	6983	7533	-	3593	-	-	5,247
100	-	7729	8370	-	3820	3613	3,328	5,830
110	-	-	-	-	-	3865	-	6,413
120	-	-	-	-	-	3892	3,528	6,996
130	-	-	-	-	-	3907	3,547	7,589
140	-	-	-	-	-	3715	3,378	8,162
150	-	-	-	-	-	3369	3,064	8,745
160	-	-	-	-	-	-	2,329	9,328
170	-	-	-	-	-	-	1,633	9,911
180	-	-	-	-	-	-	-	10,494
190	-	-	-	-	-	-	22,094	11,077
200	-	-	-	-	-	-	22,057	11,660

TABLE XXVII. COMPARISON OF EXPERIMENTAL AND CALCULATED SPANWISE STRESSES AT ROSETTE NO. 3 (UPPER SKIN OF FORWARD CELL AT BL 68.0)

Percent DUL	Condition II Stresses (psi)			Condition I Stresses (psi)				
	Test Results		Stress Analysis	Test Results				Stress Analysis
	Run No. 1	Run No. 2		Run No. 1	Run No. 2	Run No. 3	Run No. 4	
10	-2100	-1,797	-1,865	-1634	-	-	-	-1,298
20	-3929	-3,636	-3,730	-3359	-3,290	-3,368	-3,396	-2,596
30	-6027	-5,434	-5,595	-4994	-	-	-	-3,894
40	-7821	-7,235	-7,460	-6850	-6,641	-6,723	-6,743	-5,192
50	-9567	-8,941	-9,325	-8532	-	-	-	-6,490
60	-	-10,774	-11,190	-	-9,931	-10,092	-10,138	-7,788
70	-	-12,392	-13,055	-	-11,667	-	-	-9,086
80	-	-14,594	-14,920	-	-13,413	-13,422	-13,599	-10,384
90	-	-16,430	-16,785	-	-15,191	-	-	-11,682
100	-	-18,379	-18,650	-	-16,949	-16,967	-17,271	-12,980
110	-	-	-	-	-	-18,818	-	-14,278
120	-	-	-	-	-	-20,697	-21,117	-15,576
130	-	-	-	-	-	-22,732	-23,241	-16,874
140	-	-	-	-	-	-	-25,274	-18,172
150	-	-	-	-	-	-26,862	-27,262	-19,470
160	-	-	-	-	-	-	-29,190	-20,768
170	-	-	-	-	-	-	-31,195	-22,066
180	-	-	-	-	-	-	*	-
190	-	-	-	-	-	-	*	-
200	-	-	-	-	-	-	*	-

*Instrumentation limits exceeded.

TABLE XXVIII. COMPARISON OF EXPERIMENTAL AND CALCULATED SPANWISE STRESSES AT ROSETTE NO. 4 (LOWER SKIN OF FORWARD CELL AT BL 68.0)

Percent DUL	Condition II Stresses (psi)			Condition I Stresses (psi)				
	Test Results		Stress Analysis	Test Results				Stress Analysis
	Run No. 1	Run No. 2		Run No. 1	Run No. 2	Run No. 3	Run No. 4	
10	1914	1,881	2,034	1600	-	-	-	1,415
20	3718	3,765	4,068	3113	2,[illegible]91	3,002	2,979	2,830
30	5628	5,642	6,102	4712		-	-	4,245
40	7533	7,510	8,136	6307	6,[illegible]30	6,084	6,061	5,660
50	9322	9,294	10,170	7874	-	-	-	7,075
60	-	11,119	12,204	-	9,150	9,086	9,040	8,490
70	-	12,710	14,238	-	10,679	-	-	9,905
80	-	14,610	16,272	-	12,156	12,042	11,996	11,320
90	-	16,437	18,306	-	13,623	-	-	12,735
100	-	18,164	20,340	-	15,062	14,998	15,051	14,150
110	-	-	-	-	-	16,466	-	15,565
120	-	-	-	-	-	17,835	17,986	16,980
130	-	-	-	-	-	19,399	19,527	18,395
140	-	-	-	-	-	20,821	21,071	19,810
150	-	-	-	-	-	22,190	22,365	21,225
160	-	-	-	-	-	-	23,900	22,640
170	-	-	-	-	-	-	25,299	24,055
180	-	-	-	-	-	-	26,620	25,470
190	-	-	-	-	-	-	28,163	26,885
200	-	-	-	-	-	-	29,582	28,300

TABLE XXIX. COMPARISON OF EXPERIMENTAL AND CALCULATED SPANWISE STRESSES AT ROSETTE NO. 5 (UPPER SKIN OF AFT CELL AT BL 28.0)

Percent DUL	Condition II Stresses (psi)			Condition I Stresses (psi)				
	Test Results		Stress Analysis	Test Results				Stress Analysis
	Run No. 1	Run No. 2		Run No. 1	Run No. 2	Run No. 3	Run No. 4	
10	-848	-879	-1,010	-620	-	-	-	-703
20	-1668	-1726	-2,020	-1413	-1359	-1,339	-1,426	-1,406
30	-2517	-2606	-3,030	-2032	-	-	-	-2,109
40	-3417	-3478	-4,040	-2690	-2709	-2,716	-2,783	-2,812
50	-4299	-4313	-5,050	-3381	-	-	-	-3,515
60	-	-5187	-6,060	-	-4070	-4,056	-4,210	-4.218
70	-	-5902	-7,070	-	-4784	-	-	-4,921
80	-	-6909	-8,080	-	-5514	-5,469	-5,657	-5,624
90	-	-8121	-9,090	-	-6214	-	-	-6,327
100	-	-8937	-10,100	-	-6951	-7,008	-7,250	-7,030
110	-	-	-	-	-	-7,798	-	-7,733
120	-	-	-	-	-	-8,603	-8,846	-8,436
130	-	-	-	-	-	-9,410	-9,709	-9,139
140	-	-	-	-	-	-10,241	-10,603	-9,842
150	-	-	-	-	-	-11,188	-11,376	-10,545
160	-	-	-	-	-	-	-12,221	-11,248
170	-	-	-	-	-	-	-13,145	-11,951
180	-	-	-	-	-	-	-14,020	-12,654
190	-	-	-	-	-	-	-14,994	-13,357
200	-	-	-	-	-	-	-15,998	-14,060

TABLE XXX. COMPARISON OF EXPERIMENTAL AND CALCULATED SPANWISE STRESSES AT ROSETTE NO. 6 (LOWER SKIN OF AFT CELL AT BL 28.0)

Percent DUL	Condition II Stresses (psi)			Condition I Stresses (psi)				
	Test Results		Stress Analysis	Test Results				Stress Analysis
	Run No. 1	Run No. 2		Run No. 1	Run No. 2	Run No. 3	Run No. 4	
10	860	881	902	577	-	-	-	628
20	1723	1744	1804	1007	881	854	831	1,256
30	2583	2625	2706	1590	-	-	-	1,884
40	3499	3480	3608	2128	1914	1895	1835	2,512
50	4349	4340	4510	2609	-	-	-	3,140
60	-	5201	5412	-	2796	2750	2665	3,768
70	-	5878	6314	-	3199	-	-	4,396
80	-	6909	7216	-	3568	3462	3331	5,024
90	-	7407	8118	-	3838	-	-	5,652
100	-	8235	9020	-	4104	4055	3946	6,280
110	-	-	-	-	-	4317	-	6,908
120	-	-	-	-	-	4436	4553	7,536
130	-	-	-	-	-	4567	4497	8,164
140	-	-	-	-	-	4553	4614	8,792
150	-	-	-	-	-	4430	4490	9,420
160	-	-	-	-	-	-	4108	10,048
170	-	-	-	-	-	-	4071	10,676
180	-	-	-	-	-	-	3679	11,304
190	-	-	-	-	-	-	-	11,932
200	-	-	-	-	-	-	-	12,560

TABLE XXXI. COMPARISON OF EXPERIMENTAL AND CALCULATED SPANWISE STRESSES AT ROSETTE NO. 7 (UPPER SKIN OF AFT CELL AT BL 48.0)

Percent DUL	Condition II Stresses (psi)			Condition I Stresses (psi)				
	Test Results		Stress Analysis	Test Results				Stress Analysis
	Run No. 1	Run No. 2		Run No. 1	Run No. 2	Run No. 3	Run No. 4	
10	-1531	-1, 564	-1, 730	-965	-	-	-	-1, 205
20	-3044	-3, 036	-3, 460	-2091	-2, 050	-2, 063	-2, 084	-2, 410
30	-4574	-4, 600	-5, 190	-3055	-	-	-	-3, 615
40	-5988	-6, 089	-6, 920	-4072	-4, 103	-4, 062	-4, 123	-4, 820
50	-7519	-7, 532	-8, 650	-5096	-	-	-	-6, 025
60	-	-9, 061	-10, 380	-	-6, 153	-6, 125	-6, 207	-7, 230
70	-	-10, 301	-12, 110	-	-7, 204	-	-	-8, 435
80	-	-12, 035	-13, 840	-	-8, 171	-8, 098	-8, 226	-9, 640
90	-	-13, 613	-15, 570	-	-9, 178	-	-	-10, 845
100	-	-15, 058	-17, 300	-	-10, 189	-10, 135	-10, 330	-12, 050
110	-	-	-	-	-	-11, 230	-	-13, 255
120	-	-	-	-	-	-12, 306	-12, 455	-14, 460
130	-	-	-	-	-	-13, 421	-13, 657	-15, 665
140	-	-	-	-	-	-15, 545	-14, 802	-16, 870
150	-	-	-	-	-	-15, 614	-15, 742	-18, 075
160	-	-	-	-	-	-	-16, 847	-19, 280
170	-	-	-	-	-	-	-17, 720	-20, 485
180	-	-	-	-	-	-	-18, 764	-21, 690
190	-	-	-	-	-	-	-19, 967	-22, 895
200	-	-	-	-	-	-	-21, 106	-24, 100

TABLE XXXII. COMPARISON OF EXPERIMENTAL AND CALCULATED SPANWISE STRESSES AT ROSETTE NO. 8 (UPPER SKIN OF AFT CELL AT BL 68.0)

Percent DUL	Condition II Stresses (psi)			Condition I Stresses (psi)				
	Test Results		Stress Analysis	Test Results				Stress Analysis
	Run No. 1	Run No. 2		Run No. 1	Run No. 2	Run No. 3	Run No. 4	
10	-2,029	-2,096	-2,456	-1219	-	-	-	-1,708
20	-4,017	-4,005	-4,912	-2494	-2,529	-2,582	-2,624	-3,416
30	-6,046	-6,101	-7,368	-3711	-	-	-	-5,124
40	-8,029	-8,150	-9,824	-5276	-5,121	-5,185	-5,118	-6,832
50	-10,130	-10,164	-12,280	-6602	-	-	-	-8,540
60	-	-12,276	-14,736	-	-7,653	-7,771	-7,746	-10,248
70	-	-14,231	-17,192	-	-8,987	-	-	-11,956
80	-	-16,696	-19,648	-	-10,290	-10,267	-10,328	-13,664
90	-	-19,092	-22,104	-	-11,579	-	-	-15,372
100	-	-21,411	-24,560	-	-12,892	-12,956	-13,105	-17,080
110	-	-	-	-	-	-14,357	-	-18,788
120	-	-	-	-	-	-15,735	-15,950	-20,496
130	-	-	-	-	-	-17,290	-17,546	-22,204
140	-	-	-	-	-	-18,865	-19,122	-23,912
150	-	-	-	-	-	-20,636	-20,586	-25,620
160	-	-	-	-	-	-	-22,158	-27,328
170	-	-	-	-	-	-	-23,904	-29,036
180	-	-	-	-	-	-	-25,809	-30,744
190	-	-	-	-	-	-	-27,795	-32,452
200	-	-	-	-	-	-	-29,936	-34,160

TABLE XXXIII. COMPARISON OF EXPERIMENTAL AND CALCULATED SPANWISE STRESSES AT ROSETTE NO. 9 (LOWER SKIN OF AFT CELL AT BL 68.0)

Percent DUL	Condition II Stresses (psi)			Condition I Stresses (psi)				
	Test Results		Stress Analysis	Test Results				Stress Analysis
	Run No. 1	Run No. 2		Run No. 1	Run No. 2	Run No. 3	Run No. 4	
10	1993	2,022	2,193	1230	-	-	-	1,526
20	3980	4,003	4,368	2379	2,214	2,199	2,176	3,052
30	5969	6,025	6,579	3609	-	-	-	4,578
40	7851	7,908	8,772	4814	4,541	4,529	4,430	6,104
50	9775	9,747	10,965	5960	-	-	-	7,630
60	-	11,609	13,158	-	6,755	6,728	6,606	9,156
70	-	13,242	15,351	-	7,854	-	-	10,862
80	-	15,158	17,544	-	8,922	8,709	8,607	12,208
90	-	16,892	19,737	-	9,870	-	-	13,734
100	-	18,572	21,930	-	10,896	10,760	10,737	15,260
110	-	-	-	-	-	11,851	-	16,786
120	-	-	-	-	-	12,741	12,792	18,312
130	-	-	-	-	-	13,807	13,882	19,838
140	-	-	-	-	-	14,795	14,946	21,364
150	-	-	-	-	-	15,835	15,713	22,890
160	-	-	-	-	-	-	16,671	24,416
170	-	-	-	-	-	-	17,658	25,942
180	-	-	-	-	-	-	18,440	27,468
190	-	-	-	-	-	-	19,352	28,994
200	-	-	-	-	-	-	20,271	30,520

TABLE XXXIV. COMPARISON OF EXPERIMENTAL AND CALCULATED SPANWISE STRESSES AT ROSETTE NO. 10 (MAIN SPAR AT BL 28.0)

Percent DUL	Condition II Stresses (psi)			Condition I Stresses (psi)				
	Test Results		Stress Analysis	Test Results				Stress Analysis
	Run No. 1	Run No. 2		Run No. 1	Run No. 2	Run No. 3	Run No. 4	
10	18	14	-	31	-	-	-	58
20	50	67	-	-1	-47	-61	-68	116
30	68	82	-	30	-	-	-	174
40	78	103	-	31	-61	-54	-96	232
50	110	144	-	20	-	-	-	290
60	-	175	-	-	-109	-115	-162	348
70	-	194	-	-	-117	-	-	406
80	-	247	-	-	-156	-196	-243	464
90	-	273	-	-	-187	-	-	522
100	-	-111	-	-	-205	-278	-312	580
110	-	-	-	-	-	-304	-	638
120	-	-	-	-	-	-366	-406	696
130	-	-	-	-	-	-406	-467	754
140	-	-	-	-	-	-480	-541	812
150	-	-	-	-	-	-581	-635	870
160	-	-	-	-	-	-	-691	928
170	-	-	-	-	-	-	-792	986
180	-	-	-	-	-	-	-1032	1044
190	-	-	-	-	-	-	-1299	1102
200	-	-	-	-	-	-	-1728	1160

TABLE XXXV. COMPARISON OF EXPERIMENTAL AND CALCULATED SPANWISE STRESSES AT ROSETTE NO. 11 (MAIN SPAR AT BL 68.0)

Percent DUL	Condition II Stresses (psi)			Condition I Stresses (psi)				
	Test Results		Stress Analysis	Test Results				Stress Analysis
	Run No. 1	Run No. 2		Run No. 1	Run No. 2	Run No. 3	Run No. 4	
10	-120	-124	-	21	-	-	-	142
20	-94	-115	-	6	-187	-200	-207	284
30	-214	-239	-	28	-	-	-	426
40	-346	-389	-	-32	-265	-281	-268	568
50	-510	-526	-	-118	-	-	-	710
60	-	-703	-	-	-451	-481	-475	852
70	-	-835	-	-	-547	-	-	994
80	-	-955	-	-	-664	-687	-695	1136
90	-	-1180	-	-	-781	-	-	1278
100	-	-1329	-	-	-907	-967	-955	1420
110	-	-	-	-	-	-1061	-	1562
120	-	-	-	-	-	-1201	-1243	1704
130	-	-	-	-	-	-1341	-1382	1846
140	-	-	-	-	-	-1456	-1546	1988
150	-	-	-	-	-	-1605	-1699	2130
160	-	-	-	-	-	-	-1801	2272
170	-	-	-	-	-	-	-1968	2414
180	-	-	-	-	-	-	-2160	2556
190	-	-	-	-	-	-	-2387	2698
200	-	-	-	-	-	-	-2681	2840

TABLE XXXVI. COMPARISON OF EXPERIMENTAL AND CALCULATED SPANWISE STRESSES AT GAGE NO. 36 (UPPER SKIN OF FORWARD CELL AT BL 68.0)

Percent DUL	Condition II Stresses (psi)			Condition I Stresses (psi)				
	Test Results		Stress Analysis	Test Results				Stress Analysis
	Run No. 1	Run No. 2		Run No. 1	Run No. 2	Run No. 3	Run No. 4	
10	-1970	-2,000	-1,980	-1450	-	-	-	-1,380
20	-362[illegible]	-3,720	-3,960	-2920	-3,275	-3,370	-3,370	-2,760
30	-560[illegible]	-5,720	-5,940	-4370	-	-	-	-4,140
40	-7560	-7,650	-7,920	-5980	-6,420	-6,490	-6,490	-5,520
50	-9460	-9,550	-9,900	-7900	-	-	-	-6,900
60	-	-11,580	-11,880	-	-9,690	-9,850	-9,850	-8,280
70	-	-13,580	-13,860	-	-11,400	-	-	-9,660
80	-	-15,600	-15,840	-	-13,120	-13,100	-13,290	-11,040
90	-	-17,680	-17,820	-	-14,900	-	-	-12,420
100	-	-19,600	-19,800	-	-	-16,700	-17,000	-13,800
110	-	-	-	-	-	-18,580	-	-15,180
120	-	-	-	-	-	-20,350	-20,670	-16,560
130	-	-	-	-	-	-22,300	-22,750	-17,940
140	-	-	-	-	-	-24,200	-24,800	-19,320
150	-	-	-	-	-	-26,200	-26,600	-20,700
160	-	-	-	-	-	-	-30,650	-22,080
170	-	-	-	-	-	-	*	-
180	-	-	-	-	-	-	*	-
190	-	-	-	-	-	-	*	-
200	-	-	-	-	-	-	*	-

*Instrumentation limits exceeded.

Note: Modulus for data reductic [illegible] 17 x 10^6 psi.

TABLE XXXVII. COMPARISON OF EXPERIMENTAL AND CALCULATED SPANWISE STRESSES AT GAGE NO. 37 (LOWER SKIN OF FORWARD CELL AT BL 68.0)

Percent DUL	Condition II Stresses (psi)			Condition I Stresses (psi)				
	Test Results		Stress Analysis	Test Results				Stress Analysis
	Run No. 1	Run No. 2		Run No. 1	Run No. 2	Run No. 3	Run No. 4	
10	1960	1,830	2,266	1410	-	-	-	1,576
20	3700	3,700	4,532	2730	2,670	2,585	2,585	3,152
30	5660	5,530	6,798	4140	-	-	-	4,728
40	7440	7,310	9,064	5530	5,390	5,350	5,260	6,304
50	9270	9,100	11,330	6900	-	-	-	7,880
60	-	10,880	13,596	-	8,070	7,940	7,850	9,456
70	-	12,620	15,862	-	9,410	-	-	11,032
80	-	14,490	18,128	-	10,790	10,520	10,520	12,608
90	-	16,320	20,394	-	12,080	-	-	14,184
100	-	18,150	22,660	-	13,420	13,200	13,290	15,760
110	-	-	-	-	-	14,630	-	17,336
120	-	-	-	-	-	15,870	15,960	18,912
130	-	-	-	-	-	17,300	17,390	20,488
140	-	-	-	-	-	18,640	19,080	22,064
150	-	-	-	-	-	19,980	19,980	23,640
160	-	-	-	-	-	-	22,560	25,216
170	-	-	-	-	-	-	22,700	26,792
180	-	-	-	-	-	-	23,800	28,368
190	-	-	-	-	-	-	25,150	29,944
200	-	-	-	-	-	-	26,490	31,520

Note: Modulus for data reduction = 4.45×10^6 psi.

TABLE XXXVIII. COMPARISON OF EXPERIMENTAL AND CALCULATED SPANWISE STRESSES AT GAGE NO. 38 (UPPER SKIN OF MAIN SPAR AT BL 68.0)

Percent DUL	Condition II Stresses (psi)			Condition I Stresses (psi)				
	Test Results		Stress Analysis	Test Results				Stress Analysis
	Run No. 1	Run No. 2		Run No. 1	Run No. 2	Run No. 3	Run No. 4	
10	-2070	-2,030	-2,072	-1260	-	-	-	-1,442
20	-3700	-3,660	-4,144	-2480	-3,030	-3,030	-3,110	-2,884
30	-5760	-5,700	-6,216	-3740	-	-	-	-4,326
40	-7720	-7,730	-8,288	-5210	-5,800	-5,840	-5,920	-5,768
50	-9760	-9,750	-10,360	-6760	-	-	-	-7,210
60	-	-11,820	-12,432	-	-8,840	-8,870	-9,020	-8,652
70	-	-13,860	-14,504	-	-10,430	-	-	-10,094
80	-	-15,970	-16,576	-	-12,020	-11,900	-12,200	-11,536
90	-	-18,140	-18,648	-	-13,570	-	-	-12,978
100	-	-20,200	-20,720	-	-15,230	-15,160	-15,530	-14,420
110	-	-	-	-	-	-16,860	-	-15,862
120	-	-	-	-	-	-18,560	-18,930	-17,304
130	-	-	-	-	-	-20,410	-20,780	-18,746
140	-	-	-	-	-	-22,110	-22,550	-20,188
150	-	-	-	-	-	-24,030	-24,180	-21,630
160	-	-	-	-	-	-	-27,880	-23,072
170	-	-	-	-	-	-	-27,700	-24,514
180	-	-	-	-	-	-	-29,730	-25,956
190	-	-	-	-	-	-	-31,800	-27,398
200	-	-	-	-	-	-	-34,090	-28,840

Note: Modulus for data reduction = 3.69×10^6 psi.

TABLE XXXIX. COMPARISON OF EXPERIMENTAL AND CALCULATED SPANWISE STRESSES AT GAGE NO. 39 (LOWER SKIN OF MAIN SPAR AT BL 68.0)

Percent DUL	Condition II Stresses (psi)			Condition I Stresses (psi)				
	Test Results		Stress Analysis	Test Results				Stress Analysis
	Run No. 1	Run No. 2		Run No. 1	Run No. 2	Run No. 3	Run No. 4	
10	1460	1,390	2,110	970	-	-	-	1,468
20	2770	2,700	4,220	1890	1920	1,850	1,920	2,936
30	4240	4,090	6,330	2860	-	-	-	4,404
40	5620	5,430	8,440	3850	3850	3,770	3,770	5,872
50	7050	6,780	10,550	4830	-	-	-	7,340
60	-	8,200	12,660	-	5770	5,620	5,690	8,808
70	-	9,550	14,770	-	6770	-	-	10,276
80	-	10,970	16,880	-	7770	7,540	7,620	11,744
90	-	12,410	18,990	-	8740	-	-	13,212
100	-	13,720	21,100	-	9730	9,470	9,700	14,680
110	-	-	-	-	-	10,620	-	16,148
120	-	-	-	-	-	11,620	11,770	17,616
130	-	-	-	-	-	12,780	12,930	19,084
140	-	-	-	-	-	13,770	13,930	20,552
150	-	-	-	-	-	14,850	14,930	22,020
160	-	-	-	-	-	-	17,080	23,488
170	-	-	-	-	-	-	17,300	24,956
180	-	-	-	-	-	-	18,050	26,424
190	-	-	-	-	-	-	19,160	27,892
200	-	-	-	-	-	-	20,240	29,360

Note: Modulus for data reduction = 3.84×10^6 psi.

TABLE XL. COMPARISON OF EXPERIMENTAL AND CALCULATED SPANWISE STRESSES AT GAGE NO. 40 (UPPER SKIN OF AFT CELL AT BL 68.0)

Percent DUL	Condition II Stresses (psi)			Condition I Stresses (psi)				
	Test Results		Stress Analysis	Test Results				Stress Analysis
	Run No. 1	Run No. 2		Run No. 1	Run No. 2	Run No. 3	Run No. 4	
10	-2,200	-2,120	-2,576	-1270	-	-	-	-1,793
20	-3,830	-3,830	-5,152	-2510	-3,020	-3,020	-3,180	-3,586
30	-6,040	-5,950	-7,728	-3780	-	-	-	-5,379
40	-8,070	-8,070	-10,304	-5270	-5,870	-5,870	-6,040	-7,172
50	-10,150	-10,110	-12,880	-6820	-	-	-	-8,965
60	-	-12,320	-15,456	-	-8,890	-8,890	-9,220	-10,758
70	-	-14,480	-18,032	-	-10,440	-	-	-12,551
80	-	-16,720	-20,608	-	-12,030	-11,910	-12,230	-14,344
90	-	-19,080	-23,184	-	-13,580	-	-	-16,137
100	-	-20,430	-25,760	-	-15,210	-15,090	-15,580	-17,930
110	-	-	-	-	-	-16,800	-	-19,723
120	-	-	-	-	-	-18,514	-19,000	-21,516
130	-	-	-	-	-	-20,390	-20,880	-23,309
140	-	-	-	-	-	-22,190	-22,840	-25,102
150	-	-	-	-	-	-24,220	-24,470	-26,895
160	-	-	-	-	-	-	-26,200	-28,688
170	-	-	-	-	-	-	-28,100	-30,481
180	-	-	-	-	-	-	-30,420	-32,274
190	-	-	-	-	-	-	-32,710	-34,067
200	-	-	-	-	-	-	-35,150	-35,860

Note: Modulus for data reduction = 4.07×10^6 psi.

TABLE XLI. COMPARISON OF EXPERIMENTAL AND CALCULATED SPANWISE STRESSES AT GAGE NO. 41 (LOWER SKIN OF AFT CELL AT BL 68.0)

Percent DUL	Condition II Stresses (psi)			Condition I Stresses (psi)				
	Test Results		Stress Analysis	Test Results				Stress Analysis
	Run No. 1	Run No. 2		Run No. 1	Run No. 2	Run No. 3	Run No. 4	
10	2010	2,050	2,314	1390	-	-	-	1,610
20	3790	4,010	4,628	2730	2,630	2,590	2,670	3,220
30	5800	6,070	6,942	4120	-	-	-	4,830
40	7810	7,980	9,256	5510	5,350	5,350	5,350	6,440
50	9670	9,940	11,570	6870	-	-	-	8,050
60	-	11,900	13,884	-	7,980	7,940	8,030	9,660
70	-	13,730	16,198	-	9,320	-	-	11,270
80	-	15,650	18,512	-	10,660	10,440	10,610	12,880
90	-	17,520	20,826	-	11,900	-	-	14,490
100	-	19,350	23,140	-	13,200	13,020	13,290	16,100
110	-	-	-	-	-	14,440	-	17,710
120	-	-	-	-	-	15,700	15,960	19,320
130	-	-	-	-	-	17,120	17,390	20,930
140	-	-	-	-	-	18,370	18,640	22,540
150	-	-	-	-	-	19,710	19,800	24,150
160	-	-	-	-	-	-	20,900	25,760
170	-	-	-	-	-	-	22,300	27,370
180	-	-	-	-	-	-	23,630	28,980
190	-	-	-	-	-	-	24,970	30,590
200	-	-	-	-	-	-	26,310	32,200

Note: Modulus for data reduction = 4.45×10^6 psi.

TABLE XLII. COMPARISON OF EXPERIMENTAL AND CALCULATED SPANWISE STRESSES AT GAGE NO. 42 (UPPER SKIN OF MAIN SPAR AT BL 48.0)

Percent DUL	Condition II Stresses (psi)			Condition I Stresses (psi)				
	Test Results		Stress Analysis	Test Results				Stress Analysis
	Run No. 1	Run No. 2		Run No. 1	Run No. 2	Run No. 3	Run No. 4	
10	-1410	-1,550	-1,462	-1050	-	-	-	-1,020
20	-2850	-2,960	-2,924	-2080	-2,180	-2,140	-2,220	-2,040
30	-4260	-4,510	-4,386	-3140	-	-	-	-3,060
40	-5800	-6,040	-5,848	-4240	-4,400	-4,360	-4,440	-4,080
50	-7290	-7,460	-7,310	-5350	-	-	-	-5,100
60	-	-8,990	-8,772	-	-6,580	-6,510	-6,660	-6,120
70	-	-10,470	-10,234	-	-7,730	-	-	-7,140
80	-	-11,920	-11,696	-	-8,840	-8,730	-8,870	-8,160
90	-	-13,500	-13,158	-	-9,940	-	-	-9,180
100	-	-15,000	-14,620	-	-11,090	-11,020	-11,240	-10,200
110	-	-	-	-	-	-12,200	-	-11,220
120	-	-	-	-	-	-13,380	-13,610	-12,240
130	-	-	-	-	-	-14,640	-14,940	-13,260
140	-	-	-	-	-	-15,830	-16,120	-14,280
150	-	-	-	-	-	-17,080	-17,300	-15,300
160	-	-	-	-	-	-	-18,450	-16,320
170	-	-	-	-	-	-	-19,750	-17,340
180	-	-	-	-	-	-	-21,150	-18,360
190	-	-	-	-	-	-	-22,550	-19,380
200	-	-	-	-	-	-	-24,180	-20,400

Note: Modulus for data reduction = 3.69×10^6 psi.

TABLE XLIII. COMPARISON OF EXPERIMENTAL AND CALCULATED SPANWISE STRESSES AT GAGE NO. 43 (LOWER SKIN OF MAIN SPAR AT BL 48.0)

Percent DUL	Condition II Stresses (psi)			Condition I Stresses (psi)				
	Test Results		Stress Analysis	Test Results				Stress Analysis
	Run No. 1	Run No. 2		Run No. 1	Run No. 2	Run No. 3	Run No. 4	
10	1260	1,250	1,490	910	-	-	-	1,035
20	2520	2,520	2,980	1820	1690	1,690	1,690	2,070
30	3800	3,780	4,470	2720	-	-	-	3,105
40	5050	4,990	5,960	3600	3430	3,460	3,390	4,140
50	5900	6,200	7,450	4490	-	-	-	5,175
60	-	7,440	8,940	-	5120	5,160	5,080	6,210
70	-	8,320	10,430	-	6000	-	-	7,245
80	-	9,550	12,920	-	6850	6,770	6,770	8,280
90	-	10,820	13,410	-	7700	-	-	9,315
100	-	12,100	14,900	-	8540	8,460	8,540	10,350
110	-	-	-	-	-	9,390	-	11,385
120	-	-	-	-	-	10,230	10,230	12,420
130	-	-	-	-	-	11,240	11,240	13,455
140	-	-	-	-	-	12,080	12,080	14,490
150	-	-	-	-	-	12,930	12,850	15,526
160	-	-	-	-	-	-	13,650	16,560
170	-	-	-	-	-	-	14,400	17,595
180	-	-	-	-	-	-	15,240	18,630
190	-	-	-	-	-	-	16,080	19,665
200	-	-	-	-	-	-	16,780	20,700

Note: Modulus for data reduction = 3.84×10^6 psi.

TABLE XLIV. COMPARISON OF EXPERIMENTAL AND CALCULATED SPANWISE STRESSES AT GAGE NO. 44 (UPPER CAP OF MAIN SPAR AT BL 28.0)

Percent DUL	Condition II Stresses (psi)			Condition I Stresses (psi)				
	Test Results		Stress Analysis	Test Results				Stress Analysis
	Run No. 1	Run No. 2		Run No. 1	Run No. 2	Run No. 3	Run No. 4	
10	260	250	-1,580	210	-	-	-	-1,100
20	510	490	-3,160	440	430	410	450	-2,200
30	770	740	-4,740	650	-	-	-	-3,300
40	1050	1000	-6,320	870	830	780	820	-4,400
50	1300	1260	-7,900	1080	-	-	-	-5,500
60	-	1540	-9,480	-	1260	1190	1270	-6,600
70	-	1800	-11,060	-	1510	-	-	-7,700
80	-	2110	-12,640	-	1790	1720	1760	-8,800
90	-	2440	-14,220	-	2070	-	-	-9,900
100	-	2770	-15,800	-	2390	2290	2380	-11,000
110	-	-	-	-	-	2660	-	-12,100
120	-	-	-	-	-	2990	3120	-13,200
130	-	-	-	-	-	3480	3570	-14,300
140	-	-	-	-	-	3930	4020	-15,400
150	-	-	-	-	-	4430	4510	-16,500
160	-	-	-	-	-	-	5100	-17,600
170	-	-	-	-	-	-	5500	-18,700
180	-	-	-	-	-	-	6270	-19,800
190	-	-	-	-	-	-	7090	-20,900
200	-	-	-	-	-	-	8030	-22,000

Note: Modulus for data reduction = 4.09×10^6 psi.

TABLE XLV. COMPARISON OF EXPERIMENTAL AND CALCULATED SPANWISE STRESSES AT GAGE NO. 45 (LOWER CAP OF MAIN SPAR AT BL 28.0)

Percent DUL	Condition II Stresses (psi)			Condition I Stresses (psi)				
	Test Results		Stress Analysis	Test Results				Stress Analysis
	Run No. 1	Run No. 2		Run No. 1	Run No. 2	Run No. 3	Run No. 4	
10	-80	-100	1,510	81	-	-	-	1,050
20	-180	-180	3,020	110	100	100	110	2,100
30	-260	-280	4,530	190	-	-	-	3,150
40	-340	-370	6,040	260	160	150	210	4,200
50	-440	-420	7,550	290	-	-	-	5,250
60	-	-500	9,060	-	260	240	320	6,300
70	-	-580	10,570	-	320	-	-	7,350
80	-	-650	12,080	-	420	420	530	8,400
90	-	-730	13,590	-	550	-	-	9,450
100	-	-780	15,100	-	730	730	870	10,500
110	-	-	-	-	-	960	-	11,550
120	-	-	-	-	-	1240	1460	12,600
130	-	-	-	-	-	1670	1850	13,650
140	-	-	-	-	-	2210	2320	14,700
150	-	-	-	-	-	2940	2970	15,750
160	-	-	-	-	-	-	3810	16,800
170	-	-	-	-	-	-	5120	17,850
180	-	-	-	-	-	-	6720	18,900
190	-	-	-	-	-	-	8080	19,950
200	-	-	-		-	-	8080	21,000

Note: Modulus for data reduction = 4.05×10^6 psi.

TABLE XLVI. COMPARISON OF EXPERIMENTAL AND CALCULATED SPANWISE STRESSES AT GAGE NO. 46 (UPPER CAP OF MAIN SPAR AT BL 68.0)

Percent DUL	Condition II Stresses (psi)			Condition I Stresses (psi)				
	Test Results		Stress Analysis	Test Results				Stress Analysis
	Run No. 1	Run No. 2		Run No. 1	Run No. 2	Run No. 3	Run No. 4	
10	620	620	-2,240	430	-	-	-	-1,558
20	1150	1170	-4,480	820	900	900	860	-3,116
30	1770	1790	-6,720	1250	-	-	-	-4,674
40	2430	2410	-8,960	1670	1740	1760	1,720	-6,232
50	3050	3060	-11,200	2150	-	-	-	-7,790
60	-	3740	-13,440	-	2640	2660	2,580	-9,348
70	-	4440	-15,680	-	3120	-	-	-10,906
80	-	5200	-17,920	-	3610	3530	3,530	-12,464
90	-	6000	-20,160	-	4030	-	-	-14,022
100	-	6820	-22,400	-	4610	4550	4,590	-15,580
110	-	-	-	-	-	5120	-	-17,138
120	-	-	-	-	-	5700	5,700	-18,696
130	-	-	-	-	-	6310	6,350	-20,254
140	-	-	-	-	-	6920	6,920	-21,812
150	-	-	-	-	-	7580	7,500	-23,370
160	-	-	-	-	-	-	8,180	-24,928
170	-	-	-	-	-	-	8,800	-26,486
180	-	-	-	-	-	-	9,590	-28,044
190	-	-	-	-	-	-	10,290	-29,602
200	-	-	-	-	-	-	11,020	-31,160

Note: Modulus for data reduction = 4.09 x 10^6 psi.

TABLE XLVII. COMPARISON OF EXPERIMENTAL AND CALCULATED SPANWISE STRESSES AT GAGE NO. 47 (LOWER CAP OF MAIN SPAR AT BL 68.0)

Percent DUL	Condition II Stresses (psi)			Condition I Stresses (psi)				
	Test Results		Stress Analysis	Test Results				Stress Analysis
	Run No. 1	Run No. 2		Run No. 1	Run No. 2	Run No. 3	Run No. 4	
10	-340	-310	2,140	-240	-	-	-	1,488
20	-650	-650	4,280	-520	-550	-570	-610	2,976
30	-990	-960	6,420	-760	-	-	-	4,464
40	-1280	-1300	8,560	-1020	-1120	-1140	-1180	5,952
50	-1580	-1590	10,700	-1320	-	-	-	7,440
60	-	-1920	12,840	-	-1670	-1710	-1790	8,928
70	-	-2260	14,980	-	-1960	-	-	10,416
80	-	-2580	17,120	-	-2240	-2230	-2350	11,904
90	-	-2950	19,260	-	-2530	-	-	13,392
100	-	-3280	21,400	-	-2810	-2800	-2880	14,880
110	-	-	-	-	-	-3050	-	16,368
120	-	-	-	-	-	-3330	-3490	17,856
130	-	-	-	-	-	-3610	-3770	19,344
140	-	-	-	-	-	-3900	-4060	20,832
150	-	-	-	-	-	-4180	-4300	22,320
160	-	-	-	-	-	-	-4330	23,808
170	-	-	-	-	-	-	-3450	25,296
180	-	-	-	-	-	-	-5070	26,784
190	-	-	-	-	-	-	-5320	28,272
200	-	-	-	-	-	-	-5560	29,760

Note: Modulus for data reduction = 4.05×10^6 psi.

TABLE XLVIII. COMPARISON OF EXPERIMENTAL AND CALCULATED SHEAR STRESSES AT ROSETTE NO. 1 (UPPER SKIN OF FORWARD CELL AT BL 28.0)

Percent DUL	Condition II Stresses (psi)			Condition I Stresses (psi)				
	Test Results		Stress Analysis	Test Results				Stress Analysis
	Run No. 1	Run No. 2		Run No. 1	Run No. 2	Run No. 3	Run No. 4	
10	135	135	187	693	-	-	-	985
20	377	261	374	1354	1395	1,419	1,419	1,970
30	512	396	561	2045	-	-	-	2,995
40	646	530	748	2753	2790	2,767	2,859	3,940
50	791	660	935	3487	-	-	-	4,925
60	-	796	1122	-	4185	4,185	4,278	5,910
70	-	912	1309	-	4917	-	-	6,895
80	-	1078	1496	-	5636	5,648	5,765	7,880
90	-	1227	1683	-	6416	-	-	8,865
100	-	1380	1870	-	7183	7,136	7,252	9,850
110	-	-	-	-	-	7,927	-	10,835
120	-	-	-	-	-	8,717	8,833	11,820
130	-	-	-	-	-	9,555	9,671	12,805
140	-	-	-	-	-	10,438	10,484	13,790
150	-	-	-	-	-	15,823	11,297	14,775
160	-	-	-	-	-	-	12,064	15,760
170	-	-	-	-	-	-	12,992	16,745
180	-	-	-	-	-	-	14,019	17,730
190	-	-	-	-	-	-	15,064	18,715
200	-	-	-	-	-	-	16,110	19,700

TABLE XLIX. COMPARISON OF EXPERIMENTAL AND CALCULATED SHEAR STRESSES AT ROSETTE NO. 2 (LOWER SKIN OF FORWARD CELL AT BL 28.0)

Percent DUL	Condition II Stresses (psi)			Condition I Stresses (psi)				
	Test Results		Stress Analysis	Test Results				Stress Analysis
	Run No. 1	Run No. 2		Run No. 1	Run No. 2	Run No. 3	Run No. 4	
10	119	124	128	-869	-	-	-	-939
20	289	253	256	-1700	-1821	-1,860	-1,887	-1,878
30	409	378	384	-2570	-	-	-	-2,817
40	517	486	512	-3470	-3594	-3,620	-3,723	-3,756
50	631	590	640	-4399	-	-	-	-4,695
60	-	708	768	-	-5415	-5,480	-5,610	-5,634
70	-	791	896	-	-6385	-	-	-€,573
80	-	935	1024	-	-7328	-7,341	-7,548	-7,512
90	-	1045	1152	-	-8376	-	-	-8,451
100	-	1158	1280	-	-9372	-9,307	-9,540	-9,390
110	-	-	-	-	-	-10,315	-	-10,329
120	-	-	-	-	-	-11,401	-11,633	-11,268
130	-	-	-	-	-	-12,590	-12,719	-12,207
140	-	-	-	-	-	-13,778	-13,778	-13,146
150	-	-	-	-	-	-15,047	-14,969	-14,085
160	-	-	-	-	-	-	-16,060	-15,024
170	-	-	-	-	-	-	-17,350	-15,963
180	-	-	-	-	-	-	-	-
190	-	-	-	-	-	-	-	-
200	-	-	-	-	-	-	-	-

TABLE L. COMPARISON OF EXPERIMENTAL AND CALCULATED SHEAR STRESSES AT ROSETTE NO. 3 (UPPER SKIN OF FORWARD CELL AT BL 68.0)

Percent DUL	Condition II Stresses (psi)			Condition I Stresses (psi)				
	Test Results		Stress Analysis	Test Results				Stress Analysis
	Run No. 1	Run No. 2		Run No. 1	Run No. 2	Run No. 3	Run No. 4	
10	-52	-56	187	400	-	-	-	985
20	-227	-232	374	748	96	1000	977	1,970
30	-280	-289	561	1148	-	-	-	2,955
40	-311	-325	748	1618	1843	1873	1,906	3,940
50	-335	-340	935	2116	-	-	-	4,925
60	-	-363	1122	-	2808	2873	2,883	5,910
70	-	-367	1309	-	3304	-	-	6,895
80	-	-491	1496	-	3811	3883	3,924	7,880
90	-	-486	1683	-	4355	-	-	8,865
100	-	-405	1870	-	4872	4920	4,985	9,850
110	-	-	-	-	-	5454	-	10,835
120	-	-	-	-	-	6012	6,054	11,820
130	-	-	-	-	-	6593	6,635	12,805
140	-	-	-	-	-	2348	7,175	13,790
150	-	-	-	-	-	7784	7,756	14,775
160	-	-	-	-	-	-	8,190	15,760
170	-	-	-	-	-	-	8,700	16,745
180	-	-	-	-	-	-	9,428	17,730
190	-	-	-	-	-	-	10,010	18,715
200	-	-	-	-	-	-	10,583	19,700

TABLE LI. COMPARISON OF EXPERIMENTAL AND CALCULATED SHEAR STRESSES AT ROSETTE NO. 4 (LOWER SKIN OF FORWARD CELL AT BL 68.0)

Percent DUL	Condition II Stresses (psi)			Condition I Stresses (psi)				
	Test Results		Stress Analysis	Test Results				Stress Analysis
	Run No. 1	Run No. 2		Run No. 1	Run No. 2	Run No. 3	Run No. 4	
10	21	5	128	698	-	-	-	939
20	114	103	256	1387	1307	1,371	1,397	1,878
30	134	108	384	2083	-	-	-	2,817
40	103	88	512	2745	2663	2,688	2,766	3,756
50	89	57	640	3417	-	-	-	4,695
60	-	21	768	-	3967	4,060	4,163	5,634
70	-	-21	896	-	4640	-	-	6,573
80	-	-26	1024	-	5299	5,377	5,532	7,512
90	-	-41	1152	-	6050	-	-	8,451
100	-	-52	1280	-	6787	6,748	6,929	9,390
110	-	-	-	-	-	7,496	-	10,329
120	-	-	-	-	-	8,273	8,428	11,268
130	-	-	-	-	-	9,100	9,125	12,207
140	-	-	-	-	-	9,952	9,875	13,146
150	-	-	-	-	-	10,832	10,652	14,085
160	-	-	-	-	-	-	11,481	15,024
170	-	-	-	-	-	-	12,255	15,963
180	-	-	-	-	-	-	13,235	16,902
190	-	-	-	-	-	-	14,167	17,841
200	-	-	-	-	-	-	15,200	18,780

TABLE LII. COMPARISON OF EXPERIMENTAL AND CALCULATED SHEAR STRESSES AT ROSETTE NO. 5 (UPPER SKIN OF AFT CELL AT BL 28.0)

Percent DUL	Condition II Stresses (psi)			Condition I Stresses (psi)				
	Test Results		Stress Analysis	Test Results				Stress Analysis
	Run No. 1	Run No. 2		Run No. 1	Run No. 2	Run No. 3	Run No. 4	
10	-46	-60	78	516	-	-	-	799
20	-97	-111	156	1014	1046	1046	1,070	1,598
30	-145	-173	235	1530	-	-	-	2,397
40	-201	-219	313	2059	2091	2091	2,138	3,196
50	-256	-275	391	2600	-	-	-	3,995
60	-	-329	469	-	3139	3139	3,209	4,794
70	-	-380	547	-	3684	-	-	5,593
80	-	-456	626	-	4196	4232	4,301	6,392
90	-	-512	704	-	4788	-	-	7,191
100	-	-577	782	-	5335	5300	5,393	7,990
110	-	-	-	-	-	5835	-	8,789
120	-	-	-	-	-	6439	6,533	9,588
130	-	-	-	-	-	7044	7,067	10,387
140	-	-	-	-	-	7671	7,648	11,186
150	-	-	-	-	-	8230	8,253	11,985
160	-	-	-	-	-	-	8,816	12,784
170	-	-	-	-	-	-	9,338	13,583
180	-	-	-	-	-	-	10,042	14,382
190	-	-	-	-	-	-	10,717	15,181
200	-	-	-	-	-	-	11,414	15,980

TABLE LIII. COMPARISON OF EXPERIMENTAL AND CALCULATED SHEAR STRESSES AT ROSETTE NO. 6 (LOWER SKIN OF AFT CELL AT BL 28.0)

Percent DUL	Condition II Stresses (psi)			Condition I Stresses (psi)				
	Test Results		Stress Analysis	Test Results				Stress Analysis
	Run No. 1	Run No. 2		Run No. 1	Run No. 2	Run No. 3	Run No. 4	
10	-46	-46	26	740	-	-	-	846
20	-103	-103	52	1391	1589	1,576	1,654	1,692
30	-150	-150	78	2130	-	-	-	2,538
40	-197	-187	104	2895	3062	3,075	3,257	3,384
50	-233	-233	130	3692	-	-	-	4,230
60	-	-275	156	-	4653	4,653	4,912	5,076
70	-	-316	182	-	5506	-	-	5,922
80	-	-377	208	-	6360	6,308	6,618	6,768
90	-	-423	234	-	7317	-	-	7,614
100	-	-470	260	-	8233	8,091	8,479	8,460
110	-	-	-	-	-	8,996	-	9,306
120	-	-	-	-	-	10,030	10,392	10,152
130	-	-	-	-	-	11,193	11,374	10,998
140	-	-	-	-	-	12,331	12,409	11,844
150	-	-	-	-	-	13,651	13,572	12,690
160	-	-	-	-	-	-	14,448	13,536
170	-	-	-	-	-	-	15,867	14,382
180	-	-	-	-	-	-	17,993	15,228
190	-	-	-	-	-	-	20,061	16,074
200	-	-	-	-	-	-	-	16,920

TABLE LIV. COMPARISON OF EXPERIMENTAL AND CALCULATED SHEAR STRESSES AT ROSETTE NO. 7 (UPPER SKIN OF AFT CELL AT BL 48.0)

Percent DUL	Condition II Stresses (psi)			Condition I Stresses (psi)				
	Test Results		Stress Analysis	Test Results				Stress Analysis
	Run No. 1	Run No. 2		Run No. 1	Run No. 2	Run No. 3	Run No. 4	
10	-14	-14	78	549	-	-	-	799
20	-19	-28	156	1083	1139	1186	1,162	1,598
30	-32	-42	235	1632	-	-	-	2,397
40	-56	-65	313	2190	2232	2278	2,301	3,196
50	-79	-74	391	2770	-	-	-	3,995
60	-	-88	469	-	3371	3464	3,464	4,794
70	-	-102	547	-	3941	-	-	5,593
80	-	-121	626	-	4509	4603	4,626	6,392
90	-	-131	704	-	5138	-	-	7,191
100	-	-135	782	-	5742	5835	5,812	7,990
110	-	-	-	-	-	6416	-	8,789
120	-	-	-	-	-	7020	7,068	9,588
130	-	-	-	-	-	7764	7,694	10,387
140	-	-	-	-	-	7194	8,345	11,186
150	-	-	-	-	-	9159	9,043	11,985
160	-	-	-	-	-	-	9,512	12,784
170	-	-	-	-	-	-	10,208	13,583
180	-	-	-	-	-	-	11,204	14,382
190	-	-	-	-	-	-	12,018	15,181
200	-	-	-	-	-	-	12,972	15,980

TABLE LV. COMPARISON OF EXPERIMENTAL AND CALCULATED SHEAR STRESSES AT ROSETTE NO. 8 (UPPER SKIN OF AFT CELL AT BL 68.0)

Percent DUL	Condition II Stresses (psi)			Condition I Stresses (psi)				
	Test Results		Stress Analysis	Test Results				Stress Analysis
	Run No. 1	Run No. 2		Run No. 1	Run No. 2	Run No. 3	Run No. 4	
10	89	80	78	572	-	-	-	799
20	325	302	156	1213	999	1022	1,070	1,598
30	414	382	235	1785	-	-	-	2,397
40	470	437	313	2315	2127	2116	2,162	3,196
50	525	488	391	2836	-	-	-	3,995
60	-	539	469	-	3126	3138	3,232	4,794
70	-	590	547	-	3626	-	-	5,593
80	-	760	626	-	4126	4138	4,254	6,392
90	-	829	704	-	4662	-	-	7,191
100	-	909	782	-	5196	5161	5,254	7,990
110	-	-	-	-	-	5672	-	8,789
120	-	-	-	-	-	6254	6,346	9,588
130	-	-	-	-	-	6835	6,881	10,387
140	-	-	-	-	-	7439	7,439	11,186
150	-	-	-	-	-	8067	7,997	11,985
160	-	-	-	-	-	-	8,700	12,784
170	-	-	-	-	-	-	9,280	13,583
180	-	-	-	-	-	-	9,857	14,382
190	-	-	-	-	-	-	10,577	15,181
200	-	-	-	-	-	-	11,368	15,980

TABLE LVI. COMPARISON OF EXPERIMENTAL AND CALCULATED SHEAR STRESSES AT ROSETTE NO. 9 (LOWER SKIN OF AFT CELL AT BL 68.0)

Percent DUL	Condition II Stresses (psi)			Condition I Stresses (psi)				
	Test Results		Stress Analysis	Test Results				Stress Analysis
	Run No. 1	Run No. 2		Run No. 1	Run No. 2	Run No. 3	Run No. 4	
10	36	26	26	584	-	-	-	846
20	31	36	52	1152	1267	1,267	1,344	1,692
30	67	62	78	1738	-	-	-	2,538
40	94	94	104	2358	2469	2,456	2,585	3,384
50	134	124	130	2999	-	-	-	4,230
60	-	150	156	-	3736	3,723	3,929	5,076
70	-	192	182	-	4395	-	-	5,922
80	-	227	208	-	5041	5,016	5,248	6,768
90	-	268	234	-	5791	-	-	7,614
100	-	301	260	-	6463	6,360	6,592	8,460
110	-	-	-	-	-	7,058	-	9,306
120	-	-	-	-	-	7,807	7,989	10,152
130	-	-	-	-	-	8,634	8,686	10,998
140	-	-	-	-	-	9,409	9,409	11,844
150	-	-	-	-	-	10,263	10,160	12,690
160	-	-	-	-	-	-	10,207	13,536
170	-	-	-	-	-	-	11,481	14,382
180	-	-	-	-	-	-	12,641	15,228
190	-	-	-	-	-	-	13,520	16,074
200	-	-	-	-	-	-	14,425	16,920

TABLE LVII. COMPARISON OF EXPERIMENTAL AND CALCULATED SHEAR STRESSES AT ROSETTE NO. 10 (MAIN SPAR AT BL 28.0)

Percent DUL	Condition II Stresses (psi)			Condition I Stresses (psi)				
	Test Results		Stress Analysis	Test Results				Stress Analysis
	Run No. 1	Run No. 2		Run No. 1	Run No. 2	Run No. 3	Run No. 4	
10	449	445	743	-388	-	-	-	513
20	873	868	1486	-760	821	821	845	1,026
30	1322	1313	2229	-1149	-	-	-	1,539
40	1763	1749	2972	-1556	1617	1640	1,688	2,052
50	2214	2190	3715	-1970	-	-	-	2,565
60	-	2640	4458	-	2438	2462	2,532	3,078
70	-	3072	5201	-	2884	-	-	3,591
80	-	3578	5944	-	3306	3260	3,377	4,104
90	-	4061	6687	-	3763	-	-	4,617
100	-	4416	7430	-	4220	4150	4,267	5,130
110	-	-	-	-	-	4619	-	5,643
120	-	-	-	-	-	5112	5,205	6,156
130	-	-	-	-	-	5627	5,744	6,669
140	-	-	-	-	-	6167	6,237	7,182
150	-	-	-	-	-	6752	6,752	7,695
160	-	-	-	-	-	-	7,137	8,208
170	-	-	-	-	-	-	7,722	8,721
180	-	-	-	-	-	-	8,511	9,234
190	-	-	-	-	-	-	9,262	9,747
200	-	-	-	-	-	-	10,152	10,260

TABLE LVIII. COMPARISON OF EXPERIMENTAL AND CALCULATED SHEAR STRESSES AT ROSETTE NO. 11 (MAIN SPAR AT BL 68.0)

Percent DUL	Condition II Stresses (psi)			Condition I Stresses (psi)				
	Test Results		Stress Analysis	Test Results				Stress Analysis
	Run No. 1	Run No. 2		Run No. 1	Run No. 2	Run No. 3	Run No. 4	
10	496	510	743	402	-	-	-	513
20	896	901	1486	765	938	938	962	1,026
30	1392	1411	2229	1168	-	-	-	1,539
40	1914	1923	2972	1631	1794	1829	1,876	2,052
50	2424	2424	3715	2111	-	-	-	2,565
60	-	2950	4458	-	2732	2767	2,837	3,078
70	-	3456	5201	-	3236	-	-	3,591
80	-	4019	5944	-	3739	3681	3,799	4,104
90	-	4671	6687	-	4267	-	-	4,617
100	-	5212	7430	-	4783	4713	4,854	5,130
110	-	-	-	-	-	5276	-	5,643
120	-	-	-	-	-	5814	5,908	6,156
130	-	-	-	-	-	6448	6,495	6,669
140	-	-	-	-	-	7034	7,104	7,182
150	-	-	-	-	-	7644	7,644	7,695
160	-	-	-	-	-	-	7,956	8,208
170	-	-	-	-	-	-	8,541	8,721
180	-	-	-	-	-	-	9,449	9,234
190	-	-	-	-	-	-	10,153	9,747
200	-	-	-	-	-	-	10,903	10,260

TABLE LIX. COMPARISON OF EXPERIMENTAL AND CALCULATED SHEAR STRESSES AT GAGES NO. 34 AND 35 (AFT SPAR AT BL 68.0)

Percent DUL	Condition II Stresses (psi)			Condition I Stresses (psi)				
	Test Results		Stress Analysis	Test Results				Stress Analysis
	Run No. 1	Run No. 2		Run No. 1	Run No. 2	Run No. 3	Run No. 4	
10	280	280	466	-380	-	-	-	-388
20	640	630	932	-720	-890	-915	-915	-775
30	920	920	1398	-1110	-	-	-	-1163
40	1200	1180	1864	-1560	-1700	-1710	-1780	-1550
50	1470	1440	2330	-2000	-	-	-	-1938
60	-	1700	2796	-	-2590	-2630	-2700	-2326
70	-	1960	3262	-	-3050	-	-	-2713
80	-	2240	3728	-	-3500	-3560	-3610	-3100
90	-	2540	4194	-	-4000	-	-	-3488
100	-	2820	4660	-	-4480	-4530	-4600	-3875
110	-	-	-	-	-	-4960	-	-4260
120	-	-	-	-	-	-5490	-5560	-4650
130	-	-	-	-	-	-5980	-6030	-5040
140	-	-	-	-	-	-6500	-6510	-5430
150	-	-	-	-	-	-6990	-7050	-5820
160	-	-	-	-	-	-	-7920	-6208
170	-	-	-	-	-	-	-6400	-6596
180	-	-	-	-	-	-	-8400	-6984
190	-	-	-	-	-	-	-8870	-7372
200	-	-	-	-	-	-	-9340	-7760

Note: Modulus for data reduction = 1.17 x 10^6 psi.

Unclassified
Security Classification

DOCUMENT CONTROL DATA - R & D		
(Security classification of title, body of abstract and indexing annotation must be entered when the overall report is classified)		
1. ORIGINATING ACTIVITY *(Corporate author)* Goodyear Aerospace Corporation Akron, Ohio 44315		2a. REPORT SECURITY CLASSIFICATION Unclassified
		2b. GROUP
3. REPORT TITLE APPLICATION OF COMPOSITE MATERIALS TO AN AIRCRAFT WING SECTION		
4. DESCRIPTIVE NOTES *(Type of report and inclusive dates)* Final Technical Report		
5. AUTHOR(S) *(First name, middle initial, last name)* Fred E. Bauch and Robert C. Lair		
6. REPORT DATE October 1970	7a. TOTAL NO. OF PAGES 222	7b. NO. OF REFS 7
8a. CONTRACT OR GRANT NO DA 44-177-AMC-407 (T)	9a. ORIGINATOR'S REPORT NUMBER(S) USAAVLABS Technical Report 70-55	
b. PROJECT NO Task 1F162204A17003		
c.	9b. OTHER REPORT NO(S) *(Any other numbers that may be assigned this report)* GER 14892	
d.		
10. DISTRIBUTION STATEMENT This document is subject to special export controls, and each transmittal to foreign governments or foreign nationals may be made only with prior approval of U. S. Army Aviation Materiel Laboratories, Fort Eustis, Virginia 23604.		
11. SUPPLEMENTARY NOTES	12. SPONSORING MILITARY ACTIVITY U.S. Army Aviation Materiel Laboratories Fort Eustis, Virginia	

13. ABSTRACT

A 7-foot-long aircraft wing test section was fabricated with fiber glass reinforced plastic materials and subjected to static and dynamic tests. This was the third wing fabricated by Goodyear Aerospace and tested by the Naval Air Development Center (Aero Structures Department). However, this was the first wing to incorporate the higher strength, higher stiffness S glass material in roving and cloth form. The wing section performed in a very satisfactory manner with a good correlation between the predicted and actual test values.

DD FORM 1 NOV 65 1473

Unclassified
Security Classification

14. KEY WORDS	LINK A		LINK B		LINK C	
	ROLE	WT	ROLE	WT	ROLE	WT
Glass-Fiber Reinforced Sandwich Structures Aircraft Structure Design Aircraft Structure Testing Aircraft Wing						